



# Landsat 7 Science Data Users Handbook

## Foreword

The purpose of the Landsat program is to provide the world's scientists and application engineers with a continuing stream of remote sensing data for monitoring and managing the Earth's resources. Landsat 7 is the latest NASA satellite in a series that has produced an uninterrupted multispectral record of the Earth's land surface since 1972. Along with data acquisition and the USGS archival and distribution systems, the program includes the data processing techniques required to render the Landsat 7 data into a scientifically useful form. Special emphasis has been placed on periodically refreshing the global data archive, maintaining an accurate instrument calibration, providing data at reasonable prices, and creating a public domain level one processing system that creates high level products of superior quality.

\*Landsat Data is available for FREE

-Download data via the USGS at:

Glovis: <http://glovis.usgs.gov/>

Earth Explorer: <http://edcsns17.cr.usgs.gov/EarthExplorer/>

-Download data via GLCF at:

GLCF: <http://www.landcover.org/index.shtml>

The Landsat 7 Science Data User's Handbook is a living document prepared by the Landsat Project Science Office at NASA's Goddard Space Flight Center in Greenbelt, Maryland. Its purpose is to provide a basic understanding of the joint NASA/USGS Landsat 7 program and to serve as a comprehensive resource for the Landsat 7 spacecraft, its payload, the ground processing system, and methodologies for rendering Landsat 7 data into a form suitable for science.



# Landsat 7 Science Data Users Handbook

## 1.1 Background to the Landsat Program

The Landsat Program has provided over 38 years of calibrated high spatial resolution data of the Earth's surface to a broad and varied user community, including agribusiness, global change researchers, academia, state and local governments, commercial users, military, and the international community. Landsat images provide information meeting the broad and diverse needs of business, science, education, government, and national security.

The mission of the Landsat Program is to provide repetitive acquisition of high-resolution multispectral data of the Earth's surface on a global basis. Landsat represents the only source of global, calibrated, high spatial resolution measurements of the Earth's surface that can be compared to previous data records. The data from the Landsat spacecraft constitute the longest record of the Earth's continental surfaces as seen from space. It is a record unmatched in quality, detail, coverage, and value.

The Landsat platforms carry multiple remote sensor systems and data relay systems along with attitude-control and orbit-adjust subsystems, power supply, receivers for ground station commands and transmitters to send the data to ground receiving stations.

The most recent Landsat mission, Landsat 7, offers these features:

**Data Continuity:** Landsat 7 is the latest in a continuous series of land remote sensing satellites spanning 38 years.

**Global Survey Mission:** Landsat 7 data will be acquired systematically to build and periodically refresh a global archive of sun-lit, substantially cloud-free images of the Earth's landmass.

**Affordable Data Products:** Landsat 7 data products will be available through the EROS Data Center at the cost of fulfilling user requests (COFUR).

**Enhanced Calibration:** Data from the ETM+ will be calibrated to better than 5% absolute, providing an on-orbit standard for other missions.

**Responsive Delivery:** Automated request processing systems will provide products electronically within 48 hours of order.

The continuation of the Landsat Program is an integral component of the U.S. Global Change Research Program. Landsat 7 is part of a global research program known as NASA's

Earth Sciences Enterprise, a long-term program that is studying changes in Earth's global environment. The goal of Earth Sciences Enterprise is to provide a better understanding of natural and man-made environmental changes. In the Landsat Program tradition, Landsat 7 will continue to provide critical information to those who characterize, monitor, manage, explore, and observe the land surfaces of the Earth over time.

### **1.1.1 Previous Missions**

Landsat satellites have been providing multispectral images of the Earth continuously since the early 1970's. A unique 38-year data record of the Earth's land surface now exists. This unique retrospective portrait of the Earth's surface has been used across disciplines to achieve improved understanding of the Earth's land surfaces and the impact of humans on the environment. Landsat data have been utilized in a variety of government, public, private, and national security applications. Examples include land and water management, global change research, oil and mineral exploration, agricultural yield forecasting, pollution monitoring, land surface change detection, and cartographic mapping.

Landsat 7 is the latest satellite in this series. The first was launched in 1972 with two Earth-viewing imagers - a return beam vidicon and an 80-meter multispectral scanner (MSS). Landsat 2 and 3, launched in 1975 and 1978 respectively, were configured similarly. In 1984, Landsat 4 was launched with the MSS and a new instrument called the Thematic Mapper (TM). Instrument upgrades included improved ground resolution (30 meters) and 3 new channels or bands. In addition to using an updated instrument, Landsat 4 made use of the multission modular spacecraft (MMS), which replaced the Nimbus, based spacecraft design employed for Landsats 1-3. Landsat 5, a duplicate of 4, was launched in 1984 and even today after 26 years - 21 years beyond its 5-year design life - is still returning useful data. Landsat 6, equipped with a 15-meter panchromatic band, was lost immediately after launch in 1993.

Table 1.1 lists key mission characteristics of the Landsat Program while Table 1.2 compares the sensors carried aboard these satellites. A detailed [Landsat Program Chronology](#) is also available.

**Table 1.1 Landsat Mission Characteristics**

System	Launch (End of service)	I(s)	Resolution (meters)	Communications	Alt. Km	R Days	D Mbps
Landsat 1	7/23/72 (1/6/78)	RBV MSS	80 80	Direct downlink with recorders	917	18	15
Landsat 2	1/22/75 (2/25/82)	RBV MSS	80 80	Direct downlink with recorders	917	18	15
Landsat 3	3/5/78 (3/31/83)	RBV MSS	40 80	Direct downlink with recorders	917	18	15
Landsat 4*	7/16/82	MSS TM	80 30	Direct downlink TDRSS	705	16	85
Landsat 5	3/1/84	MSS TM	80 30	Direct downlink TDRSS**	705	16	85
Landsat 6	10/5/93 (10/5/93)	ETM	15 (pan) 30 (ms)	Direct downlink with recorders	705	16	85
Landsat 7	4/99	ETM+	15 (pan) 30 (ms)	Direct downlink with recorders (solid state)	705	16	150

I(s) = Instrument(s)

R = Revisit interval

D = Data rate

\*TM data transmission failed in August, 1993.

\*\* Current data transmission by direct downlink only. No recording capability.

**Table 1.2 Landsat Satellites and Sensors**

Satellite	Sensor	Bandwidths	Resolution	Satellite	Sensor	Bandwidths	Resolution	
LANDSATs 1-2	RBV	(1) 0.48 to 0.57	80	LANDSATs 4-5	MSS	(4) 0.5 to 0.6	82	
		(2) 0.58 to 0.68	80			(5) 0.6 to 0.7	82	
		(3) 0.70 to 0.83	80			(6) 0.7 to 0.8	82	
	MSS	(4) 0.5 to 0.6	79			(7) 0.8 to 1.1	82	
		(5) 0.6 to 0.7	79			TM	(1) 0.45 to 0.52	30
		(6) 0.7 to 0.8	79				(2) 0.52 to 0.60	30
		(7) 0.8 to 1.1	79				(3) 0.63 to 0.69	30
LANDSAT 3	RBV	(1) 0.505 to 0.75	40	(4) 0.76 to 0.90	30			
		(5) 0.6 to 0.7	79	(5) 1.55 to 1.75	30			
	MSS	(4) 0.5 to 0.6	79	(6) 10.4 to 12.5	120			
		(5) 0.6 to 0.7	79	(7) 2.08 to 2.35	30			
		(6) 0.7 to 0.8	79	LANDSAT 7	ETM <sup>+</sup>	(1) 0.45 to 0.52	30	
		(7) 0.8 to 1.1	79			(2) 0.52 to 0.60	30	
		(8) 10.4 to 12.6	240			(3) 0.63 to 0.69	30	
						(4) 0.76 to 0.90	30	
						(5) 1.55 to 1.75	30	
						(6) 10.4 to 12.5	60	
						(7) 2.08 to 2.35	30	
						PAN 0.50 to 0.90	15	

### 1.1.2 The EOSAT Era

In the mid 1980's, U.S. Government agencies, including NASA and NOAA, were directed to attain their commercial space objectives without the use of direct federal funding by entering into appropriate cooperative agreements with private sector corporate entities to encourage and advance private sector basic research, development, and operations.

The implementation of this policy required the transfer of government-developed space technology to the private sector in such a manner as to protect its commercial value, which included retention of technical data rights by the private sector. Commercial sector space activities developed under this mandate were to be supervised or regulated by federal agencies only to the extent required by law, national security, international obligations and public safety.

With the passage of Public Law 98-365, the "Land Remote Sensing Commercialization Act of 1984", NOAA was directed to delegate management of the Landsat 4 and 5 satellites and their data distribution to the private sector. In addition, NOAA was to pursue procurement of future remote sensing Landsat products and services from the private sector.

In 1985, NOAA solicited bids to manage the existing Landsat satellites and to build and operate future systems. The Earth Observation Satellite Company (EOSAT), a joint venture between RCA and Hughes Aircraft, now called Space Imaging Corporation, won the competitive bidding process in August 1984 and took over operation of the Landsat system on September 27, 1985.

From 1985 to 1994, EOSAT retained exclusive sales rights to all Landsat 4 and 5 Thematic

Mapper (TM) data until July 1994, at which time Landsat data over ten years old became available from the [National Archive at the EROS Data Center \(EDC\)](#). This agreement between Landsat Program management and EOSAT Corporation on cost and reproduction rights for Landsat 4 and 5 Thematic Mapper data remains in effect and was last updated in October 1996. EOSAT also won competition to produce the next satellite in the series, Landsat 6.

### **1.1.3 Basis in Law for Landsat**

By 1992, it had become clear that the high cost of commercially provided Landsat data had greatly restricted its use in research and other public sector applications. In response, the U.S. Congress passed H.R. 6133, the "[Land Remote Sensing Policy Act of 1992](#)", into law in September of that year. This law established a new national land remote sensing policy which:

- Abandoned full commercialization of the Landsat Program.
- Returned management of the Program to the Government.
- Established a data policy of distributing Landsat data at the cost of fulfilling a user request (COFUR).
- Directed that preliminary work begin on a new Landsat 7.
- Foster development of advanced land remote sensing systems and opportunities for commercialization.

The loss of [Landsat 6](#) in October 1993 suddenly made the new Landsat 7 mission imperative. A [May 5, 1994 Presidential Decision Directive](#) (NSTC-3) defined the new Landsat 7 data policy, program management strategies and implementation guidelines. Subsequent NASA and NOAA memoranda later that summer brought the current Landsat 7 mission into existence.

Other, recent legislation relevant to Landsat:

- **HR1275** Short title: "Civilian Space Authorization Act, Fiscal Years 1998 and 1999"
- **HR1278** Short title: "National Oceanic and Atmospheric Administration Authorization Act of 1997"
- **HR1702** Short title: "Commercial Space Act of 1997"

Visit [Recent and Pending Legislation Affecting the Landsat Program](#) for detailed public law information.

### 1.1.4 System Operation and Management

The Landsat 7 Program management structure changed repeatedly from 1992 through 1998, from NASA/USAF/USGS to NASA/NOAA/USGS to a bi-agency NASA/USGS partnership. As described in the [Landsat 7 Management Plan](#), NASA is responsible for the development and launch of the Landsat 7 satellite and the development of the ground system. The Landsat Project at Goddard Space Flight Center manages these responsibilities with Hughes Santa Barbara Remote Sensing building the sensor and Lockheed Martin Missiles and Space developing the spacecraft. The USGS is responsible for operation and maintenance of the satellite and the ground system for the life of the satellite. In this role the USGS captures, processes, and distributes the data and is responsible for maintaining the Landsat 7 data archive. The following web sites should be visited for additional information: [NASA Landsat 7 Project](#) developed the Landsat 7 System. Specifically, it meant designing, developing, and testing the Landsat 7 spacecraft, ETM+ instrument, and the end-to-end ground system. NASA was also responsible for the satellite launch and performing a 60-day in-orbit check out before handing operations to the USGS. NASA is still responsible for verifying data processing integrity and assuring high image quality.

The USGS Center for [Earth Resources Observation and Science \(EROS\)](#) manages the overall Landsat 7 Mission Operations. In this capacity EDC directs on-orbit flight operations, implements mission policies, directs acquisition strategy, and interacts with International Ground Stations. EDC captures Landsat 7 data and performs pre-processing, archiving, product generation, and distribution functions. EDC also provides a public interface into the archive for data search and ordering and handles billing and accounting procedures.

## 1.2 Landsat 7 Mission Objectives

The Landsat 7 Mission Objective is to provide timely, high quality visible and infrared images of all landmass and near-coastal areas on the Earth, continually refreshing an existing Landsat database. Data input into the system will be sufficiently consistent with currently archived data in terms of acquisition geometry, calibration, coverage and spectral characteristics to allow comparison for global and regional change detection and characterization.

The Landsat 7 project will continue to make Landsat data available for U.S. civil, national security, and private sector use as well as academic, foreign, and commercial uses. Another goal of the project is to expand the uses of such data.

### 1.2.1 Overall Mission Objectives

Landsat 7 is to have a design lifetime of five years. The overall objectives of the Landsat 7 Mission are:

- Provide data continuity with Landsats 4 and 5.
- Offer 16-day repetitive Earth coverage.
- Build and periodically refresh a global archive of Sun-lit, substantially cloud free, land images.
- Make data widely available for the cost of fulfilling a user request (COFUR).
- Support Government, international and commercial communities.
- Play a vital role in NASA's [Earth Observing System \(EOS\)](#) by promoting interdisciplinary research via synergism with other EOS observations. (In particular, orbit in tandem with EOS-AM1 for near coincident observations.)

▪

### 1.2.2 Specific Performance Requirements

Some specific requirements for the Landsat 7 System include the following:

- Acquire, capture, and archive the equivalent of 250 ETM+ scenes per day.
- Produce browse and metadata for all full and partial scenes acquired.
- Produce the equivalent of 100 Level 0R products and 100 Level 1 products per day, with phased expansion capabilities to handle an increased processing load.
- Accept data acquisition and product requests from users.
- Provide for rapid turnaround of priority acquisitions and processing.
- Supply data to users at the cost of fulfilling the user request.
- Provide communications downlinks for data capture by fixed and transportable X-band ground stations using the [Consultative Committee for Space Data Systems \(CCSDS\)](#) standard protocol for communication of data.



## 1.3 System Capabilities

The Landsat 7 system design can best be described as robust. New and unusual system capabilities include:

- Provides for a systematic collection of global, high resolution, multispectral data.
- Provides for a high volume of data collection (averaging 250 scenes per day into the U.S. archive).
- Uses cloud cover predicts to avoid acquiring unusable data.
- Provides data available for ordering by end users within 24 hours of capture at EDC.
- Provides delivery of up to 100 scene products per day.
- Provides improved access to International Ground Station data.

### 1.3.1 Global Survey Mission

An important operational strategy of the Landsat 7 mission is to establish and maintain a global survey data archive. Landsat 7 will be able to image the Earth's landmass systematically every 16 days, following the same "Worldwide Reference System" used for Landsats 4 and 5.

However, unlike previous Landsat missions, Landsat 7 will endeavor to systematically capture sun-lit, substantially cloud-free images of the Earth's entire land surface. A "Long Term Plan" has been developed to define the acquisition pattern for the Landsat 7 mission in order to create and periodically update this global archive. See [Chapter 5](#) for descriptions of the Worldwide Reference System and Long Term Acquisition Plan.

### 1.3.2 Rapid Data Availability

## EDC - DAAC (Distributed Active Archive Center)

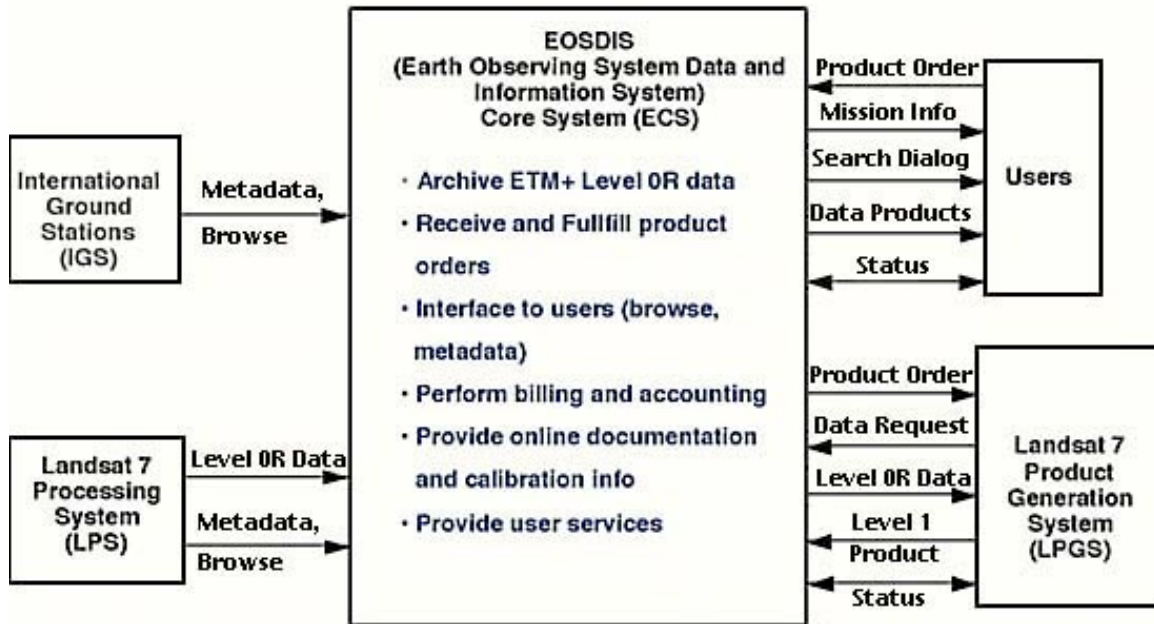


Figure 1.1 - Landsat 7 Data Distribution System

The Landsat 7 data distribution system will provide access to Landsat 7 Level 0R data products within 24 hours of collection and Level 1 processed products within 48 hours of request. Product media options include Exabyte tape (8 mm 8200, 8mm 8500), CD-ROM or electronic transfer via FTP. Billing and accounting are handled via ECS-registered prepaid accounts. New users should contact the EDC-DAAC User Services Office (605-594-6116 voice, 605-594-6963 fax, Email for assistance in setting up data purchase accounts and arranging payment method in advance.

Landsat 7 product orders may be placed electronically via the web using the [USGS Global Visualization Viewer](#) or the [Global Land Cover Facility](#).

### 1.3.3 Enhanced IGS Access

Imagery of foreign landmasses will be recorded and down linked to EDC yet the temporal depth will be a fraction of what's available at the international ground stations. Users of Landsat 7 data will have improved access to this data. As stipulated in the NOAA-IGS Memorandum of Understanding, each international ground station collecting Landsat 7 data is required to send periodic inventory information in the form of scene metadata to the LP-

DAAC. IGS metadata is structured according to the U.S. standard and as such, is available for web-based searching using tools developed for the U.S. archive. The IGSs also have the option to send browse imagery to the LP-DAAC for viewing by interested users.

The LP-DAAC will also support access to foreign products in other ways. Users will discover on EDC's web servers internet links to IGS browse systems and information on IGS product types and ordering protocols. No IGS products will be archived at EDC. They can only be discovered and then ordered directly from the IGS data distributor(s).

## 2.1 Overview

The Landsat 7 satellite was successfully launched from Vandenberg Air Force Base on April 15, 1999. The Delta II launch vehicle left the pad at 11:32 PDT and performed flawlessly. The injected spacecraft, depicted in Figure 2.2 and in this [1.8 MB Quicktime movie](#), is a 5000 pound-class satellite designed for a 705 km, sun synchronous, earth mapping orbit with a 16-day repeat cycle. Its payload is a single nadir-pointing instrument, the Enhanced Thematic Mapper Plus (ETM+). S-Band is used for commanding and housekeeping telemetry operations while X-Band is used for instrument data downlink. A 378 gigabit Solid State Recorder (SSR) can hold 42 minutes of instrument data and 29 hours of housekeeping telemetry concurrently. Power is provided by a single Sun-tracking solar array (four 74" by 89.3" panels - 184 square feet) and two 50 amp-hour Nickel-Hydrogen batteries. Attitude control is provided through four reaction wheels (pitch, yaw, roll, skewed), three 2-channel gyros with celestial drift updating, a static Earth sensor, 1750A processor, and torque rods and magnetometers for momentum unloading. Orbit control and backup momentum unloading is provided through a blow-down monopropellant hydrazine system with a single tank containing 270 pounds of hydrazine, associated plumbing, and 12 one pound-thrust jets. Spacecraft weight is approximately 4632 pounds at launch.



Figure 2.1 - Landsat 7 Launch

## 2.2 Platform Details

The satellite provides active, three axis stabilized, attitude control; NASA standard telemetry, tracking and command for narrowband communications; Landsat unique direct, and store and forward wideband data; direct energy power transfer, including a single solar array with multiple panels, with on-board power storage; on-board computing for power management, attitude control, satellite commanding and failsafe protection management; and hydrazine

reaction control for momentum compensation and orbit adjust maneuvers.

The satellite attitude control uses precision mode, which is a combination of stellar and inertial guidance sensors to maintain the spacecraft platform within 0.015 degrees of earth pointing. The capability exists for an initial attitude control rate-nulling mode, local vertical acquisition mode, yaw gyro backup mode, and an orbit adjust maneuver mode.

Narrowband communications include processing of real-time and stored commands, processing and authentication of command messages and transmission of telemetry data, which is the collection of housekeeping and satellite processor reports.

Wideband communications for payload data transmission to the ground incorporates four X-band transmitters, switchable to three steerable antennas that have a downlink beam width of 1.2 degrees. Also, an on-board solid-state recorder is used to store imagery of foreign landmasses for subsequent transmission to EDC.

The on-board processor performs autonomously executed functions for wideband communications, electrical power management, and satellite control. These include attitude control, redundancy management, antenna steering, battery management, solar array pointing maintenance, thermal profile maintenance, and stored command execution. The Satellite Segment also includes the Aerospace Ground Equipment (AGE) which is composed of all the electrical (EAGE), mechanical (MAGE), instrument and propellant ground equipment and related software used to integrate the satellite to the launch vehicle. Additionally, it consists of support system test functions and protection of the satellite during transport. One particular type of EAGE, the launch site equipment (LSE), is used to verify the readiness of the satellite during pre-launch testing and during launch operations and readiness reviews.

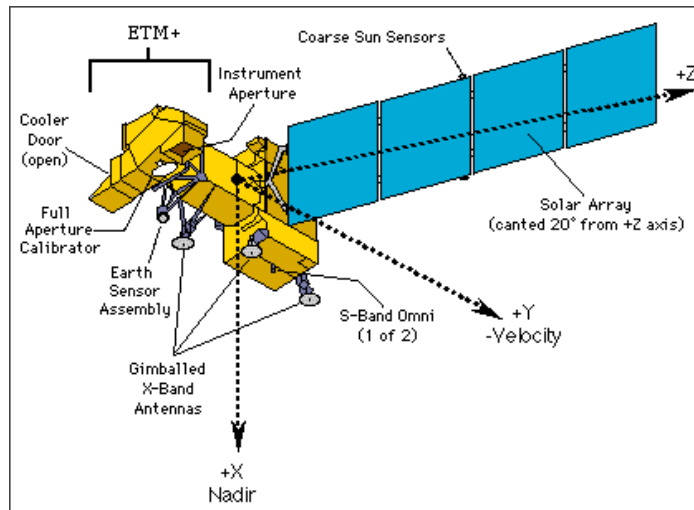


**Figure 2.2** - The Landsat 7 satellite as viewed from the sun side.

## 2.3 Functions

### 2.3.1 Scheduling

Planning and scheduling takes place in three categories; long-term planning, short-term planning, and daily scheduling.

#### Long-Term Planning

The prime goal of the Landsat 7 mission is to refresh the global archive. Because the Landsat 7 mission orbit profile operates on a repetitive 16-day cycle, the global archive refresh strategy was designed years before the Landsat 7 satellite launch. The long-term acquisition plan was generated early, to provide ample time for coordination with the science community, program management, international resources, and project elements. The long-term plan takes into account the calibration plan, planned satellite maneuvers, and international imaging needs. The MOC ingests the long-term plan prior to launch and uses the data as the main database from which to plan daily schedules of instrument and SSR activities.

#### Short-Term Planning

The objectives of short-term planning are to schedule communication contacts for telemetry, tracking and commanding services on the Landsat Ground Network (LGN), to include special requests into the scheduling process, and to generate daily reports summarizing the disposition of imaging requests and time-ordered scheduled ETM+ imaging events for the latest 48-hour period.

#### Daily Scheduling

On a daily basis, the MOC must generate a nominal 48-hour set of imaging, SSR activities, and X-band downlink services from which the MOC will generate an absolute time stored command load. The MOC will schedule the 48-hour set of activities based on a number of criteria, including global refresh requirements, request priority, SSR or other resource availability, and cloud cover predictions. After the FOT has iterated through the scheduling function and resolved all conflicts, the MOC will pass the 48-hour schedule to the load generation function for final compilation. To assist in the scheduling process, the MOC receives planning aids from the FDF (Table 2.1), a cloud cover prediction from the National Meteorological Center (NMC), and metadata on acquired or archived imagery from the EDC-DAAC.

<b>Table 2.1 MOC/FDF Product Exchange</b>		
<b>Product from MOC</b>	<b>Product to MOC</b>	<b>Frequency</b>
Telemetry and displays	-	Realtime during each pass; TBD after receipt of playback
Orbit maneuver data	-	As needed (within 30 minutes of maneuver command)
Post maneuver evaluation	-	As needed
-	Post maneuver evaluation and report	within 48 hours of maneuver completion
IGS position data	-	As needed (within 24 hours of data receipt)
-	Orbit State Vectors	Daily
-	Planning Aids	Weekly
-	Local Oscillator Frequency (LOF)	Monthly
-	Star Catalog	As needed
Maneuver planning	Maneuver planning	As needed
-	Maneuver plan	48 hours before maneuver
-	Orbit maneuver parameters	48 hours before maneuver
-	Station Acquisition data	Daily

### **2.3.2 Tracking and Spacecraft Control**

The radio frequency (RF) communications system provides S-band (narrowband) telemetry for housekeeping data and tracking ability. The S-band communications are conducted through two omni S-band antennas located on opposite sides of the spacecraft (nadir and zenith pointing). The zenith antenna is used for Tracking Data and Relay Satellite (TDRS) communications; the nadir antenna is used for LGN communications. Each antenna provides essentially hemispherical coverage.

Telemetry data is generated and recorded at all times and contains all of the information required to monitor and assess the health of the satellite, verify day-to-day operations, and assist in anomaly resolution. The on-board telemetry data formatter continually collects, formats, and outputs a telemetry data stream into a CCSDS compliant downlink protocol

and sends the encoded data to the SSR for recording. The encoded data may also be sent to the S-band transponder for transmission to the MOC via a TDRS or LGN ground station.

The MOC receives tracking telemetry on a daily basis that shows the position and velocity of the spacecraft. The Flight Dynamics Facility (FDF) is responsible for computing the actual spacecraft position and velocity for the last 61 hours and generating predicted orbit state vectors for the next 72 hours. The orbit state vectors must provide an attitude accuracy of 375 meters at 40 hours and must be uplinked daily in order to maintain the satellite within mission parameters.

The MOC receives the orbit state vectors file from the FDF and validates the information. The MOC converts the orbit state vectors data into a Landsat 7 orbit state vectors table. The new orbit state vectors are compared against the old orbit state vectors in the same way the flight software makes this comparison on the satellite after the receipt of the new orbit state vectors load. During daily scheduling, the Flight Operations Team (FOT) inserts an orbit state vectors activation command into the daily absolute command sequence.

After the MOC operators uplink and activate the absolute stored command load, the new orbit state vectors table is uplinked to a scratch buffer. At the appropriate epoch time, stored commands deactivate the active orbit state vectors table, move the orbit state vectors from the scratch buffer into active memory, and reactivate the active orbit state vectors table. On-board software interpolates this new data to generate the positional information contained in the Payload Correction Data (PCD).

### **2.3.3 Orbit Maneuvers**

During the Landsat 7 mission, the MOC operators perform two types of orbit maneuvers to ensure the satellite's orbit remains within the Landsat 7 mission parameters. The two types of orbit maneuvers are:

- In-plane Maintenance, and
- Inclination Maintenance.

The In-plane maintenance maneuver, also called a drag make-up maneuver, maintains the semi-major axis within an acceptable tolerance of the mission orbit semi-major axis. The semi-major axis is biased high and permitted to decay over time. The bias applied to the orbit varies with the amount of environmental drag, which is a function of solar activity.

The inclination maintenance maneuver involves a yaw slew by approximately +/- 90 degrees. The operators perform the inclination maneuver to keep the satellite-descending

node within a 30-minute box (09:45 to 10:15 AM). The FDF is responsible for monitoring the satellite orbit to ensure that its orbit remains within mission parameters. The FDF receives tracking data from the space network and Landsat telemetry data from the MOC that are necessary to monitor the orbit and informs the MOC when the orbit has been perturbed sufficiently to require an orbit adjust. The FDF calculates the orbit maneuver command data, including an orbit maneuver time window, and passes the command data and a maneuver plan to the MOC.

The MOC ingests the orbit maneuver command data and generates a set of absolute time commands. The Flight Operations Manager (FOM) reviews the data and the resulting commanding prior to merging the commanding into the absolute time command load for the day of the orbit maneuver. The FOT mission planner will insert an orbit state vector activation command that is timed to execute at the end of the maneuver window.

The FOT coordinates the orbit maneuver times with the NCC for TDRSs support and with the NOAA SOCC for CDAS support to facilitate the communications support needed to monitor the orbit maneuver in real-time. Additionally, the FOT schedules TDRS tracking passes to occur immediately after the maneuver.

On the day of the orbit maneuver, the FDF sends the MOC two sets of orbit state vectors: one to execute in a burn scenario and one to execute if the MOC cancels the orbit maneuver. The MOC generates orbit state vector loads for each set and make them available to the FOT.

Once the FOM makes the final decision to perform the orbit maneuver, the FOT uplinks the absolute time stored command load to the satellite. Sometime after the FOT activates the stored command load and before the orbit maneuver occurs, the FOT uplinks the appropriate orbit state vectors load. The orbit state vectors load remains in the on-board scratch buffer until after the burn takes place. At that time, the FOT executes real-time commands to activate the post-burn orbit state vectors by copying the orbit state vectors from the scratch buffer to the active orbit state vectors table and starting ephemeris processing of the new orbit state vectors.

Following the orbit adjust; the MOC conducts TDRS contacts for acquiring tracking data. The FDF calculates the new satellite orbit, using this tracking data, verifies the success of the orbit adjust, and generates new orbit state vectors for routine delivery on the day following the burn. The FDF evaluates the performance of the satellite components used during the orbit adjust and provide that information to the MOC to update the MOC-resident propulsion model. The MOC uses the MOC-resident propulsion model to calculate the remaining propellant on-board the satellite and analyze the propulsion system.



## 2.4 Communication Links

Ground sites exist at Sioux Falls, South Dakota (The Landsat Ground Station, or LGS), Poker Flat, Alaska (Alaska Ground Station, or AGS), Wallops Virginia (WPS), and Svalbard, Norway (SGS). SGS and AGS are also known as the EOS Polar Ground Sites (EPGS) and are managed by Wallops Flight Facility (WFF). All ground sites are equipped with 11-meter antennas. AGS, SGS, and LGS are capable of receiving both S-band (housekeeping) at a downlink rate of 4 Kbps and X-band (payload) data simultaneously. The figure below provides a view of the ground stations' acquisition circles.

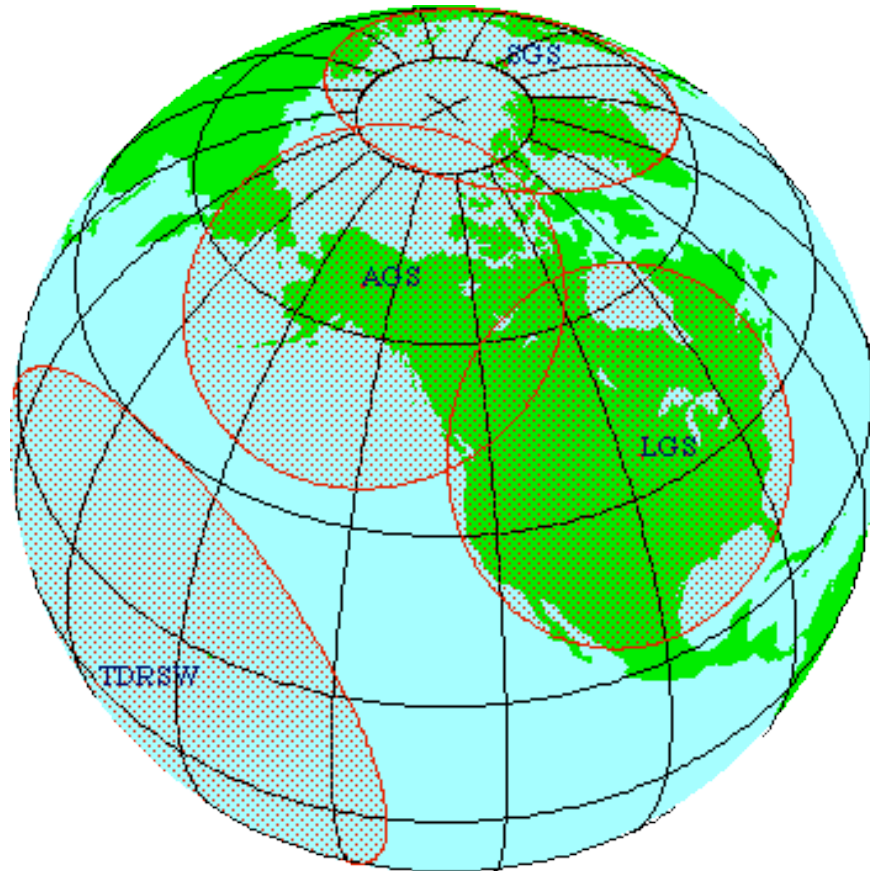


**Figure 2.3** - U.S. Ground Station Acquisition Circles

In addition to the ground sites, the [TDRS](#), operated by the Space Network, NASA code 530 is utilized. TDRS enables downlink of real-time and stored S-band data and command of the spacecraft. TDRS is also used tracking and data collection for FDF generation of Landsat 7 spacecraft ephemeris, which is subsequently uploaded, for use in precision attitude control. The NASCOM division of NASA provides all network lines.

## 2.5 Solid State Recorder

The SSR is used to capture wideband data from the ETM+. The SSR accepts two inputs at 75 Mbps. The SSR can hold up to 42 minutes (approximately 100 scenes) of data at 150

Mbps. The SSR records and plays back wideband data in numbered logical blocks, which are used by the MOC in commanding the recorder.

The SSR records ETM+ channel access data units (CADU) as two bitstreams, each at a nominal rate of 74.914 Mbps. CADUs are recorded in the same order as received from the ETM+. Partial CADUs may be recorded if the ETM+ collection interval extends beyond the commanded SSR record interval, if the ETM+ is turned off before the end of the SSR data recording area is achieved, or as a result of a ground command to disable wideband recording.

During playback, the two 75 Mbps bitstreams are read out of memory and sent to the broadband switching unit. A second pair of 75 Mbps bitstreams can also be played back for a total aggregate rate of 300 Mbps. The bitstreams include the CADUs generated by the ETM+. Record intervals, each corresponding to an ETM+ collection interval, which consists of one or more Landsat scenes, may be subdivided for playback if more than one scene is collected. In this case, each resulting subinterval is defined such that data in the vicinity of each subinterval boundary are included (redundantly) with both subintervals. Each subinterval includes all of the CADU data required to process the subinterval as a separate ETM+ collection. As a result, individual subintervals may contain partial CADUs. The SSR contains error detection and correction capability to preserve the integrity of the stored wideband and narrowband data. [Reed-Solomon encoding](#) is performed on record while Reed-Solomon decoding is performed on playback to recover data from possible dynamic RAM list errors.

Narrowband data is captured from by the SSR from the Telemetry Data Formatter. The SSR accepts two input rates of 1.216 Kbps or 4.864Kbps and plays back stored telemetry data at 256 Kbps to the S-Band transponder.

The SSR is capable of either recording or playing back wideband data (but not both simultaneously) while simultaneously recording and/or playing back narrowband telemetry data. S-Band telemetry data is stored separately from wideband image data and can be recorded during load shedding.

### 3.1 Sensor Overview

Landsat 7's sensor - the Enhanced Thematic Mapper Plus (ETM+) - was built by SBRS. The sensor is a derivative of the Thematic Mapper (TM) engineered for Landsats 4 and 5, but is more closely related to the Enhanced Thematic Mapper (ETM) lost during the Landsat 6 failure. The primary performance related changes of the ETM+ over the TM's are the addition of the panchromatic band and two gain ranges (added for Landsat 6), the improved spatial resolution for the thermal band, and the addition of two solar calibrators.



Figure 3.1 - Enhanced Thematic Mapper Plus

The ETM+ design provides for a nadir-viewing, eight-band multispectral scanning radiometer capable of providing high-resolution image information of the Earth's surface when operated from Landsat 7, a 3 axis stabilized spacecraft located in a near polar, sun-synchronous and circular orbit at a 705 km nominal altitude, with an orbit inclination of 98.2 degrees. The ETM+ is designed to collect, filter and detect radiation from the Earth in a swath 185 km wide as it passes overhead and provides the necessary cross-track scanning motion while the spacecraft orbital motion provides an along-track scan.

### 3.2 ETM+ Design

Scene energy passes through a number of major ETM+ subsystems, depicted in Figure 3.2, before the solid-state detectors at the focal plane collect it. The bidirectional scan mirror assembly (SMA) sweeps the detector's line of sight in west-to-east and east-to-west directions across track, while the spacecraft's orbital path provides the north-south motion. A Ritchey-Chretien telescope focuses the energy onto a pair of motion compensation

mirrors (i.e. scan line corrector) where it is redirected to the focal planes. The scan line corrector is required due to the compound effect of along-track orbital motion and cross-track scanning which leads to significant overlap and underlap in ground coverage between successive scans.

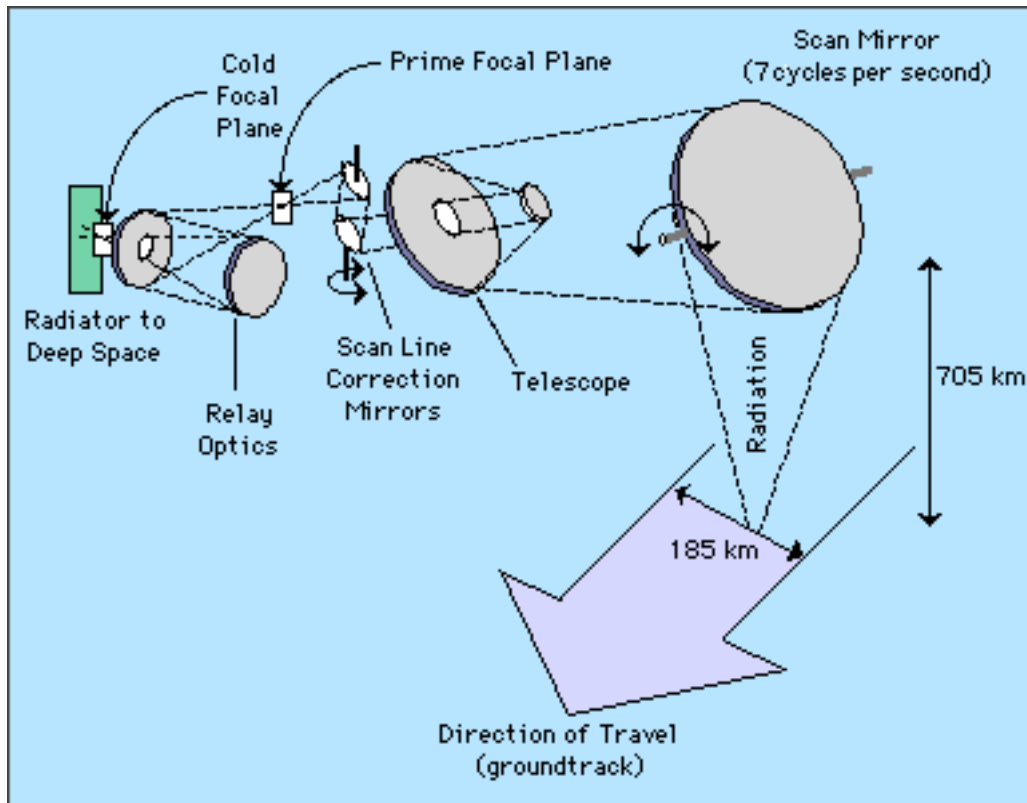


Figure 3.2 - ETM+ Optical Path

The aligned energy encounters the Primary Focal Plane (PFP), where the silicon detectors for bands 1-4 and 8 (panchromatic) are located. A portion of the scene energy is redirected from the PFP by the relay optics to the Cold Focal Plane where the detectors for bands 5, 7, and 6 are located. The temperature of the cold focal plane is maintained at a predetermined temperature of 91° K using a radiative cooler. The spectral filters for the bands are located directly in front of the detectors.

### 3.2.1 Detector Geometry

Figure 3.3 illustrates the relative position of all the detectors from both focal planes with respect to their actual ground projection geometry. The even-numbered detectors are arranged in a row normal to the scan direction while the odd-numbered detectors are arranged in a parallel row, off exactly one IFOV in the along scan direction. This arrangement provides for a contiguous bank of 32, 16, and 8 detectors for band 8, bands 1-5

and 7, and band 6 respectively. The detector arrays are swept left to right (forward) and right to left (reverse) by the scan mirror, which covers a ground swath approximately 185 kilometers wide. With each sweep or scan an additional 480 meters (32, 16, and 8 data lines at a time) of along track image data is added to the acquired subinterval.

### Band Offsets

During a scan the actual ground observed by each band's detectors is not identical due to the horizontal spacing of detector rows within and between bands. Again referring to the ground projection illustration in figure 3.3 one should note the spacing between bands as measured in 30 meter 42.5 microradian IFOVs. Taken individually, these numbers represent a band's unique leading edge preamble that occurs before coincident data is collected by a band's forward or reverse focal plane neighbor. Taken cumulatively, these numbers represent the first order zero fill offsets that LPS uses during OR processing to achieve image registration at the level 0 level. Other factors such as detector offsets within a band and sample timing must be considered to calculate registration offsets accurately.

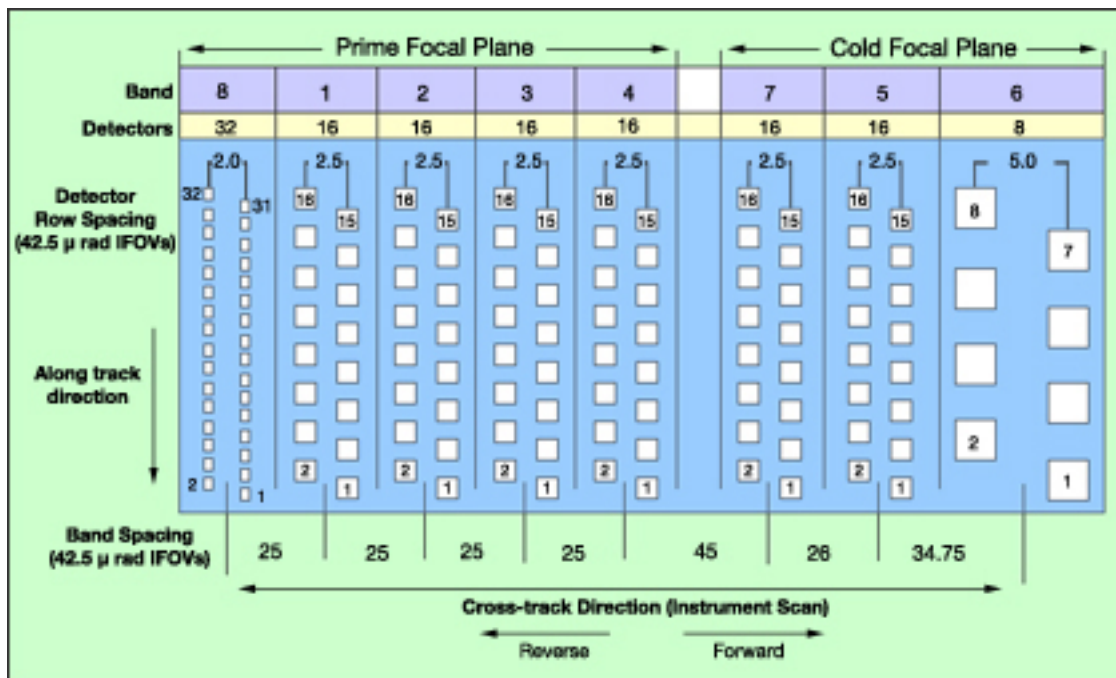


Figure 3.3 - Detector Projection at the Prime Focal Plane

### Detector Offsets

Band 8 detectors rows are separated by 2 42.5μ IFOVs which translates to 4 15 meter samples. The band 8 odd and even detectors are sampled simultaneously, twice per minor frame (i.e. one sample). The registration offsets for the odd and even detectors will therefore always differ by four samples for both forward and reverse scans.

The detector rows within bands 1-5 and 7 are separated by 2.5 42.5μ IFOVs. This seemingly

curious design makes sense because the multiplexer samples the even detectors .5 IFOV later than the odd detectors within a minor frame of data. The delay effectively separates the odd and even detectors an integral multiple of IFOV's apart in sampling space. A 2 IFOV odd-to-even detector spacing is realized on forward scans while 3 IFOV spacing occurs on reverse scans. The registration offsets for forward and reverse scans will always differ by these amounts.

The band 6 odd and even detectors are separated by 5  $42.5\mu$  IFOVs which translates to 2.5 band 6 samples. The odd and evens are sampled, however, in alternating minor frames, which separate the odd and even detectors, an integral multiple of IFOVs. A 2 band 6 IFOV odd-to-even detector spacing is realized on forward scans while a 3 band 6 IFOV spacing occurs on reverse scans. The registration offsets for forward and reverse scans will always differ by these amounts.

### **3.2.2 Registration Offsets**

Over the years, different ground system engineers have characterized Landsat focal plane offsets in different ways that resulted in negative and positive offsets depending upon the forward and reverse scan directions and origin of the image grid. For Landsat 7 we have declared all shifts as positive from column 1 in the 0R image buffers. These 8 bit buffers are 3300, 6600, and 13,200 elements in size for the 60, 30, and 15-meter bands respectively.

### **3.2.3 ETM+ Sample Timing**

The ETM+ data stream is composed of a continuous succession of major frames. A major frame contains the data for an entire period of one complete scan of the ETM+ scan mirror. A major frame is partitioned into minor frames - a specific pattern for organizing groups of ETM+ data words. This pattern is based on the architecture of the Landsat 7 auxiliary Electronics module (AEM) that samples, digitizes, and groups analog video signals from the ETM+ scanner to form scene data. The minor frame data structure is 85 words (8 bits) in length consisting of 16 separate groups of 5 words, 4 data words from band 6 and a one spare.

The line sync code is generated by the AEM at the beginning of each new scan line and inserted into minor frame zero which is also called scan line start (SLS). The time code pattern preempts all video data except band 6 although the band 6 data for the first minor frame is invalid. The six minor frames immediately following the SLS minor frame describe the spacecraft time code as illustrated in Figure 3.4. The time code data preempts all minor frame video except band 6 data. The band 6 data alternates between the odd and even detectors for each successive minor frame and are synchronized to odd pixel data for the

first minor frame. The first valid band 6 data are from the even detectors and occur in minor frame two.

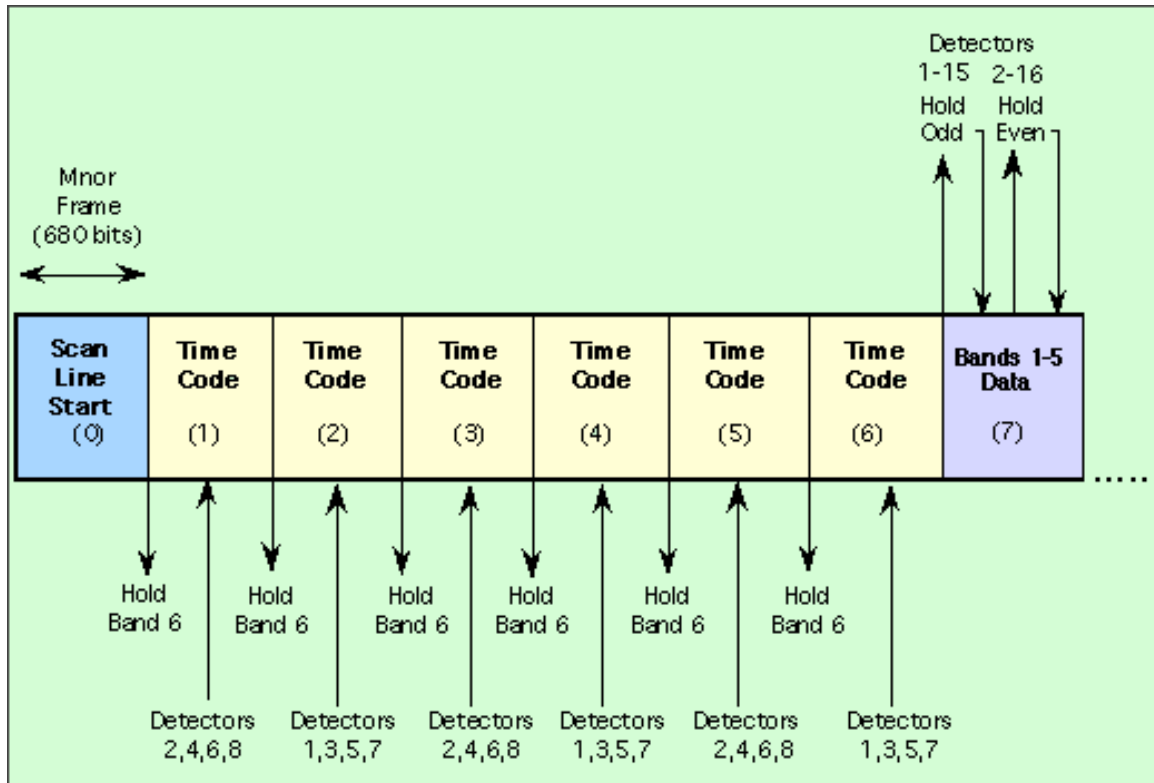


Figure 3.4 - ETM+ Sample Timing - Format 1

Scene data transmission for the other bands starts at the minor frame boundary immediately following the time code and continues until start of the next end of line pattern code, which is mechanically/optically, triggered. For reference, 6313 minor frames of scene data are nominally transmitted during any given scan cycle. The digitized scene data can be organized into either of two minor frame scene data formats as depicted in Figures 3.4 and 3.5. Bands 1-5 are allocated to format 1 while bands 7 and 8 are allocated to format 2. The two band 6 data streams allocated to formats 1 and 2 are low gain and high gain respectively.

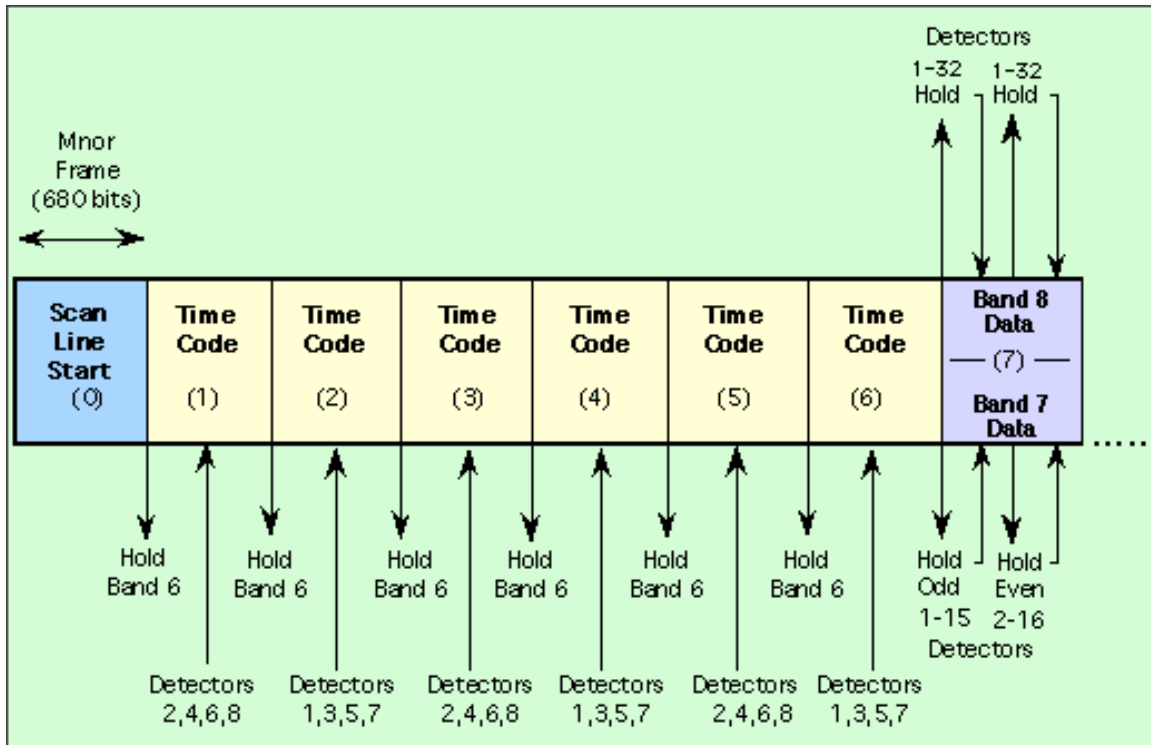


Figure 3.5 - ETM+ Sample Timing - Format 2

### 3.3 ETM+ Subsystems

#### 3.3.1 Scan Mirror Assembly

Table 3.1	
Swath width at 0 degrees North	185 km
Swath width at 40 degrees North	187 km
Scan length at 0 degrees North	480 m
Scan length at 40 degrees North	484 m
Active scan amplitude	7.695 degrees
Scan period	142.925 milliseconds
Scan Frequency	6.997 Hz
Active scan time	60.743 milliseconds
Turn around time	10.719 milliseconds
Object plane scan rate	4.42191 rad/sec
Mirror scan rate	2.21095
30 m IFOV dwell time	9.611 microseconds
Scan line length (excludes turn around)	6320 IFOVs
Inertia	< 9.4 in-lb-(sec*sec)
Clear aperture	21.050 in x 16.250 in



The Scan Mirror Assembly (SMA) provides the crosstrack scanning motion to develop the 185 km long scene swath. The SMA consists of a flat mirror supported by flex pivots on each side (which have compensators to equalize pivot reaction torque), a torquer, a scan angle monitor (SAM), 2 leaf spring bumpers and scan mirror electronics (SME). The motion of the mirror in each direction is stopped by the bumper, and is boosted by precision torque pulses during the turnaround period. The amount of torque applied is controlled by the SME microprocessor as determined from the SAM mirror angle pulses. The resulting active scan in each direction is closely controlled to 60,743  $\mu$ s. The SMA derives timing from a 10 MHz clock routed by buffers in the multiplexer. The 10 MHz is counted down from the 74.9 MHz system clock by circuits in whichever multiplexer is providing the system timing. SAM mirror angle pulses are used by the multiplexer to synchronize the detected scene data. There are redundant sets of scan mirror electronics, SME 1 and SME 2. SME 2 is an identical back up electronic package to SME 1. Additionally, both SMEs have a primary SAM mode of operation and a back up Bumper Mode of operation. SMA characteristics are listed in Table 3.1.

### 3.3.2 Telescope

<b>Table 3.2</b>	
Primary mirror clear aperture outer diameter	16.0 in (40.64 cm)
Primary mirror clear aperture inner diameter	6.56 in (16.66 cm)
Telescope effective clear aperture	1020 square cm
Effective focal length	96 in (243.8 cm)
f/#	6.0
Mirror material	Ultra-low expansion (ULE) glass
Mirror coating	Enhanced silver

The telescope is a Ritchey-Chretien configuration with a primary and secondary mirror and baffles. Both the tube-like central baffle and the outer housing have a series of annular baffles for stray light control. The telescope structure is constructed using a graphite-epoxy laminate, which has a very low coefficient of thermal expansion and thus eliminates problems due to thermal expansion. However, the graphite-epoxy laminate is hygroscopic and can change dimensions due to moisture absorption. Care was exercised during integration and test to minimize moisture absorption and to maintain knowledge of the telescope's condition. The central baffle is made from aluminum. The telescope's characteristics are summarized in Table 3.2.

### 3.3.3 Scan Line Corrector

The Scan Line Corrector (SLC) is an electro-optical mechanism composed of two parallel nickel-plated beryllium mirrors set at an angle on a shaft. The shaft, driven by a torquer, which has primary and redundant tachometers, rotates about an axis normal to the axis of the scan mirror in a saw tooth fashion. The SLC is positioned behind the primary optics and compensates for the along track motion of the spacecraft that occurs during an active SMA cross track scan. A rectilinear scan pattern is produced using the SLC instead of the zigzag pattern that would be produced without it (Figure 3.6).

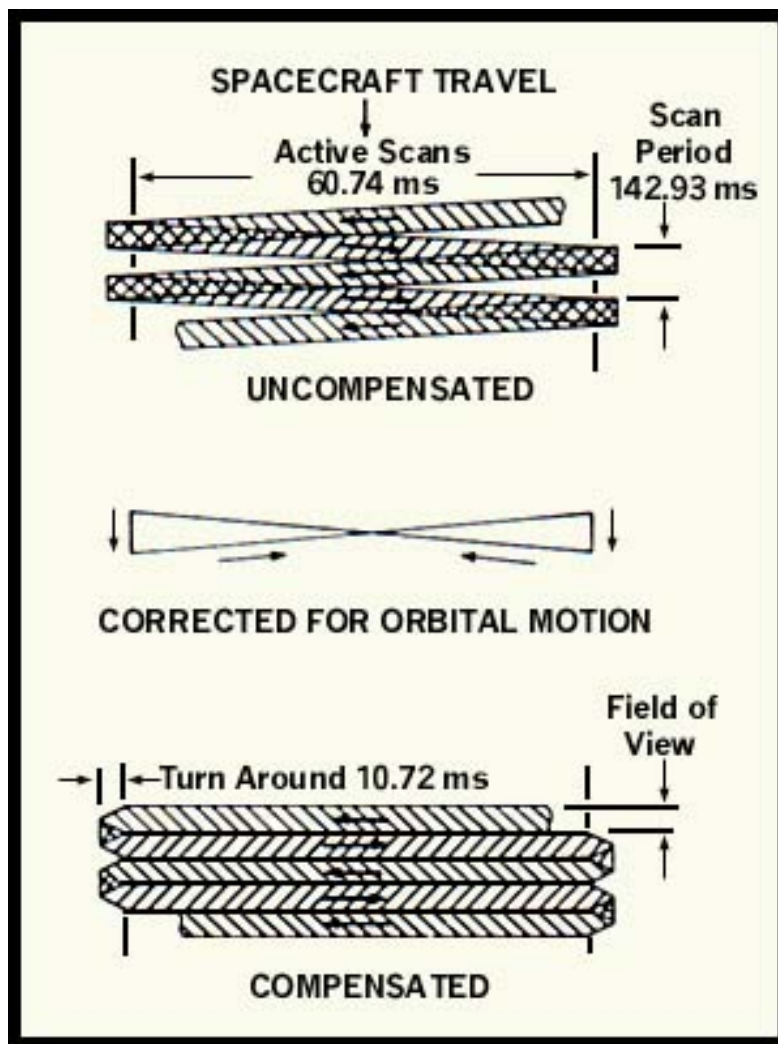


Figure 3.6 - ETM+ Scan Line Correction

A feedback control system is employed in the SLC drive electronics to achieve a constant angular rate of 576.6 mr/sec. The primary and redundant SLC drivers are implemented on the MEM A1 and A2 circuit cards respectively. The SLC driver produces a linear saw tooth

signal with a fast fly back. The SLC driver receives a 208 kHz clock and a buffered line start signal from the Timing Control Subsystem. Table 3.3 lists the SLC characteristics.

<b>Table 3.3 Scan Line Corrector Design Parameters</b>	
Scan frequency	13.99 Hz
Scan period	71.462 ms
Scan rate in object space	9.610 $\mu$ rad/sec
SLC rotation rate	576.6 $\mu$ rad/sec
SLC linear scan angle	35.02 $\mu$ rad
Linear scan angle in object space	583.7 $\mu$ rad
Mirror separation	1.600 in
Linear image displacement amplitude	.056 in
Linear image displacement rate	9.22 in/sec
Mirror material	Nickel plated beryllium
Mirror coating	Enhance silver

### 3.3.4 Primary Focal Plane

The Prime Focal Plane Assembly consists of three major subassemblies; the Prime Focal Plane Array and the two preamplifier stacks. The Prime Focal Plane Array is located at the focal plane (surface) of the telescope. Its characteristics are listed in Table 3.4. The Prime Focal Plane Array is a monolithic silicon focal plane made up of five detector arrays: Band 1 through Band 4 and the Pan Band. The arrays for Bands 1 through 4 contain 16 detectors divided into odd-even rows. The array for the Pan Band contains 32 detectors also divided into odd-even rows. The system focus is optimized for the Pan Band, which has the highest spatial resolution. The preamplifiers are mounted on the Prime Focal Plane Assembly, and consist of two stacks of flat hybrid modules. On top of each stack is a cylindrical black radiative cooling tower to help dissipate the heat from the preamplifiers.

<b>Table 3.4 Prime Focal Plane Assembly Design Parameters</b>		
<b>Parameter</b>	<b>Bands 1 through 4</b>	<b>Pan Band</b>
Number of detectors	16 per band	32
Detector Size	0.00408 in x 0.00408 in	0.00204 in x 0.00177 in
Detector Area		
I FOV size	42.5 $\mu$ rad	21.25 $\mu$ rad x 18.5 $\mu$ rad
Center to center spacing along track	0.00408 in	0.00204 in
Center to center spacing between rows	0.01020 in	0.00816 in

### 3.3.5 Relay Optics

The Relay Optics consists of a graphite-epoxy structure containing a folding mirror and a spherical mirror, which are used to relay the imaged scene from the prime focal plane to the Band 5, 6 and 7 detectors on the cold focal plane. The characteristics of the Relay Optics are listed in Table 3.5. The position and tilt of the spherical mirror may be varied during integration and test by three electro-mechanical linear actuators to provide focus of the Cold Focal Plane Array and to obtain the correct band-to-band registration of the cold focal plane detectors to the prime focal plane detectors. The Relay Optics has a magnification of 0.5. This magnification is used because of the reduced physical size of the band 6 detectors.

<b>Table 3.5 Relay Optics Design Parameters</b>	
Folding mirror clear aperture outer diameter	3.14 in
Folding mirror clear aperture inner diameter	0.537 in
Spherical mirror clear aperture diameter	5.538 in
Magnification	.5
F/#	3.0
Mirror material	ULE glass
Mirror coating	Aluminum, SiO overcoat

### 3.3.6 Cold Focal Plane

The Cold Focal Plane Assembly is mounted on the cold stage of the Radiative Cooler, and operates at a nominal temperature of 90°K~92°K and can be controlled to one of three set points (90° K, 95° K or 105° K) by a heater on the back of the substrate. The higher temperatures are backup in case the Radiative Cooler efficiency degrades. The characteristics of the Cold Focal Plane Assembly are listed in Table 3.6. The Cold Focal Plane Assembly contains the detector arrays for Bands 5, 6 and 7. Each band is a separate array. The three arrays are mounted on a monolithic substrate. The Band 5 and Band 7 arrays contain 16 detector elements, and are fabricated from indium antimonide. These photovoltaic indium antimonide arrays show very little change in responsivity from 90° K to 105° K. The nominal spatial resolution of Bands 5 and 7 is the same as Bands 1 through 4. The Band 6 array is fabricated from mercury cadmium telluride. This photoconductive array shows a significant decrease in responsivity from 90° K to 105° K. The Band 6 array contains 8 detector elements. The input stages and the feedback resistors of the preamplifier for the Band 5 and 7 (photovoltaic) detectors are mounted with the detectors on the cold stage of the Radiative Cooler. The Band 6 preamplifier and the remainder of the Bands 5 and 7 preamplifier are mounted on a circular housing adjacent to the radiative cooler. The

connections within the Radiative Cooler from the cold focal plane area to the ambient temperature connectors for the preamplifiers are made via special low thermal conductivity ribbon cables.

<b>Table 3.6 Cold Focal Plane Design Parameters</b>		
<b>Parameter</b>	<b>Bands 5 and 7</b>	<b>Band 6</b>
Number of detectors	16 per band	8
Detector Size	0.00190 in x 0.00204 in	0.00408 in x 0.00408 in
Detector Area		
IFOV size	42.5 $\mu$ rad x 39.4 $\mu$ rad	42.5 $\mu$ rad x 85.0 $\mu$ rad
Center to center spacing along track	0.00204 in	0.00408 in
Center to center spacing between rows	0.00510 in	0.01020 in

### 3.3.7 Radiative Cooler

The Radiative Cooler cools the cold focal plane by radiating heat to cold space. It has a cold stage, an intermediate stage, a radiation shield and a combination earth shield and cooler door. Temperature controlled outgas heaters (controlled to 318° K) are mounted on both the cold and intermediate stages to provide temporary heating of the cold surfaces should on-orbit contamination occur. The cold stage outgas heater also serves as a backup for the cold focal plane heater. The flat rectangular corners of the Radiative Cooler structure that extend beyond the main circular cross section serve as radiation elements to dissipate heat from the Band 5, 6 and 7 preamplifiers which are inside. Table 3.7 shows the cooler characteristics. In this table it can be seen that the Cooler has a large field of view to cold space. This field of view must remain free of any spacecraft structures, the sun, and the Earth.

<b>Table 3.7 Radiative Cooler Design Parameters</b>	
Horizontal field of view	160°
Vertical field of view	114°
Intermediate stage radiator area	660 cm squared
Cold stage radiator area	435 cm squared
Nominal intermediate stage temperature	134° K
Cold stage temperature	91° K
Cold stage minimum temperature	82° K
Outgas temperature - both temperature - both stages	318° K
Cold stage backup temperatures	95° K, 105° K

### **3.3.8 Spectral Filters**

The nominal wavelength location of the ETM+ spectral bands and the nominal ETM+ IFOV size and associated ground resolution, for a 705 km satellite altitude, are as shown in Table 3.8. The ETM+ spectral bandwidth is determined by the overall combination of all of the optical elements, the spectral filters, and the detector response. The spectral filters, located immediately in front of each detector array, are the dominant items that establish the optical bandpass for each spectral band. The prime focal plane assembly has a filter housing that contains filters for bands 1 through 4 and the panchromatic band. The cold focal plane assembly has a filter housing that contains filters for band 5, 6, and 7. The spectral filter for the ETM+ are of ion assisted deposition (IAD) design to reduce changes due to outgassing in a vacuum.

Table 3.8 ETM+ Spectral Bands, IFOV Size, and Ground Resolution			
Spectral Band	Half-Amplitude Bandwidth (μm)	IFOV Size (μm)	Sub-satellite Ground Resolution (m)
Panchromatic	0.520±0.010 - 0.900±0.010	18.5 x 21.3±4.3	13 x 15
1	0.450±0.005 - 0.515±0.005	42.5±4.3	30
2	0.525±0.005 - 0.605±0.005	42.5±4.3	30
3	0.630±0.005 - 0.690±0.005	42.5±4.3	30
4	0.775±0.005 - 0.900±0.005	42.5±4.3	30
5	1.550±0.010 - 1.750±0.010	42.5±4.3	30
6	10.40±0.100 - 12.50±0.100	85.0±9.0	60
7	2.090±0.020 - 2.350±0.020	42.5±4.3	30

### 4.1 Ground System Overview

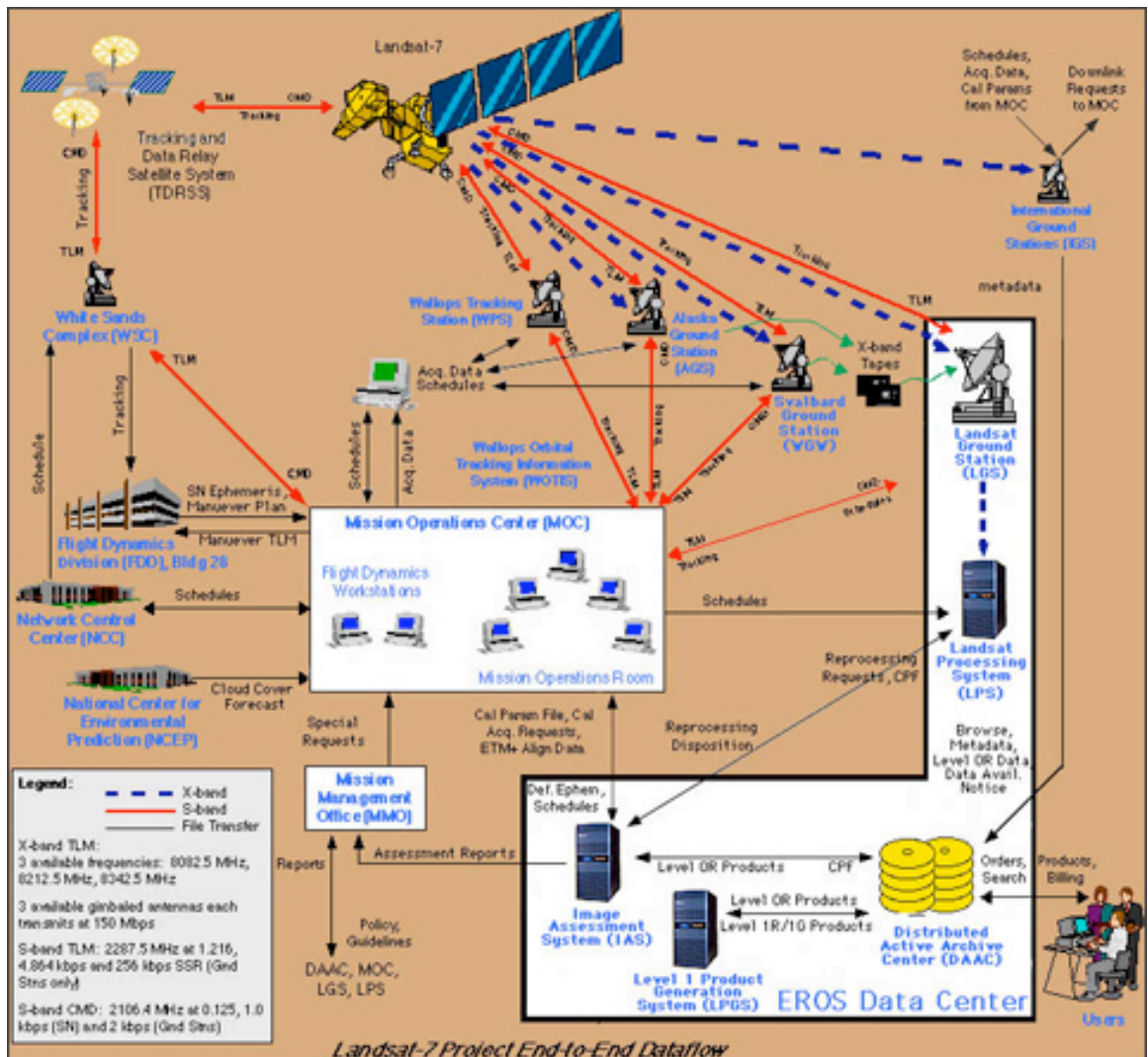


Figure 4.1 - Landsat 7 Project End-to-End Dataflow

The Landsat 7 ground system consists of both Landsat 7 unique components as well as institutional services. The unique components include the Mission Operations Center (MOC), Landsat Ground Station (LGS), Landsat Processing System (LPS), the Image Assessment System (IAS), the Level 1 Product Generation System (LPGS), the EROS Data Center Distributed Active Archive Center (LP-DAAC), and the international ground stations (IGS).

The institutional support systems consist of the Landsat Ground Network (LGN), Space Network (SN), The National Centers for Environmental Prediction (NCEP), The Flight Dynamics Facility (FDF), and the NASA Integrated Support Network (NISN).

The ground system context diagram illustrates both unique and institutional components and their data flow relationships end-to-end.

## 4.2 Unique Ground System Components

### 4.2.1 Mission Operations Center

The MOC, located at Goddard Space Flight Center (GSFC) in Greenbelt, Maryland is the focal point for all space vehicle operations. The MOC provides the facilities, hardware, software, procedures, and personnel required to accomplish Landsat 7 planning and scheduling, and to command and control the Landsat 7 space vehicle, monitor its health and status, analyze the performance of the space vehicle, and maintain flight software, and MOC ground software. The MOC also detects, investigates, and resolves spacecraft anomalies. Flight dynamics functions such as maneuver planning, planning aid generation, and orbit determination are provided by the Flight Dynamics Facility. The MOC is staffed by the Flight Operations Team (FOT), which is comprised of console analysts, mission planners, subsystem engineers, and supervisor/managers.



**Figure 4.2** - Svalbard Satellite Tracking Station (Svalsat) located on Plateau Berger, Spitsbergen Island, Svalbard. Picture taken by Trond Løkke on March 2, 1998



In addition to the ground sites, the Tracking Data and Relay Satellites (TDRS), operated by the NASA's Space Network are utilized. Together these sites provide the ability to downlink real-time and stored housekeeping data (S-band), and to command the spacecraft. In addition, tracking services and spacecraft clock maintenance capabilities are provided. The NASCOM division of NASA provides all network lines.

#### **4.2.2 Landsat Ground Stations**

The LGS, located at EDC, in Sioux Falls, South Dakota is a receive site for the wideband X-Band downlinks of payload data from the space vehicle. In addition to LGS, the Alaska Ground Station (AGS) and the Svalbard Norway Ground Station (SGS) receive payload data downlinks. Payload data downlinked to SGS and AGS is captured on tape and shipped to LGS, which serves as a front-end processor. The LGS also supports S-Band command telemetry operations, as well as tracking. The LGS is a Landsat 7 unique component of the Landsat Ground Network (LGN); the other LGN components are institutional services.

The LGS acquires ETM+ wideband data directly from the Landsat 7 spacecraft by way of two 150 megabit-per-second (Mbps) X-band return links, each at a different frequency. LGS separates each X-band data into two 75-Mbps channels ( I and Q), and transmits the acquired wideband data over four 75-Mbps LGS output channels to the LPS where they are recorded.

#### **4.2.3 Landsat Processing System**

The LPS located at EDC, in Sioux Falls, South Dakota records all wideband data, at real-time rates, into its wideband data stores. An I-Q channel pair represents a complete data set. One channel holds bands 1 through 6, and the other holds bands 7 and 8 and a second gain form of band 6. The LPS retrieves and processes each channel of raw wideband data, at lower than real-time rates, into separate accumulations of Earth image data, calibration data, mirror scan correction data (MSCD), and payload correction data (PCD). Channel accumulations represented by bands 1 through 6 and 6 through 8 become formats 1 and 2, respectively. PCD and MSCD are generated twice, once for each format. Their contents should be identical.

The LPS spatially reformats Earth imagery and calibration data into Level 0R data. This involves shifting pixels by integer amounts to account for the alternating forward-reverse scanning pattern of the ETM+ sensor, the odd-even detector arrangement within each band, and the detector offsets inherent to the focal plane array engineering design. All LPS 0R corrections are reversible; the pixel shift parameters used are documented in the IAS CPF.

During LPS processing, format 1 bands are duplicated, radiometrically corrected, and used to assess cloud cover content and to generate a browse image. Cloud cover scores are generated on a scene-by-scene and quadrant-by-quadrant basis. Metadata are generated for the entire subinterval and on a scene-by-scene basis. The image data, PCD, MSCD, calibration data, and metadata are structured into HDF-EOS for each format and sent to the LP-DAAC for long term archival in subinterval form. The two formats of data are united when a Landsat 7 0R product is ordered. The browse image is sent to the LP-DAAC separately for use as an online aid to ordering.

#### **4.2.4 Level 1 Product Generation System**

The LPGS, located at EDC, generates Level 1 products in response to user requests received from the LP-DAAC. Radiometric and geometric processing is performed by LPGS on Level 0R data to create Level 1 products. Users can order either 1R (radiometrically corrected only) or 1G (radiometrically and geometrically corrected) products. The 1G products are classified as systematic meaning the class of corrections applied is derived from spacecraft data only. Enhanced geometric accuracy is possible with the application of ground control and terrain models but these are not used by LPGS.

A number of user-selectable options exist for configuring a 1G product. These include band selection, map projection, grid cell size, resampling methodology, rotation, product size, and output format. These details can be found in the chapter on [Data Products](#).

#### **4.2.5 Image Assessment System**

The IAS, located at EDC, is responsible for the off-line assessment of image quality to ensure compliance with the radiometric and geometric requirements of the spacecraft and ETM+ sensor throughout the life of the Landsat-7 mission.

In addition to its assessment functions, the IAS is responsible for the radiometric and geometric calibration of the Landsat 7 satellite and ETM+. The IAS periodically performs radiometric and geometric calibration and updates the CPF. This file is stamped with applicability dates and sent to the LP-DAAC (EDC) for storage and eventual bundling with outbound Level 0R products. The CPF also is sent to international ground stations via the MOC. The CPF supplies the radiometric and geometric correction parameters required during Level 1 processing to create superior products of uniform consistency across the Landsat 7 system. Operational activities occur at EDC while less frequent assessments and calibration certification are the responsibility of the Landsat-7 Project Science Office at the

Goddard Space Flight Center (GSFC) in Greenbelt, Maryland.

#### 4.2.6 International Ground Stations

The IGSs are satellite data receiving stations located around the world. They provide data receive, processing, and distribution services for their user community. They receive Landsat 7 payload data via X-Band direct downlink. The acquisition circles for the IGSs depict the Earth's land areas that are regularly imaged. The X-Band direct downlink data includes the PCD required for image processing. The IGSs submit downlink requests to the MOC and receive schedule and orbital element data from the MOC. In addition, the IGSs return metadata for their station holdings to the LP-DAAC. Although catalogued at EDC, data downlinked to the IGSs must be order from these foreign stations.

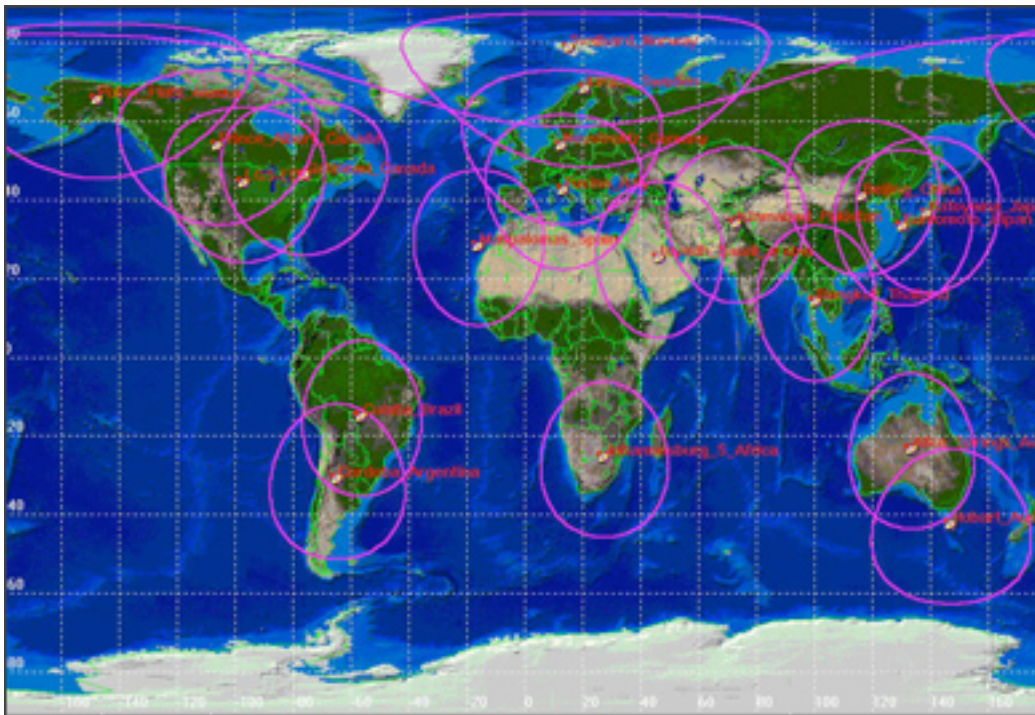


Figure 4.3 - IGS Circles

#### 4.2.7 Land Processes Distributed Active Archive Center

The LP-DAAC, located at Sioux Falls, South Dakota is part of the Earth Observing System (EOS) Data and Information System (EOSDIS). It provides information management, user interface, and data archival and distribution functions for a variety of data types including Landsat 7. In addition to the Level 0R data received from LPS, the LP-DAAC also receives calibration parameter files from the IAS. The LP-DAAC performs billing and accounting functions and serves as the repository for user-oriented documentation.

## 4.3 Institutional Ground System Components

### 4.3.1 Landsat Ground Network

LGN consists of multiple communications sites, which provide S-Band and X-Band communication support to the Landsat 7 mission. The LGN institutional services include AGS, the Wallops Island, Virginia (WPS) ground station, and the SGS in Norway. The Wallops Facility manages the AGS, WPS, and SGS.

### 4.3.2 Space Network

The SN, which includes the Tracking and Data Relay Satellites (TDRSs) and the ground terminals at the White Sands Complex, provides space-to-space and space-to-ground data relay services. These are used for Landsat 7 real-time command and telemetry monitoring during on-orbit operations on a scheduled basis and possible emergency operations on a call-up basis. The SN collects Landsat 7 space vehicle tracking data for FDF processing. The SN is managed by GSFC.

### 4.3.3 National Centers for Environmental Prediction

The National Centers for Environmental Prediction (NCEP) provide timely, accurate and continually improving worldwide forecast guidance products. NCEP, a critical part of the National Oceanic and Atmospheric Administration's National Weather Service, is the starting point for nearly all weather forecasts in the United States.

NCEP generates weather related products. For Landsat 7, the NCEP supplies cloud cover predicts data to the MOC for image scheduling.

### 4.3.4 Flight Dynamics Facility

FDF, an institutional support element located at GSFC, provides workstations in the MOC which are used by the Flight Operations Team (FOT) for orbit determination, attitude determination, ephemeris data generation, maneuver planning support, and generation of planning and scheduling aids (including in-view predictions for IGSs, SN, and the LGN). The FDF institutional facility retains responsibility for star catalog maintenance, local oscillator frequency reporting, and SN tracking data preprocessing.

### 4.3.5 NASA Integrated Support Network

NISN is a global system of communications transmission switching and terminal facilities that provide NASA with long-haul communications services. NISN was implemented to serve the needs of all of NASA's users for the transmission of digital data, voice, and video information in the most cost effective manner possible. The single integrated network project is replacing the independent special purpose networks that have served individual customers for decades. The NISN supports the above institutional facilities.

## 5.1 Orbit

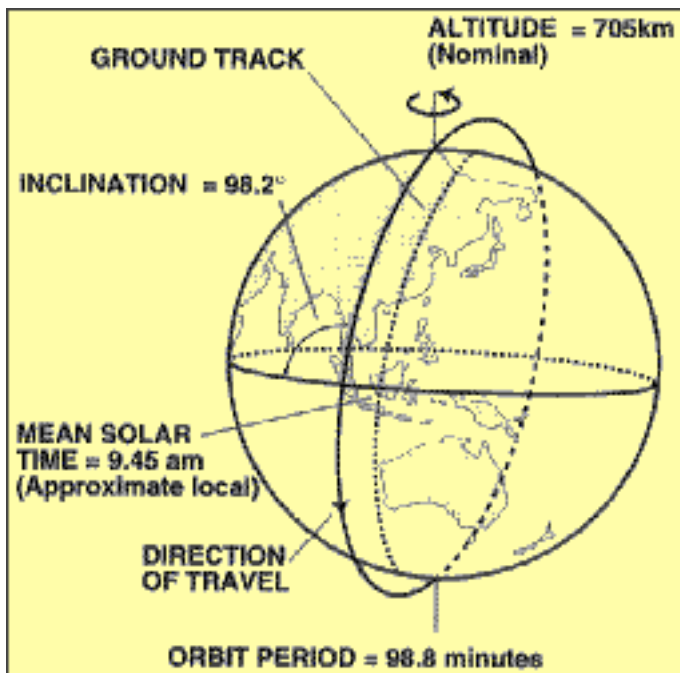


Figure 5.1 - Landsat Orbit

The orbit of Landsat 7 is repetitive, circular, Sun-synchronous, and near polar at a nominal altitude of 705 km (438 miles) at the Equator. The spacecraft crosses the Equator from north to south on a descending orbital node from between 10:00 AM and 10:15 AM on each pass. Circling the Earth at 7.5 km/sec, each orbit takes nearly 99 minutes. The spacecraft completes just over 14 orbits per day, covering the entire Earth between 81 degrees north and south latitude every 16 days. Figure 5.1 illustrates Landsat's orbit characteristics.

Landsat 7 and Terra were launched and injected into identical 705 kilometer, sun-synchronous orbits in 1999. This same day orbit configuration will space the satellites ideally 15 minutes apart (i.e. equatorial crossing times of 10:00 to 10:15 AM for Landsat 7 and 10:30 for Terra). A multispectral data set having both high (30 meter) and medium to coarse (250 to 1000 meter) spatial resolution will thus be acquired on a global basis repetitively and under nearly identical atmospheric and plant physiological conditions.

## 5.2 Swathing Pattern

Landsat 7 orbits the Earth in a preplanned ground track as illustrated in Figure 5.1. The ETM+ sensor onboard the spacecraft obtains data along the ground track at a fixed width or swath as depicted in Figure 5.2. The 16-day Earth coverage cycle for Landsat 7 is known as the swathing pattern of the satellite Figure 5.3. As seen in this figure for daytime acquisitions, Landsat 7 travels the adjacent swath to the west of a previous swath one week later (and the adjacent swath to the east occurred one week earlier and will recur nine days later). After familiarization with the data acquisition cycle or swathing pattern, it becomes straightforward to select Landsat 7 scenes or subintervals required for a specific project.

<b>Latitude (degrees)</b>	<b>Image Sidelap (%)</b>
0	7.3
10	8.7
20	12.9
30	19.7
40	29.0
50	40.4
60	53.6
70	68.3
80	83.9

At the Equator, adjacent swaths overlap at the edges by 7.3 percent. Moving from the Equator toward either pole, this sidelap increases because the fixed 185 km swath width. Table 5.1 shows the amount of sidelap from 0 to 80 degrees latitude in 10-degree increments.

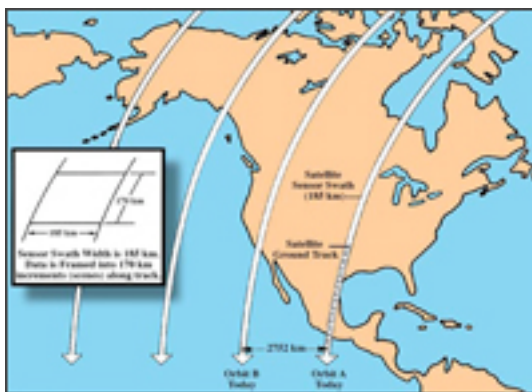


Figure 5.2 - ETM+ Swath



Figure 5.3 - ETM+ Swath Pattern

## 5.3 The Worldwide Reference System

The standard worldwide reference system as defined for Landsat 4 and 5 was preserved for Landsat 7. The WRS indexes orbits (paths) and scene centers (rows) into a global grid system (daytime and night time) comprising 233 paths by 248 rows.

The term row refers to the latitudinal centerline across a frame of imagery along any given path. As the spacecraft moves along a path, the ETM+ scans the terrain below. During ground processing, the continuous data stream or subinterval is framed into individual scenes each 23.92 seconds of spacecraft to create 248 rows per complete orbit. The rows have been assigned in such a way the row 60 coincides with the Equator (descending node). Row one of each path starts at 80° 47' N and the numbering increases southward to latitude 81° 51' S (row 122). Then, beginning with row 123, the row numbers ascend northward, cross the Equator (row 184) and continue to latitude 81° 51' N (row 246). Row 248 is located at latitude 81° 22' N, whereupon the next path begins. The Landsat satellites are not placed in a true polar orbit but rather a near polar orbit which means the path/row numbers do not coincide with latitudes 90° north and south. Figure 5.4 graphic depicts the Landsat path/row schema.

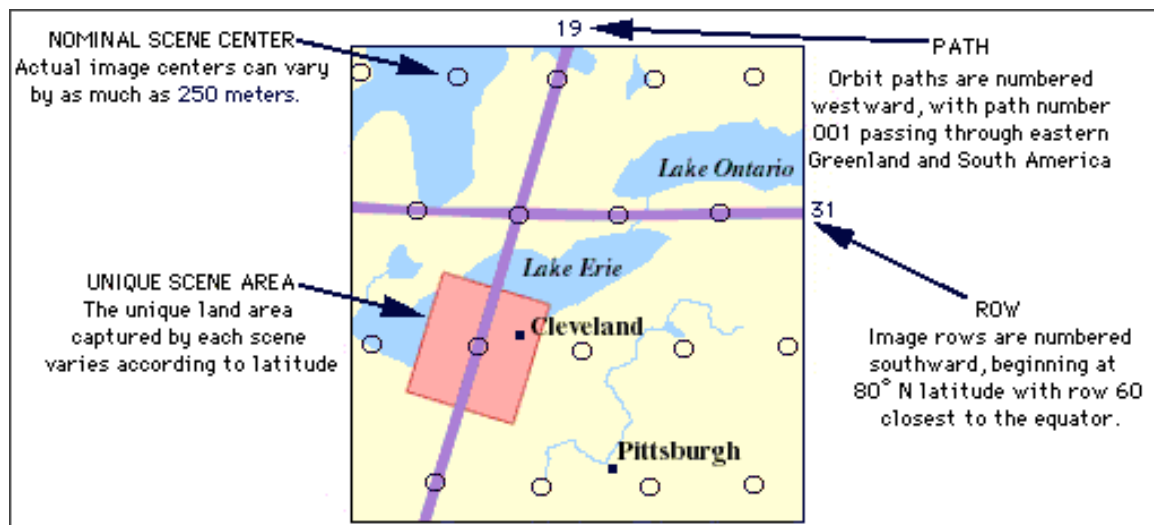


Figure 5.4 - WRS Path/Row Numbering Scheme

Successive orbits and spacecraft attitude are controlled to assure minimal variation to either side from the intended ground track and framing of scene centers is controlled through LPS processing so that successive images of a specific scene or scenes can be registered for comparison purposes.

The [WRScornerPoints.xls](#) file lists the latitude and longitude for the scene center and four corners of each WRS scene. This includes the ascending rows. Positive latitude is North, negative latitude is South. Positive longitude is East, negative longitude is West. It is sorted in Path/Row order.

WRS path/row maps are available from EROS Data Center and have the LANDSATs 1-3 WRS on one side and the LANDSATs 4-5-7 WRS on the reverse. The map sheets are at 1:10 million scale and 26 are needed for global coverage. Contact EDC Customer Services to request WRS maps:

**Customer Services**  
USGS - EROS Data Center  
Sioux Falls, SD 57198  
Tel: 605-594-6151 (7:30 am to 4:00 pm CT)  
TDD: 605-594-6933 (7:30 am to 4:00 pm CT)  
Fax: 605-594-6589 (24 hours)  
[custserv@edcmail.cr.usgs.gov](mailto:custserv@edcmail.cr.usgs.gov)

An Excel spreadsheet allows users to look up the calendar date on which a particular path will be followed by Landsat 7 (listed in blue) or by Landsat 5 (listed in red). It starts on May 27, 1999 and has been extended out to February 22, 2006. A second chart, with larger type, is also available in this file that contains the path flow/calendar dates in 3.5-month chunks. The latest revision number for these charts is 7, dated January 13, 2004. The user to extend further in the future easily updates the charts.

## 5.4 Long Term Acquisition Plan

### 5.4.1 Introduction

The Landsat-7 Long Term Acquisition Plan (LTAP) automates the selection of Landsat scenes to periodically refresh a global archive of sunlit, substantially cloud-free land images. By applying a set of algorithms on a daily basis, the LTAP is designed to ensure optimal collection of Landsat-7 Enhanced Thematic Mapper-Plus (ETM+) imagery for scientific applications, while minimizing the effects of cloud-cover and system constraints. This section provides a brief overview of the LTAP and details the specific algorithms and input files used for calculating scene acquisition priorities. Those wishing a more complete review of the LTAP, including the science justification for the approach and recent performance results, should consult Goward et al. (1999), Gasch and Campana (2000), and Arvidson et al. (2001).

### 5.4.2 LTAP Overview

The ETM+ does not acquire data continually. Instead, acquisitions are scheduled in advanced using a Long Term Acquisition Plan (LTAP) in conjunction with a software scheduler. The WRS-2 system divides the Earth into a grid of 57,784 scenes, with each scene centered on the intersection of a path (groundtrack parallel) and row (latitude parallel). The Landsat-7 observatory is operated such that it follows the WRS grid within tight tolerances,



overflying the entire global [WRS](#) scene grid every 16 days. A database of just over 14,000 scenes containing "land" was compiled for the [LTAP](#), including continental areas, shallow coastal waters, Antarctic sea-ice, and all known islands and reefs. Within any given 24-hour period, approximately 850 of these [WRS](#) land scenes (descending, sunlit paths only) are in view of the [ETM+](#) and are candidates for acquisition. Mission resource limitations (discussed later) restrict the daily acquisition volume for the U.S. archive to 250 scenes. The mission scheduler must select the "best" 250 scenes for acquisition each day within these constraints. The scheduler automatically schedules acquisitions in accordance with the [LTAP](#), basing these decisions on cloud-cover forecasts, urgency of acquisition, and availability of resources to optimize fulfillment of the Landsat mission goals.

The Landsat-7 [LTAP](#) includes several aspects that influence whether a particular scene should be acquired or not. These include:

1. Seasonality of vegetation, niche-science communities
2. Predicted vs. nominal cloud-cover
3. Sun angle
4. Missed opportunities for previous acquisitions
5. Quality (cloud-cover) of previous acquisitions
6. Scene clustering
7. System constraints (duty cycle, ground station locations, recorder capacity, etc).

Factors 1-6 feed directly to calculating the priority of each potential acquisition, while the actual acquisition list is obtained by incorporating system constraints (factor 7). Factor 4 requires feedback between the list of archived scenes and the [LTAP](#), while factor 5 requires feedback between cloud cover assessment of archived scenes and the [LTAP](#). Each of these factors is discussed in the following sections.

### **5.4.3 Seasonality**

An objective of the [LTAP](#) is to schedule acquisitions more frequently during periods of change, such as growth and senescence of vegetation, and less frequently during relatively stable periods, such as when full growth canopy exists or during winter quiescence. An 8-year [AVHRR](#) Normalized Difference Vegetation Index ([NDVI](#)) data set was used to determine where and when change was occurring (Goward, et al., 1994, 1999). To flag seasonal change within a [WRS](#) scene, a statistical test was applied to each [NDVI](#) 45-km sample mapped to that scene. Comparing each sample or pixel to the same pixel two months later revealed periods of significant change in the [NDVI](#) mean and standard deviation, when multiple acquisitions are meaningful, and periods of minimal change, when only a single acquisition is necessary.

Thus, the year is broken into a set of temporal "windows" for each path-row location. During each window, a location may be labeled as "acquire once", "acquire always", or "never acquire", and this information is stored in the [LTAP](#) seasonality file. It should be noted that "acquire always" does not imply that an actual acquisition will occur for every overpass during that time window. Rather, that scene will always be a candidate for acquisition, and other factors within the [LTAP](#) (cloud-cover, system constraints, etc) will govern whether or not an acquisition actually takes place. Conversely, "acquire once," means that once a successful acquisition occurs during the time window, that path-row location is no longer eligible for acquisition.

Niche Science Communities, defining acquisitions solely through semi-monthly [NDVI](#) change does not fully capture the science and user interest in the Landsat mission. To supplement the [NDVI](#)-based seasonality metric, specific niche science communities have requested locations for more frequent acquisitions. These locations currently include:

- 282 agriculture (acquire every season if CC predict < 60%)
- 35 calibration (acquire "always")
- 896 reefs (acquire from 2x to 6x each year)
- 30 fire (acquire "always")
- 1392 land ice (acquire once during certain months)
- 3601 Antarctica (acquire once during Jan-Feb)
- 60 oceanic islands (acquire twice each year)
- 1175 rainforest (acquire "always" all year)
- 352 sea ice (acquire from 1x to 3x each year)
- 11 Siberia (acquire "always" over 9 months)
- 72 volcanoes (acquire from 2x to 12x during year, incl. night)

The exact makeup of these niche science acquisitions varies each quarter of operations, depending on user needs and science priorities. In general, approximately 27% of the 250 scenes/day acquired by Landsat-7 are devoted to satisfying "niche" requests, approximately 70% are devoted to satisfying routine acquisitions from the seasonality file, and 3% are devoted to night images or special high-priority acquisitions (natural disasters, national needs, etc). Requirements for night imaging and high-priority acquisitions are dealt with elsewhere in the data specification.

#### **5.4.4 Predicted Cloud-cover**

The cloud-avoidance strategy is based on the relative predicted cloud cover with respect to the seasonal average cloud cover for each scene. The [LTAP](#) scheduling software compares near-term predictions to the historical average cloud cover for that scene for that month, to determine acquisition priorities each day. Scenes with better-than-average cloud-cover

predictions are given a priority boost, while those with poorer cloud cover predictions are given a lower priority. Global historical cloud data were obtained from [ISCCP](#) records (Rossow et al., 1996), that give monthly estimates of cloud-cover percentage for 2.5° grid cells from 1989 to 1993. Monthly averages over the 5 years were computed and mapped to the Landsat [WRS](#) grid to produce a cloud climatology (Figure 5). The [NOAA](#) National Centers for Environmental Prediction provide daily global forecasts of cloud-cover percentage at a 0.7° grid scale (Campana, 1994). The forecasts are compiled at 0600 UT each day and apply to each 3-hour interval up to 84 hours. Once received from [NOAA](#), these cloud predictions are translated to the Landsat [WRS](#) coordinate system. The forecast nearest in time to a candidate acquisition is compared to the [ISCCP](#) climatology to determine whether the predicted observing conditions are better or worse than typical for that location. Acquisition priority is then adjusted upward to favor the better conditions or downward to avoid the worst conditions. Figure 5.5 illustrates the cloud-free nature of the first year [ETM+](#) archive.

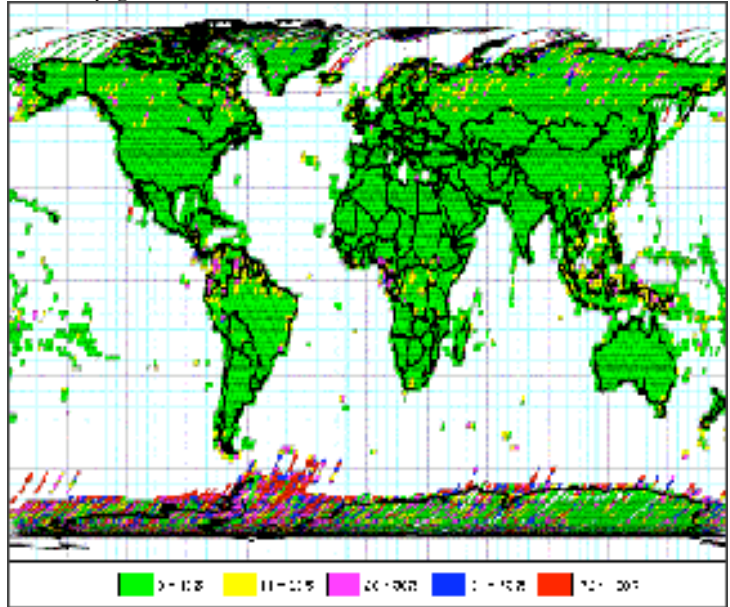


**Figure 5.5** - This map shows the lowest available cloudcover for each of the 16,514 unique path/row combinations in the U.S. Landsat 7 archive (June 28, - July 11, 2000).

### 5.4.5 Sun Angle

Requests for high-latitude scenes are rejected during local winter when the solar elevation is below a threshold. This threshold was set at 5° during the initial years of the survey. The cutoff angle was changed to 15° for the northern hemisphere on July 24, 2002 because of duty cycle concerns and the fact that snow dominates scenes acquired at lower angles. The cutoff angle remains at 5° for the southern hemisphere.

### 5.4.6 Missed Opportunities

A request is granted a priority boost as a function of the number of consecutive past cycles in which the opportunity to acquire the requested scene was not fulfilled. This occurs when the scene was not scheduled for acquisition, or when the acquired image fails to meet minimum quality standards, such as cloud cover. For example, if the last successfully acquired image of a scene was 48 days ago, then a request for this scene is granted a priority boost based on two missed opportunities from 32 and 16 days ago. In addition, all new requests (i.e. when an acquisition window opens) are given a priority boost.

### 5.4.7 Image Quality

Quality (cloud-cover) of the best or most recently acquired image of a path-row from past cycles factors into the relative demand for another acquisition. At high latitudes, the scheduler also considers the quality of the best image that could be spliced together as a mosaic of imagery of adjacent scenes acquired in the recent past. Quality is a function of cloud contamination in the image, as determined during image processing.

### 5.4.8 Clustering

Within the Landsat-7 [LTAP](#), a higher priority is given to scenes that form "clusters" - contiguous groups of along-path acquisitions. This (i) reduces the on-off cycling of the [ETM+](#) instrument and (ii) promotes the archiving of continuous swath data, which in turn allows "floating scene" subsetting of user-defined areas without regard for scene boundaries. As of July 31, 2002 the number of scenes successfully archived was 252,208 (Figure 5.6). A more recent archive scene count (as of January 31, 2003) is presented in Figure 5.7. The lowest cloud cover scores for each [WRS](#) location are plotted in Figure 5.8.

### 5.4.9 Long Term Acquisition Plan Files

The Long Term Acquisition Plan ([LTAP](#)) is used to direct the acquisition by Landsat 7 of Worldwide Reference System ([WRS](#)) scenes around the world for archiving in the U.S. [EROS](#) Data Center. The contents of the following files represent the underpinnings of the [LTAP](#):

1. seasonality file
2. [WRS](#) land data base, Rev. 3.0, October, 2002
3. nominal cloud cover file
4. nominal cloud cover daylight additions file
5. nominal gain settings file
6. maximum solar zenith angle

1. The [seasonality file](#) specifies which [WRS](#) scenes are to be acquired during which periods of time (request period), and the frequency of acquisition during those periods. This file covers the year 2001 and includes both daytime and nighttime imaging. Frequency of acquisition is defined as either "once" during the request period, or "all" opportunities during the request period. The results of ingesting this file into the scheduler and developing the daily schedule are posted daily on the web, at this [server location](#).

Here is the warning label associated with the seasonality file: The scheduler has many resources and priorities that it juggles during consideration of requests for scheduling, including:

- predicted cloud cover as compared to the nominal
- number of missed opportunities for this request since it was opened
- how good the cloud cover assessment score was for the last acquisition
- nearness to end of the request period
- availability of resources including duty cycle, onboard recorder space, and station contact time

The result of this juggling is that scenes marked with an "all" opportunities frequency are usually acquired every 4-5 cycles (64-80 days) instead of every cycle (16 days). Another outcome of this is that scenes marked with a "once" frequency may be acquired multiple times within the request period in an attempt to better the cloud cover results, should the first acquisition's cloud cover be considerably worse than the nominal. So please treat the frequency assignment in the seasonality as a guide, not a rule.

The column headings for the seasonality file are:

- first date of request period (yyyy-mm-dd)
- last date of request period (yyyy-mm-dd)
- path/row (note that rows 246-248 will be sorted to the end of the path)
- acquisition frequency (once, all)
- base priority of the request
- maximum solar zenith angle (only for night scenes, is set to 90)

2. The [WRS land database](#) identifies those WRS scenes containing land or shallow water, which will be imaged at least once every year. At the end of the file are separate tables for the niche communities and special interests. These include: [EOS](#) validation sites, glaciers, [MODIS](#) fire validation sites, political (disputed sites), volcanoes, global oceanic islands. A comprehensive reef list is a future addition.

3. and 4. The [nominal cloud cover file](#) reports the average cloud cover for each WRS scene for each month of the year. The file spans one year and addresses the descending rows only. The [nominal cloud cover daylight additions file](#) adds those ascending rows, which will be in daylight during some part of the year and therefore may be imaged. The average cloud cover is derived from the International Satellite Cloud Climatology Project D2 data set, years 1989-1993. As subsequent years are processed, this file will be updated.

The columns in the nominal cloud cover files are: first day of month | last day of month | path | row | cloud cover value all cloud cover values for row 1 across all paths are given, then for row 2, etc.

5. The [nominal gain settings file](#) identifies the gain settings that will be used as defaults for each WRS scene for each day of the year. This file spans one year. The scheduler uses the DOY value. The DD-MMM values that are included in the file are for a leap year and are guidance for those who don't easily equate a DOY value of 177 with the date 25-JUN. The file addresses both descending and ascending rows of interest to the U.S. archive. The settings are given as H for high gain or L for low gain. The order in which they are specified for each scene is bands 123456678, where band 6 is repeated twice, once for format 1 and once for format 2, and band 8 is the panchromatic band. You will notice that bands 66 are constant at LH and band 8 is constant at L. The other bands are changed in groupings, with bands 123 changed together, band 4 changed on its own merits, and bands 57 changed together. When we do night imaging, we use the following default settings: HHHHLLHLL. The file only contains entries showing when the default gain setting has changed from its previous setting. The default gain settings are generated using rules that take land cover type and sun angle into account. To understand these rules, read the file "[gain setting rules](#)". Other files referenced by this document are:

- [desert mask](#) - (ASCII text)
- [arctic mask](#) - (ASCII text)
- [monthly gain maps](#) - (Powerpoint format)

6. The maximum solar zenith angle is a single value for all scenes at all times of the year. Daylight imaging will not be scheduled if the angle is 85 degrees or more (same as 5 degrees or less in elevation from the earth's surface).

## 6.1 Scientific Theory of Measurements

When solar energy strikes an object, five types of interaction are possible. The energy is:

1. **Transmitted** - The energy passes through with a change in velocity as determined by the index of refraction for the two media in question.
2. **Absorbed** - The energy is given up to the object through electron or molecular reactions.
3. **Reflected** - The energy is returned unchanged with the angle of incidence equal to the angle of reflection. Reflectance is the ratio of reflected energy to that incident on a body. The wavelength reflected (not absorbed) determines the

color of an object.

4. **Scattered** - The direction of energy propagation is randomly changed. Rayleigh and Mie scatter are the two most important types of scatter in the atmosphere.
5. **Emitted** - Actually, the energy is first absorbed, and then re-emitted, usually at longer wavelengths. The object heats up.

The Landsat-7 system is designed to collect 7 bands or channels of reflected energy and one channel of emitted energy. A well-calibrated ETM+ enables one to convert the raw solar energy collected by the sensor to absolute units of radiance. Radiance refers to the flux of energy (primarily irradiant or incident energy) per solid angle leaving a unit surface area in a given direction. Radiance corresponds to brightness in a given direction toward the sensor, and is often confused with reflectance, which is the ratio of reflected versus total power energy. Radiance is what is measured at the sensor and is somewhat dependent on reflectance.

The eight bands of ETM+ data are used to discriminate between Earth surface materials through the development of spectral signatures. For any given material, the amount of emitted and reflected radiation varies by wavelength. These variations are used to establish the signature reflectance fingerprint for that material. The basic premise of using spectral signatures is that similar objects or classes of objects will have similar interactive properties with electromagnetic radiation at any given wavelength. Conversely, different objects will have different interactive properties. A plot of the collective interactive mechanisms (scattering, emittance, reflectance, and absorption) at wavelengths on the electromagnetic spectrum should, according to the basic premise, result in a unique curve, or spectral signature, that is diagnostic of the object or class of objects. A signature on such a graph can be defined as reflectance as a function of wavelength. Four such signatures are illustrated in Figure 6.1.

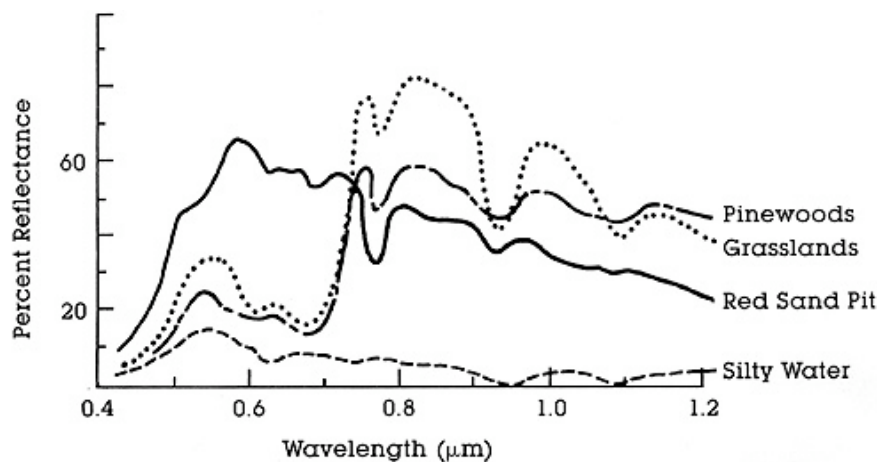


Figure 6.1 - Spectral Reflectance Curves of Four Different Targets

ETM+ data can be used to plot spectral signatures although the data are limited to eight data points within the spectral range of .45 to 12.5  $\mu\text{m}$ . More useful is plotting the ETM+ spectral signatures in multi-dimensional feature space. The four surface materials shown in Figure 6.1 are plotted in Figure 6.2 using just two of the ETM+ spectral bands. (GL representing grasslands, PW representing pinewoods, RS representing red sand, and SW representing silty water) may be characterized as distinct.

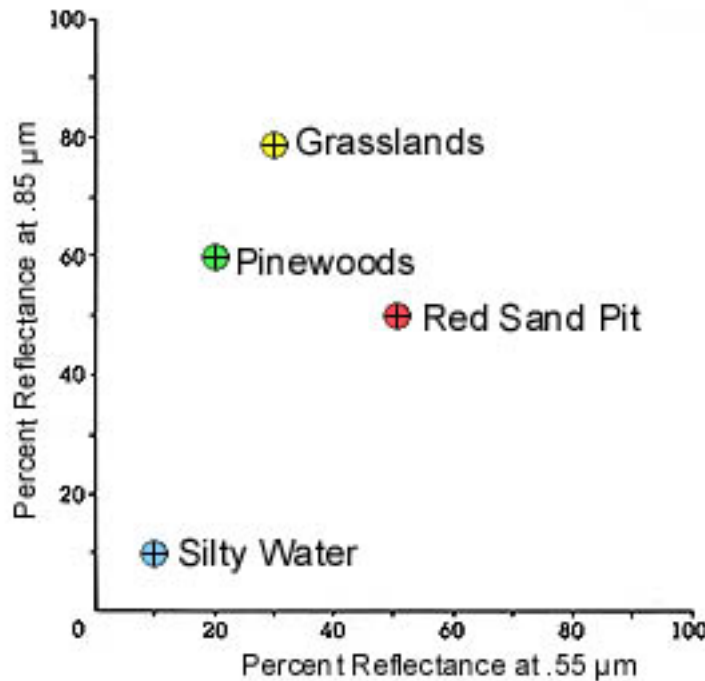


Figure 6.2 - Spectral Separability Using Just Two Bands

Each of the materials has been plotted according to its percent reflectance for two of the wavelengths or spectral bands. When more than two wavelengths are involved, the plots in multi-dimensional space tend to increase the separability among different materials. This spectral separation forms the basis for multispectral analysis where the goal is to define the bounds of accurately identified data point clusters.

## 6.2 Spatial Characteristics

Spatial resolution is the resolving power of an instrument needed for the discrimination of features and is based on detector size, focal length, and sensor altitude. More commonly used descriptive terms for spatial resolution are ground sample distance (GSD) and instantaneous field of view (IFOV). The IFOV, or pixel size, is the area of terrain or ocean covered by the field of view of a single detector. The ETM+ ground samples at three different resolutions; 30 meters for bands 1-5, and 7, 60 meters for band 6, and 15 meters for band 8. Figure 6.3 illustrates the ETM+ IFOV for bands 1-5 and 7 relative to other sensors and a football field. IKONOS, the recently launched Space Imaging sensor, has an IFOV of 1 meter. The French SPOT panchromatic sensor has an IFOV of 10 meters whereas the SPOT multispectral (XS) sensor has an IFOV of 20 meters. ETM+ has an IFOV of 30



meters for bands 1-5, and 7 of 30 meters while the Indian Remote Sensing Satellite (IRS) has an IFOV of 36.25 meters.

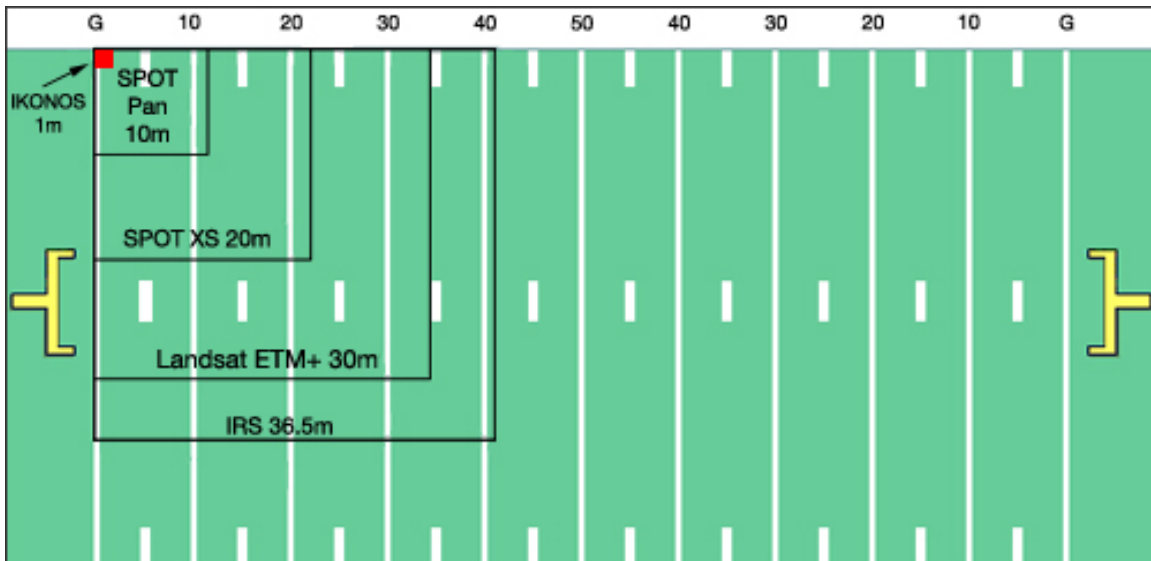


Figure 6.3 - ETM+ Spatial Resolution Relative to Other Sensors

A standard WRS scene covers a land area approximately 185 kilometers (across-track) by 180 kilometers (along-track). A more precise estimate for actual scene size can be calculated from the [0R product](#) image dimensions. These are listed in table 6.1

<b>Band Number</b>	<b>Resolution (meters)</b>	<b>Samples (columns)</b>	<b>Data Lines (rows)</b>	<b>Bits per Sample</b>
1-5, 7	30	6,600	6000	8
6	60	3,300	3,000	8
8	15	13,200	12,000	8

It is natural to assume that one could determine a scene's spatial extent by multiplying the rows and columns of a scene by the IFOV. This would lead to a scene width of 198 kilometers (6600 samples \* 30 meters) and a scene length of 180 kilometers (6000 lines \* 30 meters). While this calculation applies to scene length, the scene width calculation is more complicated due to the presence of image buffers and the staggered image bands in the 0R product. Left and right image buffers were placed in the 0R product to accommodate a possible increase in scan line length over the mission's life. The staggered image bands result from the [focal plane design](#), which LPS accounts for by registering the bands during 0R processing. The end result is an increasing amount of zero-fill preamble according to the band order on the ground projected focal plane array.

The detector offsets determine the amount of zero fill preamble for each band. These are listed in Table 6.2 and can also be found in the [Calibration Parameter File](#). Coincident imagery for all 8 bands starts at pixel location 247 for the 30-meter bands. One need only to look at the reverse scan odd detector offset for band 6 to see that this is true. This number, 116, is actually in 60 meter IFOVs, which translates to 232 30-meter pixels. Another 14 pixels must be added to this number to account for the seven minor frames of image data pre-empted by time code. Coincident imagery for all 8 bands ends at pixel location 6333 for the 30-meter bands. This number is determined by looking at the reverse even detector offset for band 8. Add to this number the value 12,626 that represents the number of band 8 pixels per line (6313 minor frames times 2). The total, 12,666, is halved to put the ending pixel number into 30-meter units. The number of coincident images pixels in a scan is therefore 6087 (6333 - 247 + 1). The nominal width for a scene is therefore 182.61 kilometers (6087 \* 30 meters).

<b>Table 6.2 ETM+ Detector Shifts</b>				
<b>Band Number</b>	<b>Forward Scan Even Detectors</b>	<b>Forward Scan Odd Detectors</b>	<b>Reverse Scan Even Detectors</b>	<b>Reverse Scan Odd Detectors</b>
1	49.0	51.0	45.0	48.0
2	74.0	76.0	70.0	73.0
3	99.0	101.0	95.0	98.0
4	124.0	126.0	120.0	123.0
5	195.0	197.0	191.0	194.0
6	110.0	113.0	114.0	116.0
7	169.0	171.0	165.0	168.0
8	50.0	54.0	40.0	44.0

## 6.3 Temporal Characteristics

### 6.3.1 Orbit Times

The Landsat 7 orbit is sun synchronous, as shown in figure 6.4. Consequently, the geometric relationship between the orbit's descending, or southbound, track and the mean projection of the sun onto the equatorial plane will remain nearly constant throughout the mission. As a result, the mean sun time at each individual point in the orbit will remain fixed, and in fact, all points at a given latitude on descending passes will have the same mean sun time. For Landsat 7, the nominal mean sun time of the descending node at the Equator is 10:00 AM.

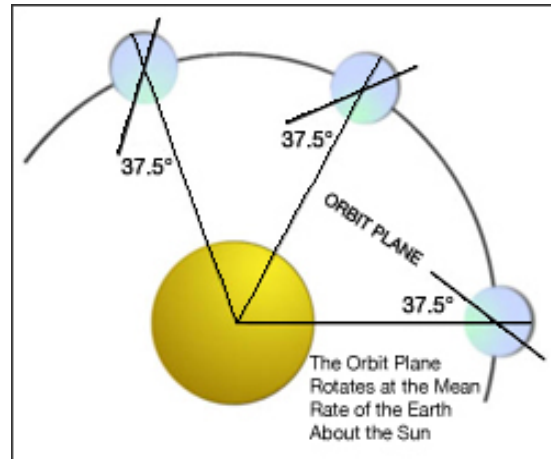


Figure 6.4 - Sun Synchronous Orbit Landsat 7

A fixed mean sun time does not mean that local clock time will remain fixed for all points at a given latitude, since discrete time zones are used to determine local time throughout the world. The local time that the satellite crosses over a given point at latitudes other than at the equator also varies due to the time the satellite takes to reach the given point (nearly 99 minutes are required for one complete orbit), and the time zones crossed by the satellite relative to its equatorial crossing point.

### 6.3.2 Sun Elevation Effects

While the orbit of Landsat 7 allows the spacecraft to pass over the same point on the Earth at essentially the same local time every 16 days, changes in sun elevation angle, as defined in figure 6.5, cause variations in the illumination conditions under which imagery is obtained. These changes are due primarily to the north-south seasonal position of the sun relative to the Earth (Figure 6.6).

The actual effects of variations in sun elevation angle on a given scene are very dependent on the scene area itself. The

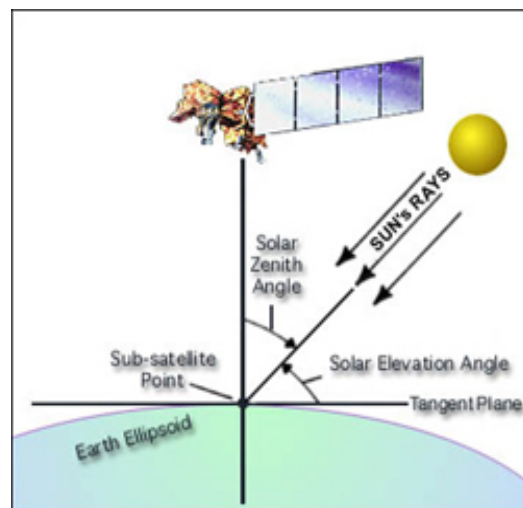
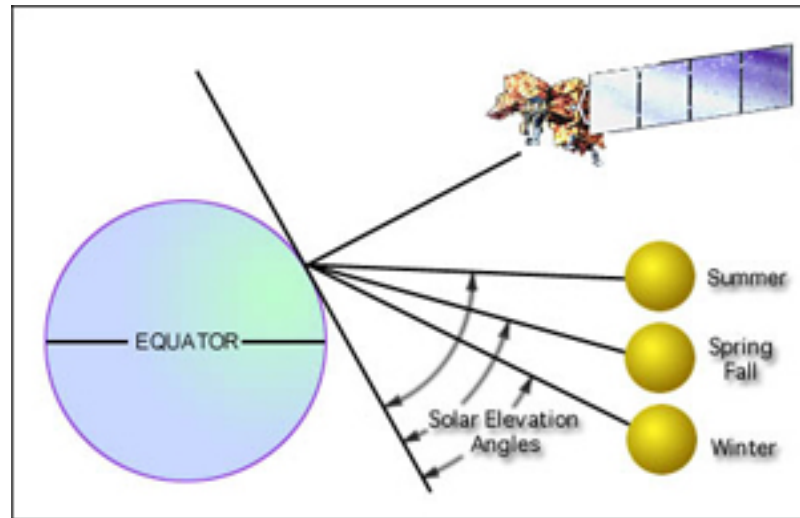


Figure 6.5 - Sun Elevation Angle

reflectance of sand, for example, is significantly more sensitive to variations in sun elevation angle than most types of vegetation. Atmospheric effects also affect the amount of radiant energy reaching the Landsat sensor, and these too can vary with time of year. Because of such factors, each general type of scene area must be evaluated individually to determine the range of sun elevation angles over which useful imagery can be realized.

Depending on the scene area, it may or may not be possible to obtain useful imagery at lower sun elevation angles. At sun elevation angles greater than 30 degrees, one should expect that all image data can be fully exploited. A sun elevation angle of 15 degrees, below which no imagery is acquired, has been established for the Landsat 7 mission.



**Figure 6.6** - Effects of Seasonal Changes on Solar Elevation Angle

Apart from the variability of scene effects, sun elevation angle is itself affected by a number of perturbing forces on the Landsat orbit. These include forces such as atmospheric drag and the sun's gravity. They have the effect of shifting the time of descending node throughout the year, and this results in changes to the nominal sun elevation angle. The effects of orbit perturbations, however, can be considered minor for most applications.

### 6.3.3 Revisit Opportunities

Repeat imaging opportunities for a given scene occur every 16 days (see [Chapter 5](#) for details). This does not mean every scene is collected every 16 days. Duty cycle constraints, limited onboard recorder storage, the use of cloud cover predictions, and adherence to the [Long Term Acquisition Plan](#) make this impossible. The goal, however, is to collect as much imagery as possible over dynamically changing landscapes. Deserts do not qualify and thus are imaged once or twice per year. Temperate forests and agricultural regions qualify as dynamic and are imaged more frequently. Figure 6.7 illustrates archived imagery during the mission's first 112 days. Although the

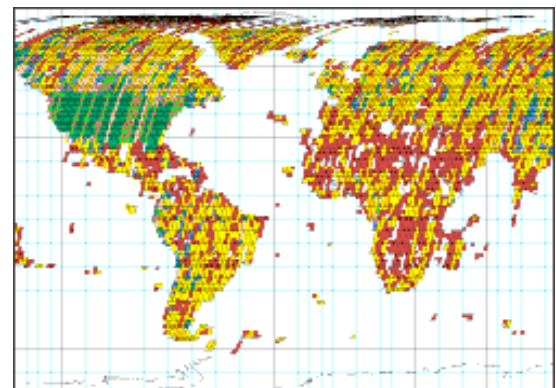


**Figure 6.7** - Landsat 7 data archived during the first 112 days of operation.

mission is still young, certain trends are emerging. The U.S including Alaska is quite green because every imaging opportunity is exploited. North Africa is mostly desert and appears red. Northern Asia is mostly red and yellow due to recorder constraints.

The importance of imaging dynamically changing landscapes frequently is illustrated in Figure 6.8. The image on the left was acquired over Salt Lake City on August 14, 1999 while the other was acquired four cycles later on October 17, 1999. The band combination for both images is 5-4-2. The dramatic color changes in the mountains to the east of Salt Lake City indicate the montaine growing season is over. A multi-temporal analysis using images such as these allows one to resolve, with greater accuracy, key landscape components such as biomass, species components, and phenological growth patterns.



**Figure 6.8** - August 14, 1999 (left) and October 17, 1999 (right) images of the Salt Lake City area

## 6.4 Radiometric Characteristics

### 6.4.1 Gain States

The ETM+ images are acquired in either a low or high gain state (Figure 6.9). Gain selection for a scene is controlled by the MOC and is performed by changing the reference voltage for the analog to digital convertor. This occurs in the preceding scene. The science goal in switching gain states is to maximize the instrument's 8-bit radiometric resolution without saturating the detectors. This requires matching the gain state for a given scene to the expected brightness conditions. For all bands, the low gain dynamic range is approximately 1.5 times the high gain dynamic range. It makes sense, therefore, to image in low gain mode when surface brightness is high and in high gain mode when surface brightness is lower. Table 6.3 lists the target/specification minimum saturation levels for all bands in both the low and high gain states.

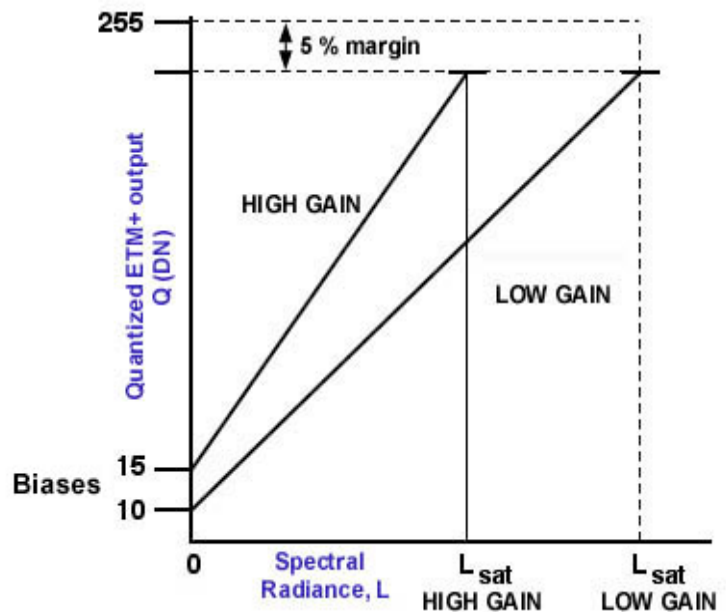


**Figure 6.9** - Design ETM+ Reflective Band High and Low gain Dynamic Ranges

<b>Table 6.3 ETM+ Dynamic Range watts / (meter squared * str * <math>\mu\text{m}</math>)</b>			
	<b>Low Gain</b>	<b>High Gain</b>	
<b>Band</b>	<b>Minimum Saturation Level</b>	<b>Minimum Saturation Level</b>	
1	285.7	190.0	
2	291.3	193.7	
3	225.0	149.6	
4	225.0	149.6	
5	47.3	31.5	
6	17.21	12.78	
7	16.7	11.10	
8	235.0	156.3	

### 6.4.2 Gain Settings

The currently implemented gain setting strategy for the Landsat-7 Long Term Acquisition Plan (LTAP) took effect July 13, 2000 (2000/195:22:40z) superseding the [at-launch plan](#) and the December 2, 1999 operational decision to acquire band 4 in low gain when the sun elevation angle exceeds 45 degrees. It consists of a fixed categorization of the surface cover types of the Earth, and gain setting rules that are surface cover and sun angle based. Within the Long Term Acquisition Plan, the gains for bands 1-3 are currently always changed together as are the gains for bands 5 and 7. The earth surface categories are as follows:

1. Land (non-desert, non-ice)
2. Desert
3. Ice/Snow
4. Water
5. Sea Ice
6. Volcano/Night

Each Landsat-7 WRS Path/Row location is categorized into one of these six types. For each surface cover type the gain setting rules are different:

### **1. Land (non-desert, non-ice):**

- a. Bands 1-3 set to high gain
- b. Band 4 set to high gain except where sun elevation is greater than  $45^{\circ}$  (set to low gain) - to avoid dense vegetation (reflectance  $> 0.66$ ) saturation. (At this sun angle high gain in band 4 saturates at about a reflectance of 0.66, so switching to low gain keeps targets at this reflectance or below from saturating.)
- c. Bands 5, 7 set to high gain
- d. Band 8 set to low gain

### **2. Desert:**

- a. Bands 1-3 set to high gain except where sun elevation is greater than  $28^{\circ}$  - to avoid bright desert target (reflectance  $> 0.65$  in band 3, [ $> 0.66$  in band 1,  $> 0.71$  in band 2]) saturation
- b. Band 4 set to high gain except where sun elevation is greater than  $45^{\circ}$  (set to low gain) - to avoid bright desert (reflectance  $> 0.66$ ) saturation.
- c. Band 5,7 set to high gain except where sun elevation is greater than  $38^{\circ}$  -- to avoid bright desert target (reflectance  $> 0.70$  in band 5, [ $> 0.68$  in band 7] saturation
- d. Band 8 set to low gain

### **3. Ice/Snow and Sea Ice:**

- a. Bands 1-3 set to high gain except where sun elevation is greater than  $19^{\circ}$  - to avoid snow ice (reflectance  $> 0.95$  in band 3, [ $> 0.94$  in band 1,  $> 1.03$  in band 2]) saturation.
- b. Band 4 set to high gain except where sun elevation is greater than  $31^{\circ}$  - to avoid snow/ice (reflectance  $> 0.92$ ) saturation.
- c. Band 5, 7 set to high gain
- d. Band 8 set to low gain

#### **4. Water/Coral Reefs:**

- a. Bands 1-5,7 set to high gain
- b. Bands 8 set to low gain

#### **5. Volcano/Night** - nighttime imaging (sun elevation $< 0$ ) is only routinely performed for sights identified as "Volcano"

- a. Bands 1-4, set to high gain
- b. Bands 5, 7 set to low gain to reduce saturation of volcanic hot spots
- c. Band 8 set to low gain

The actual saturation reflectance corresponding to a given sun angle are influenced by the Earth-Sun distance, which varies by  $\pm 1.5\%$  over the year producing a  $\pm 3\%$  irradiance variation. The current implementation does not incorporate this variability. Band 8 is in low gain for all routine acquisitions as the noise level in this band is such that high gain provides very little improvement in performance. This implementation is currently under review and the band 8 gain settings may be altered in the future.

Several additional changes have been made to the gain strategy plan implemented on July 13, 2000. On April 20, 2001 gain changes for scenes in Northern Africa are now made several rows earlier so they occur over the Mediterranean. On May 8, 20002 gain change locations starting moving as necessary to avoid impacting high priority or potentially clear scenes. When not over the U.S. gain changes are made during flywheel periods prior to scene requiring the change and during the lowest priority scene in that period. When over the U.S. gain changes are made during the cloudiest scene prior to the scene requiring the change. Also, no single scene gets a gain change two acquisitions in a row.

#### **6.4.3 At-launch Gain Setting Strategy Rationale**

The following paragraph was extracted from a paper that describes the rationale behind the at-launch gain setting strategy (Goward, et. al., 1999)

"The 8-year monthly averages of AVHRR visible and near infrared planetary reflectance measurements from the AVHRR data set, at the original 15 km spatial resolution, were used to evaluate the gain settings. Visible (bands 1-3), near infrared (band 4), and shortwave infrared (5 and 7) gains were considered separately. The at-



satellite planetary reflectance was converted to at-satellite radiance, based on the solar zenith angle at the time of satellite overpass. For each Landsat WRS scene, the observed spectral radiance was subjected to the two gain states. For each gain state, an entropy statistic was calculated to determine the potential scene contrast in each setting. Where low gain was found to provide substantially greater scene contrast (e.g. glaciers in summer), this setting was selected. For all other cases the high gain was selected. This decision process will no doubt yield less than optimum results for some applications, but it was the best compromise to meet the requirement to minimize gain changes while providing generally high quality measurements".

#### **6.4.4 Gain Change Location Rationale**

The gain change commands at the time of launch were issued at the start time of a scene, which due to various error accumulations was placing the gain change 1 to 2 seconds into the start of the scene. The MOC was informed that the U.S. ground processing system could not handle this band change location. A scheduler modification was subsequently made to move the gain change commanding back by 4 seconds, so it would occur during the trailing end of the preceding scene. This was initially incorporated between July 14 to July 26, 1999. This change was made permanent starting on August 2, 1999.

The rationale for setting the offset to -4 seconds was:

1. Payload command timing error: up to 1-second quantization error because the SCP executes commands on integer second boundaries.
2. Gain change command execution time:  $0.1 \text{ second/band} \times 8 \text{ bands} = 0.8 \text{ seconds}$
3. Orbital along-track position uncertainty: typically  $< 1.0 \text{ km}$ , equivalent to 0.2 seconds (except on days following delta-V orbit correction maneuver, in which the along track error could reach 2 seconds).
4. Scene center-to-center time variance: typically  $23.92 \pm 0.09 \text{ seconds}$  due to orbital eccentricity.

The -4 second gain change offset exists for all scenes acquired after August 2, 1999 (1999/128:22:07 zulu). A [list of scenes](#) with leading edge gain changes (i.e. pre August 2, 1999) was compiled for the record.

## 6.5 Radiometric Characteristics

The ground footprint, spatial resolution, and the spectral channels of today's sensors characterize the civilian space-based remote sensing industry. On one end of the scale are the low-resolution, large footprints, multi-spectral sensors such as NOAA's polar orbiters that have one-kilometer resolution and a 2000-kilometer swath or footprint. On the other end are high resolution, small footprint, and panchromatic snapshot sensors such as IKONOS, which was recently launched by Space Imaging. As depicted in Figure 6.10, Landsat 7 occupies a unique niche between these two extremes.

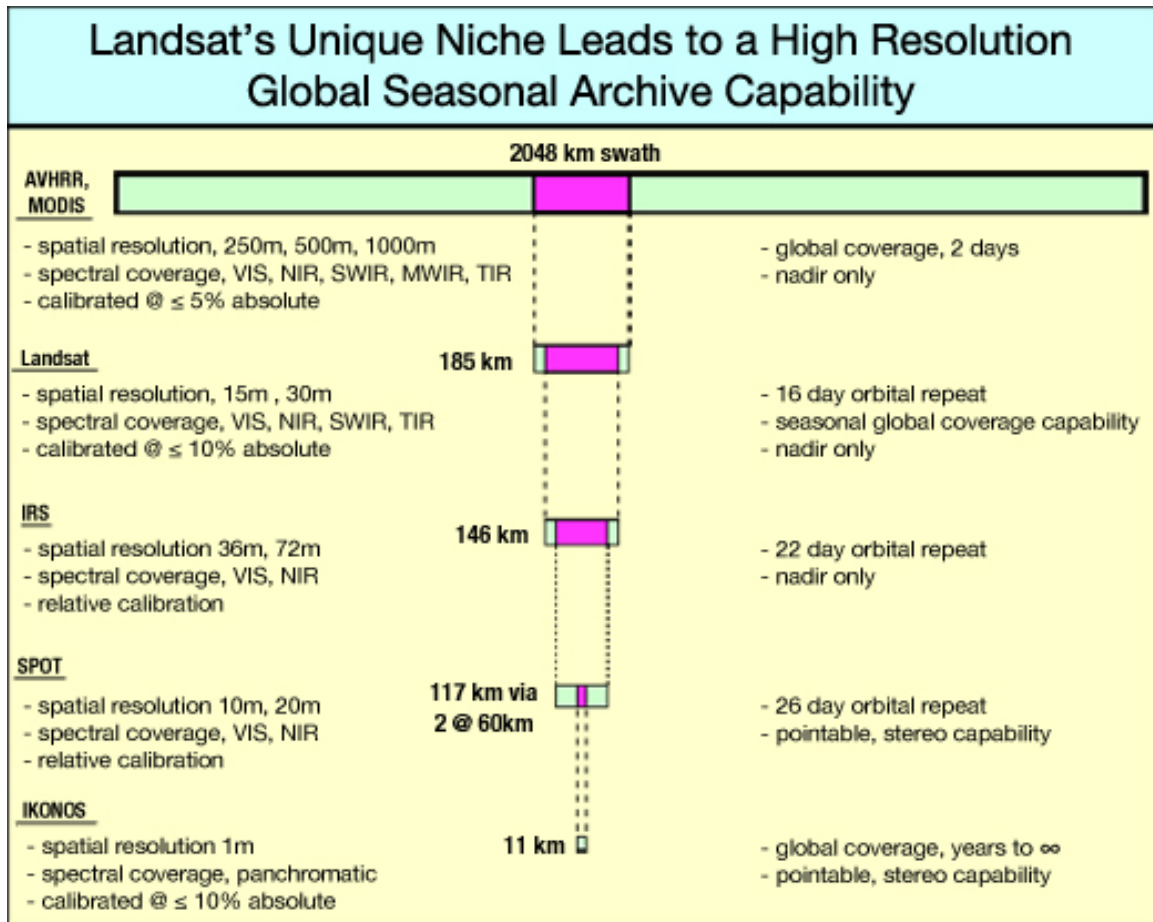


Figure 6.10 - Landsat Sensing Characteristics Relative to Other Satellite Systems

The horizontal bars represent proportionately scaled footprints of the sensors on the left. Listed with each sensor is its spatial resolution, spectral coverage, and radiometric calibration accuracy. The right side of the chart lists the sensor's temporal resolution and pointing capability. Upon careful examination of this chart, one can quickly ascertain Landsat's unique niche. No other sensor can match Landsat's uncommon characteristics, which include repetitive, broad-area, and global coverage at high spatial resolution in all four passive optical regions of the electromagnetic spectrum (i.e. visible, near IR, short-wave IR, and thermal IR regions), and accurate radiometric calibration. In addition, Landsat's retrospective archive stretches back 25 years.

## 7.1 Overview

Analyses performed on Landsat 5 data over the years has revealed the existence of imperfections or image artifacts caused by the instrument's electronics, dead or dying detectors, and downlink errors. As a descendant of the Thematic Mapper, the ETM+ generates data with similar characteristics. In the past, these effects were ignored or artificially removed using cosmetic algorithms such as histogram equalization during radiometric processing. A proactive approach is in place for Landsat 7. The goal of the ground system is to remove image artifacts prior to radiometric processing. Remnant artifacts, if they exist, are subsequently removed in a post-processing step using cosmetic algorithms.

The known ETM+ image artifacts are scan correlated shift, memory effect, modulation transfer function, and coherent noise. Dropped lines and inoperable detectors also exist as a result of decommutating errors and detector failure. Remnant artifacts, which may exist, include banding and striping. A discussion of each of these effects and characterization methodologies follows. Eliminating their presence from data products is addressed in a later chapter on Level 1 processing.

## 7.2 Scan Correlated Shift

Scan Correlated Shift (SCS) is a sudden change in bias that occurs in all detectors simultaneously. The bias level switches between two states. Not all detectors are in phase; some are 180 degrees out of phase (i.e. when one detector changes from low to high, another may change from high to low). All detectors shift between two states that are constantly time varying, or slowly time varying on the order of days to months. Measurement of SCS levels is affected by another instrument artifact known as Memory Effect (ME).

Characterization of SCS is performed at three levels. First, SCS levels are obtained for each detector in each line of the scene. This must be done to all scenes that require removal of SCS. Second, the value for the SCS levels is calculated for each detector. Third, the exact location of the transition from one SCS state to another within a scan line is determined, (assuming that a continuous flow of data from the detectors is available).

## 7.3 Memory Effect

Thematic Mapper data was rife with the artifact known as ME. It is manifested in a noise pattern commonly known as banding. It can be observed as alternating lighter and darker

horizontal stripes that are 16 pixels wide in data that has not been geometrically corrected. These stripes are most intense near a significant change in brightness in the horizontal (along scan) direction, such as a cloud/water boundary. Because of this, it was formerly termed 'Bright Target Saturation' or 'Bright Target Recovery.' Another artifact known as Scan Line Droop' was originally thought to be a separate phenomenon, but has since been shown to be simply another manifestation of ME. Because of its nature, ME have historically been the cause of significant error in calibration efforts since its effect on IC calibration data is scene dependent. It is present in Bands 1 through 4 of the Primary Focal Plane, and nearly absent in the Cold Focal Plane.

ME is known to be caused by circuitry contained in the pre-amplifiers immediately following the detectors in the instrument electronics. It is primarily due to a portion of a feedback circuit that contains a resistor/capacitor combination with a time constant of approximately 10 ms. This directly corresponds to time constants of approximately 1100 minor frames that have been derived from night scenes. Therefore, ME has been modeled as a simple first order linear system and only three model parameters need to be identified to characterize it (actually one of the three is simply detector bias).

$$g(mf) = b - k(1 - \exp(t/\tau))$$

where: **g(mf)** = the ME pulse response  
**b** = detector bias  
**k** = ME magnitude  
**tau** = the ME time constant

Although the exact approach taken to characterize ME is dependent on data type, response of the detector to some type of pulse is measured and averaged over many scan lines. Since the response will be exponential in form, the data are manipulated by subtracting out the appropriate bias level, linearized via the natural logarithm, and linearly regressed to determine the model parameters.

## 7.4 Coherent Noise

In TM reflective band data, coherent noise (CN) manifested itself in various ways. It is difficult to characterize and correct for as a consequence. Some CN components are locked to the start of the scan, but the more dominant components are not. The most persistent and dominant component is scan-free and has a varying frequency. Analysis of a swath of L5 TM night data showed the frequency of this component generally increasing as a function of time with episodic and strong jumps occurring at lamp state transitions. In addition, there is a bursting broadband component that is also not locked to the start of the scan. The power of this component varies strongly even within a scan, with a maximum amplitude of 1 DN.

In addition, its peak frequency varies widely over a range of 0.1 inverse minor frames (imf). Consequently, this component is difficult to filter out. A common scan-locked component manifests as a spike every 16 minor frames. Its amplitude may reach up to .1-2 DN. Another scan-locked component appears in only a few detectors. It is quite strong in one detector, having an amplitude of 0.6 DN. Interestingly; the power of this component varies significantly. Analysis of the swath of night data previously referred to, reveals its power to decrease exponentially from an amplitude of 0.6 DN to an amplitude of 0.3 DN over a timescale of about one thousand scan cycles. Finally, the power of most, if not all, CN components and the background noise (DN) correlates positively with SCS state.

The set of parameters characterizing a CN component in a detector will be the phase relative to a reference minor frame, the frequency, and the total power in the line in excess of that of the background noise. These parameters will be obtained per scan. In order to obtain the total power in excess of the background noise, the background noise must be characterized. Thus, it is necessary to characterize the continuum of the power density spectrum before identifying CN components. Analysis of the night data swath showed a strong dependence of the continuum on detector and SCS state. It also showed a dependence on lamp state, but the effect is weak. Thus, it is assumed that the continuum depends only on detector, scan direction, and SCS state.

## 7.5 Dropped Lines

Dropped lines occur in OR data due to decommutating errors in the raw data stream ingested by Landsat Processing System. During LPS processing a fill pattern is used to distinguish good data from bad data. Odd detectors are filled with zeros, while even detectors are filled with 255s. Data filling is performed on a minor frame basis - if data are missing from part of a minor frame, the entire minor frame is filled. Dropped lines can thus be entire or partial scans. Statistics on dropped lines (occurrence count, frequency) are stored in the metadata that accompanies all subintervals transferred to the LP-DAAC.

Dropped lines are characterized by examining the raw input image for the 0-255 fill pattern on a line-by-line basis. Known inoperable detectors are excluded from this operation. Filled minor frames are tallied by scan and for the entire image and compared to LPS counts reported in their metadata. During processing filled minor frames are flagged in the label mask, which is referenced during level 1 processing.

## 7.6 Inoperable Detectors

Image artifacts caused by dead or dying detectors require characterization. In addition to the obvious case of a "dead detector," one, which provides no change in output DN for changes in input radiance it is also important to determine when a detector channel has fallen out of acceptable performance, limits. A starting point for such a determination is a test to see if

each detector meets the performance criteria established in the Landsat-7 System Specification, Para. 3.7.8.1.3.1. This specification provides a detector to be classified as degraded, if its Signal to Noise Ratio (SNR) or dynamic range are below the specification levels.

This is a distributed algorithm that evaluates the outputs of several of the characterizations. One piece takes the indications of dead detectors from the output of performance in the IC to determine detector "aliveness". A second piece takes the outputs of random noise characterization to determine "in-spec" or out of spec behavior of the detector noise levels. This latter piece has two portions: one of which can operate on any scene using the shutter data, the other operates only on the output of FASC scenes. The final piece of the algorithm takes the output of the current gain selection and the currently indicated saturation bins, to assess the dynamic range of the channels. If any portion of the algorithm detects a change in performance (e.g. a new dead detector, noise level below spec or dynamic range below specs) flags will be set for an analyst to examine the results and potentially update the parameter file.

## 7.7 Banding

Banding or "scan-to-scan striping", is a sometimes visible noise pattern caused by memory effect. After scanning past a bright target such as clouds or snow, detector response is reduced due to memory effect. Thus if the region past the bright target is uniform, data values obtained from the sensor will be slightly lower than corresponding values obtained on the following scan (since the following scan is in the opposite direction and therefore, has yet to encounter the bright target.) The result is that scans in one direction will be noticeably darker than adjacent scans in the opposite direction. The banding pattern is very small in intensity, typically on the order of 1 to 2 counts.

Banding characterizations are performed after artifact removal and radiometric correction. The operation is cosmetic in nature as it recognizes and removes striping patterns left over from an ineffective ME correction process.

The approach employs an algorithm that applies a filter optimized for detection of the banding pattern. Because of the small amplitude inherent to banding, the filter is adaptive so that it only operates on those portions of the image where banding is detectable (i.e. in homogeneous or "smooth" image regions.) The filtering operation produces an output image where banding has been removed, as well as a difference image that gives an indication of where banding was detected, and its amplitude. An overall figure of merit is also calculated.

## 7.8 Striping

Striping is a line-to-line artifact phenomenon that appears in individual bands of radiometrically corrected data. Its source can be traced to individual detectors that are calibrated incorrectly with respect to one another. The application of the calibration coefficients to the ETM+ data, i.e. the generation of the level 1R data, is intended to remove the detector to detector variations in gain and offset, effectively de-striping the data. As detector to detector variations are already explicitly taken into account through the generation of relative gains and bias from histograms, and these are included in the process of generating the applied gains and biases, the striping characterization and correction should not be required in routine processing.

Nonetheless, a post processing characterization and removal process is in place should a cosmetic fix become necessary. This is achieved by linearly adjusting the 1R data to match the means and standard deviations of each detector to a reference detector, or to the average of the detectors. This actual processing algorithm applies the relative gains and biases calculated by the histogram analysis performed on every image just prior to radiometric correction.

## 8.1 Radiometric Calibration Overview

A major objective of the Landsat-7 program is to upgrade the radiometric quality of the data to be commensurate with the other sensors in the Earth Observing System (EOS). Unlike its predecessors, a specific goal of the Landsat-7 program is to achieve radiometric calibrations of the data to  $\pm 5\%$  uncertainty over the 5-year life of the mission. Pre-launch, the mission design supports this requirement through hardware design changes, and instrument characterizations. Post-launch or on-orbit, this 5% requirement is supported by a monitoring and calibrations program, and the implementation of any necessary changes to the ground processing of the data.

### 8.2 Pre-Launch

#### 8.2.1 Spectral Characterization

The measured wavelength locations of the ETM+ spectral bands are compared to Landsat 5's TM in Table 8.1. The spectral bandwidths are determined by the combined response of all optical path mirrors (i.e. primary, secondary, scan line corrector, scanning), the spectral filters, and the individual detectors. The spectral filters, located immediately in front of each detector array, are the dominant items that establish the optical bandpass for each spectral band. The prime focal plane assembly has a filter housing that contains filters for bands 1 through 4 and the panchromatic band. The cold focal plane assembly has a filter housing

that contains filters for bands 5 through 7.

<b>Table 8.1 TM and ETM+ Spectral Bandwidths</b>								
<b>Bandwidth (<math>\mu</math>) Full Width - Half Maximum</b>								
<b>Sens or</b>	<b>Band 1 Plot Data</b>	<b>Band 2 Plot Data</b>	<b>Band 3 Plot Data</b>	<b>Band 4 Plot Data</b>	<b>Band 5 Plot Data</b>	<b>Band 6 Plot Data</b>	<b>Band 7 Plot Data</b>	<b>Band 8 Plot Data</b>
TM	0.45 - 0.52	0.52 - 0.60	0.63 - 0.69	0.76 - 0.90	1.55 - 1.75	10.4 - 12.5	2.08 - 2.35	N/A
ETM +	0.45 - 0.52	0.53 - 0.61	0.63 - 0.69	0.78 - 0.90	1.55 - 1.75	10.4 - 12.5	2.09 - 2.35	.52 - .90

A discrete spectral shift occurred on Landsat 5 TM has been largely attributed to filter outgassing. The ETM+ filters were made using a process called ion assisted deposition (IAD) which presumably makes the filters resistant to this phenomenon. In addition, the new filters have shown significant improvement in band edge responses as compared to Landsats 4 and 5.

## 8.2.2 Radiometric Calibration

### Reflective Band Calibration and Monitoring

Two [spherical integrating sources \(SIS\)](#) were used to calibrate the ETM+ prior to launch. The first - a 100 cm source (SIS100) is equipped with 18 200-watt lamps; 6 45-watt lamps, and 10 8-watt lamps. It provides radiance levels covering the full dynamic range of the instrument in all bands, and at least 10 usable radiance levels for each band for each gain state. The SIS100 was used to perform the primary radiometric calibration of the ETM+ in August 1997 and was also used for the pre-launch calibration of AM-1's Moderate Resolution Imaging Spectroradiometer (MODIS). The second source is a 122 cm (48") SIS with 6 200-watt lamps; 2 100-watt lamps, and 4 25-watt lamps. The SIS48 was used for monitoring the radiometric calibration of the ETM+ five times during instrument and spacecraft level testing. During SIS calibrations the Bench Test Cooler (BTC) was used to maintain the temperature of the Cold Focal Plane at 105°K. This was the only one of the three temperature set points for the cold focal plane that could be obtained in ambient pressure and temperature conditions.



The calibration data reduction is performed as follows:

- (1) The ETM + band weighted spectral radiances,  $L_{\lambda}(b,s)$ , for band "b" and sphere level "s" are calculated as:

$$L_{\lambda}(b,s) = \frac{\int RSR(b,\lambda)L_{\lambda}(s,\lambda)d\lambda}{\int RSR(b,\lambda)d\lambda}$$

Where:

$RSR(b,\lambda)$  is the Relative Spectral Response for band "b" at " $\lambda$ " calculated from component level transmission, reflectance and responsivity measurements,

$L_{\lambda}(s,\lambda)$  is the measured spectral radiance of sphere level "s" at " $\lambda$ "

- (2) The quantized detector (d) by detector responses,  $Q(d,b,s)$ , are regressed against the integrating sphere band weighted radiance level,  $L_{\lambda}(b,s)$ , per the calibration equation:

$$Q(d,b,s) = G(d,b)L_{\lambda}(b,s) + B(d,b)$$

The slopes of these regression lines are the responsivities or gains,  $G(d,b)$ , and the intercepts are the biases,  $B(d,b)$ . The Landsat Project Science Office (LPSO) will review the various integrating sphere calibrations and their effective transfer to the ETM+ before deciding which calibration should go the IAS to represent the pre-launch IAS.

### Thermal Band Calibration

The radiometric calibration of band 6, the thermal band, is fundamentally different than the reflective bands as the instrument itself contributes a large part of the signal. A model of this temperature dependent instrument contribution has been developed by SBRS. The calibration for band 6 is formulated as:

$$Q_{sc} - Q_{sh}(d) = G(d)(L_{\lambda,sc} - L_{\lambda,esh})$$

Where:

$Q_{sc}(d)$  is the quantized response of band 6 detector d to the scene,

$Q_{sh}(d)$  is the quantized response of band 6 detector d to the shutter,

$G(d)$  is the gain of detector d

$L_{\lambda,sc}$  is the spectral radiance of the scene

$L_{\lambda,esh}$  is the scene-equivalent spectral blackbody radiance of the shutter:

$$L_{\lambda,esh} = L_{sh} + \sum a_j(L_{sh} - L_j)$$

where  $L_{sh}$  is the blackbody radiance of the shutter,  $L_j$  is the blackbody radiance of the jth component of the ETM + instrument, and  $a_j$  is the emissivity adjusted view factor for the jth ETM + component of the  
 $j = 1$  for scan line corrector;  $j = 2$  for the central baffle;  
 $j = 3$  for the secondary mirror and mask;  $j = 4$  for the primary mirror and mask;  $j = 5$  for the scan mirror. Each of these components is in front of the shutter and contributes to the apparent scene radiance when the shutter is open.

The pre-launch calibration of band 6 is primarily a calibration of this model. The radiometric calibration of the thermal band occurs during thermal vacuum testing. During this test the ETM+ is aligned to the Thematic Mapper Calibrator (TMC), a collimator with selectable sources at its focus. During the band 6 calibration, blackbody sources will be used in the TMC. The band 6 detectors' responses to combinations of various TMC blackbody and instrument temperatures are used to calibrate the instrument and to refine emitted radiance contributions from various internal ETM+ components. The results of this calibration are nominal gains and biases for band 6, and the emissivity adjusted view factors ( $a(j)$ ) for the various internal components of the ETM+ that affect the band 6 calibration. The gains and biases are included in the CPF as pre-launch values for band 6.

### 8.2.3 ETM+ Spherical Integrating Source

A spherical integrating source is a hollow sphere with the entire inner surface uniformly coated with a material, which has a high diffuse reflectance. The basic concept behind the spherical shape is that light from the internal source has a chance to perform multiple bounces thereby randomizing its original direction before it exits a small aperture. The sphere's interior coating is designed to have a very high degree of diffuse reflectance. A perfect diffuse reflector can behave like a perfect (i.e. Lambertian) diffuse source which means energy is distributed in all directions

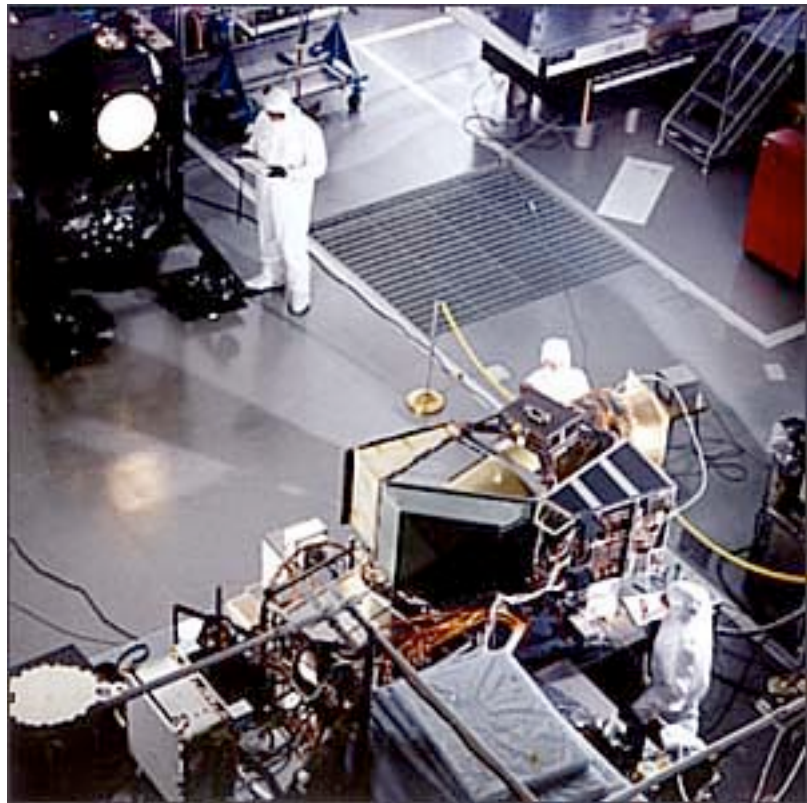


Figure 8.1 - SIS in clean room

equally. A Lambertian source is a source whose radiance is independent of viewing angle. Radiance is defined as the energy flux per unit projected area per unit solid angle leaving a source, or a surface.

Each SIS is calibrated by SBRS to National Institute of Standards and Technology (NIST) traceable standards of spectral irradiance. In addition, EOS cross calibration activities

include comparison of the SBRS radiometric scale to the NIST, University of Arizona, NASA's Goddard Space Flight Center, and Japan's National Research Laboratory of Metrology (NRLM) radiometric scales.

The Landsat Transfer Radiometer (LXR), a visible and near infrared radiometer designed for stability by NIST, is used to monitor the output of each sphere during each calibration and calibration check. This radiometer has also been calibrated by NIST to provide an independent check on the radiometric calibration of the two sources.

## 8.3 Post-Launch

The post-launch radiometric calibration of the ETM+ is accomplished by regularly examining the instrument's response when illuminated by known sources that are relatively stable. The ETM+ has 3 on-board calibration devices, namely, the Internal Calibrator (IC), the Partial Aperture Solar Calibrator (PASC), and the Full Aperture Solar Calibrator (FASC). The IC is useful for calibrating all ETM+ bands, while the PASC and FASC are mainly useful for the reflective bands. Changes to the ETM+ calibration have occurred since launch and can be viewed using this graphical [timeline](#) (Table 8.2).

Ground look calibrations are occasionally performed to confirm, via independent analysis, the accuracy of the calibration using on-board sources.

### 8.3.1 Internal Calibrator

The IC consists of a shutter flag, 2 tungsten lamps, and a blackbody source. The shutter flag, located immediately in front of the prime focal plane, oscillates in synchronization with the scan mirror. At the end of each scan the shutter blocks light from the Earth, from the focal planes. In addition, the shutter flag relays light from the IC lamps and blackbody, to the detectors. The two IC lamps are situated near the base of the internal calibrator flag. Light from either or both lamps is directed through optics at the pivot point of the flag, into a sapphire rod contained within the flag. This rod transfers the light up the shutter flag and splits it into separate paths for each of the spectral bands. The light is directed out of the shutter flag and onto the focal planes by additional optics in the head of the instrument. The light separated for each band is aligned so that it impinges on the appropriate detectors.

The IC lamps are supplied with a regulated voltage across a combination of the lamp and a resistor, resulting in quasi-constant power being supplied to the lamp. Each lamp can be commanded "on" or "off", such that 4 lamp states are possible (both "off" [0,0], one "on" [0,1] or [1,0] or both "on" [1,1]). The IC was designed to have one lamp produce a usable signal in all bands. Note, both lamps "on" will saturate some bands particularly in high gain mode.

The IC blackbody is situated off the optical axis of the instrument. When the shutter flag passes in front of the primary focal plane, radiation from the blackbody is reflected off of a toroidal mirror on the flag, into the aft optics of the ETM+ and onto the band 6 detectors. The portion of the shutter flag imaged by band 6, exclusive of the area where the toroidal mirror is located, is coated with a high emissivity paint and acts as the second source for band 6 calibration. This portion of the shutter flag is also instrumented with a thermistor. The blackbody has three set point temperatures namely, 30°C, 37°C and 46°C.

The ETM+ IC, although similar to the IC on the Landsat-6, differs from the IC's on Landsat-4 and Landsat-5, in 5 principal ways: (1) the ETM+ uses 2 lamps (4 states) instead of 3 lamps (8 states), (2) a more compact filament results in a higher flux incident on the IC optics, though the lamps are nearly identical in terms of current and voltage ratings, (3) the control circuit for ETM+ uses voltage regulation in the primary operation mode, whereas TM used radiance stabilization in the primary mode, and voltage regulation in the backup mode, (4) ETM+ uses sapphire rods to transmit the energy from the base of the flag to the head of the shutter flag, while the TM's used fiber optics in an attempt to improve the uniformity of the calibration flux at the focal plane, (5) the ETM+ does not retain the lamp sequencer used on TM to automatically cycle through the lamp states.

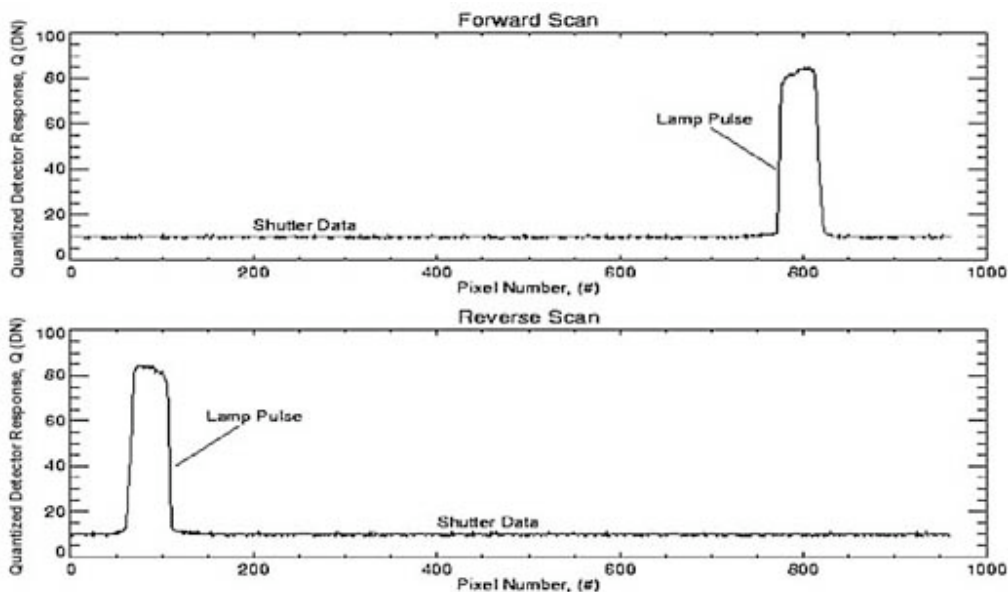
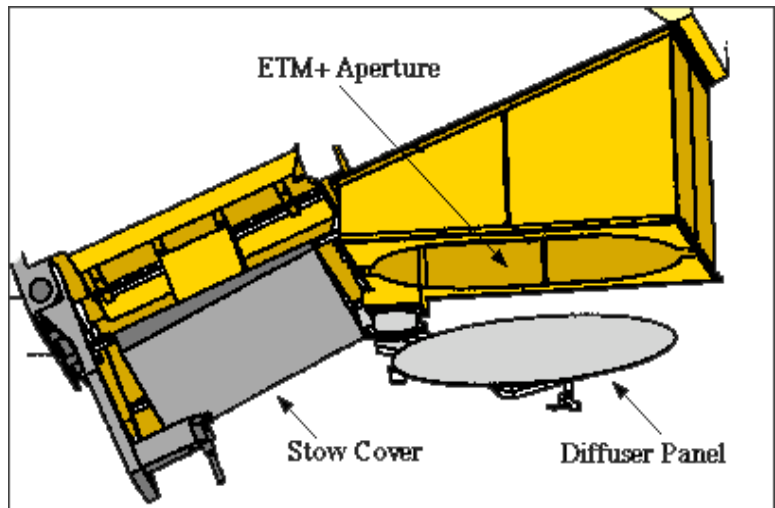


Figure 8.2 - ETM+ Band 4, Detector 1, Low gain, IC data, 12/7/96, primary lamp.

When the ETM+ is operating, the shutter flag oscillates in synchronization with the scan mirror. The size of the shutter flag and its speed of movement combine to provide obscuration of the light to each detector for about 8.2 msec, or 750 pixels, for the 30 meter channels; the light pulse for the reflective bands, has a width of approximately 40 pixels (Figure 8.2). For band 6, the calibration signal is similar with the blackbody pulse about 20 pixels wide.

### 8.3.2 Full Aperture Solar Calibrator

The Full Aperture Solar Calibrator (FASC) is a white painted panel that is deployed in front of the ETM+ aperture and diffusely reflects solar radiation into the full aperture of the instrument as illustrated in Figure 8.3. With known surface reflectance, solar irradiance and geometry conditions, this device behaves as an independent, full aperture calibrator. The device consists of an octagon shaped, aluminum honeycomb paddle on a motorized arm. On command,



**Figure 8.3** - ETM+ FASC in deployed position in front of ETM+ aperture.

the motor rotates the panel from its stowed position away from the ETM+ aperture, to an inclined position in front of the ETM+. When stowed the panel rests adjacent to the stow cover which reduces the exposure of the panel to contaminants and UV radiation. The center 51 cm of the FASC panel is painted with the classic formulation of YB71, an inorganic flat white paint designed for spacecraft thermal control. This paint was selected for its near Lambertian properties, high reflectance, and apparent stability in a space environment. When in the calibrate position the angle between the sensor nadir vector, and the panel normal, is specified to be 23.5°. In use, the panel can be illuminated by the sun from 90° zenith angle (i.e. sunrise on panel) to about 67° zenith angle. Below 67°, the instrument begins to shade the panel. Depending on the time of year the solar azimuth angle with respect to the velocity vector of the ETM+, varies from 23° to 37°. The relative azimuth between the nadir view vector and the solar illumination varies across the same range.

ETM+ image data acquired with the FASC will appear to be an essentially flat field with vignettted cross track edges. The image will increase in brightness along track as the solar

zenith angle (SZA) on the panel decreases (roughly at  $1/\cos(\text{SZA})$ ). Specifications require the FASC to fill the ETM+ aperture for the central 1000 pixels (approx 1/6 of each scan line); the design nominally fills the aperture for the central ~50% of the scan line. As the mirror scans, the view angles to the FASC panel change. If the nadir viewing pixel has the nominal  $23.5^\circ$  view angle and a  $0^\circ$  view azimuth angle, then at the extreme ends of the scan, the view zenith angle increases by about  $1^\circ$ , and the view azimuth angle varies by  $\pm 30^\circ$ . Pre-launch BRDF measurements indicate that the radiance change across the scan, should be a 1% effect across the full scan assuming the aperture is filled. Across the central 1000 pixels, this translates into a 0.1% effect.

### 8.3.3 Partial Aperture Solar Calibrator

The Partial Aperture Solar Calibrator (PASC) is used for calibrating bands 1-5, 7 and 8 and consists of a small passive device that allows the ETM+ to image the sun while viewing a 'dark earth'. It is attached to the ETM+ sunshade and permanently obscures a small portion (~0.5%) of the aperture. It consists of four essentially identical sets of optical elements each in a slightly different orientation. Each set (or facet) consists of an uncoated silica reflector, a  $45^\circ$  mirror, and an aperture plate with a precision drilled small aperture (~4 mm) (Figure 7). The combination of the small aperture and the uncoated silica reflector reduces the signal amplitude

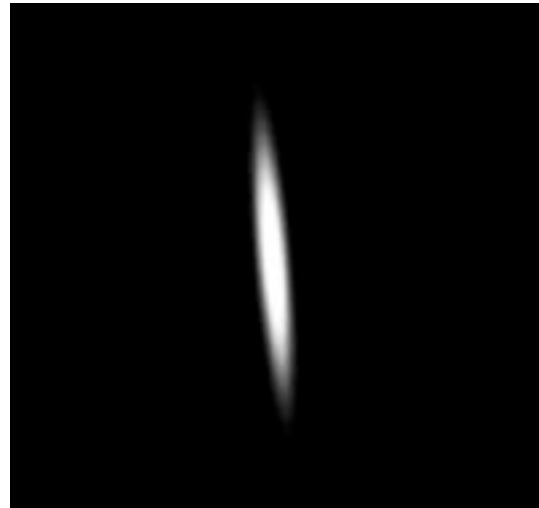


Figure 8.4 - Simulated ETM+ PASC scene.

sufficiently to bring it into the ETM+ dynamic range. The four facets are duplicated to account for angular variations of Sun position with season. They are oriented such that in any given orbit, as the satellite passes out of solar eclipse (i.e. space vehicle sunrise) in the vicinity of the north pole, at least one facet will reflect sunlight directly into the ETM+ aperture and the ETM+ will image the sun.

Recent SBRS measurements of the alignment between the PASC and scanner assembly, have revealed a design misalignment, which resulted in a nominal declination angle of the PASC (relative to spacecraft nadir) of 20 degrees, versus the prescribed 18 degrees. This increase in declination effectively forces the Spacecraft to acquire PASC scenes earlier in its orbit (i.e. closer to spacecraft sunrise). Although the spacecraft solar panel undergoes a period of thermal instability during sunrise, an analysis of the resultant spacecraft jitter has shown minimal impact ( $< 1\%$ ) to the acquisition of PASC data.

The PASC will generate a reduced resolution image of the sun, the resolution being limited by diffraction from the small apertures. This diffraction effect is wavelength dependent. For

example, in band 1 the blur will extend across about 7 pixels (at the first dark ring of the diffraction pattern), and in band 7 the extent is about 32 pixels. In addition to the blur, the image will be elongated in the "along-track" direction. The "along-track" movement across the solar disk can best be expressed in terms of the spacecraft pitch rate (i.e. 360 degrees in ~100 minutes or ~3.6 degrees/minute). By comparison, the ground is normally scanned at 16 instantaneous field of views (IFOV's). This equates to .039 degrees ( $16 * .0024$  degrees) per 72 msec scan or ~32.5 degrees/minute. Thus the sun image will be oversampled along track by a factor of about 9. One other contributor to the rendition of the solar image, is the scanning direction, which is not perpendicular to the motion of the sun - the angle between the two can be as small as 45 degrees. These combined effects of oversampling, and a non-orthogonal scan pattern, produce an elongated, skewed image of the sun as seen in Figure 8.4.

Within a PASC processed image, it is anticipated that most uniform portions of the solar disk center will be approximately 200 pixels in width for bands 1-5, 7, 105 pixels for band 6, and 410 pixels for band 8.

PASC calibration is performed once a day, every day, on the orbit specified by the IAS. The IAS orders the resulting data from the EDC-DAAC for calibration processing and assessment.

### **8.3.4 ETM+ Calibration Actions**

Presented in Table 8.2 are the actions taken by the Landsat Project Science Office (NASA/GSFC) and the Image Assessment Team (USGS/EDC) to provide the best possible calibration for Landsat ETM+ imagery.

Definition of Terms:

Acquisition Date - date image was acquired by the satellite

Processing Date - date image was processed to Level 1 by the Processing System; this date should be close to the date the scene was ordered and received by the customer

Table 8.2 Calibration Action Time Line

Problem/ Update	Bands Affected	Acquisition Dates	Processing Dates																							
			1999						2000												2001					
			J u l	A u g	S e p	O c t	N o v	D e c	Jan	Feb	Mar	A p r	M a y	J u n	J u l	A u g	S e p	O c t	N o v	D e c	J a n	F e b	M a r	A p r	M a y	J u n
B6 Calibration	6	all	bias error in calibration procedure, subtract 0.31 radiance units for calibrated imagery																		calibration corrected					
B6 Gain Swap Period	6	11/24/99 to 12/08/99				B6 out of calibratio n	bias error in calibration procedure, subtract 0.31 radiance units						B6 out of calibration						B6 calibrati on correct ed							
Lmin/Lmax update	all	all	use first set of Lmin/Lmax's to scale Level 1 DN to radiance												use second set of Lmin/Lmax to scale Level 1 DN to radiance											

**Summary of Required Actions**

Problem/Update	Details/For more details...
B6 Calibration	Independent calibration teams discovered an offset error in the B6 calibration. This was corrected through processing on 21 DEC 2000. For users with data processed before 21 DEC 2000, subtract 0.31 W/m2 sr um from the radiance image for calibrated data.
B6 Gain Swap	An error caused the two B6 gains to be swapped, resulting in an intermediate gain state. Attempts to correct the problem were implemented then lost and implemented again on 01 Jul 2001.
Lmin/Lmax update	Using updated information on the pre-launch calibration, the scaling factors were adjusted beginning 01 Jul 2000 to make better use of the dynamic range.
Links to Landsat Updates at NASA: <a href="http://landsat.gsfc.nasa.gov/news/">http://landsat.gsfc.nasa.gov/news/</a> and USGS: <a href="https://landsat.usgs.gov/about_Landsat_Updates.php">https://landsat.usgs.gov/about_Landsat_Updates.php</a>	



## 8.4 TM Cross Calibration

### 8.4.1 Introduction

#### Calibrating the Landsat Data Record

The Landsat data record is important for terrestrial remote sensing and global change research because it covers a 30-year time when significant anthropogenic terrestrial change has occurred. In order to benefit from this data record, steps are needed to ensure that the data are self-consistent and not significantly affected by artifacts of the various Landsat sensors. In anticipation of a successful Landsat 7 mission, renewed efforts were made to ensure radiometric calibration across the Landsat series of sensors and with other Earth observation sensors. A critical step in such a process is sensor radiometric calibration to an absolute scale, yielding image data at the top of the atmosphere in physical units. Additional processing steps to retrieve surface parameters such as reflectance and temperature then become possible.

Consistency between the Landsat sensors starts with sound calibration of the individual sensors, including the development of a stable sensor (i.e. ETM+), detailed prelaunch characterization, and on-orbit calibration. Post-launch radiometric calibrations are based on reference to onboard standards and ground-based test sites. ETM+ cross-calibration with earlier Landsat sensors begins by making use of near-simultaneous imaging of common Earth surface targets. Typically, there is a limited overlap period when more than one of the sensors is operating at the same time. Such an overlap period with Landsat 5 was designed into the initial phases of the Landsat-7 mission. The resulting opportunity for radiometric cross-calibration between ETM+ and Landsat 5's TM is the main subject of this chapter. This material was extracted from a paper that covers the subject in greater detail (Teillet, et. al., 2001).

#### The Tandem Configuration

The launch of Landsat-7 on April 15, 1999 placed the spacecraft temporarily in an orbit very close to that of the Landsat-5 spacecraft. The mean altitude of Landsat-7 was 699 km, 6 km below the 705-km mean altitude of Landsat-5. At this altitude, the Landsat-7 ground track drifted slowly relative to the nearly fixed Landsat-5 pattern. The key period for the tandem configuration was June 1-4, 1999 when the tracks were almost exactly the same, but with a temporal offset on the order of 10 to 30 minutes. This unusual and valuable opportunity was specifically designed to facilitate the establishment of data consistency between the Landsat ETM+ and TM sensors. During the tandem configuration period when there was useful

overlap in coverage between the two sensors, image sequences corresponding to 791 matching scenes were recorded by both the Landsat-7 ETM+ and, in cooperation with Space Imaging EOSAT and international ground stations, the Landsat-5 TM (Table 8.3). Subsequently, the Landsat-7 orbit was changed for nominal operations such that its 16-day repeat coverage cycle is now offset from that of Landsat-5 by 8 days. Given cloud cover and possible problems with data reception and recording, the number of useful tandem data scene pairs is roughly estimated to be on the order of 400 scenes.

<b>Table 8.3 Landsat 7 ETM+ and Landsat 5 Tandem Data Coverage</b>							
<b>Tandem Scene Coverage (June 1-4, 1999)</b>							<b>Stations</b>
<b>June</b>	<b>P</b>	<b>R</b>	<b>Station</b>	<b>June</b>	<b>Path</b>	<b>Row</b>	<b>Station</b>
3	6	21-29	GNC	3	159	-	RSA
3	6	57-71	CUB	3	159	69-78	JSA
3	6	67-71	COA	2	168	19-27	KIS
2	15	12-44	GNC	2	168	-	RSA
2	15	27-45	NOK	2	168	62-83	JSA
3	22	10-43	GNC	3	175	19-26	KIS
3	22	26-49	NOK	3	175	23-42	FUI
2	31	7-40	PAC	3	175	-	RSA
2	31	25-46	NOK	3	175	62-85	JSA
3	38	6-39	PAC	2	184	22-44	FUI
3	38	25-40	NOK	2	184	44-77	LBG
1	40	25-38	NOK	3	191	14-24	KIS
2	47	4-30	PAC	3	191	17-43	FUI
2	47	25-30	NOK	2	200	17-40	FUI
3	54	4-25	PAC	3	207	19-24	FUI
2-3	95	65-87	ASA	2	216	63-76	CUB
3	102	69-83	ASA	3	223	60-86	CUB
2	104	62-82	ASA	3	223	68-98	COA
3-4	111	64-84	ASA	2	232	54-85	CUB
2	152	-	RSA	2	232	66-97	COA

**ASA** ACRES, Alice Springs, Australia

**COA** Cordoba, Argentina

**CUB** INPE, Cuiaba, Brazil

**FUI** ESA, Fucino, Italy

**GNC** CCRS, Gatineau, Canada

**JSA** Johannesburg, South Africa

**KIS** ESA, Kiruna, Sweden

**LBG** DLR, Libreville, Gabon

**NOK** SI/EOSAT, Norman, Oklahoma

**PAC** CCRS, Prince Albert, Canada

**RSA** Saudia Arabia (for SI/Dubai)

The cross-calibration methodology documented here is applicable to tandem image pairs and presents specific results for two different pairs of nearly coincident matching scenes from the tandem configuration period. The main results consist of TM responsivities in the six solar reflective spectral bands referenced against well-calibrated ETM+ responsivities in corresponding spectral bands. The formulation includes adjustments for differences in illumination regimes as well as for differences in spectral response profiles between the two sensors.

### 8.4.2 Tandem Data Sets Selected for Analysis

Attention was focused on two particular tandem image pairs for cross-calibration methodology development and analysis because of the availability of ground reference data. Both Landsat sensors imaged the Railroad Valley Playa (RVPN), Nevada on 1 June 1999, when a team from the University of Arizona made measurements of surface spectral reflectance and atmospheric aerosol optical depth the same day. Similarly, a team from South Dakota State University acquired the same types of ground reference data at a grassland test site in the area of Niobrara, Nebraska (NIOB) on 2 June 1999, the day of the tandem Landsat overpasses for that site.

**Table 8.4 Characteristics of the Two Tandem Data Sets**

	<b>Railroad Valley Playa</b>	<b>Niobrara, Nebraska</b>
Image Date	June 1, 1999	June 2, 1999
WRS Path/Row	40/33	31/30
Landsat 7 Offset from WRS	76.56 km East	18.15 km East
ETM+ Data Level	Level-0R	Level-0R
TM Data Level	Level-0	Level-0
ETM+ Solar Zenith Angle	24.28 °	26.60 °
TM Solar Zenith Angle	27.23 °	28.67 °
Terrain Elevation	1.425 km	0.760 km
ETM+ A0D550*	0.1046	0.059
TM A0D550*	0.1035	0.059
Area Common to ETM+ & TM	10.7 km by 4.4 km	106 km by 66 km
* A0D550 represents aerosol optical depth at 0.550 micrometers		

Table 8.4.2 provides information on the characteristics of the two data sets and Figure 8.4 shows both Landsat image pairs. The RVPN test site is a dry-lake playa that is very homogeneous and consists of compacted clay-rich lacustrine deposits forming a relatively smooth surface compared to most land covers. The NIOB test site is characterized primarily by grasslands grazed by cattle and by a smaller proportion of agricultural crops.

### 8.4.3 Cross Calibration Methodology

The cross-calibration methodology assumes that the Landsat-5 TM calibration is to be updated with respect to the Landsat-7 ETM+ sensor, which serves as a well-calibrated reference sensor with a radiometric calibration uncertainty of  $\pm 3$  percent (Barker et al., 1999). Because data acquisitions were only 10 to 30 minutes apart during the tandem configuration period, it is assumed that the surface and atmospheric conditions did not change significantly between the two image acquisitions. Cross-calibration methodologies in general should consider adjustments as appropriate for bi-directional reflectance factor (BRF) effects due to differences in illumination and observation angles. For Landsat sensor image data pairs acquired during the tandem configuration period, the expectation is that such BRF adjustments are not necessary. The solar illumination geometries are very similar (within three degrees), satellite zenith angles are predominantly near-nadir, and relative azimuth angles between solar and satellite directions do not differ significantly from one Landsat overpass to the other. Nevertheless, there are geometric, radiometric, and spectral considerations to be addressed.

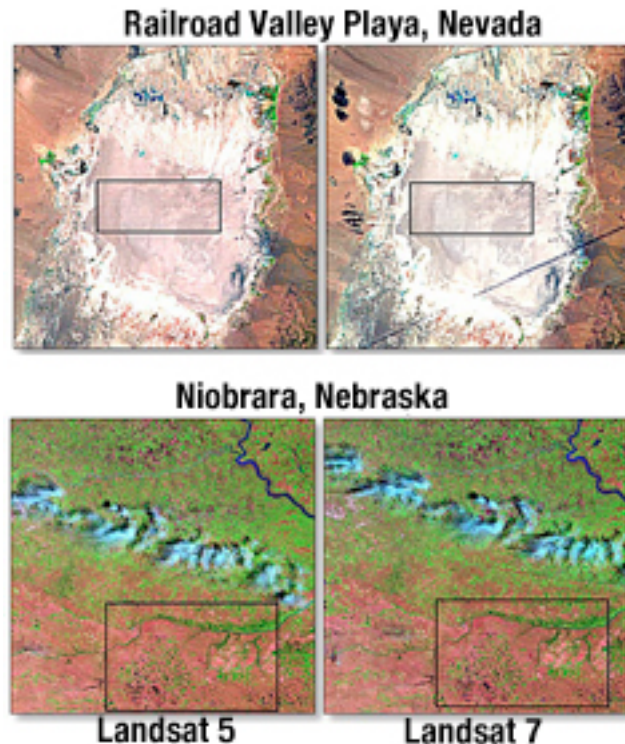


**Figure 8.5** - Landsat 5 and 7 Cross Calibration Data Sets of Railroad Valley Playa, Nevada WRS 40/33 acquired June 1, 1999 and of Niobrara, Nebraska, WRS 31/30 acquired June 2, 1999 using bands 5,4,2.

#### Geometric Matching

Geometrically, the Landsat-7 and Landsat-5 sensors differ in their along-track and across-track pixel sampling. Due to wearing of the bumpers used by the Landsat-5 TM scanning mirror, along-track gaps between scans are longer than they are for Landsat-7 ETM+. For the same reason and because the ETM+ scan time is slightly longer than the specification, there are also across-track differences in the ground coverage. In addition, slight mismatches will arise in the imagery because of the altitude difference. In particular, there is variation in the ETM+ scanning pattern and its effect on the scan line corrector due to the lower-than-

nominal orbit during the tandem configuration time period. These considerations make it very difficult to establish sufficient geometric control to facilitate radiometric comparisons on a point-by-point and/or detector-by-detector basis. Therefore, the analysis approach was developed to make use of image statistics based on large areas in common between the image pairs.

### Radiometric Formulation

Radiometric raw data are assumed (Level 0 for TM and Level 0R for ETM+). In spectral band  $i$ , the image quantized level  $Q_i$  (in counts) is related to top-of-atmosphere (TOA) radiance  $L_i^*$  (in Watts/(m<sup>2</sup> sr mm)) by

where: (1)

$G_i$  is band-averaged sensor responsivity (in counts per unit radiance)

$Q_{0i}$  is the zero-radiance bias (in counts) in spectral band  $i$ .

Quantized levels of  $Q = 0$  and  $Q = 255$  are excluded to avoid saturation effects. The zero-radiance biases are based on dark current restore values computed on a line-by-line basis. Radiometric detector normalizations based on full-scene statistics are applied in each spectral band, for each particular scene in the case of TM and for many scenes in the case of ETM+. The normalizations are with respect to the band average and the process is not expected to bias the cross-calibration. Normalized and bias-corrected image values are then given by

$$\Delta Q_i = Q_i - Q_{0i} = G_i L_i^* \tag{2}$$

Thus, TOA radiances  $L_i^*$  (in Watts/(m<sup>2</sup> sr μm)) are related to image data by

$$L_i^* = \Delta Q_i / G_i \tag{3}$$

TOA reflectance is related to TOA radiance by

$$\rho^*_i = \pi L^*_i d_s^2 / (E_{0i} \cos\theta) , \quad (4)$$

where:

$E_{0i}$  is the exo-atmospheric solar irradiance in spectral band  $i$  (in Watts/(m<sup>2</sup> mm)) based on the Modtran-3 spectrum

$\theta$  is the solar zenith angle

$d_s$  is the Earth-Sun distance in Astronomical Units

A combination of equations (2), (3), and (4) yields

$$\Delta Q_i = G_i \rho^*_i E_{0i} \cos\theta / (\pi d_s^2) . \quad (5)$$

There are two advantages to using reflectance instead of radiance. One advantage is to remove the cosine effect of different solar zenith angles due to the 10- to 30-minute time difference between data acquisitions. For example, the three-degree difference in solar zenith angles for the RVPN image pair leads to a 2.5 percent effect in the ratio of the cosines of the respective angles. The other advantage is to compensate for different values of exo-atmospheric solar irradiance arising from spectral band differences. If differences in atmospheric conditions are not a factor, then the TOA reflectance comparisons have the potential to yield the best possible calibration comparisons between the TM and ETM+ based on the tandem data sets.

### Cross Calibration

Equation (5) can be defined separately for image data from the Landsat-5 TM ("5") and for image data from the Landsat-7 ETM+ ("7"):

$$\Delta Q_{i5} = G_{i5} \rho^*_{i5} (E_{0i} \cos\theta)_5 / (\pi d_s^2) ; \quad (6)$$

$$\Delta Q_{i7} = G_{i7} \rho^*_{i7} (E_{0i} \cos\theta)_7 / (\pi d_s^2) . \quad (7)$$

The combination of equations (6) and (7) yields

$$\Delta Q_{i5A} = A_i \Delta Q_{i5} = (G_{i5} / G_{i7}) \Delta Q_{i7} = M_i \Delta Q_{i7} , \quad (8)$$

where the adjustment factor  $A_i$  adjusts Landsat-5 TM radiance data for illumination and spectral band difference effects. In particular,  $M_i$  is the slope of the linear equation that characterizes  $\Delta Q_{i5A}$  as a function of  $\Delta Q_{i7}$  and

$$A_i = B_i (E_{0i} \cos\theta)_7 / (E_{0i} \cos\theta)_5 , \quad (9)$$

Where

$$B_i = \rho_{i7}^* / \rho_{i5}^* . \quad (10)$$

$B_i$  is essentially a spectral band [adjustment factor](#), given that the  $\rho_{i7}^*$  in equations (6) and (7) are not necessarily the same because of the differences in relative spectral response profiles between corresponding ETM+ and TM spectral bands. Landsat-5 TM responsivity  $G_{i5}$  is then given in spectral band  $i$  (in counts per unit radiance (CPUR)) by

$$G_{i5} = M_i G_{i7} . \quad (11)$$

With this updated value of TM responsivity, users can obtain TOA radiance  $L_i^*$  (in Watts/(m<sup>2</sup> sr μm)) from raw image quantized levels  $Q_i$  (in counts) using

$$L_i^* = a_i Q_i + b_i , \quad (12)$$

where  $a_i = 1 / G_i$  and  $b_i = -Q_{0i} / G_i$ . Thus, image pairs from the tandem configuration period make it possible to use well-calibrated Landsat-7 ETM+ image data to update the radiometric calibration of the Landsat-5 TM.

#### 8.4.4 Image Processing and Analysis

Standard image processing and statistical analysis steps were used to obtain the  $M_i$  slopes in equation (8) for use in equation (11). The  $\Delta Q_{i5A}$  and  $\Delta Q_{i7}$  for use in equation (8) were obtained from large areas, depicted in Figure 8.5, common to the ETM+ and TM data pairs. As noted before, sub-pixel geometric registration is not critical in this case, but care was



taken to capture the common area as accurately as possible.

The image processing steps in each solar-reflective spectral band  $i$  was as follows.

Set up a 5 by 5 grid of contiguous image windows or cells and extract  $\Delta Q_i$  means and standard deviations from each of the 25 grid cells for an area common to both the ETM+ and TM image data.

Repeat step 1 for a series of one-pixel shifts in a 5 by 5 pattern, yielding 25 subsets of means and standard deviations per grid cell. This "jitter" pattern makes it possible to assess the sensitivity of grid-cell data to these shifts as an indicator of misregistration effects. The additional sets of values resulting from this jitter exercise are not used for any other purpose.

Keep grid-cell mean results only if sensitivity to shifts is low (within one percent). The value retained is the one obtained for the geometric centre of the jitter pattern.

Compute  $\Delta Q_{i5A}$  from  $\Delta Q_{i5}$  using equations (8) - (10) to adjust for spectral band differences and illumination regime differences between acquisitions.

Plot grid-cell  $\Delta Q_{i5A}$  and  $\Delta Q_{i7}$  means and obtain the slopes  $M_i$  (equation (8)).

Use equation (11) to compute Landsat-5 TM responsivity  $G_{i5}$ .

The jitter exercise revealed low sensitivity to possible misregistration between the sub-scenes selected as areas common to both images in each tandem pair. For the majority of grid cells, the coefficient of variation for the 25 jitter values of  $\Delta Q_i$  is a small fraction of a percent, reaching 0.3 percent in a few cases for the Niobrara scene and just over one percent for one grid cell for the Railroad Valley playa scene. The average coefficient of variation for the RVPN case is 0.24 percent. Therefore, no image cells were excluded on the basis of the jitter exercise.

After preprocessing in accordance with the radiometric formulation described earlier, sub-scene grid-cell means for  $\Delta Q_{i5A}$  and  $\Delta Q_{i5}$  were plotted to obtain the slopes  $M_i$  (Equation (8)). Figure 8.4 shows a plot for the Railroad Valley playa and Table 8.5 lists the slope results for the RVPN and NIOB sub-scene pairs analyzed separately and in combination (Figure 8.7). Because the quantized levels

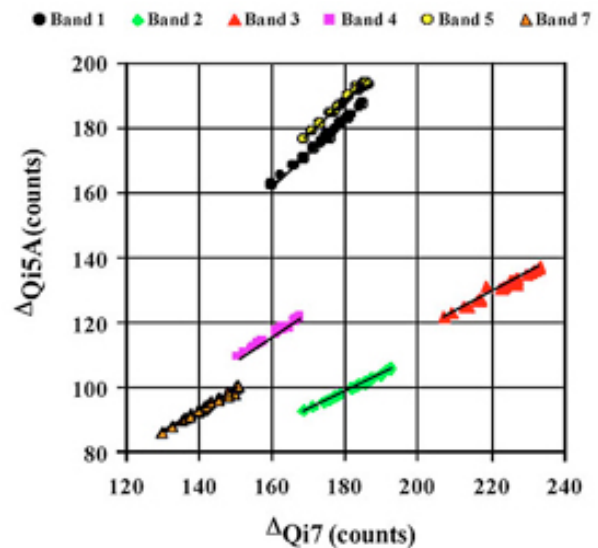


**Figure 8.6** - Plot of grid cell  $\Delta Q_{i5A}$  and  $\Delta Q_{i7}$  means combined for the Railroad Valley sub-scene. The lines are linear fits with zero-intercepts.

are bias-subtracted, the linear fits were forced to have zero intercepts. Nevertheless, with the exception of band 4 for the Niobrara case, the unaccounted for variances in percent,  $100(1-R^2)$ , with the linear fits are low (Table 8.5), where R is the correlation coefficient. No explanation has been found for the greater scatter in spectral band 4. Table 8.5 also indicates that the  $M_i$  slopes obtained for the two different image pairs generally differ by a few percent only, which provides some degree of confidence in the cross-calibration methodology.

<b>Table 8.5 Slopes (<math>M_i</math>) and Sensor Responsivities (<math>G_{i5}</math> and <math>G_{i7}</math>)</b>				
<b>Spectral Band</b>	<b><math>M_i</math> (zero-intercept)</b>	<b><math>100(1-R^2)</math> (zero-intercept)</b>	<b><math>G_{i7}</math> (CPUR)</b>	<b><math>G_{i5}</math> (CPUR)</b>
<b>Railroad Valley Playa Sub-Scene Data</b>				
1	1.014	0.40	1.225	1.243
2	0.5509	0.45	1.191	0.6561
3	0.5884	2.5	1.538	0.9050
4	0.7235	1.2	1.496	1.082
5	1.047	1.3	7.589	7.944
7	0.6662	1.2	21.80	14.52
<b>Niobrara, Nebraska Sub-Scene Data</b>				
1	1.030	1.7	1.225	1.261
2	0.5659	0.77	1.191	0.6740
3	0.5812	0.49	1.538	0.8939
4	0.7226	36	1.496	1.081
5	1.040	0.22	7.589	7.891
7	0.6424	0.061	21.80	14.00
<b>Combined Tandem Pair Sub-Scene Data</b>				
1	1.017	0.026	1.225	1.246
2	0.5525	0.039	1.191	0.6580
3	0.5879	0.017	1.538	0.9042
4	0.7233	0.60	1.496	1.082
5	1.045	0.052	7.589	7.931
7	0.6608	0.26	21.80	14.41

### 8.4.5 Spectral Band Differences

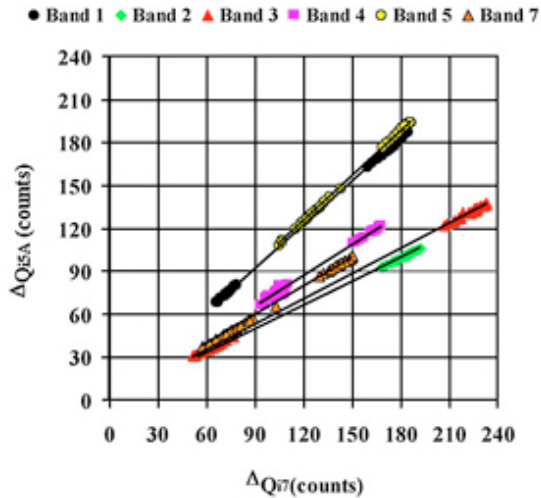


**Figure 8.7** - Plot of grid cell  $\Delta Q_{15A}$  and  $\Delta Q_{17}$  means combined for the two sub-scenes. The lines are linear fits with zero-intercepts.

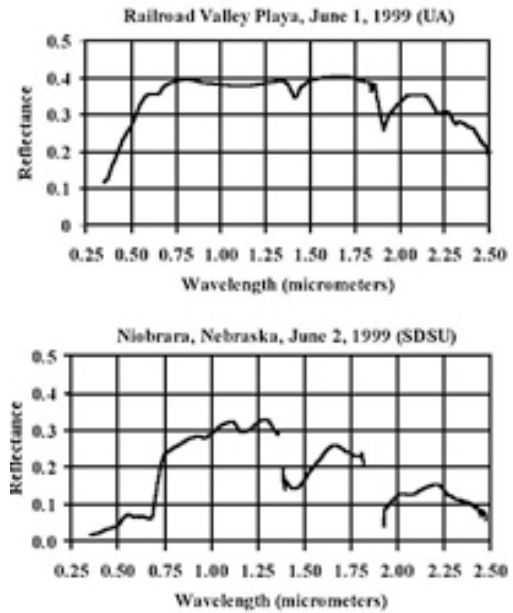


**Figure 8.8** - Surface Reflectance Spectra.

There are significant [differences](#) in relative spectral response profiles between corresponding Landsat-7 ETM+ and Landsat-4/5 TM spectral bands. The effects these spectral band differences have on measured TOA reflectances depend on spectral variations in the exo-atmospheric solar illumination, the atmospheric transmittance, and the surface reflectance. Because surface spectral reflectance (Figure 8.6) and atmospheric aerosol optical depth data are available for the RVPN and NIOB test sites on June 1 and 2, 1999, respectively, B<sub>i</sub> factors were generated for the image data pairs under consideration in this study (Table 8.6). For each test site, these data were used as inputs to a radiative transfer code to compute the TOA reflectance in corresponding solar reflective ETM+ and TM band. Standard values were assumed for other atmospheric input parameters (mid-latitude summer profile and continental aerosol model), but solar illumination angles pertinent to each Landsat image acquisition under consideration were used. The results in Table 8.6 show that the spectral band difference effect is on the order of two percent, except in the two short-wave infrared bands where it is larger, ranging from 3 to 7 percent depending on the band and the test site. The direction of the effect is also opposite between the two sites in bands 1 and 2, which is attributable to the significantly different reflectance spectra of the playa and grassland surfaces. Deriving spectral adjustment factors for other tandem data pairs would be less straightforward because of the lack of ground reference data.

<b>Table 8.6 Spectral Band Quantities used for Cross-calibration.</b>						
<b>Spectral Band</b>	<b>1</b>	<b>2</b>	<b>3</b>	<b>4</b>	<b>5</b>	<b>7</b>
<b>TM <math>E_o(W / (m^2\mu m))</math></b>	1954	1826	1558	1047	217.2	80.29
<b>ETM+ <math>E_o(W / (m^2\mu m))</math></b>	1968	1839	1555	1054	228.4	81.59
<b><math>A_i</math> for RVPN</b>	1.013	1.013	1.017	1.035	1.106	0.994
<b><math>B_i</math> for RVPN</b>	0.981	0.981	0.994	1.003	1.026	0.964
<b><math>A_i</math> for NIOB</b>	1.051	1.053	0.997	1.044	1.118	0.969
<b><math>B_i</math> for NIOB</b>	1.020	1.022	0.977	1.014	1.039	0.932
<p><math>E_o</math> is the exo-atmospheric solar irradiance, <math>A_i</math> is the illumination adjustment factor, and <math>B_i</math> is the spectral adjustment factor.</p> <p>RVPN = Railroad Valley Playa, Nevada. NIOB = Niobrara, Nebraska.</p>						

#### 8.4.6 Cross Calibration Results

The  $M_i$  slopes derived from the two image pairs (RVPN and NIOB) separately and combined were used in equation (11) to generate TM responsivity coefficients. Figure 8.7 compares results from the two image pairs with Railroad Valley playa arbitrarily chosen as the reference case. The consistency between results from the two image pairs varies from negligible differences in spectral band 4 to almost four percent difference in band 7. The average difference is 1.6 percent, which, although based on only 12 spectral band cases, is a measure of the repeatability of the cross-calibration approach.

Figure 8.7 also shows differences in TM responsivities if spectral band difference adjustments are excluded ( $B_i = 1$ ). Overall, adjustments for spectral band difference appear to be on the order of two percent or less in the visible and near infrared bands, but greater than that in the short-wave infrared bands. As noted in an earlier part of the paper, the implication is that cross-calibration comparisons that do not benefit from the surface reflectance spectra and atmospheric optical parameters needed to compute the spectral band difference effect will potentially have an inherent additional uncertainty of several percent. A starting point for estimating the uncertainty of the tandem-based cross-calibration method is the  $\pm 3$  percent uncertainty of the ETM+ radiometric calibration (Barker et al., 1999). Additional sources of uncertainty include residual geometric misregistration, small changes in atmospheric conditions between tandem image pair acquisitions, artifacts in the TM image radiometry, and residual uncertainty from spectral band difference adjustments. The jitter analysis indicated a misregistration effect on the order of 0.24 percent and, although no corroborative analyses have been carried out, experience suggests that the other uncertainties are also well within one percent. If these additional sources of uncertainty amount to a 1-2 percent effect, the overall root-sum-squared uncertainty for the cross-calibration method is approximately  $\pm 3.5$  percent. The near-simultaneity of image acquisition and the similarity of

imaging geometry afforded by the tandem configuration are definite advantages in this context. If the spectral signature of the common test site surface is unknown and the spectral band difference effect is 5 percent, say, then the overall uncertainty approaches  $\pm 6$  percent.

An evaluation of the tandem cross-calibration would be incomplete without a comparison against results obtained from the two TM vicarious calibrations and to pre-launch responsivity coefficients for Landsat 5.

<b>Spectral Band</b>	<b>1999 RVPN ETM+ Cross Calibration Gi5 (CPUR)</b>	<b>1999 UAZ Vicarious Calibration Gi5 (CPUR)</b>	<b>Difference Relative to Cross-Cal Gi5 (CPUR)</b>	<b>1999 NIOB ETM+ Cross Calibration Gi5 (CPUR)</b>	<b>1999 SDSU Vicarious Calibration Gi5 (CPUR)</b>	<b>Difference Relative to Cross-Cal Gi5 (CPUR)</b>	<b>1999 RVPN ETM+ Cross Calibration Gi5 (CPUR)</b>	<b>Prelaunch Calibration Gi5 (CPUR)</b>	<b>Difference Relative to Prelaunch Gi5 (CPUR)</b>
<b>1</b>	1.243	1.211	-2.6%	1.261	1.221	-3.2%	1.243	1.555	-20%
<b>2</b>	0.6561	0.6270	-4.4%	0.6740	0.6620	-1.8%	0.6561	0.786	-17%
<b>3</b>	0.9050	0.8953	-1.1%	0.8939	0.9040	1.1%	0.9050	1.020	-11%
<b>4</b>	1.082	1.111	2.7%	1.081	0.980	-9.3%	1.082	1.082	0.00%
<b>5</b>	7.944	8.097	1.9%	7.891	7.681	-2.7%	7.944	7.875	0.88%
<b>7</b>	14.52	13.17	-9.3%	14.00	16.91	21%	14.52	14.77	-1.7%

The TM vicarious calibration result for the RVPN test site on June 1, 1999 has kindly been provided by UAZ in advance of publication. These results are presented in Table 8.7 together with the RVPN ETM+/TM cross-calibration results. The average difference between the cross-calibration and vicarious calibration results is 1.8 percent for bands 1-4 and 3.7 percent overall, the minimum and maximum differences being 1.1 and 9.3 percent in spectral bands 3 and 7, respectively. Error bars are not shown in Figure 12, but uncertainties in the vicarious calibration results are reported to be  $\pm 5$  percent in the visible and near-infrared bands and approximately 50 percent greater in the short-wave infrared bands (Thome et al., 1997). The results in the figure are consistent with the possibility that there were no major changes in the Landsat-5 TM responsivity in any of the spectral bands between 1994 and 1999. For spectral bands 5 and 7, it should be noted that there is an additional 5 percent peak-to-peak variation in the general responsivity trend, likely due to the periodic build up of ice on the window in front of the cold focal plane (Markham et al., 1998).

South Dakota State University (SDSU) has kindly provided in advance of publication vicarious calibration results for Landsat-5 TM obtained at the NIOB test site on June 2, 1999, when the tandem data were acquired (Black et al., 2000). Table 8.7 presents a comparison of the TM responsivity results from the cross-calibration work and the SDSU vicarious calibration. Agreement to within 3.2 percent is found in spectral bands 1-3 and 5. SDSU also carried out a vicarious calibration for the Landsat-7 ETM+ at Niobrara on the same day and the ETM+ band 4 results is approximately 10 percent lower than the nominal ETM+ responsivity provided by the Landsat Project Science Office. This is a possible explanation for the difference between the tandem cross-calibration and SDSU results for TM band 4 (-9.3 percent). Similarly, the SDSU result for ETM+ band 7 responsivity is approximately 6 percent higher than the nominal ETM+ value, which could explain part of the 21-percent difference found between the TM band 7 results. On-orbit calibration updates for spectral bands 5 and 7 have always been characterized by greater uncertainties and so the results in Table 8.4.5 for these bands, although unsatisfactory, are not unexpected.

Table 8.7 also compares the 1999 TM calibration update to prelaunch responsivity coefficients for the six solar reflective spectral bands. Differences ranging from -11 to -20 percent exist for spectral bands 1, 2, and 3, whereas the differences are only a few percent or less in spectral bands 4, 5, and 7. Clearly, the use of prelaunch calibration coefficients for the visible bands would lead to significant errors in TOA radiances and any quantities derived from TOA radiances, including surface reflectances retrieved from the TM imagery via atmospheric correction for example.

### **8.4.7 Summary**

The work described here indicates that the tandem cross-calibration approach provides a valuable "contemporary" calibration update for Landsat-5 TM solar reflective bands based on the excellent radiometric performance of Landsat-7 ETM+. Initial trials of the approach with two different tandem image pairs yielded repeatable results for TM responsivity coefficients. Users, however, should use the  $M_i$  slopes derived from the RVPN tandem pair for updating the radiometry for Landsat 5 level 0 data. This work is ongoing and any improved cross-calibration updates will be made in the Handbook as necessary.

### **REFERENCES**

Barker, J.L., Dolan, S.K., Sabelhaus, P.A., Williams, D.L., Irons, J.R., Markham, B.L., Bolek, J.T., Scott, S.S., Thompson, R.J., Rapp, J.J., Arvidson, T.J., Kane, J.F., and Storey, J.C. 2000. "Landsat-7 Mission and Early Results", Proceedings of SPIE Conference 3870, Europto SPIE Conference on Sensors, Systems, and Next-Generation Satellites V, Florence, Italy, pp.

299-311.

Teillet, P.M., Barker, J.L., Markham, B.L., Irish, R.R., Fedosejevs, G., J.C. Storey, J.C., "Radiometric Cross-Calibration of the Landsat-7 ETM+ and Landsat-5 TM Sensors Based on Tandem Data Sets", *Remote Sensing of Environment*, in press.

Thome, K., Markham, B., Barker, J., Slater, P., and Biggar, S. 1997. "Radiometric Calibration of Landsat", *Photogrammetric Engineering and Remote Sensing*, 63(7):853-858.

## 8.5 Geometric Calibration Overview

This chapter describes the geometric characterization and calibration activities that will be performed over the life of the Landsat 7 mission using the software tools developed as part of the [Landsat 7 Image Assessment System](#). The IAS provides the capability to routinely perform four types of geometric characterization to verify and monitor system geometric performance, and three types of geometric calibration to estimate improved values for key system geometric parameters.

The geometric characterizations include:

1. geodetic accuracy assessment to measure the absolute accuracy of Level 1Gs (systematic) corrected products;
2. geometric accuracy assessment to qualitatively and quantitatively evaluate residual internal geometric distortions within Level 1Gs images;
3. band to band registration assessment to measure and monitor the relative alignment of the eight ETM+ spectral bands; and
4. image-to-image registration assessment to measure and monitor multi-temporal image registration accuracy.

The geometric calibration capabilities provided by the IAS include:

1. sensor alignment calibration to provide improved knowledge of the geometric relationship between the ETM+ optical axis and the Landsat 7 attitude control reference system;
2. scan mirror calibration to measure and correct any systematic deviations in the ETM+ scan mirror along and across scan profiles; and
3. focal plane calibration to measure and provide improved estimates of the eight band center locations on the two ETM+ focal planes relative to the ETM+ optical axis. Techniques for measuring and estimating improved values for individual detector locations and delays are being researched and may be added to the IAS as a post-launch capability.

The most critical geometric calibration activities involve measuring and verifying the Landsat 7 ETM+ system performance during the Initial On-orbit Checkout (IOC) period using the geodetic, geometric, band-to-band, and image-to-image characterization capabilities, and to perform the initial sensor alignment calibration. Refining the pre-launch sensor alignment knowledge is critical to ensure that the Level 1Gs product geodetic accuracy specification can be met. Sufficient supporting data sets (e.g., ground control, terrain data) to perform these characterization and calibration activities must be available at launch. The second priority during the IOC period will be to verify and, if necessary, update the pre-launch focal plane (particularly band placement) and scan mirror profile calibrations. The results of these initial calibration activities will be used to verify that the system is performing within specifications and to create an initial post-launch release of the Calibration Parameter File, which can be used by the IAS or the Landsat 7 Level-1 Product Generation System (LPGS) to create Level 1G products, which meet the Landsat 7 geodetic accuracy requirements.

After the IOC period, ongoing calibration activities will monitor the stability of the Landsat 7 ETM+ system's geometric performance and attempt to identify and characterize any systematic variations in the system's geometric parameters. This will include processing additional calibration scenes under a variety of acquisition conditions (e.g., orbital position, ETM+ time on) to measure the system's geometric performance as a function of time, temperature, and location.



## 8.6 Sensor Alignment Calibration

The goal of the sensor alignment calibration is to improve the in-flight knowledge of the relationship between the ETM+ instrument and the Landsat 7 navigation base reference. The IAS is required to estimate this alignment to an accuracy of 24 arc seconds (per axis) at least once per calendar quarter. This calibration will use discrete ground control points in a set of pre-defined calibration reference scenes.

The primary challenge in alignment calibration is the need to estimate the underlying alignment trend (assumed initially to be a bias) from a series of precision correction solutions, which measure a combination of orbit, attitude, and alignment errors. Landsat 7 will have more accurate (estimated to be in the 10-50 meter range versus 133 meter accuracy for the ephemeris downlinked in the Payload Correction Data) post-pass definitive ephemeris data available for the alignment calibration test scenes, reducing the uncertainty due to orbital errors. The GSFC Flight Dynamics Facility (FDF) upon request provides this precise ephemeris from the IAS. Multiple precision correction solutions will be integrated using a Kalman filter algorithm to estimate the best-fit systematic alignment bias. As the Kalman processes additional precision correction solutions filter, the filter's estimates of the alignment biases will improve.

Periodically, an IAS analyst will decide that the alignment knowledge has changed enough to warrant generating an updated sensor alignment matrix for inclusion in the Calibration Parameter File. Initially, this decision is based on the alignment bias covariance estimates generated by the Kalman filter. A new set of CPF parameters are generated as soon as the bias estimate standard deviation move below the 24-arc second alignment accuracy requirement threshold. During normal operations, a new alignment matrix is generated whenever a new version of the CPF was scheduled for release.

### **Definitive Ephemeris**

If available, the Landsat 7 definitive ephemeris is used for geometrically correcting ETM+ data. Definitive ephemeris substantially improves the positional accuracy of the Level 1G product over predicted ephemeris.

An ephemeris is a set of data that provides the assigned places of a celestial body (including a manmade satellite) for regular intervals. In the context of Landsat 7, ephemeris data shows the position and velocity of the spacecraft at the time imagery is collected. The position and velocity information are used during product generation.

The Landsat 7 Mission Operations Center receives tracking data on a daily basis that shows the position and velocity of the Landsat 7 spacecraft. This information comes from the three US operated ground-receiving stations and is augmented by similar data from NASA's Tracking and Data Relay Satellites. The Flight Operations Team processes this information to produce a refined or "definitive" ephemeris that shows the position and velocity of Landsat 7 in one-minute intervals. Tracking data are used to compute the actual spacecraft position and velocity for the last 61 hours and to predict these values for the next 72 hours. The predicted ephemeris data are uploaded to the spacecraft daily. On-board software interpolates from this data to generate the positional information contained in the Payload Correction Data (PCD).

Engineers with the Landsat Program have completed a predicted versus definitive ephemeris analysis. Comparisons to ground control points demonstrate the definitive ephemeris is, in fact, reliably more accurate than the predicted ephemeris. Geometric accuracy on the order of 30-50 (1 sigma) meters, excluding terrain effects, can be achieved when the definitive ephemeris is used to process the data. Level 1G products produced after March 29, 2000 use definitive ephemeris if available. The .MTL field "ephemeris\_type" in the product metadata files identifies whether a product was created with definitive or predicted ephemeris. Daily definitive ephemeris profiles have been archived since June 29, 1999 and are available for [downloading](#).

## 8.7 Scan Mirror Calibration

The behavior of the ETM+ scan mirror is measured and, if necessary, calibrated using the IAS scan mirror calibration capability. This process compares a terrain corrected image to a high accuracy reference image constructed from a higher resolution source, to detect systematic deviations of the scan mirror motion from its nominal profile. The support data used to construct the terrain corrected image is used to generate test points which can be related to a particular time within a particular forward or reverse scan. By comparing these test points to the reference image and analyzing the measured deviations as a function of scan direction and scan time, it will be possible to estimate corrections to the pre-launch scan mirror profiles, if needed. Any significant deviations detected will be folded back into the Calibration Parameter File as updates to the mirror profile polynomial coefficients.

Scan mirror calibration applies to both the along and across scan directions so it will detect and compensate for [Scan Line Corrector \(SLC\)](#) deviations as well. In practice, SLC deviations will be indistinguishable from scan mirror deviations so we have chosen to model the deviations as part of the scan mirror motion. Detecting systematic deviations which can be attributed to mirror motion requires reference points which can be uniquely associated with individual forward and reverse ETM+ scans and which provide a good distribution of observations as a function of scan angle. The current approach to acquiring such a control reference is to use spatially accurate reference imagery for one or more calibration areas. The scan mirror calibration procedure will compare a precision and terrain corrected ETM+

panchromatic band image with the reference image constructed from USGS Digital Orthophoto Quadrangle (DOQ) data to detect within-scan mirror deviations. This involves constructing an array of points in the ETM+ scan geometry, which are mapped to the output terrain corrected product. These points, with known scan number and time in scan coordinates will be correlated with the reference image to measure the (sub-pixel) residual distortion. The distortion patterns from many scans will be analyzed to detect systematic deviations from the pre-launch forward and reverse scan mirror profiles.

## 8.8 Focal Plane Calibration

The focal plane calibration operations involve measuring the alignment of the eight ETM+ bands to ensure that band registration accuracy meets the 0.28 pixel requirement as stated in the system specification. If the band-to-band comparisons detect any uncompensated misalignment the band placement calibration procedure will be used to update the band center location parameters in the Calibration Parameter File accordingly. Detector to detector alignment will also be monitored to ensure that image discontinuities are not introduced by using incorrect detector locations and delays in the Level 1G image resampling process.

Landsat 7 ETM+ images of focal plane calibration test sites will be used to measure and calibrate the internal alignment of the detectors on the two ETM+ focal planes. These test sites are selected based on image content rather than the availability of supporting data. Band to band registration assessment requires scenes which contain significant high spatial frequency content that is common to all eight ETM+ bands. Although it is anticipated that scenes with long linear features would be used to assess the alignment of individual detectors, detector placement calibration techniques are still under investigation and at this time are not a part of the focal plan calibration procedure.

## 9.1 File Description

The IAS is responsible for the sustained radiometric and geometric calibration of the Landsat 7 satellite and ETM+ and passing this knowledge to the user community. This is achieved by assessing new imagery on a daily basis, performing both radiometric and geometric calibration when needed, and developing new processing parameters for creating level 1 products. Processing parameters are stored in the Calibration Parameter File (CPF), which is stamped with applicability dates and sent to the LP-DAAC for storage and eventual bundling with outbound Level 0R products. The CPF is also sent to international ground stations via the Landsat 7 Mission Operations Center.

### 9.1.1 Calibration Parameter File Updates

IAS updates and distributes the calibration parameter file at least every 90 days. Updates will likely be more frequent during early orbit checkout and will also occur between the regular 90-day cycles whenever necessary. Irregular updates, however, will not affect the regular 90-day schedule. The timed release of a new calibration parameter file must be maintained because of the UT1 time corrections and pole wander predictions included in the file. These parameters span a 180-day interval time centered on the effective start date of the new IAS CPF. The IAS maintains a CPF archive. At this [web site](#), you can download and view all CPFs since launch.

#### Time Stamps

The calibration parameter file is time stamped by IAS with an effective date range. The first two parameters in the file, Effective\_Date\_Begin and Effective\_Date\_End, designate the range and are of the form YYYY-MM-DD. The Effective\_End\_Date for the most recent parameter file is its Effective\_Date\_Begin plus 90 days. After this date the file is without applicable UT1 time predictions. The parameter file that accompanies an order has an effective date range that includes the acquisition date of the image ordered.

#### File Naming Conventions

Through the course of the mission, a serial collection of CPFs is generated and sent to the LP-DAAC for coupling to OR products. A distinct probability exists that a CPF will be replaced due to improved calibration parameters for a given period or perhaps due to file error. The need for unique file sequence numbers becomes necessary as file contents change. IAS to name the CPF uses the following file naming procedure:

<b>L7CPFyyyymmdd_yyyymmdd.nn</b>	
where:	L7 = Constant for Landsat 7 CPF = 3-letter CPF designator yyyy = 4-digit effectivity starting year mm = 2-digit effectivity starting month dd = 2-digit effectivity starting day _ = Effectivity starting/ending date separator yyyy = 4-digit effectivity ending year mm = 2-digit effectivity ending month dd = 2-digit effectivity ending day nn = Sequence number for this file

As an example, suppose four calibration files were created by the IAS on 90-day intervals and sent to the LP-DAAC during the first year of the mission. Further suppose that the first file was updated twice and the second and third files were updated once. The assigned file names would be as follows:

<b>File 1</b>	L7CPF19980601_199808210.00 L7CPF19980601_199808210.01 L7CPF19980601_199808210.02
<b>File 2</b>	L7CPF19980830_19981127.01 L7CPF19980830_19981127.02
<b>File 3</b>	L7CPF19981128_19990225.01 L7CPF19981128_19990225.02
<b>File 4</b>	L7CPF19990226_19990526.01

It is worth noting the **00** sequence number assigned to the original CPF. This reserve sequence number uniquely identifies the pre-launch CPF. Sequence numbers for subsequent time periods all begin with 01. New versions or updates are incremented by one.

This example assumes the effectivity dates do not change. The effectivity date range for a file can change, however, if a specific problem (e.g. detector outage) is discovered somewhere within the nominal 90-day effectivity range. Assuming this scenario, two CPFs with new names and effectivity date ranges are spawned for the time period under consideration. The `effective_date_end` for a new pre-problem CPF would change to the day before the problem occurred. The `effective_date_begin` remains unchanged. A post-problem CPF with a new file name would be created with an `_effective_date_begin` corresponding to the imaging date the problem occurred. The `effective_date_end` assigned would be the original `effective_date_end` for the time period under consideration. New versions of all other CPFs affected by the erroneous parameter also would be created.

Using this example, suppose a dead detector is discovered to have occurred on January 31, 1999. Two new CPFs are created that supersede the time period represented by file number three, version 2, and a new version of file number four is created. The new file names and sequence numbers become:

<b>File 3</b>	L7CPF19981128_19990225.01 L7CPF19981128_19990225.02 L7CPF19981128_19990131.03 L7CPF19990201_19990225.03
<b>File 4</b>	L7CPF19990226_19990526.01 L7CPF19990226_19990526.02

## 9.1.2 File Structure

All calibration parameters are stored as American Standard Code for Information Interchange (ASCII) text using the ODL syntax developed by JPL. ODL is a tagged keyword language developed to provide a human-readable data structure to encode data for simplified interchange. The body of the file is composed of two statement types:

1. Attribute assignment statement used to assign values to parameters.
2. Group statements used to aid in file organization and enhance parsing granularity of parameter sets.

To illustrate consider the first three parameters in the file: `Effective_Date_Begin`, `Effective_Date_End`, and the `CPF_File_Name`. These three parameters form their own group, which is called `FILE_ATTRIBUTES`. The syntax employed for this collection of parameters in the CPF appears as:

```
GROUP = FILE_ATTRIBUTES  
    Effective_Date_Begin = 1999-02-26  
    Effective_Date_End = 1999-05-26  
    CPF_File_Name = L7CPF19990226_19990526.01  
END_GROUP = FILE_ATTRIBUTES
```

## 9.2 File Content

The CPF supplies the radiometric and geometric correction parameters required during Level 1 processing to create superior products of uniform consistency across the Landsat 7 system. They fall into one of three major categories: geometric parameters, radiometric parameters, or artifact removal parameters.

### 9.2.1 Geometry Parameters

The geometric parameters are classified into 11 first tier groups. A brief description of each group and their use various Landsat 7 systems follows. The heading for each group is the actual ODL group name used in the CPF.

- **Earth Constants**
- **Orbit Parameters**

- **Scanner Parameters**
- **Spacecraft Parameters**
- **Mirror Parameters**
- **Scan Line Corrector**
- **Focal Plane Parameters**
- **Attitude Parameters**
- **Time Parameters**
- **Transfer Function**
- **UT1 Time Parameters**

## **9.2.2 Radiometric Calibration Parameters**

The radiometric parameters are classified into 15 first tier groups. A brief description of each group and their use in various Landsat 7 systems or by user follows. The heading for each group is the actual ODL group name used in the CPF.

- **Detector Status**  
The Detector Status parameters provide a five-element code that describes the current health status of each ETM+ detector. The five codes indicate detector status (live or dead), low gain signal noise, high gain signal noise, low gain dynamic range quality, and high gain dynamic range quality.
- **Detector Gains**  
Analysis of the SIS calibration transfer to the IC and output from the CRAM model used by IAS results in the Detector Gain parameter set. For each detector there is a prelaunch gain, post launch gain, and a current gain for each of the two gain settings. The prelaunch and post launch gains are based on the

SIS calibration and remain static while the current gain is updated as a function of CRAM model improvement and detector responsivity over time. The Detector Gain parameters are used to radiometrically correct ETM+ image data prior to LPS automatic cloud cover assessment (ACCA) algorithm and optionally by LPGS for as an alternative to computing gains on the fly from the IC data.

- **Bias Locations**

The bias location parameters refer to the IC data. They specify the starting pixel location for the bias (dark current restore), the length in pixels of the bias region, and the length of useable IC data including the pulse. A set of parameters exists for each of the three band groups - reflective, panchromatic, and thermal. They are used during radiometric correction for rapid retrieval of calibration pulse and shutter data.

- **Detector Biases B6**

During level 1 processing band 6 biases are generally computed from the IC for the image being processed. This is a complex task and may be subject to anomalies. This parameter group is computed both prelaunch and at regular intervals over the life of the mission. These are baseline band 6 biases and are used during level 1 processing if the image specific IC-derived biases prove unreliable.

- **Scaling Parameters**

The Scaling Parameter set consists of the lower and upper limit of the post-calibration dynamic range for each band in each gain state. These are the LMIN and LMAX values and are expressed in units of absolute spectral radiance. These values are used by LPGS to convert 1G products to scaled 8-bit values and by users for the reverse transformation. There is an LMIN/LMAX pair per band for each of the gain modes.

- **MTF Compensation**

All image systems, including Landsat 7, cause a blurring of the scene radiance field during image acquisition. Accurate characterization of this blurring is referred to as the modulation transfer function (MTF). Restoration processing compensates and corrects for systemic degradations to yield greater radiometric accuracy. The MTF compensation parameters are weighting functions for each band. Five weighting parameters for both pixel and line directions were selected to best fit the optimal MTF response. These are applied to the components of the piecewise cubic convolution kernel to generate the optimal MTF reconstruction kernel.



- Sensitivity Temperatures**

The temperature of the detectors on the primary focal plane of the ETM+ is not controlled and tends to warm up as the instrument operates. The cold focal plane is controlled but may operate at different set points. Most detectors show some dependence of responsivity with temperature. The sensitivity temperature parameters describe the relationship between gain change and operating temperature for each detector and are used to adjust the gains derived from multi-calibration sources. Gains derived solely from IC data are not temperature adjusted.
- Reference Temperatures**

The sensitivity temperature coefficients just described are used to adjust gains for varying focal plane temperatures. The reference temperatures are used to normalize the gains to a stable temperature. A single reference temperature is calculated prelaunch and post launch for each band at both gain states.
- Lamp Radiance**

The lamp radiance parameters contain the actual radiance of the two IC lamps in three possible configurations (i.e. lamp 1 on - lamp 2 off, lamp 1 off - lamp 2 on, lamp 1 on - lamp 2 on). For each reflective band there are pre-launch, post-launch, and current values for the low and high gain settings. Pre-launch values are established by transferring the SIS calibration to the IC lamps via the ETM+. Post launch are determined using PASC and FASC calibration data. The lamp radiance parameters used to compute the gains used for converting raw ETM+ data to units of absolute radiance.
- Reflective IC Coefficients**

Radiance levels produced by the internal calibrator, or seen by the detectors vary as a function of instrument state. Several parameters affecting instrument state are tracked and used for correcting this effect. These parameters are instrument on time, position in orbit, and temperatures of the internal calibrator components and focal plane arrays. The reflective IC coefficients are used in the model that corrects for these effects. For each detector there are 18 coefficients for both the low and high gain states.
- Lamp Reference**

As explained above, the radiance levels produced by the internal calibrator, or seen by the detectors vary as function of instrument state. The model that compensates for these effects requires as input 14 temperatures of the internal calibrator components and focal plane arrays. In general, these temperatures are extracted from the PCD for the image being processed. However, the IAS also performs a pre-launch calibration of the ETM+ and a post calibration using the combined radiometric model. The lamp reference parameters represent the instrument state at the time of calibration.

- **B6 View Coefficients**  
The band 6 view coefficients are used in computing the actual shutter (i.e. bias) values when processing the emissive IC data. The offset algorithm takes into account radiance of the shutter flag as well as contributions from other instrument components such as the scan mirror and scan line corrector. Each band 6 detector has a different view of the contributing components. The band 6 view coefficients capture this view and are used to adjust the contributing spectral radiances accordingly.
- **B6 Temp Model Coefficients**  
The Band 6 temperature coefficients are used to calculate the temperature of the scan mirror. The emissive IC algorithm requires scan mirror temperature for computing band 6 gains and offsets. The scan mirror's contribution to the band 6 response must be calculated and accounted for.
- **Lamp Current Coefficients**  
Included in the PCD are the currents for the two IC lamps. The currents are in a raw data format and require conversion to engineering units (i.e. milli-amps) prior to their use. The lamp coefficient parameters are used to linearly transform the raw counts to milli-amps. There are two coefficients for each lamp.
- **Thermistor Coefficients**  
Included in the PCD are a variety of ETM+ component temperatures. The temperatures are in a raw data format and require conversion to valid numbers prior to their use. The thermistor coefficients parameters are used for this purpose. Six conversion coefficients are supplied for each of the 28 different temperatures that accompany the PCD.

### 9.2.3 Artifact Parameters

The artifact parameters are classified into 9 first tier groups. A brief description of each group and their use in various Landsat 7 systems follows. The heading for each group is the actual ODL group name used in the CPF.

- **Memory Effect**  
Memory effect is a noise pattern commonly known as banding. It's observed as alternating lighter and darker horizontal scan-wide stripes. The memory effect parameters were derived by the IAS and are static. They consist of a magnitude and time constant for each detector. These are used in an inverse filtering operation to remove the memory effect artifact.

- Ghost Pulse**

The ghost pulse is a faint secondary image of the internal calibrator lamp pulse. It appears in bands 5 and 7. The ghost pulse parameters identify the beginning and ending minor frames that bound this ghost image.
- Scan Correlated Shift**

Scan correlated shift is a sudden change in bias that occurs in all detectors simultaneously. The scan correlated shift parameters are derived by the IAS and are static. They consist of a bias magnitude for each detector and are used to compensate for the shift when it occurs.
- Striping**

Striping is defined as residual detector-to-detector gain and offset variations within a band of radiometrically corrected (1R) data. The 1R process is intended to remove detector-to-detector variations through the generation of relative gains and bias from histograms. These are included in the absolute gains and biases eventually applied. Nonetheless, the possibility of residual striping remains. The striping parameters are correction methodology flags. Two processing options are possible: linearly adjust the 1R data to match the means and standard deviations of each detector to a reference detector or to an average of all the detectors. There is one striping parameter per band for each of the gain modes.
- Histogram**

Histogram analysis estimates the relative gains and biases for all detectors by characterizing the response behavior of individual detectors in a band relative to the other detectors in a band. Results are used to adjust the gains and biases applied during radiometric correction. The histogram parameters control the algorithm by specifying detector noise, a normalization reference detector for each band, saturation metrics, and histogramming window size.
- Impulse Noise**

Impulse noise within a digital signal manifests itself in a sample as a departure from the signal trend far in excess of that expected from random noise. The impulse noise parameters specify a median filter width and an impulse noise threshold for each detector. The IAS employs these parameters for identifying and trending impulse noise in otherwise homogeneous data such as night scenes and FASC imagery.
- Coherent Noise**

Coherent noise is a low-level periodic noise pattern that was found in all Landsat 5 imagery and characterized by the IAS for Landsat 7. The coherent noise parameters consist of the number of noise components and a set of waveform characteristics that describe each component for each band. The

waveform characteristics are the mean, sigma, minimum, and maximum for each component's frequency, phase, and magnitude.

- **Detector Saturation**

In addition to normally observed saturation (i.e. 0, 255) two other types of detector saturation can occur. An analog to digital converter may saturate below 255 counts at the high end, or above 0 at the low end. The detector saturation parameters identify these levels for each detector. The analog electronic chain may saturate at a radiance corresponding to a level below 255 counts and above 0 counts on the low end. The detector saturation parameters also identify these levels for each detector.

- **Fill Patterns**

LPS uses two values to fill minor frames to distinguish missing or bad band data from good data. The two fill values used are zeros for odd detectors and 255s for even detectors. The fill data is placed on a minor frame basis - if data is missing from part of a minor frame the whole minor frame is filled. The alternating 0/255 fill pattern was selected to unambiguously flag artificial fill from reflectance values that naturally could occur.

#### **9.2.4 ACCA Parameters**

Each scene processed by LPS undergoes automatic cloud cover assessment prior to being archived. The cloud cover scores become searchable metadata and are used to filter out undesirable scenes from an archive interrogation. The ACCA algorithm uses a variety of threshold and band indices for cloud identification. These may change during the mission and are therefore included in the CPF for LPS use.

- **ACCA Biases**

The LPS automatic cloud cover recognition (ACCA) algorithm requires radiometrically corrected image data. The ACCA Biases parameter set is used in conjunction with the Detector Gains described above for converting raw digital numbers to units of absolute radiance. There is one bias parameter per detector per band for each of the two gain modes. Although ACCA uses only bands 2 through 6, the other band biases are included for completeness. Biases are reported in units of digital counts.

- **ACCA Thresholds**

The LPS ACCA algorithm uses bands 2 through 6 in a combination of thresholds, ratios, and indices to separate clouds from land. Results are reported in metadata that eventually is used in client data searches. LPS and possibly IGSs list the ACCA Threshold parameters in the CPF for use.

- **Solar Spectral Irradiances**

The LPS ACCA algorithm converts radiometrically corrected data to units of planetary reflectance prior to cloud filtering. This involves normalizing image data for solar irradiance, which reduces between-scene variability. The parameter values listed in Table 9.1 are the mean solar spectral irradiances for bands 1 through 5, 7 and 8. There is one value for each band.

<b>Table 9.1 Solar Spectral Irradiances</b> (watts/m <sup>2</sup> /nm)	
band 1	1969.000
band 2	1840.000
band 3	1551.000
band 4	1044.000
band 5	225.700
band 7	82.07
band 8	1368.000

- **Thermal Constants** ACCA converts Band 6 from spectral radiance to a more physically useful variable, namely the effective at-satellite temperatures of the viewed Earth-atmosphere system. The transformation equation requires two calibration constants, which are listed in table 9.2.

<b>Table 9.2 ETM+ Thermal Constants</b>		
<b>Constant</b>	<b>Value</b>	<b>Units</b>
K1	666.09	watts/(meter squared * ster * m <sup>2</sup> )
K2	1282.71	temperature degrees (Kelvin)

## 10.1 Overview

The geometric algorithms used by Level 1 processing system at EDC were originally developed for the Landsat 7 Image Assessment System. The overall purpose of the IAS geometric algorithms is to use Earth ellipsoid and terrain surface information in conjunction with spacecraft ephemeris and attitude data, and knowledge of the Enhanced Thematic Mapper Plus instrument and Landsat 7 satellite geometry to relate locations in ETM+ image space (band, scan, detector, sample) to geodetic object space (latitude, longitude, and height). These algorithms are used for purposes of creating accurate Level 1 output products, characterizing the ETM+ absolute and relative geometric accuracy, and deriving improved estimates of geometric calibration parameters such as the sensor to spacecraft alignment.

## 10.2 Level 1 Algorithms

The Level 1 processing algorithms include:

1. Payload Correction Data (PCD) processing
2. Mirror Scan Correction Data (MSCD) processing
3. ETM+/Landsat 7 sensor/platform geometric model creation
4. sensor line of sight generation and projection
5. output space/input space correction grid generation
6. image resampling
7. geometric model precision correction using ground control
8. terrain correction.

The diagrams that follow describe the high-level processing flows for the IAS Level 1 processing algorithms. [Figure 10.1](#) describes the process involved in initialization and creation of the Landsat 7 geometry model. [Figure 10.2](#) shows the process of creating a geometric correction grid and the application of that grid in the resampling process. [Figure 10.3](#) describes the process of refining the Landsat 7 geometry model with ground control, resulting in a precision geometry model. [Figure 10.4](#) again describes the creation of a geometric correction grid (this time precision), and resampling with terrain correction.

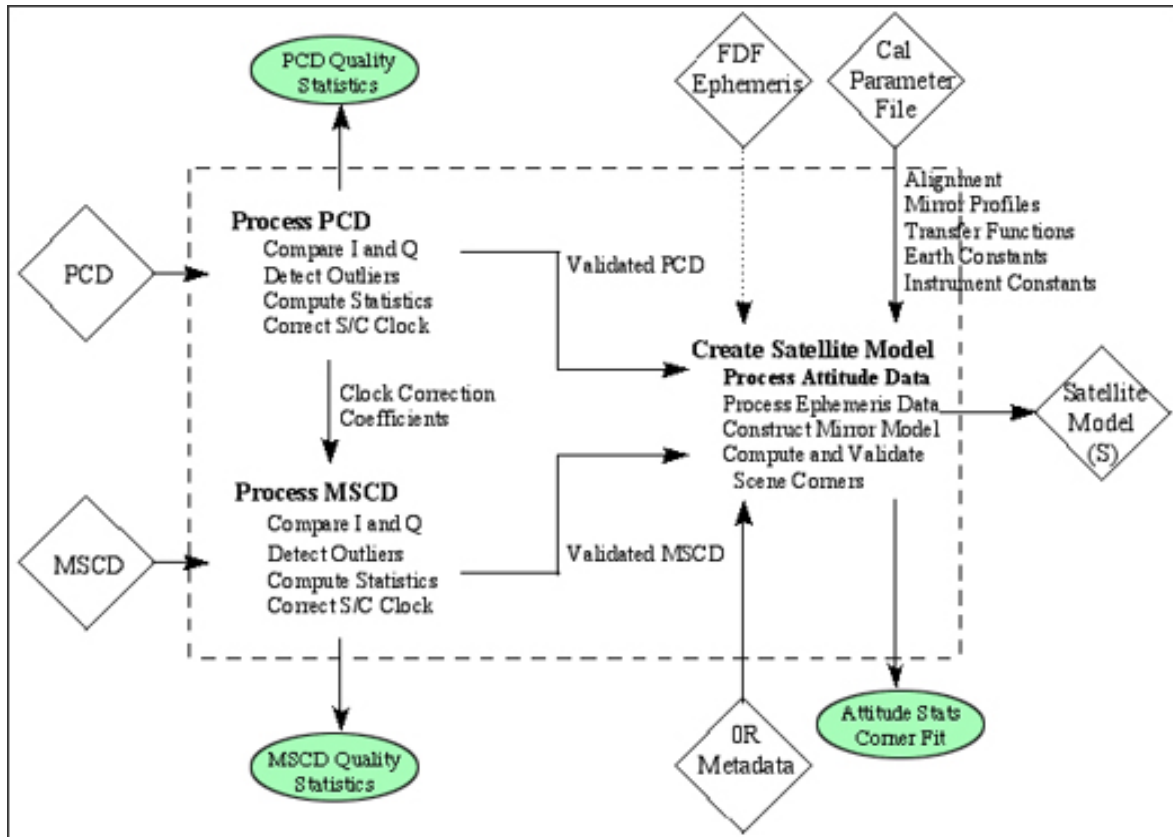


Figure 10.1 - Geometry Model Initialization Flow Chart

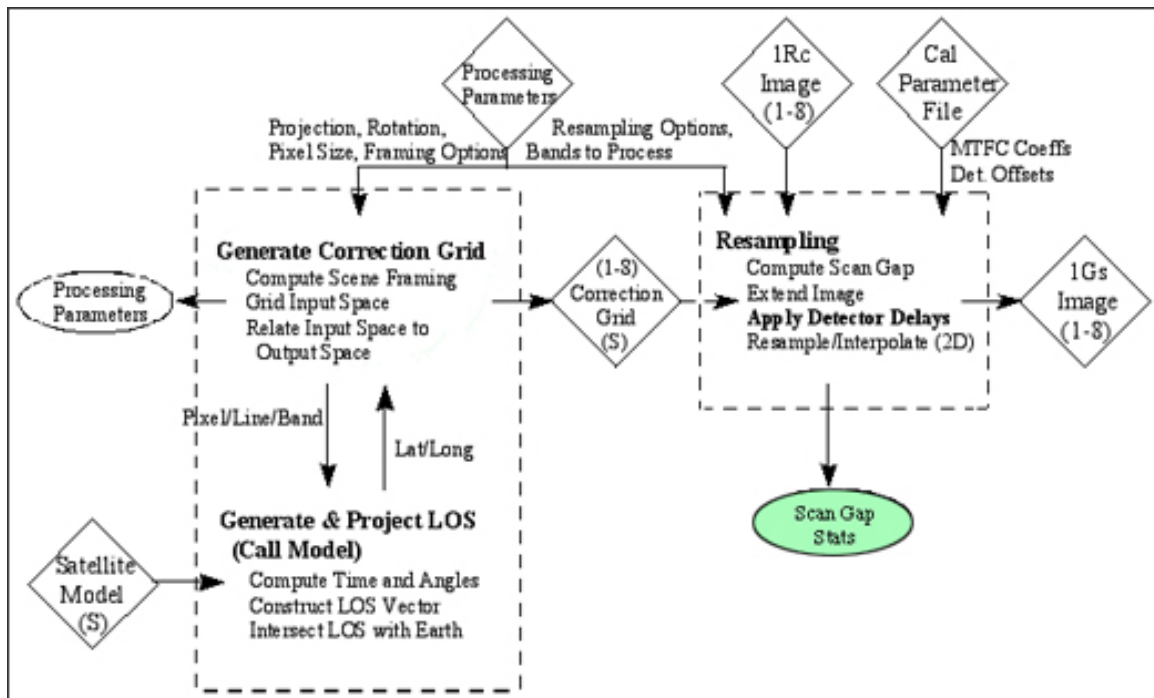


Figure 10.2 - Rectification and Resampling Flow Chart

Detailed algorithm descriptions for each of main process boxes in these diagrams can be found in the Landsat 7 Image Assessment System (IAS) Geometric Algorithm Theoretical Basis Document (PDF). In this document are supporting theoretical concepts and mathematics of the IAS geometric algorithms, a review of the Landsat 7 ETM+ viewing geometry, a discussion of the coordinate and time systems used by the algorithms and the relationships between them, the mathematical development of, and solution procedures for the Level 1 processing, geometric calibration, and geometric characterization algorithms and finally an examination of the estimates of uncertainty (error analysis) associated with each of the algorithms.

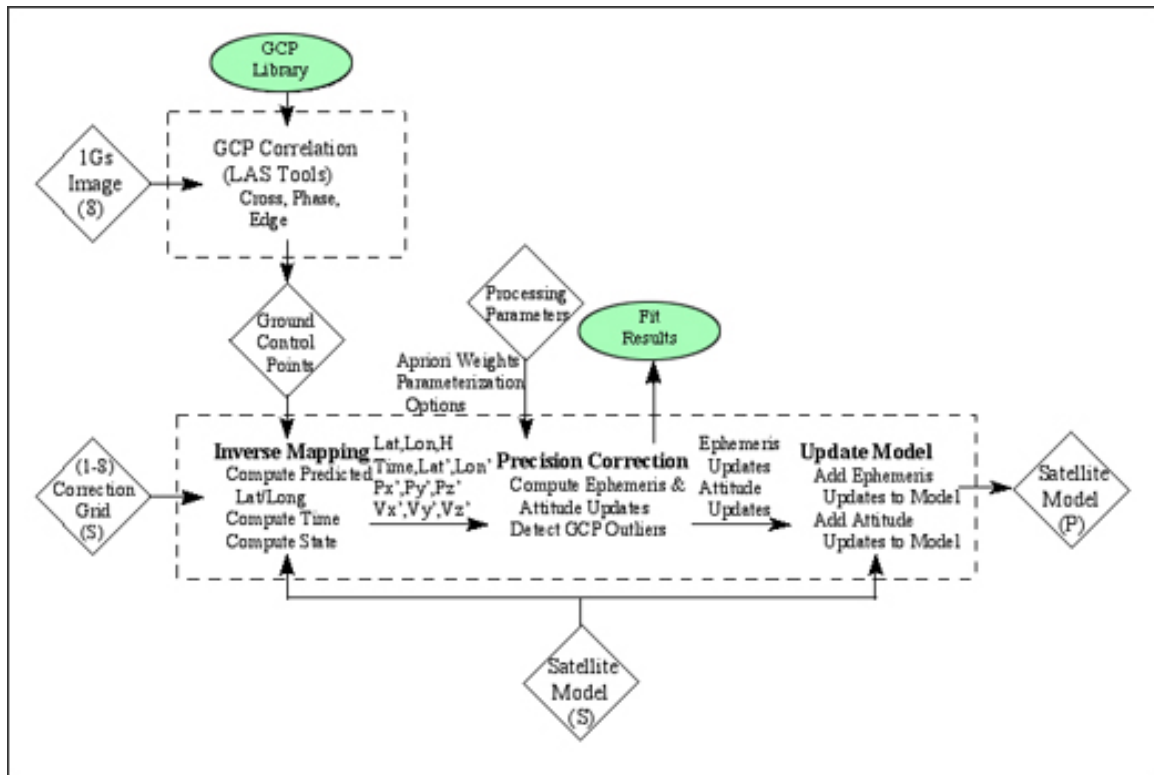


Figure 10.3 - Precision Correction Flow Chart





timing, scan mirror profiles, and attitude sensor data transfer functions (gyro and ADS), to be used in the generation of the initial Calibration Parameter File.

5. Earth parameters including: static Earth model parameters (e.g., ellipsoid axes, gravity constants) and dynamic Earth model parameters (e.g., polar wander offsets, UT1-UTC time corrections) - used in systematic model creation and incorporated into the Calibration Parameter File.

## 11.1 Level 0R Product

Unlike earlier Landsat programs, the Landsat 7 system was not originally designed to produce high level (i.e. Level 1) products users. The baseline program philosophy was to provide raw data only, which would leave the value added domain for commercial companies. A prevailing "wait and see" position by commercial vendors prompted NASA add a systematic correction capability to ensure product availability. The primary product for users and vendors seeking higher level processing, however, 0R data - an essentially raw data form that is marginally



Figure11.1 - Simulated Level 0R Image

useful prior to radiometric and geometric correction. This is readily apparent when viewing a simulated 0R image. A Landsat 7 0R product, however, does contain all the ancillary data required to perform these corrections including a calibration parameter file (CPF) generated by the Landsat 7 IAS.

LPS spatially reformats earth imagery and calibration data into Level 0R data. This involves shifting pixels by integer amounts to account for the alternating forward-reverse scanning pattern of the ETM+ sensor, the odd-even detector arrangement within each band, and the

detector offsets inherent to the focal plane array engineering design. All LPS 0R corrections are reversible; the pixel shift parameters used are documented in the IAS CPF.

The LPS 0R output is HDF-EOS formatted and archived. Details of the archival format can be found in the [Landsat 7 System Wideband DFCB, Vol. 4](#).

### 11.1.1 Product Size

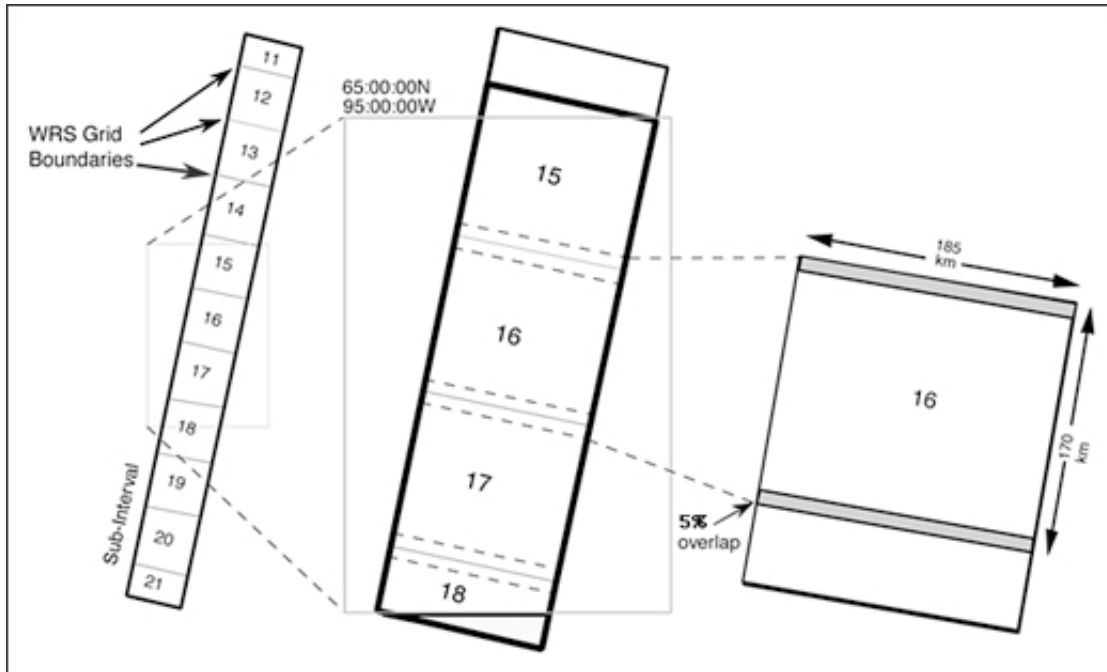


Figure 11.2 - Level 0R Product Alternatives

Three options, depicted in Figure 11.2, exist when defining the size or spatial extent of a Landsat level 0R product ordered from the LP-DAAC.

- **Standard Worldwide Reference System (WRS) Scene.** The standard WRS scene as defined for Landsats 4 and 5 was preserved as a product for Landsat 7. The WRS indexes orbits (paths) and scene centers (rows) into a global grid system comprising 233 paths by 248 rows. The path/row notation was originally employed to provide a standard designator for every nominal scene center and allow straightforward referencing without using longitude and latitude coordinates. The distance between WRS center points along a path is 161.1 kilometers. A path distance of 90 kilometers before and after a WRS center point defines the standard scene length of 180 km. This length includes 20 scans of overlap with neighboring scenes. The standard WRS scene overlaps neighboring scenes along a path by 5% at the equator and has a width or cross track distance of 185 kilometers. Landsat 7 browse is framed according to WRS scenes. An ordered scene will cover the same geographic

extent observed in the browse with the following caveat. Standard WRS scenes have 375 scans. Partial scenes (less than 375 scans) may exist at the beginning or end of a subinterval due to the fact that imaging events do not always start and end on scene boundaries. Browse and scene metadata for these occurrences accurately reflect their partial scene nature and geographic extent although partials are currently not offered due to complexities associated with level 1 processing.

- **Subinterval.** An interval is a scheduled ETM+ image period along a WRS path, and may be from one to 90 scenes in length. A subinterval is a contiguous segment of raw wideband data received during a Landsat 7 contact period. Subintervals are caused by breaks in the wideband data stream due to communication dropouts and/or the inability of the spacecraft to transmit a complete observation (interval) within a single Landsat 7 contact period. The largest possible subinterval is 35 scenes long. The smallest possible subinterval is a single ETM+ scene.
- **Partial Subinterval** A partial Landsat 7 subinterval can also be ordered. The partial subinterval is dimensioned according to standard WRS scene width, is at least one WRS scene in length, and can be up to 10 scenes in length if ordered in 0R form or 3 scenes in length in 1G form. A partial subinterval can float or be positioned at any scan line starting point within a subinterval. Partial subintervals are defined by either contiguous WRS locations or a bounding longitude/latitude rectangle. In the latter case, all scan lines touched by the bounding rectangle are included in their entirety.

### 11.1.2 Product Components

A complete scene-sized 0R product consists of 19 data sets derived from the wideband telemetry, an IAS-generated calibration parameter file, a product specific metadata file, a geolocation index generated by EOSDIS Core System (ECS), and an HDF directory. Therefore, if you order a complete (i.e. all bands) scene-based 0R product it will have 23 distinct files. A brief description of each follows.

- 1 - **9. Earth Image Data** - The unique bands of ETM+ image data comprise nine of the data sets. The data is laid out in a scan line sequential format in descending detector order (i.e. detector 16 followed by detector 15 and so on for the 30 meter bands). Band 6 is captured twice - once in low and the other in high gain mode. Under nominal satellite configuration the low gain form of band 6 will be present in format 1. All image samples or pixels are 8 bits in size.

- 10. Internal calibrator (IC) data - format 1** - IC data for format 1 consists of scan line ordered internal lamp and shutter data for bands 1-5 and blackbody radiance and shutter data for low gain band 6. The data is collected once per scan and structured in a band sequential format in descending detector order (e.g. detector 16 followed by detector 15 and so on for the 30 meter bands).
- 11. Internal calibrator (IC) data - format 2** - IC data for format 2 consists of scan ordered internal lamp and shutter data for bands 7 and 8 and blackbody radiance and shutter data for high gain band 6. The data is collected once per scan and structured in a band sequential format in descending detector order (e.g. detector 16 followed by detector 15 and so on for the 30 meter bands).
- 12. MSCD - format 1.** A logical record of MSCD exists for each data scan present in the 0R product ordered. Each logical record consists of 3 MSCD data values - the first half scan error, the second half scan error, and the scan line direction. This information, which actually applies to the previous scan, is used to compute deviations from nominal scan mirror profiles as measured on the ground and reported in the calibration parameter file. Also included in the MSCD file are scan based values such as time code, gain status and processing errors encountered by LPS. The MSCD is trimmed to fit the product ordered although one additional record is added to the file during the subsetting process due to the fact that scan error and direction information corresponds to the prior scan.
- 13. MSCD - format 2.** A duplicate set of MSCD is generated when format 2 is processed and is kept with the product in the event format 1 MSCD is lost or corrupted.
- 14. PCD - format 1** The PCD for format 1 consists of attitude and ephemeris profiles as well high frequency jitter measurements. PCD for the entire subinterval is included with the 0R product regardless of the size of the data set ordered.
- 15. PCD - format 2** A duplicate set of PCD is generated when format 2 is processed and is kept with the product in the event format 1 is lost or corrupted.
- 16. Scan line offsets - format 1.** During LPS processing image data is shifted in an extended buffer to account for predetermined detector and band shifts, scan line length, and possible bumper wear. The scan line offsets represent the actual starting and ending pixel positions for valid (non-zero fill) Earth image data on a data line by data line basis for bands 1 through 6 low gain. The left starting pixel offsets also apply to the IC data.

- 17. Scan line offsets - format 2.** During LPS processing image data is shifted in an extended buffer to account for predetermined detector and band shifts, scan line length, and possible bumper wear. The scan line offsets represent the actual starting and ending pixel positions for valid (non-zero fill) earth image data on a data line by data line basis for bands 6 high gain through 8. The left starting pixel offsets also apply to the IC data.
- 18. Metadata - format 1.** During LPS format 1 processing metadata is generated that characterizes the subinterval's spatial extent, content, and data quality for bands 1 through 6 low gain. This file, in its entirety and original form, accompanies the 0R product.
- 19. Metadata - format 2.** Format 2 metadata is similar but not identical to format 1 metadata. The subinterval-related metadata contents are identical; the scene-related metadata is specific to bands 6 - high gain, 7, and 8. Also, the format 2 metadata does not include cloud cover assessment data or references to browse data products. This file, in its entirety and original form, accompanies the 0R product.
- 20. Metadata - ECS.** A third metadata file generated by ECS during order processing. This file contains product specific information such as corner coordinates and number of scans.
- 21. Geolocation Index.** The geolocation index is also produced by ECS. This table contains scene corner coordinates and their product-specific scan line numbers for bands at all three resolutions. Its purpose is provide for efficient subsetting of a 0R product.
- 22. Calibration parameters.** The IAS regularly updates the CPF to reflect changing radiometric and geometric parameters required for level 1 processing. These are stamped with applicability dates and sent to the LP-DAAC for storage and bundling with outbound 0R products.
- 23. HDF Directory.** A file containing all the pointers, file size information, and data objects required to open and process the 0R product using the HDF library and interface routines.

A user may order a subset of the available bands, which will affect the actual file, count in a 0R product. In all cases, however, every product includes two PCD files, two MSCD files, three metadata files, the CPF, and the HDF directory. Only the internal calibrator, scan line offset, and earth image file counts are affected by a product possessing less than the full complement of bands.

### 11.1.3 Product Format

The product delivered to Landsat 7 data users is packaged in HDF - an open standard selected by NASA for Earth Observing System (EOS) data products. HDF is a self-describing format that allows an application to interpret the structure and contents of a file without outside information. HDF allows Landsat 0R products to be shared across different computer platforms without modification and is supported by a public domain software library consisting of access tools and various utilities.

Product users are directed to the [Landsat 7 0R Distribution Product Data Format Control Book, Volume 5 \(PDF\)](#) for details regarding the HDF design used for the 0R product. Included are references to NCSA-authored documentation. New users should begin with **Getting Started with HDF** while the **HDF User's Guide** and **HDF Reference Manual** are excellent resources for the HDF programmer.

### 11.2 Level 1R Product

The 2008 single-product data policy changes at EROS made the Level 1R product option obsolete. The following paragraphs are only relevant only from a historical perspective.

The Level 1R product is a radiometrically corrected 0R product. Radiometric correction is performed using either the CRAM gains in the CPF or gains computed on the fly from the IC data. The choice is available to a user when the product is ordered. The biases used are always calculated from the IC data. Image artifacts such as banding, striping, and scan-correlated shift are removed prior to radiometric correction. Radiometric corrections are not reversible. The 1R product geometry is identical to the input Level 0R data.

During 1R product rendering image pixels are converted to units of absolute radiance using 32 bit floating-point calculations. Pixel values are then multiplied by 100 and converted to 16 bit integers prior to media output. Two digits of decimal precision are thus preserved. One merely divides each pixel value by 100 to convert the 1R image data back to radiance units. The 16-bit 1R product is twice the data volume of an alike 0R product. **Note for band 6:** A bias was found in the pre-launch calibration by a team of independent investigators post launch. This was corrected for in the LPGS processing system beginning Dec 20, 2000. For data **processed** before this, the 16 bit image radiances are 0.31 w/m<sup>2</sup> ster um too high.

#### Official Announcement

In the fall of 2000, two Landsat 7 science team investigator groups discovered a band 6-calibration bias in Level 1 ETM+ data products emanating from the EDC (i.e.

LPGS) at the EROS Data Center. This bias apparently results from limitations in the pre-launch calibration of the ETM+. The magnitude of the correction is estimated to be  $0.31 \text{ W}/(\text{m}^2 \text{ sr } \mu\text{m})$  or about 3-4% radiance error at typical surface temperatures. This apparent systematic error in Band 6 radiance calibration translates into estimated temperatures derived from Landsat 7 ETM+ being about 3°C too high for typical Earth surface temperatures.

To remedy the situation, several changes were made to the product generation software and CPF. The band 6 biases and instrument component view coefficients were changed in the October 1, 2000 release of the CPF. The calibration equation used by LPGS software was operationally updated on December 20, 2000. Users need to be aware of the impact these changes have on level 1 products.

#### **LPGS Level 1 products - pre 12/20/00**

Users should subtract the bias value ( $0.31 \text{ W}/(\text{m}^2 \text{ sr } \mu\text{m})$ ) from the radiances obtained from Level 1R and Level 1G data products generated since launch by LPGS for both high and low gain band 6 data. The changes made to the October 1, 2000 CPF effectively remove the temperature bias but only if the product generation software uses the changed CPF values. The LPGS software in place prior to December 20th does not.

#### **LPGS Level 1 products - post 12/20/00**

Users can safely use temperatures derived from band 6 radiance values. No bias correction is necessary.

#### **Other Systems - pre 10/01/00**

If the CPF gains and biases are used then the band 6 radiance values should be adjusted for the bias described in paragraph three above.

#### **Other Systems - post 10/01/00**

If the CPF gains and biases are used then no adjustments are necessary after this date.

Other systems that employ a band 6-calibration equation are outside NASA/USGS configuration and control. For accurate processing, please consult with your product provider.



### 11.2.1 Product Size

Two options existed for users when defining the size or spatial extent of a Landsat level 1R product ordered from the LP-DAAC.

- **Standard Worldwide Reference System (WRS) Scene.** The standard WRS scene, as defined above for the 0R product, could be ordered in 1R form. Partial scenes that may exist at the beginning and end of subintervals could also be ordered.
- **Partial Subinterval** A partial subinterval could also be ordered in 1R form. Unlike the 0R product the 1R was limited to a maximum of 3 WRS scenes in size. The variably sized 1R product could float or be positioned at any scan line starting point within a subinterval. Alternatively, the product could be defined by up to three contiguous WRS locations.

### 11.2.2 Product Components

A complete scene-sized 1R product consists of 17 data sets derived from the wideband telemetry, an IAS-generated calibration parameter file, a product specific metadata file, a geolocation index generated by EOSDIS Core System (ECS), and an HDF directory. Therefore, if you order a complete (i.e. all bands) scene-based 0R product it will have 21 distinct files. There are two fewer data files than an alike 0R product due to the fact that the multiple PCD and MSCD files are merged into single consensus files. Please reference the 0R file product for individual file descriptions.

A user could order a subset of the available bands, which affected the actual file, count in a 1R product. In all cases, however, every product included one consensus PCD file, one consensus MSCD files, three metadata files, the CPF, and the HDF directory. Only the internal calibrator, scan line offset, and earth image file counts were affected by a product possessing less than the full complement of bands.

### 11.2.3 Product Format

The 1R product was delivered to users only in the HDF format. The HDF 0R and 1R formats are nearly identical. Exceptions include the united PCD and MSCD files and an enhanced product specific metadata file that reflects 1R correction characteristics. Please refer to the [Landsat 7 0R Distribution Product Data Format Control Book, Volume 5 \(PDF\)](#) for details regarding HDF specifics. Additional information unique to the 1R product can be found in the [ESDIS Level 1 Product Generation system Output Files DFCB \(PDF\)](#).

## 11.3 Level 1G Product

The 1G product available to users from EROS is a radiometrically and geometrically corrected Level 0R image. The correction algorithms employed model the spacecraft and sensor using data generated by onboard computers during imaging events. Primary inputs are the PCD, which includes the attitude and ephemeris profiles, the [definitive ephemeris](#) (if available) and the MSCD. Refined parameters from the CPF, ground control points and a digital elevation model are also used to improve the overall geometric fidelity of the standard level-one terrain-corrected (L1T) product.

The L1T correction process utilizes both ground control points (GCP) and digital elevation models (DEM) to attain absolute geodetic accuracy. The WGS84 ellipsoid is employed as the Earth model for the Universal Transverse Mercator (UTM) coordinate transformation. Associated with the UTM projection is a unique set of projection parameters that flow from the USGS General Cartographic Transformation Package. The end result is a geometrically rectified product free from distortions related to the sensor (e.g. jitter, view angle effects), satellite (e.g. attitude deviations from nominal), and Earth (e.g. rotation, curvature, relief).

Geodetic accuracy of the L1T product depends on the accuracy of the GCPs and the resolution of the DEM used\*. The 2005 Global Land Survey is used as the source for GCPs while the primary terrain data is the Shuttle Radar Topographic Mission DEM. Scenes that have a quality scores of 99 and less than 40 percent cloud cover are automatically processed, and any archived scene, regardless of cloud cover, can be ordered through one of two EROS web portals ([Product Ordering](#)).

**Table 11.1 Landsat 7 1G Projection Parameters**

Table 11.1 Landsat 7 1G Projection Parameters													
Projection Name	Required Parameters												
	1	2	3	4	5	6	7	8	9	10	11	12	13
Universal Transverse Mercator (UTM)	SMajor	SMinor	Zone										
Lambert Conformal Conic	SMajor	SMinor	STDPR1	STDPR2	Cent Mer	OriginLat	FE	FN					
Polyconic	SMajor	SMinor			Cent Mer	OriginLat	FE	FN					
Transverse Mercator	SMajor	SMinor	Factor		Cent Mer	OriginLat	FE	FN					
Polar Stereographic	SMajor	SMinor			LonPol	TrueScale	FE	FN					
Hotine Oblique Mercator A	SMajor	SMinor	Factor			OriginLat	FE	FN	Long1	Lat1	Long2	Lat2	zero
Hotine Oblique Mercator B	SMajor	SMinor	Factor	AziAng	AzmthPt	OriginLat	FE	FN					one
Space Oblique Mercator B	SMajor	SMinor	Satnum	Path			FE	FN					one
Projection Parameter Definitions													
<b>AziAng</b>	azimuth angle east of north for center projection line												
<b>AzmthPt</b>	longitude of point on central meridian where <b>AziAng</b> occurs.												
<b>CentMer</b>	Longitude of the projection's central meridian												
<b>Factor</b>	scale factor at the central meridian (transverse mercator) or center of projection (Oblique Mercator)												
<b>FE</b>	false easting in the same units as the semi-major axis												
<b>FN</b>	false northing in the same units as the semi-major axis												
<b>Lat1</b>	latitude of first point on the projection's center line												
<b>Lat2</b>	latitude of second point on the projection's center line												
<b>Long1</b>	longitude of first point on the projection's center line												
<b>Long2</b>	longitude of second point on the projection's center line												
<b>LongPol</b>	longitude down below pole of map												
<b>OriginLat</b>	latitude of the projection origin												
<b>Path</b>	path number for Landsat 7 using the World Reference System #2												
<b>Satnum</b>	number of the Landsat satellite (i.e. 7)												
<b>SMajor</b>	semi-major axis of the projection's ellipsoid												
<b>SMinor</b>	semi-minor axis of the projection's ellipsoid												
<b>STDPR1</b>	latitude of the first standard parallel												
<b>STDPR2</b>	latitude of the second standard parallel												
<b>TrueScale</b>	latitude of the true scale												

The Landsat 7 level 1G product projection parameters are listed in Table 12.1. Most projections do not require 13 parameters as evidenced by the empty table cells. Parameter definitions are listed in Table 12.2.

During L1T processing the 0R image data undergoes two-dimensional resampling according to the following set of parameters:

- Correction level - L1T\*
- Pixel Size - 15, 30, 60 meters for panchromatic, VNIR/SWIR, and thermal
- Resampling kernel - Cubic Convolution (CC)
- Map projection - UTM  
with Polar Stereographic projection used for Antarctica scenes
- Ellipsoid - WGS84
- Image orientation - north up
- Output format - GeoTIFF
- File transfer protocol (FTP) download only

\* While most scenes are processed to L1T, some lack GCPs and/or DEMs required for precision and terrain correction processing. In these cases, the best level of correction will be applied - Level 1GT-systematic terrain (GCPs absent) or Level 1G-systematic (DEMs and GCPs absent).

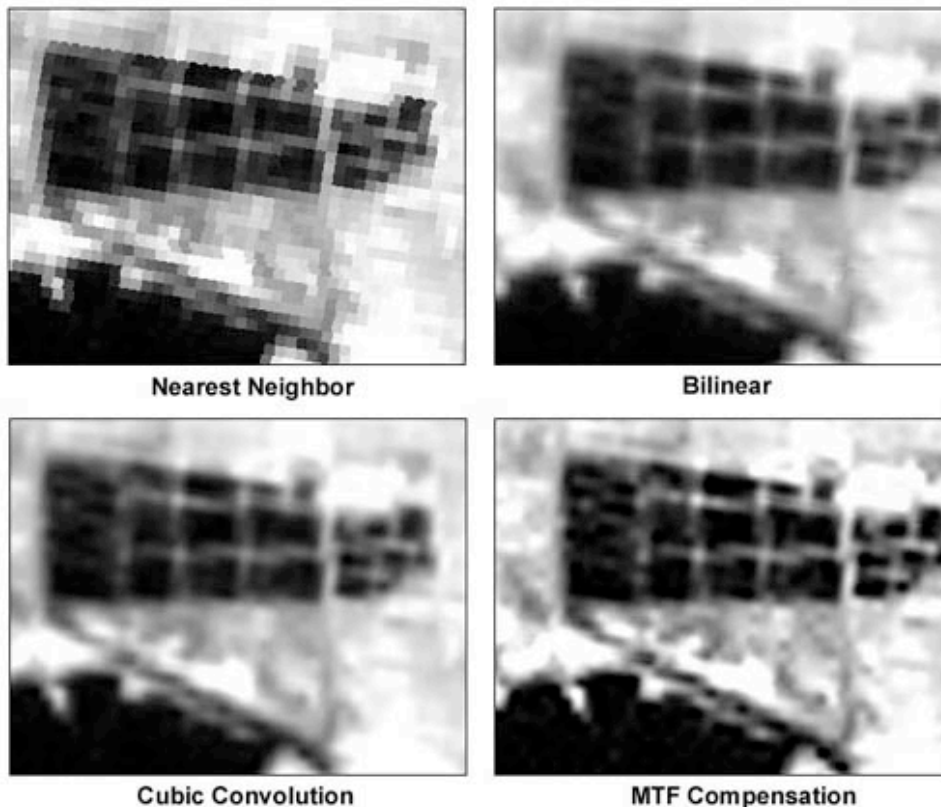


**Figure 11.3 - Landsat 7 Resampling Kernel (CC) Versus Other Methods**

The Landsat 7 level 1G product projection parameters are listed in Table 12.1. Most projections do not require 13 parameters as evidenced by the empty table cells. Parameter definitions are listed in Table 12.2.

### 11.3.1 Conversion to Radiance

During 1G-product rendering image pixels are converted to units of absolute radiance using 32 bit floating-point calculations. Pixel values are then scaled to byte values prior to media output. The following equation is used to convert DN's in a 1G product back to radiance units:

$$L_{\lambda} = \text{Grescale} * \text{QCAL} + \text{Brescale}$$

which is also expressed as:

$$L_{\lambda} = ((LMAX_{\lambda} - LMIN_{\lambda}) / (QCALMAX - QCALMIN)) * (QCAL - QCALMIN) + LMIN_{\lambda}$$

where:

- $L_{\lambda}$  = Spectral Radiance at the sensor's aperture in watts/(meter squared \* ster \*  $\mu\text{m}$ )
- Grescale** = Rescaled gain (the data product "gain" contained in the Level 1 product header or ancillary data record) in watts/(meter squared \* ster \*  $\mu\text{m}$ )/DN
- Brescale** = Rescaled bias (the data product "offset" contained in the Level 1 product header or ancillary data record ) in watts/(meter squared \* ster \*  $\mu\text{m}$ )
- QCAL** = the quantized calibrated pixel value in DN
- LMIN <sub>$\lambda$</sub>**  = the spectral radiance that is scaled to QCALMIN in watts/(meter squared \* ster \*  $\mu\text{m}$ )
- LMAX <sub>$\lambda$</sub>**  = the spectral radiance that is scaled to QCALMAX in watts/(meter squared \* ster \*  $\mu\text{m}$ )
- QCALMIN** = the minimum quantized calibrated pixel value (corresponding to LMIN <sub>$\lambda$</sub> ) in DN
  - = 1 for LPGS products
  - = 1 for NLAPS products processed after 4/4/2004
  - = 0 for NLAPS products processed before 4/5/2004
- QCALMAX** = the maximum quantized calibrated pixel value (corresponding to LMAX <sub>$\lambda$</sub> ) in DN
  - = 255

The **LMINs** and **LMAXs** are the spectral radiances for each band at digital numbers 0 or 1 and 255 (i.e. QCALMIN, QCALMAX), respectively. LPGS used 1 for QCALMIN while NLAPS used 0 for QCALMIN for data products processed before April 5, 2004. NLAPS from that date now uses 1 for the QCALMIN value. Other product **differences** exist as well. One LMIN/LMAX set exists for each gain state. These values will change slowly over time as the ETM+ detectors lose responsivity. Table 11.2 lists two sets of LMINs and LMAXs. The first set should be used for both LPGS and NLAPS 1G products created **before** July 1, 2000 and the second set for 1G products created **after** July 1, 2000. Please note the distinction between acquisition and processing dates. Use of the appropriate LMINs and

LMAXs will ensure accurate conversion to radiance units. **Note for band 6:** A bias was found in the pre-launch calibration by a team of independent investigators post launch. This was corrected for in the LPGS processing system beginning Dec 20, 2000. For data **processed** before this, the image radiances given by the above transform are 0.31 w/m<sup>2</sup> ster um too high. See the [official announcement](#) for more details. **Note for the Multispectral Scanner (MSS), Thematic Mapper (TM), and Advanced Land Imager (ALI) sensors:** the required radiometry constants are tabulated in this [PDF](#) file.

Table 11.2 ETM+ Spectral Radiance Range watts/(meter squared * ster * μm)								
Band Number	Processed Before July 1, 2000				Processed After July 1, 2000			
	Low Gain		High Gain		Low Gain		High Gain	
	LM IN	LMAX	LM IN	LMAX	LM IN	LMAX	LM IN	LMAX
1	- 6.2	297.5	- 6.2	194.3	- 6.2	293.7	- 6.2	191.6
2	- 6.0	303.4	- 6.0	202.4	- 6.4	300.9	- 6.4	196.5
3	- 4.5	235.5	- 4.5	158.6	- 5.0	234.4	- 5.0	152.9
4	- 4.5	235.0	- 4.5	157.5	- 5.1	241.1	- 5.1	157.4
5	- 1.0	47.70	- 1.0	31.76	- 1.0	47.57	- 1.0	31.06
6	0.0	17.04	3.2	12.65	0.0	17.04	3.2	12.65
7	- 0.3 5	16.60	- 0.3 5	10.932	- 0.3 5	16.54	- 0.3 5	10.80
8	- 5.0	244.00	- 5.0	158.40	- 4.7	243.1	- 4.7	158.3

### 11.3.2 Radiance to Reflectance

For relatively clear Landsat scenes, a reduction in between-scene variability can be achieved through a normalization for solar irradiance by converting spectral radiance, as calculated above, to planetary reflectance or albedo. This combined surface and atmospheric reflectance of the Earth is computed with the following formula:

Where:

- = Unitless planetary reflectance
- = Spectral radiance at the sensor's aperture
- = Earth-Sun distance in astronomical units from an [Excel file](#) or interpolated from values listed in Table 11.4
- = Mean solar exo-atmospheric irradiances from Table 11.3
- = Solar zenith angle in degrees

<b>Table 11.3 ETM+ Solar Spectral Irradiances</b> (generated using the <a href="#">Thuillier</a> solar spectrum)	
<b>Band</b>	<b>watts/(meter squared * <math>\mu\text{m}</math>)</b>
1	1997
2	1812
3	1533
4	1039
5	230.8
7	84.90
8	1362.

<b>Table 11.4 Earth-Sun Distance in Astronomical Units</b>									
Day of Year	Distance	Day of Year	Distance	Day of Year	Distance	Day of Year	Distance	Day of Year	Distance
1	.98331	74	.99446	152	1.01403	227	1.01281	305	.99253
15	.98365	91	.99926	166	1.01577	242	1.00969	319	.98916
32	.98536	106	1.00353	182	1.01667	258	1.00566	335	.98608
46	.98774	121	1.00756	196	1.01646	274	1.00119	349	.98426
60	.99084	135	1.01087	213	1.01497	288	.99718	365	.98333

### 11.3.3 Band 6 Conversion to Temperature

ETM+ Band 6 imagery can also be converted from spectral radiance (as described above) to a more physically useful variable. This is the effective at-satellite temperatures of the viewed Earth-atmosphere system under an assumption of unity emissivity and using pre-launch calibration constants listed in Table 11.5. The conversion formula is:

$$T = \frac{K2}{\ln \left( \frac{K1}{L_{\lambda}} + 1 \right)}$$

Where:

- T = Effective at-satellite temperature in Kelvin
- K2 = Calibration constant 2 from Table 11.5
- K1 = Calibration constant 1 from Table 11.5
- L = Spectral radiance in watts/(meter squared \* ster \* μm)

<b>Table 11.5 ETM+ and TM Thermal Band Calibration Constants</b>		
	<b>Constant 1 - K1</b> watts/(meter squared * ster * μm)	<b>Constant 2 - K2</b> Kelvin
Landsat 7	666.09	1282.71
Landsat 5	607.76	1260.56

### 11.3.4 Product Size

The same two 1R options exist for users when defining the size or spatial extent of a Landsat level 1G product ordered from the LP-DAAC.

- **Standard Worldwide Reference System (WRS) Scene.** The standard WRS scene, as defined above for the 0R product, can be ordered in 1G form. Partial scenes that may exist at the beginning and end of subintervals may be also be ordered.
- **Partial Subinterval.** A partial subinterval can also be ordered in 1G form. Unlike the 0R product the 1G is limited to a maximum of 3 WRS scenes in size. The variably sized 1G product can float or be positioned at any scan line starting point within a subinterval. Alternatively, the product can be defined by up to three contiguous WRS locations.



### 11.3.5 Product Components

The 1G product ordered from the LP-DAAC consists of the corrected image files and descriptive metadata. All other ancillary files delivered with the 0R and 1R products are not included. A user may order a subset of the available bands, which affects the actual file, count in a 1G product.

### 11.3.6 Product Format

The 1G product can be packaged into one of following user-specified output formats:

- **Hierarchical Data Format.** The HDF packaging format used for the 0R and 1R products is also used for structuring the 1G. The design employs external elements for the band files and metadata. These are standalone files that are referenced via tags and pointers residing in an HDF directory. External elements provide users with two processing options - exploit the NCSA HDF libraries for data access or process the data files directly using homegrown code.

The number of files comprising an HDF-formatted 1G product will vary according to the number of bands ordered. A product with a full band complement has 11 files - the HDF directory, a metadata file, and a separate file for each band. The HDF directory and metadata files are always present regardless of bands ordered. Please refer to the [Landsat 7 0R Distribution Product Data Format Control Book, Volume 5 \(PDF\)](#) for details regarding band file specifics. The 1R metadata file description can be found in the [ESDIS Level 1 Product Generation System Output Files DFCB \(PDF\)](#). The HDF format can be specified for any type of 1G product ordered from the LP-DAAC.

- **Fast.** The Fast Format was originally developed by EOSAT as a means for quickly accessing Landsat 4 and 5 image data. Its structure is straightforwardly simple. Each band is self-contained in its own file (i.e. external element style). A header file containing three records accompanies the image data. The three records in order of appearance are labeled administrative, radiometric, and geometric respectively. Sensor specific information is placed in the administrative record, gains and biases can be found in the radiometric record while projection information and image coordinates are stored in the geometric record. A single header file along with the image files constitutes the Fast product.

A derivative of the Fast Format (Fast-L7) used by EOSAT for Landsat (FAST-B) and Indian Remote Sensing products (Fast-C) was created for Landsat 7. Several differences are worth noting. File names are now included in the administrative record which allows for direct file access. A separate header file now accompanies the panchromatic, thermal and VNIR/SWIR band groups for Landsat 7. For Fast-B and Fast-C all bands were resampled to a common grid cell size thus permitting a single header file. In all likelihood each of the band groups for Landsat 7 will be resampled to a common resolution (i.e. 15, 30, & 60 meters) thus requiring a distinct header file for each.

All critical fields required for product ingest were left unchanged in the Fast L-7A Format. As a consequence Heritage Fast readers residing on user systems can be used for the Landsat 7 Fast formatted product. A full layout of the Fast L-7A Format can be found in [the ESDIS Level 1 Product Generation system Output Files DFCB](#). The Fast-L7 format supports all variations of the 1G product.

- **GeoTIFF.** Geographic tagged image file format (GeoTIFF) is based on Adobe's TIFF - a self-describing format developed to exchange raster images such as clipart, logotypes, and scanned images between applications and computer platforms. Today, the TIFF image file format is used to store and transfer digital satellite imagery, scanned aerial photos, elevation models, and output from digital cameras. TIFF is the only full-featured format in the public domain, capable of supporting compression, tiling, and extension to include geographic metadata.

The TIFF file consists of a number of label (tags), which describes certain properties of the file (such as gray levels, color table, byte format, compression size). After the initial tags comes the image data which may be interrupted by more descriptive tags. GeoTIFF refers to TIFF files which have geographic (or cartographic) data embedded as tags within the TIFF file. The geographic data can then be used to position the image in the correct location and geometry on the screen of a geographic information display.

Baseline TIFF image types can be bi-level, greyscale, palette color, and full color (24 bit). For simplicity's sake the greyscale model was implemented for the Landsat 7 GeoTIFF product. Under this implementation each ordered band is delivered as its own 8-bit greyscale GeoTIFF image. A standard WRS scene possessing the full band complement would thus be comprised of nine separate GeoTIFF images or files. No other files accompany the product. For detailed

information regarding the Landsat 7 GeoTIFF implementation please refer to the [ESDIS Level 1 Product Generation system Output Files DFCB \(PDF\)](#). For GeoTIFF details, please download the [GeoTIFF Format Specification \(PDF\)](#) or visit this [web site](#).

At the present time GeoTIFF format cannot be used for the Space Oblique Mercator and Oblique Mercator projections. Products projected into these reference systems must be formatted using HDF or Fast-L7.

An instrument malfunction occurred onboard Landsat 7 on May 31, 2003. The problem was caused by failure of the Scan Line Corrector (SLC), which compensates for the forward motion of the satellite. Subsequent efforts to recover the SLC have not been successful, and the problem is permanent.

The Landsat 7 Enhanced Thematic Mapper Plus (ETM+) is still capable of acquiring useful image data with the SLC turned off, particularly within the central portion of any given scene. Landsat 7 ETM+ will therefore continue to acquire image data in the "SLC-off" mode.

EDC has recently released several Landsat 7 ETM+ SLC-off data products. The first, a gap-present product became available on October 22, 2003. This product release includes all image data acquired by Landsat 7 in SLC-off mode from July 14, 2003 to present, excluding a 2-week interval from 9/3/03 to 9/17/03.

The center of a gap-present SLC-off data product is very similar in quality to previous Landsat 7 data. However, the scene's edges will contain alternating scan lines of missing data (Level 1G) or duplicated data (Level 0Rp or L1R). The precise location of the affected scan lines will vary from scene to scene, and these gaps will not be visible on the browse image preview when ordering SLC-off data. A preliminary report regarding the utility of Landsat 7 SLC-off data is available in PDF form. This report includes input from scientists affiliated with the USGS, NASA, and the Landsat 7 Science Team.

The gap-present SLC-off data product is available as a single scene entity in Level 1G terrain corrected (L1T) form. As of November, 2008, the USGS offers all archived Landsat scenes to the public at no charge. Newly acquired Landsat 7 ETM+ SLC-off and Landsat 5 TM images with less than 40 percent cloud cover are automatically processed and made freely available for immediate download. SLC-off data products can be searched and ordered via the [Earth Explorer](#), and [Global Visualization L7 Image Browser](#).

The second product now being offered (as of May 10, 2004) is in 1G form and has the gap areas filled with Landsat 7 data acquired at a similar time of year and prior to the SLC failure. The two scenes are geometrically registered, and a histogram matching technique is applied to the fill pixels, which provides the best-expected radiance values for the missing data.



**Figure 11.4** - Top image: pre-SLC anomaly, middle of image. Middle image: scene after SLC anomaly. Bottom image: scene after SLC anomaly with data gaps filled.

The USGS, in conjunction with NASA, is continuing to research other methods of providing merged data products and will continue to provide information resulting from this work as it becomes available. Various methodologies have been examined to fill the data gaps with observations acquired during prior or later than the target scene of interest. An example of a gap-filled product is illustrated in Figure 11.4.

### **11.3.7 Definitive Ephemeris**

If available, the Landsat 7 definitive ephemeris is used for geometrically correcting ETM+ data. Definitive ephemeris substantially improves the positional accuracy of the Level 1G product over predicted ephemeris.

An ephemeris is a set of data that provides the assigned places of a celestial body (including a manmade satellite) for regular intervals. In the context of Landsat 7, ephemeris data shows the position and velocity of the spacecraft at the time imagery is collected. The position and velocity information are used during product generation.

The Landsat 7 Mission Operations Center receives tracking data on a daily basis that shows the position and velocity of the Landsat 7 spacecraft. This information comes from the three US operated ground-receiving stations and is augmented by similar data from NASA's Tracking and Data Relay Satellites. The Flight Operations Team processes this information to produce a refined or "definitive" ephemeris that shows the position and velocity of Landsat 7 in one-minute intervals. Tracking data are used to compute the actual spacecraft position and velocity for the last 61 hours and to predict these values for the next 72 hours. The predicted ephemeris data are uploaded to the spacecraft daily. On-board software interpolates from this data to generate the positional information contained in the Payload Correction Data (PCD).

Engineers with the Landsat Program have completed a predicted versus definitive ephemeris analysis. Comparisons to ground control points demonstrate the definitive ephemeris is, in fact, reliably more accurate than the predicted ephemeris. Geometric accuracy on the order of 30-50 (1 sigma) meters, excluding terrain effects, can be achieved when the definitive ephemeris is used to process the data. Level 1G products produced after March 29, 2000 use definitive ephemeris if available. The .MTL field "ephemeris type" in the product metadata files identifies whether a product was created with definitive or predicted ephemeris. Daily definitive ephemeris profiles have been archived since June 29, 1999 and are available for [downloading](#).

### **11.3.8 Radiometric Scaling Parameters for Landsat 7 ETM+ Level 1G Products**

The LMIN's and LMAX's are a representation of how the output Landsat ETM+ Level 1G data products are scaled in radiance units. The LMIN corresponds to the radiance at the minimum quantized and calibrated data digital number (QCALMIN), which is typically "1" or "0" and LMAX corresponds to the radiance at the maximum quantized and calibrated data digital number (QCALMAX), typically "255".

#### **Reflective bands:**

The LMIN's are set so that a "zero radiance" scene will still be on scale in the 8-bit output product, even with sensor noise included. LMIN should result in "zero " radiance being about 5 DN in low gain and 7.5 DN in high gain. The LMAX's are set so that LMAX corresponds to slightly less than the saturation radiance of the most sensitive detector. This is done so that in the output product all "pixels" saturate at the same radiance. Currently the LMAX is set to be 0.99 of the pre-launch saturation radiance of the most sensitive detector in each band.

Normally, there is no need to change the LMIN's or LMAX's, unless something changes drastically on the instrument. If the sensitivity of the instrument increases, which is not expected, there is no need to change the LMIN and LMAX values. If the sensitivity decreases, the LMAX values can be increased which in turn increases the usable dynamic range of the product (this will not occur unless the change is large). The changes that have taken place to date have been mostly due to the adoption of "improved" pre-launch gains for the instrument that have, in effect, "increased" its sensitivity. The Landsat Project Science Office also detected a few errors in the original numbers, which were corrected.

## 11.4 Level 1 Product Differences

The two USGS Landsat 7 Level 1 product generation systems, LPGS and the National Landsat Archive Processing System (NLAPS), create products that are similar but not identical. LPGS products are ordered through the EOS Data Gateway while Earth Explorer is used to order NLAPS products. Users should be aware of the following differences.

### Scaling

After radiometric correction the LPGS system scales the output values of the ETM+ 1G image data within the range of 1-255. The zero value is reserved for fill data. NLAPS, prior to **April 5, 2004**, scaled the 1G image data from 0-255 and also used 0 for fill data. NLAPS now scales (post April 5, 2004) ETM+ 1G data from 1-255 to match LPGS (the output scale for TM and MSS remains unchanged (0-255)). This change was made to assist in identifying the potential gaps for SLC-off products. Users must be cognizant of which system was used **and** the date of processing if a conversion back to radiance, as described in Chapter 11, is desired.

### Gain Change Scenes

Earlier, it was reported that the LPGS and NLAPS have different scaling procedures for scenes with gain state changes. This isn't the case. Both systems always utilize the low gain LMAX value when scaling the radiance of a scene.

### Edge Trimming

The two systems also treat the scenes scan line edges differently. NLAPS trims the band offsets while LPGS does not. This distinguishing characteristic (Figure 11.5) can be used when system origin is unknown.

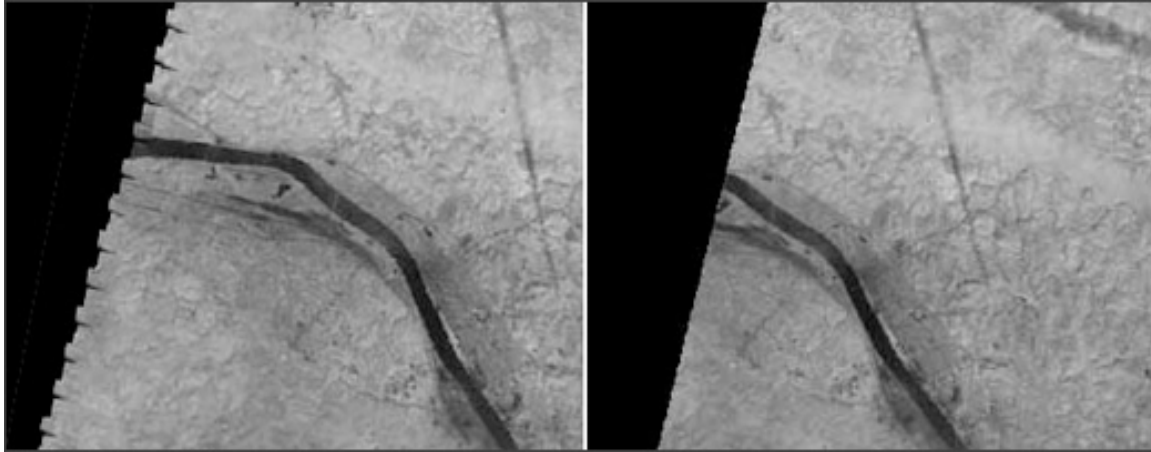


Figure 11.5 - The LPGS (left) does not trim scan edges like NLAPS (right).

### Map Projection Coordinates

The two systems also use slightly different output projection pixel placement schemes. LPGS products have map coordinates that are pixel center based. NLAPS coordinates assigns coordinates to the upper left corner. These differences are illustrated in figure 11.5 where the upper left corner pixel is depicted for all three band resolutions.

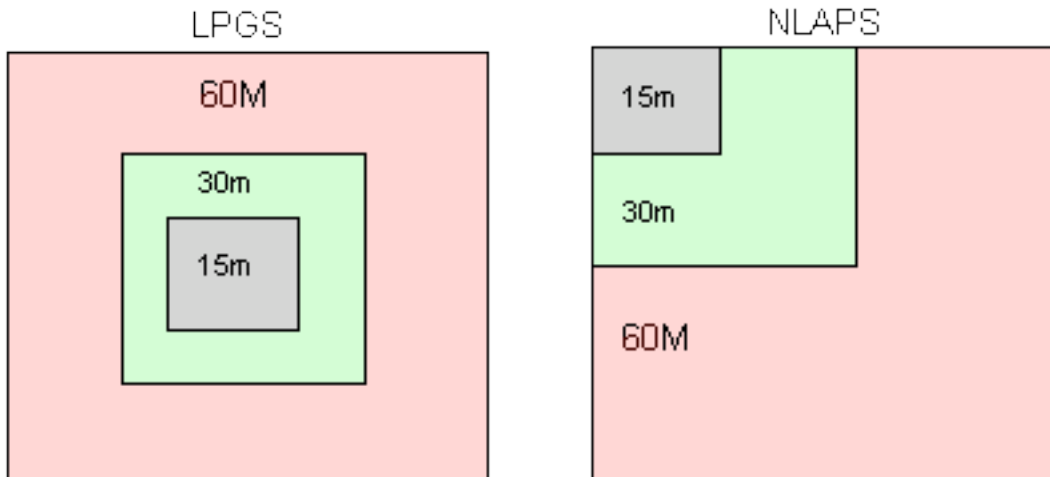


Figure 11.6 - Upper left corner pixel alignment for LPGS versus NLAPS 1G products.

### GeoTIFF Header

There is also a difference in the TIFF header for GeoTIFF formatted products. Both systems have the BitsPerSample tag set to 8. The NLAPS product also has the SampleFormat tag set to unsigned integer format. The LPGS does not use the SampleFormat tag for its GeoTIFF formatted products.

## **GXA Slewing**

Data anomalies that manifest as scan line offsets can occur when the Gimbaled X-band Antenna (GXA) is redirected from one ground station to another. Level 1 processing algorithms attempt to correct this problem but are not always successful. When not, LPGA estimates an end-of-line (EOL) and processes the damaged scans. The scans will be offset but available. NLAPS assumes an absent EOL means no data and will zero fill the affected scans.

## **12.1 Data Holdings**

The primary receiving station for ETM+ data is the US Geological Survey's Center for Earth Resources Observation and Science (EROS) in Sioux Falls, South Dakota. Substantially cloud-free, land and coastal scenes are acquired by EROS through real-time downlink, and by playback from the on-board solid-state recorder. Approximately 200 scenes are downlinked or played back per day. Another 50-60 scenes arrive each day on tape from the northern latitude ground stations in Norway and Alaska. These scenes consist of Alaskan coverage as well as recorder dumps from foreign land masses.

On April 21, 2008, the USGS announced plans to provide all archived Landsat scenes to the public at no charge. Newly acquired Landsat 7 ETM+ SLC-off and Landsat 5 TM images with less than 40 percent cloud cover are automatically processed and made freely available for immediate download. The downloadable inventory reaches back one year. Older scenes and imagery with more than 40 percent cloud cover can still be ordered, however, delivery takes days, not minutes. Only the L1T product is available. Previously offered USGS Landsat products with customer-defined projection options on various media are no longer available.

There are a number of organizations and data centers that have made their ETM+ data holdings available online. This data is generally free or available at a nominal reproduction cost.



<b>Additional ETM+ Data Sources</b>	
<b>Source</b>	<b>Geographic Area</b>
<a href="#">OhioView</a>	Ohio, Montana, SE Alaska, Turkey, Ethiopia
<a href="#">Tropical Rain Forest Information Center</a>	U.S., Northern South America, Central Africa, SE Asia
<a href="#">Global Land Cover Facility</a>	Chesapeake Bay, Canada, Caribbean, Northern South America, Philippines
<a href="#">Arizona Regional Image Archive</a>	Sonoran desert region, including the US Southwest and northern Mexico
<a href="#">Landsat.org</a>	Assorted scenes worldwide
<a href="#">Landsat4u</a>	Southwestern U.S.
<a href="#">W. M. Keck Earth Sciences and Mining Research Information Center</a>	Nevada
<a href="#">EOS-WEBSTER</a>	Sparse U.S. and Russian collections
<a href="#">Landsat 7 Data Sets</a>	Educational Image Downloads

### 12.1.1 Product Prices

Landsat data is free and can be downloaded from the USGS's website [GloVis](#) and the Global Land Cover Facility's [ESDI](#) website.

### 12.1.2 Product Media

Landsat products (both online and ordered) are distributed via FTP electronic transfer only. Once ordered scenes are processed, an email notification is sent to the customer with instructions for downloading.

## 12.2 Online Aids

The Landsat 7 satellite is part of NASA's [Earth Observing System \(EOS\)](#). The EOS Data and Information System component ([EOSDIS](#)) provides a structure for data management and user services for products derived from launched EOS satellite instruments, future missions and relevant NASA Earth science data for the foreseeable future. Within the EOSDIS framework, the Distributed Active Archive Centers (DAACs) are responsible for providing data and information services to support the customer community.

These centers are responsible for data archival, product development and distribution along with user support. They are distinguished from one another by their data subject area. The [LP DAAC](#) is responsible for land processes data of which Landsat 7 is a part. The DAACs are linked by the Warehouse Inventory Search Tool ([WIST](#)) web portal which allows users to submit cross-discipline data (e.g. MODIS, ASTER) queries using spatial and temporal criteria, examine search results for relevancy using built-in tools, and submit orders via the EOS ClearingHouse (ECHO) to the appropriate data providers.

Landsat archive searching and downloading is now performed through the [EarthExplorer](#) and [Global Visualization Viewer \(GloVis\)](#) - two web portals developed by the EROS to replace the dated Global Land Information System (GLIS). EarthExplorer allows searches from Macs, PCs and Unix computers across multiple USGS maintained data sets. These data sets include Landsat 7, Landsats 1 - 5, AVHRR and aerial photography. GloVis simplifies the scene selection process via efficient retrospective examination of all acquisitions for a given WRS location.

Two different product generation systems are used by EDC; the NASA-built Level 1 Product Generation System (LPGS) and the EDC-procured National Landsat Archive Production System (NLAPS). The two systems generate similar Landsat 7 Level 1 products but [differences](#) do exist. The user is allowed to choose the level 1 product rendering system.

### **12.2.1 Search Types**

An EarthExplorer search is performed by identifying the Landsat holding and then specifying a location via world map or place/address name. Additional criteria may include acceptable cloud cover, date range, and data type. A search commences and a results page is presented that lists all scenes meeting the search criteria. A set of links appears with each scene that allows one to examine the [browse](#), download the scene, examine the scene's Earth footprint, and view the scene's metadata. Of particular metadata interest to users of [ETM+](#) data are the [cloud cover](#), [data quality scores](#) and the gain states for the individual bands, which are needed to convert the scaled digital numbers to radiance units.

The GloVis portal provides a rapid way of examining the entire acquisition history for a specific WRS location. Once a collection type is selected from a pull-down menu, a user either enters a longitude-latitude coordinate or clicks on a world map to zero-in on the desired land area. A 3 by 3 Landsat browse grid appears with compass keys that allow scene-shifting navigation to the WRS of interest. A pull-down Map Layer menu allows for the overlay of land features such as major cities, rivers, roads, railways, and country boundaries. Search limits (e.g. cloud cover, date range) can be set using the Tools pull-down menu. Once

a scene is selected and added to the order box it can be downloaded or ordered. A downloadable message is splashed on the browse if the scene is currently online. Otherwise, an on-demand order must be submitted.

### 12.2.2 ETM+ Scene-based Browse

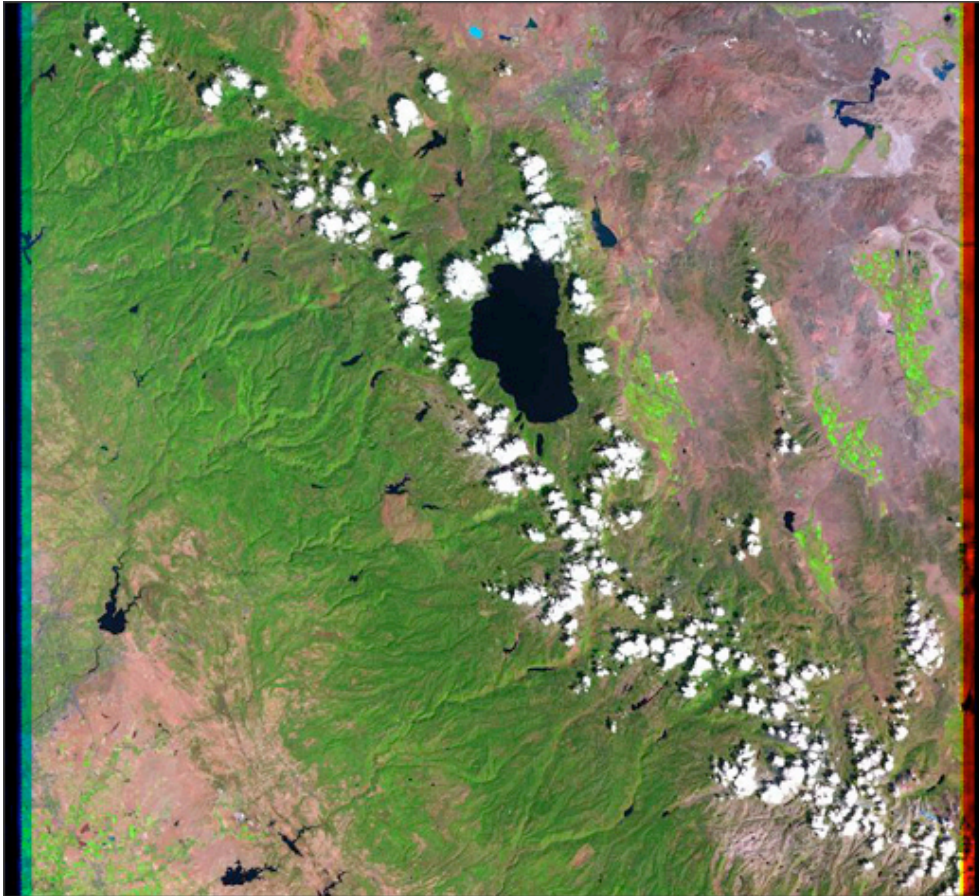


Figure 12.1 - ETM+ Sample Browse

The land area seen in an ETM+ browse is not common to all bands. The image planes are actually staggered according to the following band order arrangement: 8, 1, 2, 3, 4, 7, 5, and 6. For an image collected on a descending pass, band 8 covers more land area to the west than band 1 while band 1 covers more land area to the east. This band staggering effect can be seen in the browse image above. The browse image bands, 5,4,3 are placed in RGB color space. Band 5 reaches furthest to the east as evidenced by the red margin on the right side of the image. Though not as clear, a blue margin exists on the left side of the browse due to band 3's more western position.

When viewing a browse for geographic coverage it's important to keep the band staggering effect in mind. For example, the panchromatic band starts approximately 500 meters before band 5 but also ends 500 meters earlier. Knowledge of band offsets will prevent coverage

surprises when examining a product for the first time.

A wavelets based technique, which preserves visual detail, was used as an alternative to sub-sampling in creating the Landsat 7 browse (Ellison, Milstein).

### 12.2.3 Automated Cloud Cover Assessment

The Landsat 7 Automated Cloud Cover Assessment (ACCA) algorithm recognizes clouds by passing through the scene data twice (Irish, 2000). This two-pass approach differs from the single pass algorithm employed for Landsat-5. The algorithm is based on the premise that clouds are colder than Earth surface features. While true in most cases, temperature inversions do occur. Unexpected cloud cover calculations will occur in these situations.

The first pass through the data is designed to trap clouds and only clouds. [Twenty-six different filters](#) are deployed for this purpose. Omission errors are expected. The pass one goal is to develop a reliable cloud signature for use in pass two where the remaining clouds are identified. Commission errors, however, create algorithm havoc and must be minimized. Three class categories result from pass one processing - clouds, non-clouds, and an ambiguous group that is revisited in pass two.

After pass one processing, descriptive statistics are calculated from the cloud category using band 6. These include mean temperature, standard deviation, and distribution skew. New band 6 thresholds are developed from these statistics for use during pass two. Only the thermal band is examined during this pass to capture the remaining clouds. Image pixels that fall below the new threshold qualify. After processing, the pass one and two cloud cover scores are compared. Extreme differences are indicative of cloud signature corruption. When this occurs, the pass two results are ignored and the cloud score reverts to the pass one result.

During processing, a cloud cover mask is created. After the two passes through the data, a filter is applied to the mask to fill in cloud holes. This filtering operation works by examining each non-cloud pixel in the mask. If 5 of the 8 neighbors are clouds then the pixel is reclassified as cloud. The final cloud cover percentage for the image is calculated based on the filtered cloud mask.

The images in Figure 12.3 demonstrate an example of the improved power the Landsat 7 ACCA algorithm has over the Landsat 5 algorithm. In this case, clouds are successfully separated from the desert terrain below.

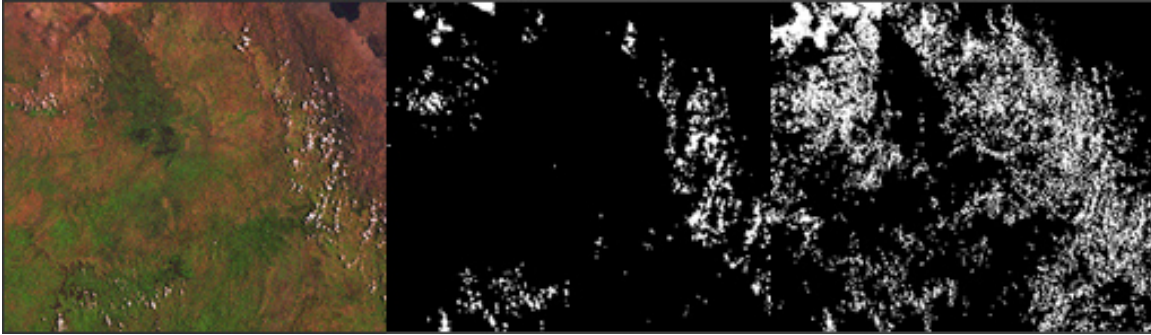


**Figure 12.2 Landsat 5 and 7 Cloud Cover Mask Comparison** - This desert area in Sudan (left, bands 5, 4, 2) represents terrain where the heritage algorithm misclassified rocks as clouds due to their high reflectance in band 5. This can be viewed in the cloud mask to the right. In the middle is the cloud mask generated using the Landsat 7 algorithm. Here the clouds are captured while the rocks are recognized for what they are.

#### **12.2.4 ETM+ Automated Cloud Cover Assessment (ACCA) Algorithm**

##### **Documentation of the ACCA Algorithm**

The operational Landsat-7 ETM+ Automated Cloud-Cover Assessment (ACCA) algorithm is described here. It has been divided into five processes, which parallel the five flow chart figures:

- Pass-1 Spectral Cloud Identification (filters 1-11)
- Band-6 Cloud Signature Development (filters 12-16)
- Pass-2 Thermal Band Cloud Separation (filters 17-20)
- Image-Based Cloud-Cover Assignments and Aggregation (filters 21-15)
- Nearest-Neighbor Cloud-Filling (filter 26)

Most of the computer-intensive part of the processing is in Pass-1 and therefore most of the ACCA algorithm documentation below addresses the processes within Pass-1. Additionally, outputs from all 26 filters are presented for a path 28, row 31 scene in Table 5.

##### **A. PASS-1 SPECTRAL CLOUD IDENTIFICATION**

The algorithm handles the cloud population in each scene uniquely by examining the raw uncalibrated Level-0R image data twice. Data preparation involves converting Bands-2 through -5 to planetary reflectance and Band-6 to apparent at-satellite radiance temperature.

For each spectral band, the 8-bit observed raw uncalibrated image quantized level  $Q$ , in units of digital number (DN), is related to Top-of-the-Atmosphere (TOA) spectral radiance  $L_i$  (in Watts/(m<sup>2</sup> sr μm)) by

$$Q_i = G_i L_i^* + Q_{0i}$$

Where

$G_i$  is sensor responsivity (in DN per unit spectral radiance) for each detector in the band and  $Q_{0i}$  is the average zero-radiance shutter background (in DN) from the Calibration Parameter File (CPF).

Sensor responsivity and the zero-radiance bias for each detector is maintained by the Image Assessment System (IAS) and recorded in the Calibration Parameter File (CPF) at the U. S. ground processing system at EDC. Radiometric detector normalization is applied in each spectral band. Bias-corrected image values are then given by

$$\Delta Q_i = Q_i - Q_{0i} = G_i L_i^*$$

Thus, TOA spectral radiances ( $L_i^*$ ) are related to image data by

$$L_i^* = \Delta Q_i / G_i$$

TOA planetary albedo or reflectance ( $r$ ) for Bands-2 through -5 is related to TOA spectral radiance ( $L_i^*$ ) in each band by

$$r = L_i^* d^2 / (E_{0i} \cos q)$$

where  $E$  is the exo-atmospheric solar irradiance in each spectral band in Watts/(m<sup>2</sup>m), which are referenced in Table 1 and the Landsat Science Data Users Handbook (Irish, 1999),  $q$  is the solar zenith angle, and  $d$  is the Earth-Sun distance in Astronomical Units. At-satellite temperature for Band-6 ( $T$ ) is related to TOA spectral radiance ( $L_i$ ) by

$$T = K2 / \ln ((K1 / L_i) + 1)$$

where

$T$  is the at-sensor temperature in Kelvin,  $K2$  is the calibration constant 1282.71 in degrees

Kelvin,  $K_1$  is the calibration constant 666.09 in Watts/(m<sup>2</sup> sr m), and  $L^*$ ; is spectral radiance from equation 3.

The first pass through the data is designed to capture pixels that are unambiguously clouds and not something on the ground. Eight different filters are used to isolate clouds and to eliminate cloudless areas including problem land surface features such as snow and sand. The pixels of clouds from pass one are used to develop a Band-6 thermal profile and thresholds for clouds for use in pass two where the remaining clouds are identified. Five categories result from pass one processing warm clouds, cold clouds, desert, non-clouds, and an ambiguous group of image pixels that are reexamined in pass two.

The Band-6 temperature profile is formulated from the observed pass one cloud population if it exists. The profile is defined by the cloud populations mean, variance, and skewness, and undergoes modulation if snow or desert features are present in a scene.

A description of each filter, presented in the order implemented follows:

a. Filter 1 Brightness Threshold

Each Band-3 pixel in the scene is first compared to a brightness threshold. Pixel values that exceed the Band-3 threshold, which is set at .08, are passed to filter 3. Pixels that fall below this threshold are identified as are passed to filter 2.

b. Filter 2 Non-cloud/Ambiguous Discriminator, Band3

Comparing each pixel entering this filter to a Band-3 threshold set at .07 identifies potential low-reflectance clouds. Pixels that exceed this threshold are labeled as ambiguous and are re-examined in pass-2. Those falling below .07 are identified as non-clouds and are flagged as such in the cloud mask.

c. Filter 3 Normalized Difference Snow Index

The normalized difference snow index (NDSI) is used to detect snow (Hall et al., 1995). The NDSI filter is expressed as:  $NDSI = (r_2 - r_5) / (r_2 + r_5)$  This filter is designed to eliminate snow. The reflectances of clouds and snow are similar in Band-2. However, in Band-5, reflectance for clouds is high while snow is low. Hall discovered that NDSI values greater than .4 represent snow cover quite well. This value was initially tried for ACCA to eliminate snow but clouds composed of ice crystals (e.g. cirrostratus) were also eliminated. The threshold was raised to .7 to capture potential clouds of this type. Pixels that fall between an NDSI range of -.25 and .7 qualify as potential clouds and are passed to filter 5. Pixels outside this NDSI range are labeled as non-cloud and passed to Filter 4. Snow pixels that slip through are generally trapped later.

d. Filter 4 Snow Threshold

Knowledge of snow in a scene is important for pass two processing so a tally of snow pixels is retained. NDSI values above a .8 threshold qualify as snow and are recorded as non-cloud in the cloud mask.

e. Filter 5 Temperature Threshold

The Band-6 temperature (T) values are used to identify potential clouds. If a pixel value exceeds 300K, a realistic cloud temperature maximum, it is labeled as non-cloud. Pixels with a temperature a value less than 300K are passed to filter 6.

f. Filter 6 Band 5/6 Composite

The low values of the product of values are sensitive to the detection of clouds. The Band 5/6 Composite is expressed as: **Band 5/6 Composite = (1 r5) T** This filter works because clouds have cold temperatures (< 300K) and are highly reflective in Band-5 and therefore have low values of (1 r5) T. It is particularly useful for eliminating cold land surface features that have low Band-5 reflectance such as snow and tundra. Sensitivity analysis demonstrated that a threshold setting of 225 works optimally. Pixels below this threshold are passed to filter 8 as possible clouds. Pixel values above this threshold are examined using filter 7.

g. Filter 7 Non-cloud/Ambiguous Discriminator, Band5

Comparing each pixel entering this filter to a Band-5 threshold set at .08 identifies potential low-reflectance clouds. Pixels that exceed this threshold are labeled as ambiguous and are re-examined in pass-2. Those falling below .08 are identified as non-clouds (probably water) and are flagged as such in the cloud mask.

h. Filter 8 Band 4/3 Ratio for Growing Vegetation

This filter eliminates highly reflective vegetation and is simply Band-4 reflectance divided by Band-3 reflectance. In the near-infrared (Band-4), reflectance for green leaves is high because very little energy is absorbed. In the red region (Band-3), the chlorophyll in green leaves absorbs energy so reflectance is low. The 4/3 ratio results in higher values for vegetation than for other scene features, including clouds. A threshold setting of 2.0 is used. Pixels that exceed this threshold are labeled ambiguous and are revisited in pass-2. Pixels with ratios below this threshold are passed to filter 9.

i. Filter 9 Band 4/2 Ratio for Senescing Vegetation

This filter eliminates highly reflective senescing vegetation and is formed by dividing the Band-4 reflectance by the Band-2 reflectance. In the near-infrared (Band-4), green leaves that are dead or dying absorb even less energy and are thus highly



reflective. In the green region (Band-2), the leaves absorb less energy because of chlorophyll loss and exhibit increased reflectivity. The 4/2 ratio values are higher for vegetation than other scene features including clouds. A threshold setting of 2.16248 works effectively. The at-launch setting was 2.16 but was change in May of 2001(?) when the operational decision was made to Band-4 in low gain. Pixels that exceed this number are ambiguous and are revisited in pass-2. Pixels with ratios below this threshold are passed to filter 10.

j. Filter 10 Band 4/5 Ratio for Soil

This filter eliminates highly reflective rocks and sands in desert landscapes and is formed by dividing the Band-4 reflectance by the Band-5 reflectance. Rocks and sand tend to exhibit higher reflectance in Band-5 than in Band-4, whereas the reverse is true for clouds. A threshold setting of 1.0 works effectively. Pixels that fall below this threshold are labeled ambiguous and are revisited in pass two. Knowledge of desert pixels in a scene is important for pass-2 processing. Therefore, a desert pixel tally is retained. Pixels with ratios that exceed this threshold are passed to filter 11.

k. Filter 11 Band 5/6 Composite for Warm and Cold Clouds

All pixels reaching this filtering level are classified as clouds. A further separation into two classes is achieved by again using the Band 5/6 Composite filter. For each cloud pixel, the Band 5/6 Composite is compared against a threshold setting of 210. Pixels above and below this threshold are classified as warm and cold clouds, respectively. These two cloud classes are recorded in the cloud mask and used to develop two cloud signatures, one for the cold clouds and the other conjoined cloud classes.

## **B. BAND-6 CLOUD SIGNATURE DEVELOPMENT**

Pass-2 processing requires two new band 6 thresholds against which all ambiguous pixels are compared. These thresholds are computed using the pass-1 cloud temperature statistics. Only the cold clouds are used if snow or desert soil is present, otherwise the cold and warm clouds are combined and treated as a single population. The cloud thermal profile developed includes key statistics including the maximum cloud temperature, mean, standard deviation and histogram skewness.

a. Filter 12 Snow and Desert Indicator

An infrared/short-wave infrared ratio is used identify highly reflective rocks and sands in desert landscapes. Snow was previously accounted for. If snow or desert rocks are present, the warm cloud class is eliminated. The desert indicator employed is simply the ratio of potential cloud pixels exiting and entering filter 10 compared against a threshold value of 0.5. If the remaining pixels are less than 50% the warm

clouds are removed. The snow percentage for the scene is computed and compared against a threshold of 1%. If the scene is more than 1% snow the warm clouds are removed.

b. Filter 13 Pass-1 Cloud-free Indicator

The pass-1 cloud tally is compared against zero. If no clouds were tallied processing ends and the scene is declared cloud-free.

c. Filter 14 Pass-1 Cold Cloud, Desert and Mean Cloud Temperature Indicator

Three conditions have to exist to continue pass-2 processing. The cold cloud scene percentage must be greater than 0.4%, the pass-1 cloud temperature mean must less than 295K and desert conditions must not exist. If any of these tests are not met processing passes to filter 22. If all three test are met pass-2 processing continues at filter 15.

d. Filter 15 Temperature Histogram Negative Skewness

Prior to computing the Band-6 thresholds a skew factor is computed from the skewness of the cloud temperature histogram. If the histogram skewness is negative the cloud population is biased towards the left or colder tail of the distribution. No skew factor is necessary because the thresholds are set at appropriate levels for identifying clouds that skew colder. The shift factor is set to 0.0

e. Filter 16 Temperature Histogram Positive Skewness

If the histogram skewness is positive the cloud population is biased towards the right or warmer tail of the cloud temperature distribution. Because of the upward bias in temperature an upward threshold adjustment is necessary. The skewness becomes the skew factor if it is less than 1.0, otherwise it is set to 1.0.

### **C. PASS-2 THERMAL BAND CLOUD SEPARATION**

One of the thresholds is set low and is used to generate a conservative estimate of clouds in a scene. The other is set high and is used to compute a less restrictive estimate of cloud cover. The thresholds are determined from the pass-1 cloud temperature histogram. The histogram's 97.5 and 83.5 percentiles are the starting points for the two temperature thresholds and adjustments are made if necessary. All ambiguous pixels are tested against the two thresholds. If a pixel falls below the high threshold it is labeled as a warm cloud. It is re-labeled cold cloud if it also falls below the lower threshold.

If a pixel temperature falls below the upper threshold, the cloud mask is flagged with a unique number that identifies a class of warmer clouds. If the pixel temperature also falls below the lower threshold, the cloud-mask value is changed to a colder cloud-class identifier.

a. Filter 17 Threshold Shift Deployment

If the skew factor is positive, upward adjustments are made to compensate for the warm cloud bias. The threshold shift is the product of the skew factor and cloud temperature standard deviation. Both thresholds are adjusted by this amount. If the skew factor is 0.0 processing continues at filter 19.

b. Filter 18 Band-6 Maximum Threshold

A final check is made to see if the new upper threshold exceeds the histogram's 98.75 percentile (a threshold above or near the cloud temperature maximum is unwanted). If so, the 98.75 percentile becomes the new upper threshold and the lower threshold is adjusted by the amount of skewness compensation actually allowed.

c. Filter 19 Band-6 Warm Cloud Indicator

Each ambiguous pixels Band-6 temperature is tested against the higher threshold and is labeled a warm cloud if it is lower. Pass-2 then processing continues at filter 20. If it is higher it is skipped and the next ambiguous pixel is likewise examined. The process continues until all ambiguous pixels are accounted for.

d. A3.20. Filter 20 Band-6 Cold Cloud Indicator

Each pass-2 warm cloud is tested against the lower threshold and is re-labeled cold cloud if it is lower. Processing continues at filter 19 until all ambiguous pixels are accounted for.

#### **D. IMAGE-BASED CLOUD-COVER ASSIGNMENTS AND AGGREGATION**

After Band-6 is processed the scene percentages for the warm and cold cloud classes are computed. The integrity of the two additional cloud classes is then appraised. The presence of snow or desert features, and the magnitude of the two new cloud classes are used to accept or reject one or both classes. Cloud classes that qualify as legitimate are combined with the pass one clouds to form a single unified cloud class in the mask.

- a. Filter 21 Pass-2 Cloud-free Indicator  
The pass-2 cloud tally is compared against zero. If no clouds are tallied, an event unlikely to happen, the final scene cloud cover score reported is the cold cloud % from Pass-1. Processing resumes at filter 26.
- b. Filter 22 Pass-1 Cloud Temperature Mean  
This filter is used when the three pass-1 criteria are not met in filter 14. The cold cloud scene percentage might be less than 0.4%, the pass-1 cloud temperature might be greater than 295K and desert conditions may exist. The mean of the pass-1 cold cloud population is again tested against the limit of 295K. If it is less the clouds are accepted as real but with less certainty. If any of these tests are not met processing passes to filter 22. The final scene cloud cover score reported is the cold cloud % from Pass-1. Processing resumes at filter 26. If the mean is greater than 295K uncertainties exists. The final scene cloud cover score is set to zero and processing ends.
- c. Filter 23 Pass-1 Cloud Acceptance Indicator  
If the snow or desert conditions determined earlier exist the pass-1 cloud percentage is determined using the pass-1 cold clouds only. If the scene is free from snow and desert soil the pass-1 cloud percentage is determined using both the cold and warm pass-1 clouds.
- d. Filter 24 Pass-2 Cold and Warm Cloud Acceptance  
The temperature means and maximums are computed for the pass-2 cold and warm cloud populations. Additionally, the percentages of the scene represented by the pass-2 cold class and combined classes (cold and warm) are computed. The pass-2 cold and warm clouds are united with the pass 1 if four conditions are met. The pass-2 cold and warm cloud contribution cannot be more than 35%, snow cannot be greater than 1% of the scene, the mean temperature for combined cloud population cannot be greater than 295K and the between the combined cloud maximum temperature and the upper threshold cannot be less than two degrees. If these four conditions are met all of the clouds identified in pass-2 are united with the pass-1 clouds and processing proceeds to filter 26. If any one condition is breached processing passes to filter 25.

e. Filter 25 Pass-2 Cold Cloud Acceptance

The pass-2 cold clouds are used if their contribution to scene cloud percentage is less than 25% and their mean temperature is less than 295 degrees. If these two conditions are satisfied the cold clouds are united with the pass-1 clouds and processing advances to filter 26. Uncertainty exists if either rule is breached and the pass-1 cold clouds are used in computing the final scene score. Processing continues at filter 26.

## **E. NEAREST-NEIGHBOR CLOUD-FILLING**

A final step involves identifying and filling cloud mask holes. This operation boosts the cloud-cover content to more accurately reflect the amount of unusable image data in a scene. Afterwards, the cloud pixels in the mask are tabulated and a final cloud cover percentage score for the scene is computed.

a. Filter 26 Threshold Shift Deployment

Each non-cloud image pixel is examined and converted to cloud if at least 5 of its 8 neighbors are clouds. Filled pixels qualify as cloudy neighbors in subsequent tests.

### **12.2.5 Algorithm for Calculation of Scene Quality**

A two-digit number that separates image and payload correction (PCD) quality is used by the LPS for Landsat 7. The first digit represents image data quality and can range in value from 0 to 9. The second digit represents PCD quality and can range in value from 0 to 9. The formula for the combined score is:

image score \* 10 + PCD score

The following paragraphs describe how the image quality and PCD quality scores are assigned.

#### **Image Quality Component**

The image quality digit is based on the number and distribution of bad scans or equivalent bad scans in a scene. It is computed by dividing the total number of filled minor frames for a scene by 6313 (the nominal number of image data minor frames in a major frame for 30 meter bands). This will give a number of equivalent bad scans.

The distribution of filled minor frames is characterized as being either clustered or scattered. A cluster of 128 bad scans will still yield a scene with a cluster 246 good scans which is almost 2/3 of a scene. A scattering of 128 bad scans may make the entire image worthless.

What defines clustering versus scattering? It is proposed that bad scan lines are clustered if they occur within a grouping of 128 contiguous scans (approximately 1/3 of a scene). Errors are characterized as scattered if they occur outside the bounds of 128 contiguous scans. The image score is assigned according to the rules in Table 12.1.

<b>Table 12.1 Scene Quality Score - Image Quality Component</b>	
<b>Score</b>	<b>Image Quality</b>
9	no errors detected, a perfect scene
8	<= 4 equivalent bad scans, clustered
7	<= 4 equivalent bad scans, scattered
6	<= 16 equivalent bad scans, clustered
5	<= 16 equivalent bad scans, scattered
4	<= 64 equivalent bad scans, clustered
3	<= 64 equivalent bad scans, scattered
2	<= 128 equivalent bad scans, clustered
1	<= 128 equivalent bad scans, scattered
0	> 128 equivalent bad scans, scattered (> 33% of the scene is bad)

### **PCD Quality Component**

The PCD quality digit is based on the number and distribution of filled PCD minor frames. There are approximately 7 PCD major frames for a standard WRS scene comprised of 375 scans. Each PCD major frame consists of 128 minor frames or 16,384 bytes. Clustering of filled PCD minor frames indicates that errors are localized whereas scattering indicates that numerous or all major frames may be affected.

What defines clustering versus scattering? Each PCD minor frame has 16 jitter measurements and corresponds to 30 milliseconds or approximately 1/2 of a scan. Two minor frames correspond to a single scan while 256 minor frames (i.e., 2 PCD major frames) correspond to 128 scans or approximately 1/3 of a scene.

Like the image data, it is proposed that bad PCD minor frames are clustered if they occur within a grouping of 2 contiguous PCD major frames (1/3 of a scene). Errors are characterized as scattered if they occur outside the bounds of contiguous PCD major frames. The PCD score is assigned according to the rules in Table 12.2.

<b>Table 12.2 Scene Quality Score - PCD Quality Component</b>	
<b>Score</b>	<b>PCD Quality</b>
9	no PCD errors detected
8	<= 8 bad minor frames, clustered
7	<= 8 bad minor frames, scattered
6	<= bad minor frames, clustered
5	<= 32 bad minor frames, scattered
4	<= 128 bad minor frames, clustered
3	<= 128 bad minor frames, scattered
2	<= 256 bad minor frames, clustered
1	<= 256 bad minor frames, scattered
0	> 256 bad minor frames, scattered (> 33% of the scene is bad)

### Scene Quality

The score calculated using the methods described above is recorded in the scene level metadata under the keyword **SCENE\_QUALITY**. Using this scoring system the highest possible rating for an image would be 99, the lowest 00. The score treats missing image data more critically than missing or filled PCD data. For example, an image with 16 filled scans that are scattered and with errorless PCD would have a 59 score whereas an image with intact image data and a 32 filled PCD minor frames that are scattered would receive a score of 95. The rationale is that PCD is less important because missing values can always be extrapolated or interpolated to enable level 1 processing. Missing image data cannot be retrieved and thus impacts the user more severely than missing PCD. The score construct unambiguously alerts the user to image data deterioration.

## 12.3 IGS Landsat Data Archives

The **IGSs** represent an evolving worldwide network of Landsat 7 data collection and product generation centers. IGS data policy and product types may differ from those in the US. While foreign landmasses will be imaged for onboard storage and eventual downlink to US controlled ground stations the depth of ETM+ coverage at participating IGSs will be much deeper. Most, if not all, IGSs will capture every scene imaged by Landsat 7 within their respective acquisition circles. Table 12.3 lists the participating IGSs and provides points of contact and web site addresses for online catalogs.

<b>Table 12.3 IGS Web Sites and Points of Contact</b>			
<b>Country</b>	<b>WWW and Mailing Address</b>	<b>Contact</b>	<b>Comments</b>
Argentina <a href="http://www.conae.gov.ar/">http://www.conae.gov.ar/</a>	Comision Nacional de Actividades Espaciales (CONAE) Ruta C 45 Km 8 Falda del C�rmen (5187) Provincia de C�rdoba ARGENTINA	Lic. Antonio MENESCARDI Station Manager  Phone: 54- 547- 20090 Fax: 54- 547- 25999 Email: <a href="mailto:menes@conae.gov.ar">menes@conae.gov.ar</a>	Operational - 7/15/99  <a href="#">Online Catalog</a>
Australia <a href="http://www.auslig.gov.au/acres/index.htm">http://www.auslig.gov.au/acres/index.htm</a>	Australian Center for Remote Sensing (ACRES) P.O. Box 28 Belconnen , ACT 2616 AUSTRALIA	Mr. Paul Trezise Manager  Phone: 61-2-62014100 Fax: 61-2-62516326 Email: <a href="mailto:P.trezise@auslig.gov.au">P.trezise@auslig.gov.au</a>	Operational - 7/15/99  <a href="#">Digital Catalog</a>
Brazil <a href="http://www.inpe.br/">http://www.inpe.br/</a>	National Institute for Space Research (INPE) Rodovia Presidente Dutra, Km 40 P.O. Box 01 Cachoeira Paulista, Sao Paulo BRAZIL	Mr. Paulo Roberto Martins Serra Head  Phone: 55-12-560-9330 Fax: 55-12-561-2088 Email: <a href="mailto:Serra@cptec.inpe.br">Serra@cptec.inpe.br</a>	Operational - 7/15/99  <a href="#">Digital Catalog</a>
Canada <a href="http://www.ccrs.nrcan.gc.ca/">http://www.ccrs.nrcan.gc.ca/</a>	Canadian Centre for Remote Sensing 588 Booth Street Ottawa, Ontario K1A 0Y7 CANADA	Dr. Susan Till Director, Data Acquisition Division  Phone: 613-947-1217 Fax: 613-947-8201 Email: <a href="mailto:Susan.Till@ccrs.nrcan.gc.ca">Susan.Till@ccrs.nrcan.gc.ca</a>	Operational - 7/15/99  <a href="#">Online Catalog</a>
Ecuador <a href="http://www.clirsenc.com/principal.html">http://www.clirsenc.com/principal.html</a>	Centro de Levantamientos Integrados de Recursos Naturales Por Sensores Remotos Edificio del Instituto Geografico Militar - 4to Piso Apartado 17-08-8216 Quito ECUADOR	Dr. Filemon Valencia Executive Director  Phone: 593-2-582447 Fax: 593-2-581066 Email: <a href="mailto:ecotoecu@uiosatnet.net">ecotoecu@uiosatnet.net</a>	Operational - 7/15/99  <a href="#">Online Catalog</a>
European Space Agency <a href="http://odisseo.esrin.esa.it/">http://odisseo.esrin.esa.it/</a>	European Space Agency (ESA) via Galileo Galilei Casalla Postale 67 Frascati Rome 00046 ITALY	Mr. Mario Albani Executive Director  Phone: 39-06-941-80610 Fax: 39-06-941-80612 Email: <a href="mailto:Malbani@esrin.esa.it">Malbani@esrin.esa.it</a>	Operational - 7/15/99  <a href="#">Online Catalog</a>
Germany <a href="http://www.nz.dlr.de/">http://www.nz.dlr.de/</a>	German Aerospace Center (DLR) German Remote Sensing Data Center (DFD) D-82234 Oberpfaffenhofen GERMANY	Mr. Gunter Schreier Executive Director Phone: 49-8153-28-1375 Fax: 49-8153-28-1313 Email: <a href="mailto:Gunter.Schreier@dlr.de">Gunter.Schreier@dlr.de</a>	Operational - 12/1999  <a href="#">Online Catalog</a>



<p>Indonesia  <a href="http://www.lapanrs.com/">http://www.lapanrs.com/</a></p>	<p>Remote Sensing Application Center  Indonesian National Institute of Aeronautics and Space (LAPAN) JL Lapan No. 70 Pekayon, Pasar Rebo Jakarta 13710 INDONESIA</p>	<p>Mr. Bambang Tejasukmana Executive Director   Telephone: 021-8717714 Fax: 021-871771 Email:  <a href="mailto:bankdata@lapanrs.com">bankdata@lapanrs.com</a> or  <a href="mailto:inderaja@pu.go.id">inderaja@pu.go.id</a></p>	<p>Online Catalog</p>
<p>Japan  <a href="http://www.nasda.go.jp/index_e.html">http://www.nasda.go.jp/index_e.html</a></p>	<p>National Space Development Agency (NASDA) 1401, Numanoue , Ohashi, Hatoyama - machi Hiki -Gun Saitama - ken, 350-0393 JAPAN</p>	<p>Mr. Takashi Nakazawa Associate Senior Engineer   Phone: 81-492-98-1235 Fax: 81-492-98-1001 Email: <a href="mailto:nakazawa.takashi@nasda.go.jp">nakazawa.takashi@nasda.go.jp</a></p>	<p>Operational - FY 2000  Online Catalog</p>
<p>People's Republic of China  <a href="http://www.rsgs.ac.cn/">http://www.rsgs.ac.cn/</a></p>	<p>China Remote Sensing Satellite Ground Station (CRSSGS) Chinese Academy of Sciences No. 45 Bei -Shan- Huan -Xi Road Beijing 100086 PEOPLE'S REPUBLIC OF CHINA</p>	<p>Prof. Pan Xizhe General Director   Phone: 86-10-625-87019 Fax: 86-10-625-61215 Email:  <a href="mailto:Xzpan@ne.rsgs.ac.cn">Xzpan@ne.rsgs.ac.cn</a></p>	<p>Operational - 12/1999  Online Catalog</p>
<p>South Africa  <a href="http://www.sac.co.za/">http://www.sac.co.za/</a></p>	<p>CSIR Satellite Applications Centre (CSIR/SAC) Mikomtek , CSIR P.O. 395 Pretoria 0001 SOUTH AFRICA</p>	<p>Mr. Ike Marais Director   Phone: 27-12-334-5055 or 334-5000 Fax: 27-12-334-5001 Email:  <a href="mailto:Ike.marais@csir.co.za">Ike.marais@csir.co.za</a></p>	<p>Operational - FY2000  Online Catalog</p>
<p>Thailand  <a href="http://www.nrct.go.th/">http://www.nrct.go.th/</a></p>	<p>National Research Council (NRC)  National Research Council 196 Phahonyothin Road Ladyao , Chatuchak Bangkok 10900 THAILAND</p>	<p>Mr. Nares Chamboonroot Director of Remote Sensing Division   Phone: 808-956-3499 Fax: 808-956-9399 Email:  <a href="mailto:UserService@fc.nrct.go.th">UserService@fc.nrct.go.th</a></p>	<p>Operational - FY 2000  Online Catalog</p>
<p>United States  <a href="http://www.soest.hawaii.edu/">http://www.soest.hawaii.edu/</a></p>	<p>University of Hawaii at Manoa (UHM)  University of Hawaii at Manoa School of Ocean, Earth Science and Technology 2525 Correa Road Honolulu, HI 96822 USA</p>	<p>Dr. Torben N. Nielsen Director   Phone: 66-2-579-5218 Fax: 66-2-561-3035 Email: <a href="mailto:Torben@hawaii.edu">Torben@hawaii.edu</a></p>	<p>Operational - 7/15/99</p>

## 13.1 Geometric Performance

### 13.1.1 Requirements

The geometric performance of the ETM+ is judged against three key requirements placed on the Landsat 7 system. They are:

#### **Absolute Geodetic Accuracy**

- Geometrically corrected products shall be accurate to 250 meters (1 sigma), excluding terrain effects, without ground control.
- Limited by spacecraft/instrument geometric model accuracy (e.g., ephemeris, attitude, alignment knowledge).

#### **Band-to-Band Registration**

- Geometrically corrected products shall have the multispectral bands registered to 0.17 pixels (1 sigma)
- Limited by focal plane alignment and stability

#### **Image-to-Image Registration**

- Geometrically corrected images from multiple dates shall be capable of being registered to an accuracy of 7.3 meters (1 sigma)
- Limited by high frequency distortions within images (e.g., uncompensated attitude jitter, scan mirror instability)

### 13.1.2 Geodetic Accuracy

Geodetic accuracy is monitored using calibration scenes containing ground control points. Scenes are first radiometrically and geometrically corrected. Control point locations are then measured on the processed imagery and compared to known ground locations. Any terrain effects are removed analytically in the comparison. The product's geodetic accuracy depends on the accuracy of four data inputs. These are:

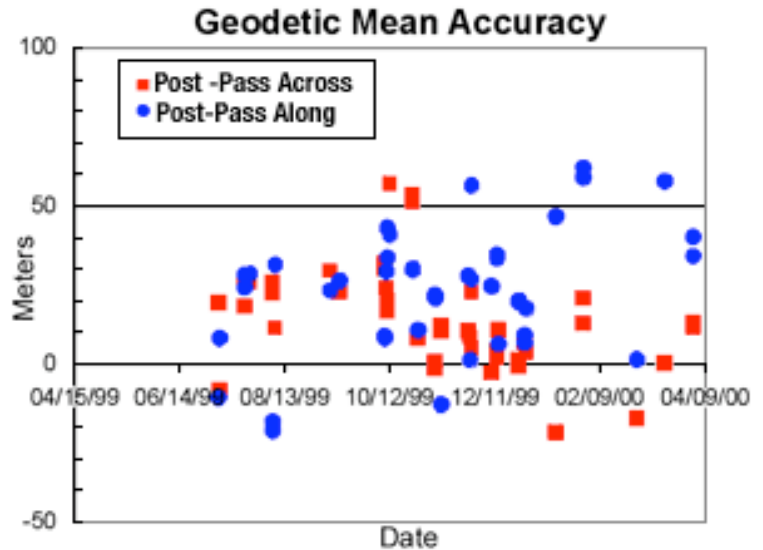


Figure 13.1 - Across and Along Track Mean Geodetic Accuracy of ETM+ Products Since Launch

1. Ephemeris data - spacecraft position and velocity
2. Attitude data - spacecraft orientation (roll, pitch, yaw)
3. Spacecraft clock - links image data to ephemeris and attitude
4. ETM+ alignment - orientation of payload to the spacecraft

The ephemeris is estimated post-pass using tracking data. On-board star trackers and gyros measure attitude. The clock performance is monitored by the Landsat 7 mission operations center and the ETM+ alignment is determined by ground processing calibration.

The ETM+ alignment is determined by measuring the orientation of the ETM+ payload relative to the L7 spacecraft attitude control system reference. Multiple scenes with ground control are used to measure the systematic biases attributable to ETM+ alignment. During the initial on-orbit calibration during first ninety days, seven different calibration scenes were used. Periodic geodetic accuracy testing showed a slow build-up of along-track bias (Figure 13.1) after July, 1999. A sensor alignment calibration update was performed in June, of 2000.

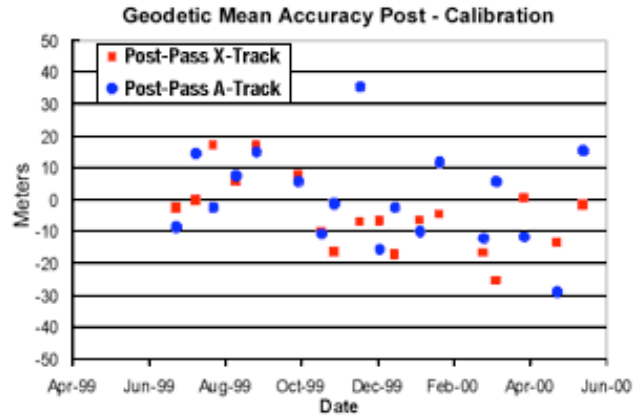


Figure 13.1 - Across and Along Track Mean Geodetic Accuracy of ETM+ Products Since Launch

Twenty-four scenes acquired since July, 1999 (~1 per cycle) were used to perform the calibration. A separate independent set of eighteen scenes covering same time span were used to verify the results. The ETM+ alignment shows time-varying behavior and will continue to be monitored during the course of the mission. Current trending reveals post-calibration (Figure 13.2) geodetic accuracy of systematic ETM+ products is approximately 80 meters (1 sigma), which is much better than 250 meter specification, placed on the system.

### 13.1.3 Band-to-Band Registration

Band-to-band registration assessment is performed periodically throughout the mission's life. The purpose of this assessment is to measure the relative alignment of the eight ETM+ spectral bands after processing to Level 1Gs for verification that the 0.17 pixel band-to-band registration requirement is being met. If not, the IAS remedies the band alignment by deriving new band center locations via band-to-band registration calibration and updating the CPF.

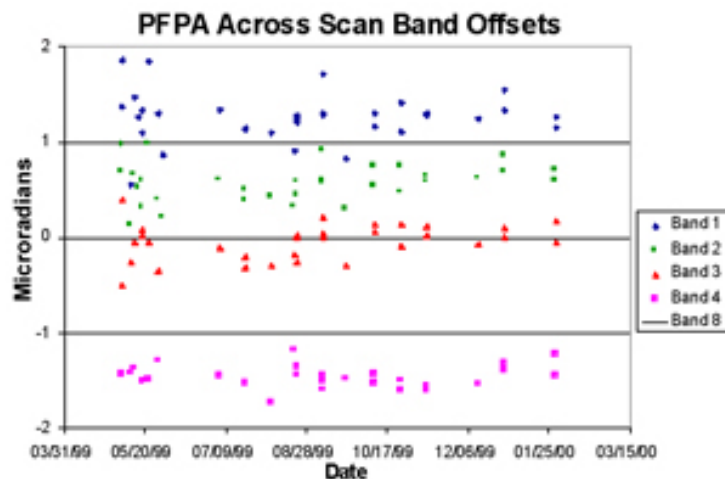


Figure 13.3 - Primary Focal Plane Assembly Across Scan Band Offsets Since Launch

Band registration is monitored using desert scenes as they provide the best cross-band correlation performance. The band center locations measured prelaunch were evaluated using on-orbit data were updated using calibration scenes during the in-orbit checkout period (first 90 days). The measured band registration accuracy was 0.06-0.08 pixels. However, the registration accuracy degraded after July, 1999. Measurements revealed that registration between the primary and cold focal planes in the line direction increased to 0.08-0.10 pixels.

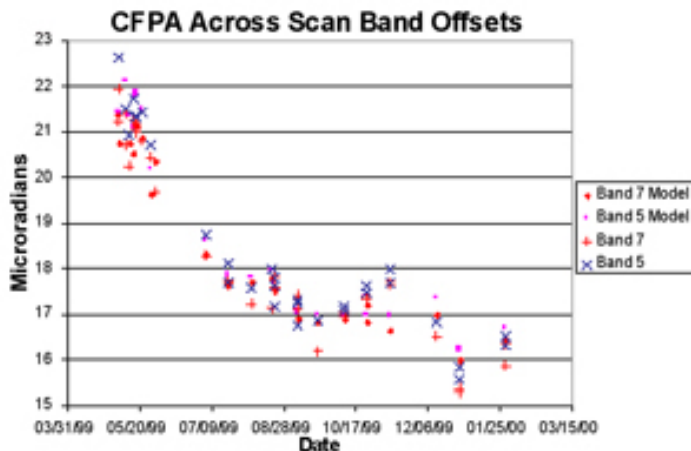


Figure 13.4 - Cold Focal Plane Assembly Across Band Offsets Since Launch

Band calibration analysis showed a systematic shift in the band 5, 6, 7 locations after July, 1999. The primary focal plane band centers (Figure 13.3) are very stable but the focal plane band centers (Figure more variable with a 3-4 microradian mean shift. The cold focal plane offsets coincide with change in ETM+ operating temperature range which is hotter than during the 90-day checkout. The band center calibration was updated for data acquired after July, 1999 although analysis revealed that band center estimates from individual scenes are still highly correlated with temperature telemetry. The current calibration is time-dependent pending development of a temperature dependent model. Nonetheless, registration performance (Figure 13.5) was well within 0.17 pixel specification.

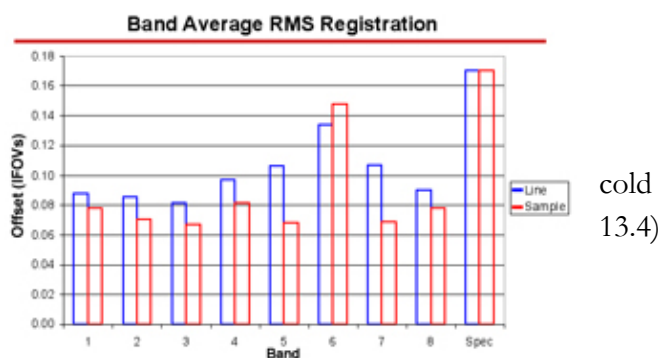


Figure 13.5 - ETM+ Band Center Offsets Versus Specifications

cold  
13.4)

### 13.1.4 Multi-Temporal Image Registration

The multi-temporal registration accuracy was determined using cloud-free scenes of the geometric calibration "super-sites". The term "geometric super-site" is used to describe those pre-selected WRS path-row locations for which ground control, digital terrain data, and reference imagery have been collected. This supporting data set makes it possible to produce precision and terrain corrected ETM+ images, and to compare them to accurately geo-registered reference images.

The required ground control, terrain models, and reference images were derived from digital orthophoto (DOQ) data. The one meter resolution DOQs were mosaicked and reduced to 15 meter resolution. Five cloud-free images of two separate calibration sites were used to measure registration accuracy. The image registration assessment was performed in two ways. First, the ETM+ images were compared against the DOQ reference images. This provides a measure of image distortion relative to an absolute reference. Second, two ETM+ scenes were cross correlated. This provides a measure of image distortion that changes scene-to-scene although systematic calibration distortions may cancel out.

Coupled with the image registration analysis is the need to measure the ETM+ scan mirror performance to ensure the pre-launch profile is correct. The geometric calibration super-site scenes were also used for this purpose. A DOQ reference image was constructed to provide full-width coverage of a Landsat 7 scene so that measurements at all scan angles could be obtained.

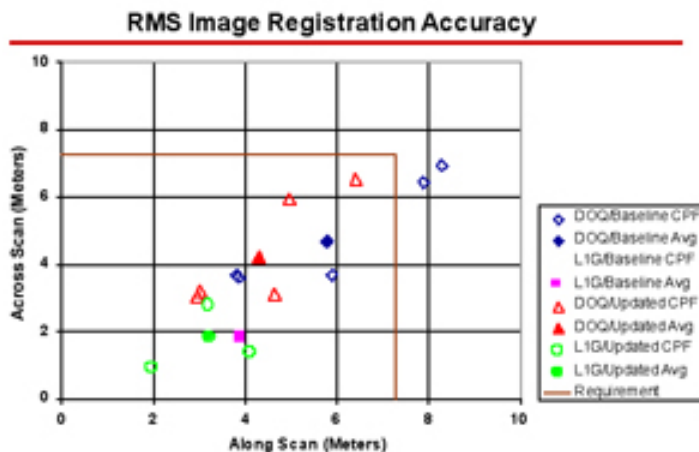


Figure 13.6 - Pre and Post Scan Mirror Calibration Registration Accuracy

Mirror deviations as a function of scan angle were obtained by ??? These were cross-correlating the ETM+ scene to the reference image.

No apparent problem was observed with the along scan mirror profile. A minor adjustment to the cross scan profiles was made to model slightly non-linear scan line corrector behavior. Also, an adjustment to the prelaunch scan angle monitor start/stop angles was made to improve image-to-image registration accuracy. The scan mirror calibration update was made to the CPF in the fourth quarter of 1999.

Image registration accuracy (Figure 13.6) was measured before and after the scan mirror calibration. Results revealed that the required image registration accuracy was achieved using the baseline prelaunch scan mirror calibration parameters. Specifically,

- All-scene average registration to DOQ:
  - meters along scan and 4.7 meters across scan (1 sigma)
- All-scene average ETM+ to ETM+ registration:
  - meters along scan and 1.8 meters across scan (1 sigma)
- Two individual scenes fell outside specification versus DOQ.

The image registration also improved using the updated scan mirror calibration parameters. Analysis yielded the following results.

- Registration to DOQ:
  - meters along scan and 4.2 meters across scan (1 sigma)
- ETM+ to ETM+ registration:
  - 3.2 meters along scan and 1.9 meters across scan (1 sigma)
- All scenes were within specification.

### 13.1.5 ETM+ Scan Mirror Stability

Regular monitoring has revealed the ETM+ scan period is increasing with time due to growth in turnaround time, probably caused by bumper wear. However, the active scan time is showing increased variability, especially in the forward scans. The rate of growth (Figure 13.7) of turnaround time, however, appears to be stable. The impact to ETM+ data is that scan gaps will gradually increase with time. Also, the scan mirror could, theoretically, lose synchronization with the calibration flag if scan time gets too long. This would effectively end the Landsat 7 mission. However, this mirror behavior is similar to that observed in Landsat 5 TM.

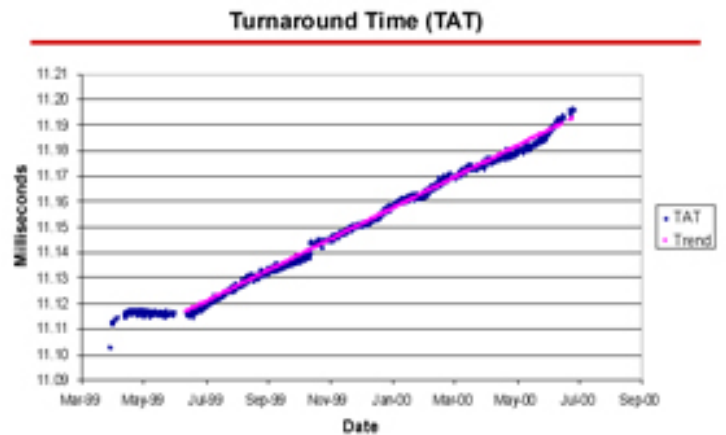
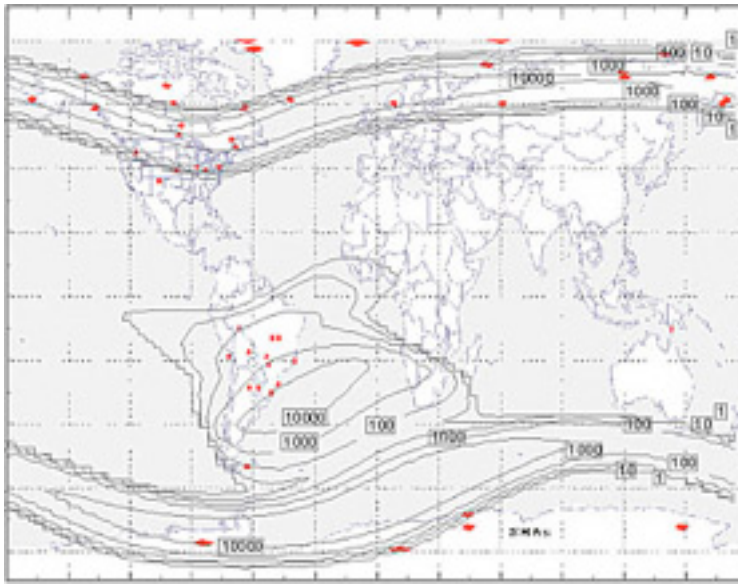
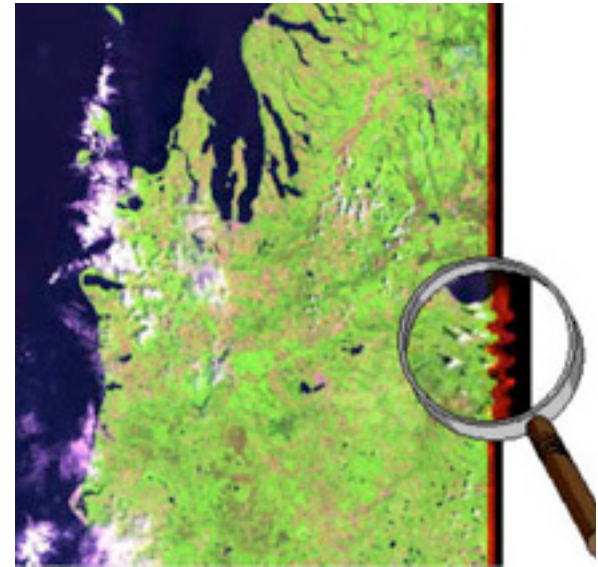


Figure 13.7 - ETM+ Scan Mirror Period Growth



**Figure 13.8** - Regions of High Electron Flux at 708 Kilometers



**Figure 13.9** - ETM+ GXA Data Anomaly

The gimbaled X-band antenna (GXA), when maneuvered in an across-track slew, sometimes disturbs the ETM+ scan mirror. This occurs when GXA the stepper motor frequencies correspond to scan mirror harmonics. The impact to ETM+ data is a wider than normal (Figure 13.9) variation in scan line length. Most extreme examples exceed the maximum allowable scan length leading which leads to dropped scans. This phenomenon was not observed on earlier missions as pointable X-band antennae are new on Landsat 7.

The scan mirror may lose synchronization or, in extreme cases, restart during imaging. Such an occurrence is correlated with regions of high electron flux (Figure 13.8) at 705 km orbital altitude particularly in polar regions and within the South Atlantic anomaly. The correlation was confirmed by a July, 2000 solar flare which resulted in 14 anomalies in a single day. The impact to ETM+ Data is dropped scans and calibration flag incursions (Figure 13.10) into the Earth imaging area. The scan mirror controller sees an "extra" timing pulse and thus loses synchronization with calibration flag. This phenomenon may have occurred on Landsat 5.



**Figure 13.10** - ETM+ GXA Data Anomaly



### 13.1.6 Scan Line Corrector (SLC) Anomaly

On May 31, 2003 the [scan line corrector](#) (SLC), which compensates for the forward motion of the satellite, failed at approximately 21:45. Subsequent efforts to recover the SLC have not been successful, and the problem appears to be permanent.

Landsat 7 Enhanced is still capable of acquiring useful image data with the SLC turned off, particularly within the central portion of any given scene. Various interpolation and compositing schemes are currently being investigated to expand the coverage of useful data. An interpolation example can be seen in Figure 13.13. Landsat 7 ETM+ will therefore continue to acquire image data in the "SLC-off" mode and has so since July 14, 2003. More information on the SLC-off anomaly can be found in [Chapter 11](#).

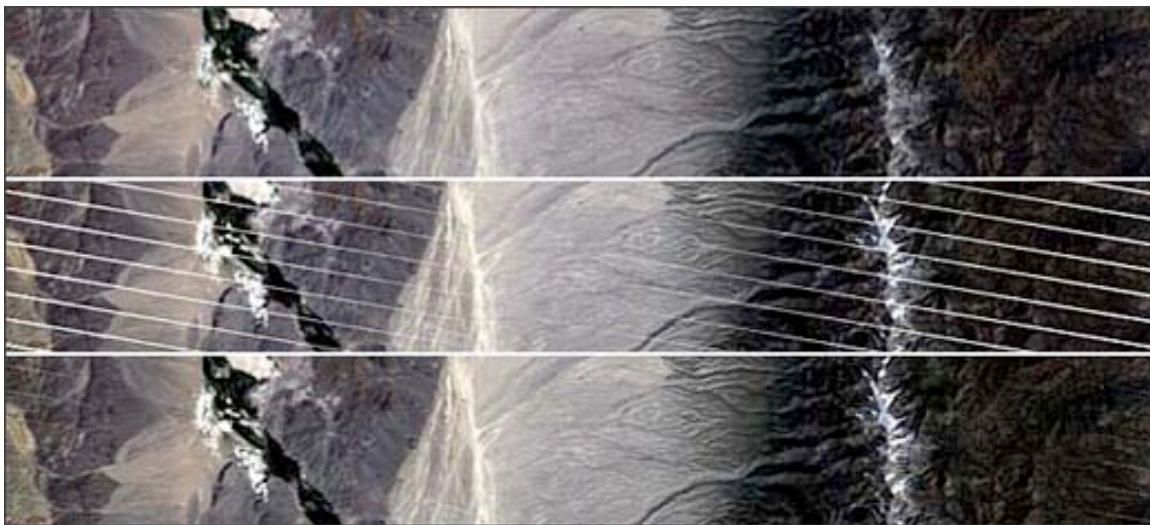


**Figure 13.11** - Top image: Pre-SLC anomaly scene, middle of image.  
Middle image: Scene after SLC anomaly.  
Bottom image: Scene after SLC anomaly, with interpolation.

### 13.1.7 Modulation Transfer Function (MTF) Characterization

The MTF of the ETM+ is regularly measured for comparison to the pre-launch test results and for monitoring long-term instrument performance. The MTF characterization methodology involves the analysis of cloud free scenes (Figure 13.12) over the Lake Ponchartrain bridge (Figure 13.13) in Louisiana. The bridge is long, straight, double-spanned (two 10m spans, separated by 24.4m) is approximately aligned with the Landsat ground track ( $<1^\circ$ ), and offers high signal contrast to the waters below.



Figure 13.12 - ETM+ Image of the MTF Characterization Site

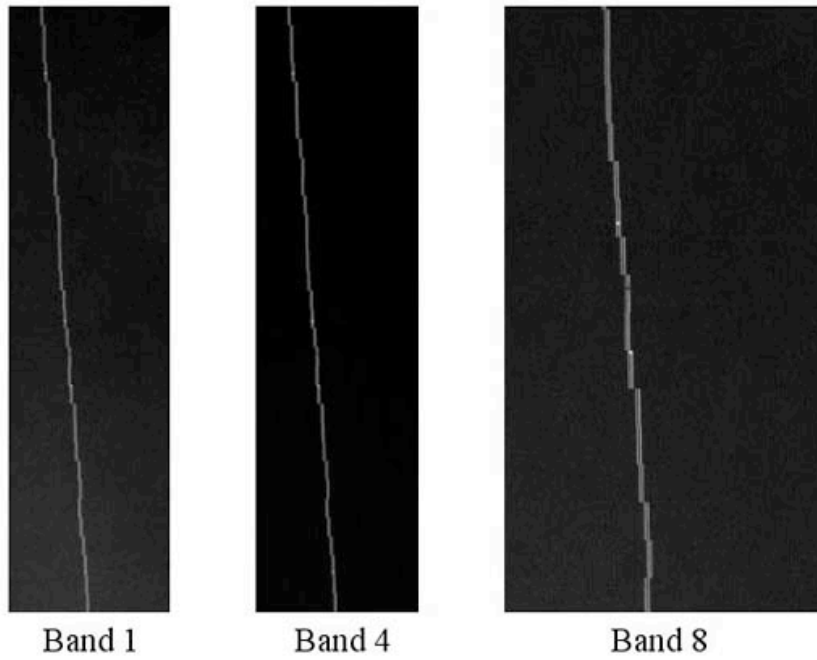


Figure 13.13 - ETM+ Images of Lake Ponchartrain Bridge

The MTF characterization is performed on level 1R data. The 1R data is in 16-bit scaled radiance form with image artifacts removed. The data undergoes no geometric resampling. A 256x2048 image window covering the bridge is manually identified and extracted. The image line numbers containing bridge crossovers (Figure 13.14) are identified and removed from the extracted image. The corresponding windows for the 30-meter bands are then extracted.

A bridge profile is then built by extracting the bridge segments from each data line. Each segment consists of 16 pixels centered about a 3-point moving average. The forward and reverse scans are separated and classified according to bridge segment phase. Phase is determined by correlating each bridge segment to bridge templates (Figure 13.15) templates shifted at 0.125 pixel increments from -1 to +1 pixels (17 total). Each segment is assigned to a phase "bin" based on the offset of the best matching template. The range of 8 consecutive bins with the most segments is then identified. The segments within this bin range are then averaged resulting in 8 mean bin segments containing 16 samples each. The samples from the mean bins are interleaved and the end result is a 128 pixel oversampled bridge profile.

An analytical bridge model was constructed in the frequency domain using the bridge span width, gap between spans and the intensities of the two spans and background water as model parameters. An optical transfer function (OTF) that borrows from previous Landsat 5 TM work was developed for ETM+. The OTF is a mathematical statement that describes the relationship between the input and output of an imaging system. It provides a complete measure of system performance in that it includes the phase relationship as well as the amplitude degradation of the bridge as the frequency changes.

The OTF is then used to compare the bridge models with the actual data. The forward and reverse scan bridge models are multiplied by the OTF model in the frequency domain. An inverse FFT is applied to convert the models to the space domain. The root sum square (RSS) differences between the models and the data for both forward and reverse scans are then computed. To minimize the RSS difference the bridge intensities were adjusted while keeping the span width and separation fixed. Adjusting the variable OTF parameters while keeping the detector model fixed also minimized the RSS differences. Numerous iterations yielded a final OTF model.

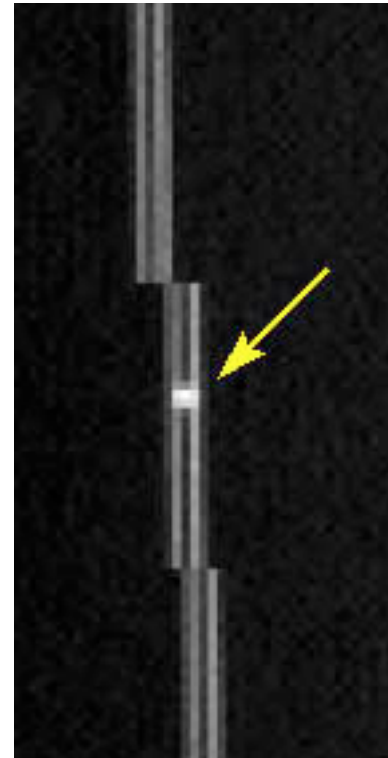


**Figure 13.14 - Lake Ponchartrain**  
Bridge Crossover

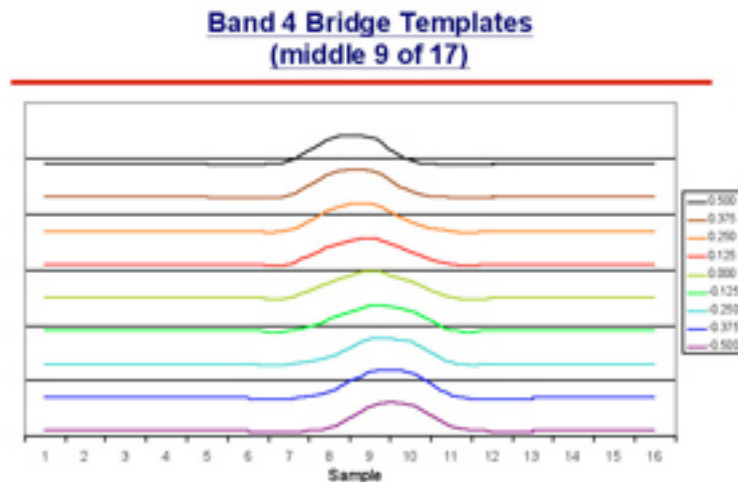


Figure 13.15 - Lake Ponchartrain Bridge Crossover

## 13.2 Radiometric Performance

A significant improvement in the Landsat-7 system is the addition of the IAS Image as part of the ground processing system. The IAS has the role of monitoring the performance and calibration of the ETM+ instrument and providing updates to the calibration parameter file (CPF). The NASA/GSFC Landsat Project Science Office (LPSO) works with the IAS (located at EDC) in analyzing the calibration information and updating the algorithms used within the IAS. Additional funding from NASA supports vicarious radiometric calibration efforts at NASA/JPL, Rochester Institute of Technology, South Dakota State University and the University of Arizona.

Approximately every 6 months the scientists and analysts involved in characterizing ETM+ radiometric calibration meet and present their results. The results form the basis for updating the radiometric gain calibration parameters in the calibration parameter file. The most recent results are presented below.

### 13.2.1 On-orbit Calibration Methods

The three on-board ETM+ calibration devices are the Full Aperture Solar Calibrator (FASC) which is a white painted diffuser panel, a Partial Aperture Solar Calibrator (PASC) which is a set of optics that allow the ETM+ to image the sun through small holes and an Internal Calibrator (IC), which consists of two lamps, a black body, a shutter and optics to transfer the energy from the sources to the focal plane. Details on the devices can be found in [Chapter 8](#).

The FASC is deployed in front of the ETM+ aperture approximately monthly. Based on the orientation of the panel relative to the sun and instrument and the pre-launch measured reflectance of the panel, a calibration can be determined. The IC provides a signal to the ETM+ detectors once each scan line as well as a view of the black shutter. The shutter provides the dark reference for the reflective bands and a low temperature source for the thermal band. The lamps and black body provide the high radiance source for the bands. At the short wavelengths, the IC has shown both short term and long-term instabilities. Results will not be discussed for wavelengths less than  $0.7\mu\text{m}$ . Performance of the PASC has been anomalous and results are not included here. On-orbit performance of the calibrators can be found in a paper that covers the subject in great detail (Markham, B.L., et al.).

### 13.2.2 Ground Look Calibration (GLC) Methods

There are four investigations evaluating the ETM+ radiometric calibration using GLC or vicarious methods. Each of these investigations predicts the radiance at the sensor aperture using a combination of ground- and/or aircraft-based reflectance, radiance or temperature measurements, coupled with measured and/or modeled atmospheric parameters. Two investigations are looking primarily at the reflective band calibrations: those of Helder and Thome (Thome, K.J., et al.). The investigations of Palluconi and Schott are concentrating on the thermal band (Schott, J.R., et al.).

### 13.2.3 Radiometric Performance Results

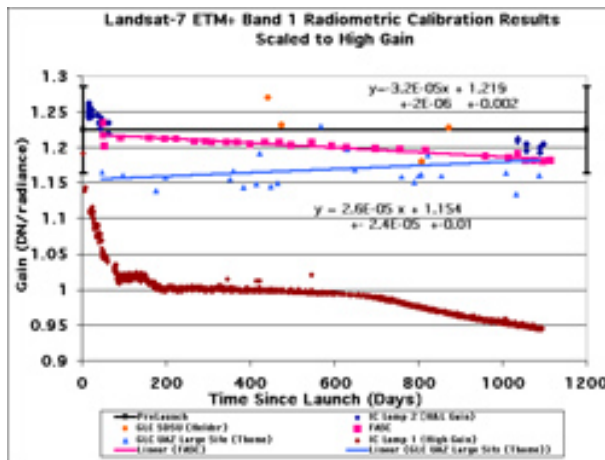


Figure 13.16 - ETM+ Band 1 Band Average High Gain Calibration Results from On-board and Ground-Look compared to Pre-launch values.

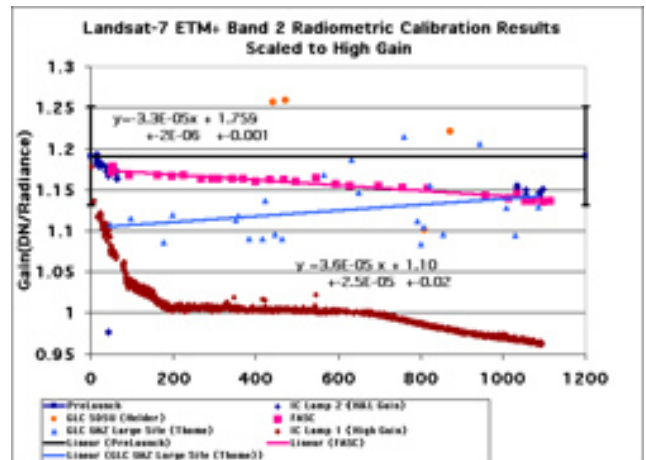


Figure 13.17 - ETM+ Band 2 Band Average High Gain Calibration Results from On-board and Ground-Look compared to Pre-launch values.

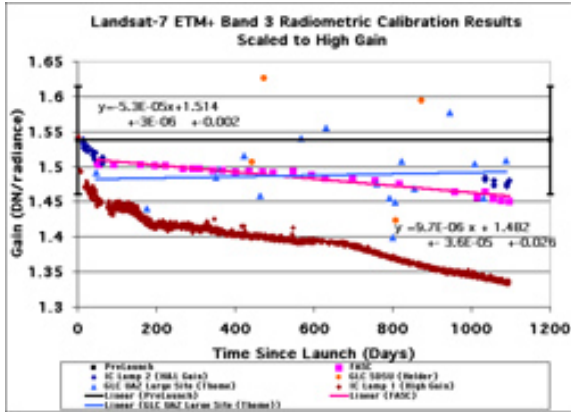


Figure 13.18 - ETM+ Band 3 Band Average High Gain Calibration Results from On-board and Ground-Look compared to Pre-launch values.

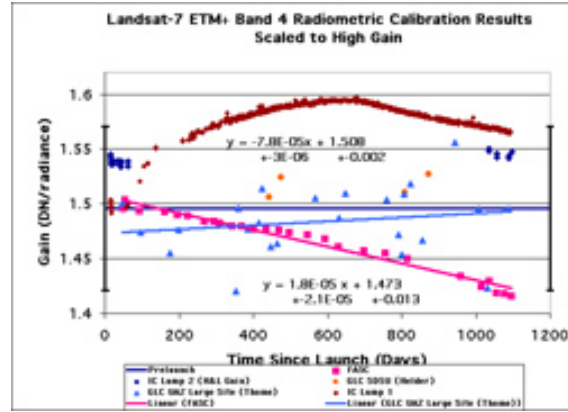


Figure 13.19 - ETM+ Band 4 Band Average High Gain Calibration Results from On-board and Ground-Look compared to Pre-launch values.

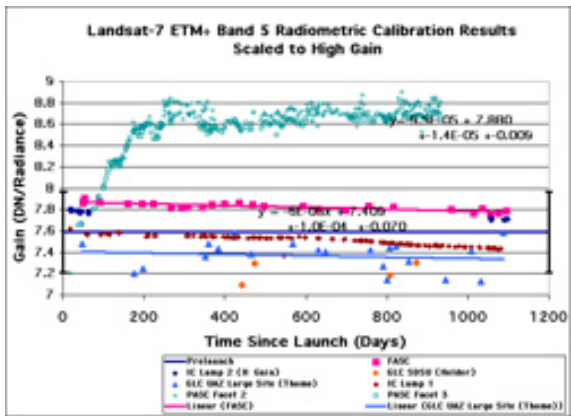


Figure 13.20 - ETM+ Band 5 Band Average High Gain Calibration Results from On-board and Ground-Look compared to Pre-launch values.

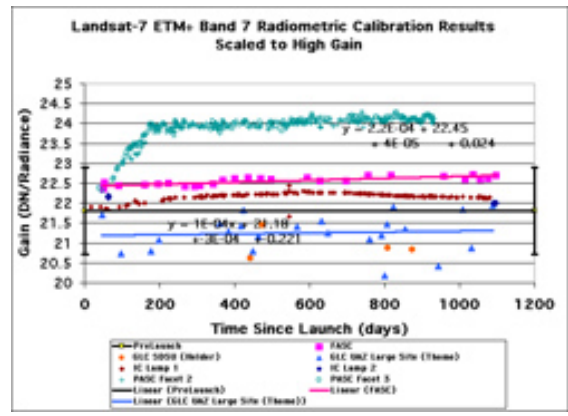
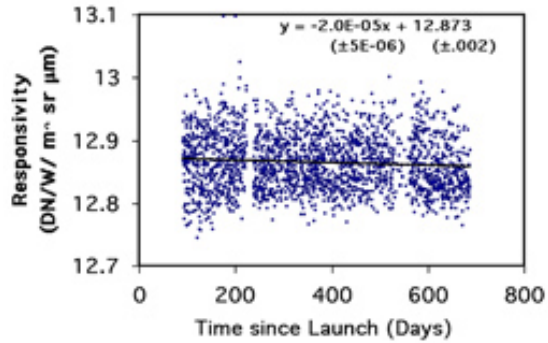


Figure 13.21 - ETM+ Band 7 Band Average High Gain Calibration Results from On-board and Ground-Look compared to Pre-launch values.

The combined calibration results for bands 1 -5, 7 and 8 are presented in Figures 13.16, 13.17, 13.18, 13.19, 13.20, 13.21, 13.22, respectively. In each case the pre-launch calibration currently in the calibration parameter file is presented along with error bars representing <5%. The FASC results presented are based on the "best" portion of the FASC panel and have been adjusted based on an apparent 1° difference in the orientation of the panel from pre-launch measurements (Markhan, B. L., et al). The IC results have also been included, recognizing that part of the variability present is related to the IC itself. Note that in all bands, the vicarious results agree to within 5% of the FASC and pre-launch values and that the trends in the GLC results are not significant. The FASC results do show significant trends, but the trends are small (less that 1.5%/year). The FASC trends are believed to be largely due to changes in the FASCs reflectance and not representative of the instrument. Note, however, that there is some consistency between the FASC, GLC and IC trends, e.g.,

in band 7 all are increasing. If the consistency continues and the vicarious trends become significant, a calibration update will be performed.

In band 6 the IC is the only on-board calibration device. The response to the IC over the life of the mission is shown in Figure 13.23. The slope of the responsivity, though significant, shows a change of less than 0.06%/year. This system is remarkably stable, particularly relative to the Landsat 4 and 5 TM thermal bands. The ETM+ instrument also appears stable relative to the vicarious measurements, though a significant bias was detected (Figure 13.24). This bias was originally measured as 0.31 W/m<sup>2</sup> sr mm and this correction was applied to the calibration parameter file on



**Figure 13.23** - ETM+ Band 6 Band Average Low Gain Mode Responsivity as Determined by Use of the Internal Calibrator.

October 1, 2000. Updated measurements indicate the bias was closer to 0.29. Altering the shutter view coefficients in the calibration parameter file and changing the calibration equation implemented the 0.31 correction. Although the coefficients were changed October 1, 2000, there was no effect on the U.S. Landsat Product Generation System (LPGS) product until December 20, 2000 when the software was revised. Depending on how data are calibrated in non-US processing systems, the calibration change may have been effective October 1, 2000 or may have been later. After correction for the bias, the calibrated product radiance has a scatter of about 1% around the vicarious results (Figure 13.25).

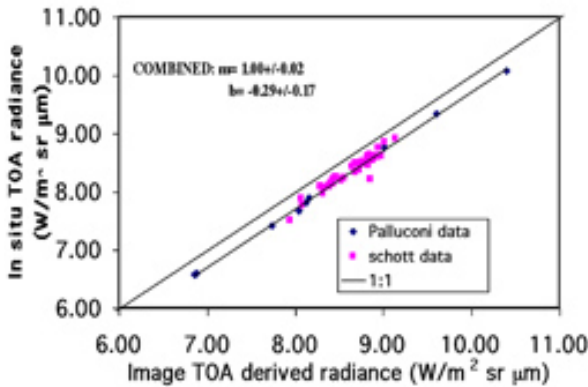


**Figure 13.24** - ETM+ Band 6 In-situ Derived Top of Atmosphere (TOA) Radiances Versus Image Toe before bias correction for July 1999 to Present.

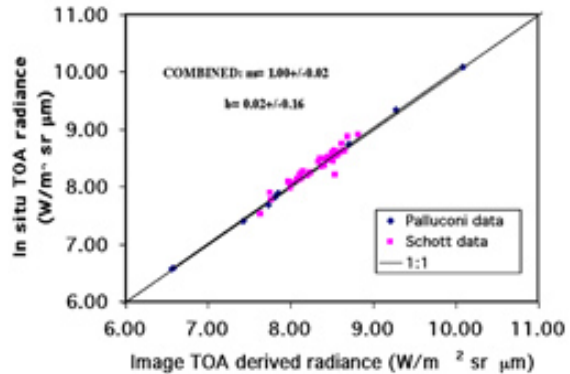


**Figure 13.25** - ETM+ Band 6 In-situ Derived Top of Atmosphere (TOA) Radiances Versus Image TOA after bias correction for July 1999 to Present.

### 13.2.4 Summary

On-orbit results indicate that the Landsat-7 ETM+ absolute radiometric calibration is stable to better than 1.5%/year in the reflective bands and 0.1%/year in the thermal band. The uncertainty in the calibration is estimated at <5% in the reflective and ~1% in the thermal regions.

## 14.1 Monitoring Temperate Forests

**Curtis E. Woodcock - Boston University**

[curtis@bu.edu](mailto:curtis@bu.edu)

Fire, drought, and humans all can destroy forests and their ecosystems. While much attention is paid to deforestation in tropical rainforests, very few comprehensive studies have been done to address changes in the Earth's temperate conifer forests. Temperate conifer forests lie at latitudes above tropical forests and below boreal forests and account for much of the forested area in the United States and Europe.

Understanding changes occurring in temperate conifer forests is important for understanding environmental issues including wildlife habitat protection, watershed management, timber harvest, and understanding the role of human activities on changes in regional climates.

Previously, researchers have only been able to monitor changes in specific locations with Landsat data due to its limited availability. Boston University geographer Curtis E. Woodcock and colleagues used Landsat to monitor how drought in the late 1980s and early 1990s affected forests in California's Sierra Nevada. During the drought, Woodcock found that Landsat images could recognize areas where trees were dying due to lack of water, a factor making the trees more susceptible to disease and the forest more susceptible to fire.

The practice of clearcutting sections of Washington's Olympic National Forest and other state forests in the Pacific Northwest was prevalent up until the late 1980s when changes in public policy caused logging to move from public to private land.

With the help of the frequent and comprehensive coverage of Landsat 7, Woodcock and colleagues plan to create a global monitoring system for temperate conifer forests. The monitoring system will measure the rates of destruction of conifer forests due to natural causes such as drought and fire and anthropogenic clearing due to harvest or development of forest lands. The monitoring system will also track the regrowth of forests and successional change in vegetation.



The new system will work in conjunction with NASA EOS land cover change studies based on the EOS Moderate-resolution Imaging Spectroradiometer (MODIS). The MODIS instrument will fly aboard the Terra satellite set for launch in July 1999, and will be used to identify large areas of significant changes in forest lands. Following up with the finer spatial resolution data from Landsat will allow determination of the type of changes and their geographic extent.

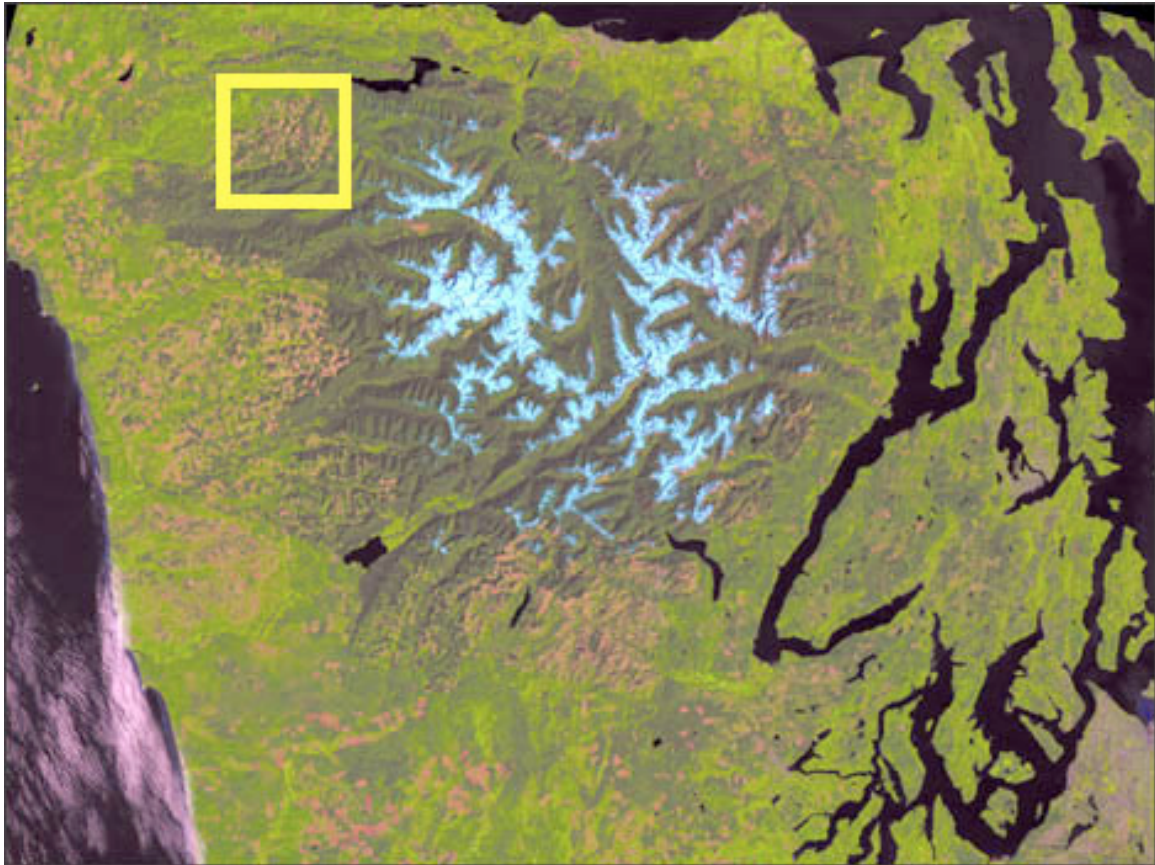


**Figure 14.1**

Using Landsat images of Washington's Olympic Peninsula (above), Boston University researchers can keep track of what areas are being cut, and what areas of forest are regrowing. The square box in this 1986 image represents a square kilometer area within the Olympic National Forest.

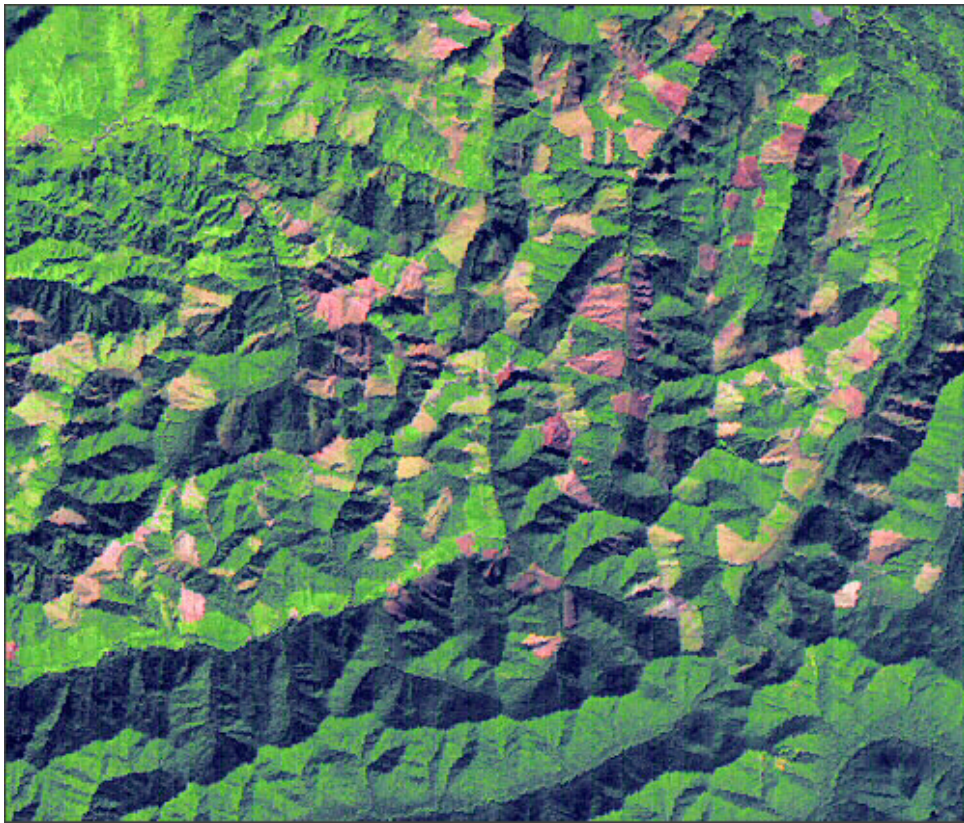


Figure 14.2

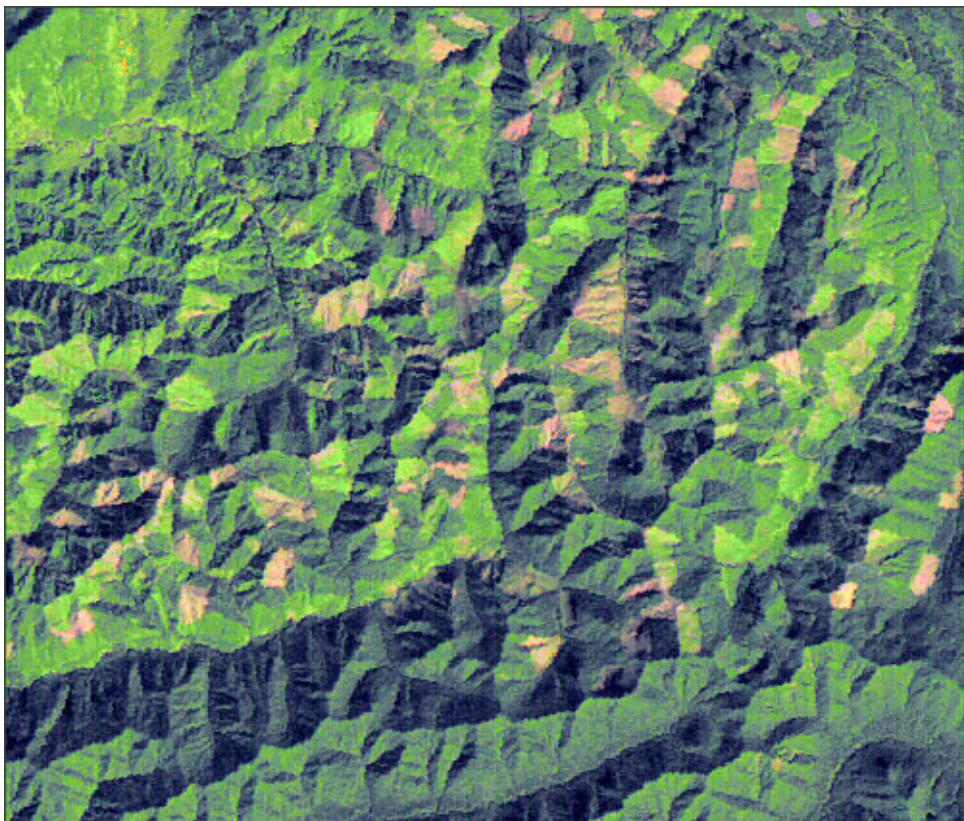


Figure 14.3

The two sub-scenes above are from September, 1987 (top) and September, 1995 (bottom). In each sub-scene, there are clearcut patches (red) in the northern two thirds of the image. Much of the clearcutting occurred prior to 1984. However, new clearcuts are evident in images of this area through 1987. After 1987, there is evidence of regrowing vegetation in the clearcut patches. In the southern portion of the images, the forest is undisturbed; this portion lies within the Olympic National Park.

## 14.2 Mapping Volcanic Surface Deposits

**Luke Flynn - University of Hawaii**

[flynn@pgd.hawaii.edu](mailto:flynn@pgd.hawaii.edu).

To understand the complex "plumbing" beneath active volcanic lava lakes and determine the amount of lava flowing from them, Luke Flynn of the University of Hawaii has been using time series of Landsat images. Much of his work has focused on the persistence of volcanic eruptions at Hawaii's Kilauea volcano, which has been continually erupting since 1983. Another objective of Flynn's research - and one critical to many residents of Hawaii - is to map active lava flows and provide advance warning to public safety officials about these natural hazards.

Flynn and other volcanologists have been using remote-sensing data from the geostationary [GOES](#) satellite to monitor volcanic eruptions in remote areas in real time. The higher resolution of Landsat data (30 meters as compared to 4 kilometers for GOES) can produce maps of lava flows with pinpoint accuracy, according to Flynn. With these maps researchers can study the evolution of individual eruptions while they are taking place.

With Landsat observations of the heat emitted during eruptions, Flynn can distinguish active lava flows from older flows that have already begun to cool. With this data, Flynn's colleague Andrew Harris is generating estimates of the amount of lava erupting onto the surface. Using similar Landsat data, Flynn produces maps of the leading edges of wildfires.

Flynn and Harris have also been working with Landsat data of active volcanic lava lakes around the world. In addition to their work in Hawaii, they are studying long-term observations of eruptions in Mexico (Popocatepetl) and Guatemala (Santaguito and Pacaya). Once they have compiled extensive observations of an individual volcano, they create a database of areas on the volcano that are most prone to lava flow hazards. Flynn plans to produce even higher resolution maps of active lava flows (15 m) with Landsat 7.

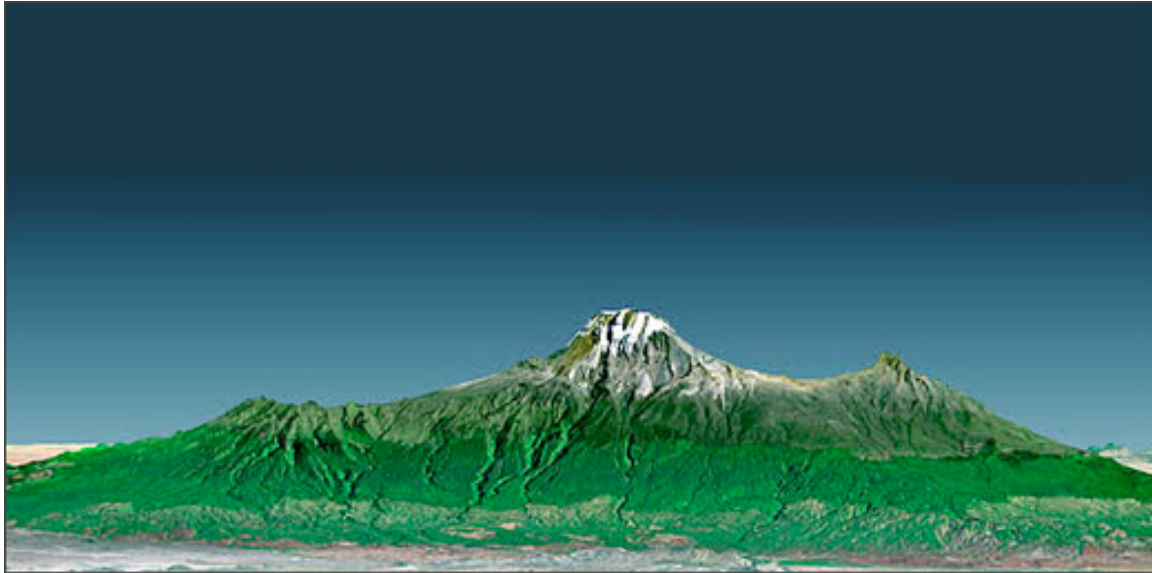
Flynn plans to collect Landsat 7 data at a ground station in Hawaii as the satellite passes over the state. He plans to produce new Landsat 7 volcano (and wildfire) hazard maps for the State of Hawaii every 8 days.



Figure 14.4 Landsat 7 and Land-based Views of Two Guatemalan Volcanoes.

### 14.3 Three Dimensional Land Surface Simulations

This 3-D view was generated using topographic data from the Shuttle Radar Topography Mission (SRTM), a Landsat 7 satellite image, and a false sky rendering. Topographic expression is vertically exaggerated two times.



**Figure 14.5** - Mount Kilimanjaro Perspective View Volcanoes. Date acquired: February 2000 (SRTM); February 21, 2000 (Landsat 7)

### 14.4 Coral Reef Mapping

Serge Andrefouet, a remote sensing specialist at the University of South Florida (USF), has been observing reefs around the world for the past five years. This [powerpoint presentation](http://newlandsathandbook.gsfc.nasa.gov/apps/prog_sect14_4.html) (41.6 MB) found at [http://newlandsathandbook.gsfc.nasa.gov/apps/prog\\_sect14\\_4.html](http://newlandsathandbook.gsfc.nasa.gov/apps/prog_sect14_4.html) describes his coral reef mapping and classification efforts using space-based imagery.

## Glossary

### A

**absorption.** The process by which electromagnetic radiation (EMR) is assimilated and converted into other forms of energy, primarily heat. Absorption takes place only on the EMR that enters a medium. A substance that absorbs EMR may also be a medium of refraction, diffraction, or scattering; however, these processes involve no energy retention or transformation and are distinct from absorption.

**absorption band.** A range of wavelengths (or frequencies) of electromagnetic radiation that is assimilated by the atmosphere or other substance.

**acquisition.** (1) Image captured by satellite sensor. (2) The process of searching for and locking onto a received signal.

**albedo.** (1) The ratio of the amount of electromagnetic energy reflected by a surface to the amount of energy incident upon it, often expressed as a percentage. (2) The reflectivity of a body as compared to that of a perfectly diffusing surface at the same distance from the Sun, and normal to the incident radiation. Albedo may refer to the entire solar spectrum or merely to the visible portion.

**alignment data.** Angular measurement of the physical position of the optical axis with respect to the primary space vehicle reference axes.

**altitude.** Height above a datum, the datum usually being mean sea level. Refers to point above the Earth's surface rather than those on it (elevation).

**analog-to-digital conversion.** The process of sampling continuous analog signals in order to convert them into a stream of digital values. ETM+ data undergo such a conversion prior to downlinking. Abbreviated as A/D conversion.

**angular velocity.** Also called rotational velocity, it is the amount of rotation that a spacecraft undergoes per unit time. For Landsat 7 it is equal to 1.059 mrad/sec ((233 paths/cycle \*  $2\pi$ \*1000 mrad/path) / (16 days/cycle \* 86400 sec/day)).

**angle of drift.** The angle between the heading of the axis of a craft and its ground track.

**anomaly.** A deviation from the norm.

**aperture.** An opening that admits electromagnetic radiation to a detector or film. An example would be the lens diaphragm opening in a camera.

**apogee.** The point in the orbit of a heavenly body, especially of a manmade satellite, at which it is farthest from the Earth.

**ascending node.** The point at which the orbit of an earth satellite intersects the plane of the equator going from south to north.

**at-aperture-radiance.** The radiance at the aperture of the sensor.

**attenuation.** The reduction in the intensity of radiation with distance from its source due to atmospheric absorption and/or scattering. It does not include the inverse-square decrease of intensity of radiation with distance from the source.

**attitude.** The angular orientation of a spacecraft as determined by the relationship between its axes and some reference line or plane or some fixed system of axes. Usually, Y is used for the axis that defines the direction of flight, x for the crosstrack axis, perpendicular to the direction of flight, and z for the vertical axis. Roll is the deviation from the vertical (the angle between the z-axis of the vehicle and the vertical axis, or angular rotation around the y-axis). Pitch is the angular rotation around the x-axis. Yaw is rotation around the z-axis.

**azimuth.** The arc of the horizon measured clockwise from the north point to the point referenced. Expressed in degrees. Azimuth indicates direction, not location.

## **B**

**background.** Any effect in a sensor or other apparatus or system above which the phenomenon of interest must manifest itself before it can be observed.

**band sequential.** A format that arranges the data by band such that all of the data from band 1 followed by all of the data from band 2, etc.

**band, spectral.** An interval in the electromagnetic spectrum defined by two wavelengths, frequencies, or wave numbers. With Landsat, bands designate the specific wavelength intervals at which images are acquired.

**BCH.** An error detection and correction scheme named after its inventors Bose, Chanduri, and Hochergan.

**black body.** An ideal body which, if it existed, would be a perfect absorber and a perfect radiator, absorbing all incident radiation, reflecting none, and emitting radiation at wavelengths. In remote sensing, the exitance curves of black bodies at various temperatures can be used to model naturally occurring phenomena like solar radiation and terrestrial emittance.

**brightness value.** In Landsat parlance, a number in the range of 0-255 that is related to the amount of planetary radiance striking a sensor's detector.

## C

**calibration data.** In remote sensing, measurements pertaining to the spectral or geometric characteristics of a sensor or radiation source. Calibration data are obtained through the use of a fixed energy source such as a calibration lamp, a temperature plate, or a geometric test pattern. The application of calibration data to restore measurements to their true values is called rectification.

**coherent noise.** The noise associated with periodic signals arising from power supplies, transmitters and clock signal typically.

**color.** That property of an object, which is dependent on the wavelength of the light, it reflects or, in the case of a luminescent body, the wavelength of the light it emits. If, in either case, this light is of a single wavelength, the color seen is a pure spectral color, but, if the light of two or more wavelengths is emitted, the color will be mixed. White light is a balanced mixture of all the visible spectral colors.

**color composite.** A color image produced by the combination of three individual monochrome images in which each is assigned a given color. For ETM+ data, if blue is assigned to band 1, green assigned to band 2, and red assigned to band 3, a true color image will result.

**cubic convolution.** A high-order resampling technique in which the brightness value of a pixel in a corrected image is interpolated from the brightness values of the 16 nearest pixels around the location of the corrected pixel.



## D

**data capture.** The receipt and storage of return link mission data at the CADU level.

**data continuity.** A NASA requirement to ensure that Landsat 7 data are compatible to those obtained by earlier Landsat satellites.

**data granule.** The increment of image data stored in the archive, i.e. an interval, swath, or WRS scene.

**data loads.** Data and command transfers from the MOC to the onboard computer.

**dark shutter image data.** The image data obtained from ETM+ detectors when the calibration shutter obscures the detectors from incident electromagnetic radiation.

**descending node.** The point at which the orbit of an earth satellite intersects the plane of the equator going from north to south.

**detector.** The composite circuitry supporting the development of a single output data sample.

**detector sample.** The process of determining the transfer characteristics (detector mean output as a function of incident exposure) for each detector element.

**digital terrain elevation data (DTED).** Digital information produced by DMA, which provides a uniform matrix of terrain elevation values. DTED is commonly used to terrain correct Landsat data.

**distortion.** A change in scale from one part of an image to another.

**dwell time.** Refers to the momentary time interval during which a detector is able to, or allowed to, sense incoming electromagnetic radiation within its intended instantaneous field of view.

**dynamic range.** The ratio of the maximum signal to the smallest measurable signal.

## E

**EDC.** Earth Resources Observation System Data Center is a national archive, production, distribution and research facility for remotely sensed data and other geographic information. (see EROS)

**electromagnetic radiation.** Energy emitted as result of changes in atomic and molecular energy states and propagated through space at the speed of light.

**electromagnetic spectrum.** The system that classifies, according to wavelength, all energy (from short cosmic to long radio) that moves, harmonically, at the constant velocity of light.

**elevation.** Vertical distance from the datum, usually mean sea level, to a point or object on the Earth's surface.

**emission.** With respect to electromagnetic radiation, the process by which a body emits electromagnetic radiation as a consequence of its kinetic temperature only.

**emissivity.** Ratio of radiation emitted by a surface to the radiation emitted by a black body at the same temperature under similar conditions. May be expressed as total emissivity (for all wavelengths), spectral emissivity (as a function of wavelength), or goniometric emissivity (as a function of angle).

**Enhanced Thematic Mapper Plus (ETM+).** The ETM+ is a fixed-position nadir viewing whisk-broom instrument. The viewing swath is produced by means of an oscillating mirror system that sweeps across track as the sensor field of view moves forward along-track due to satellite motion.

**ETM+ scene.** A set of ETM+ observations that covers 170 km in width by 185 km in length and is centered about a WRS vertex.

**engineering data.** All data available on-board about health, safety, environment or status of the platform and instruments.

**ephemeris.** A set of data that provides the assigned places of a celestial body (including a manmade satellite) for regular intervals. Ephemeris data help to characterize the conditions under which remote sensing data are collected and may be used to correct the sensor data prior to analysis.

**EROS.** The Earth Resources Observation System was established in the early 1970s under the Department of Interior's U.S. Geological Survey, to receive, process and distribute data from the United States' Landsat satellite sensors and from airborne mapping cameras.

## F

**field-of-view.** The solid angle through which an instrument is sensitive to radiation. See effective resolution element, instantaneous field of view, and resolution.

**focal length.** In a camera, the distance measured along the optical axis from the optical center of the lens to the plane at which the image of a very distant object is brought into focus.

**focal plane.** In a sensor, the plane occupied by the detectors, and on which the radiances sensed are incident.

**frame.** For Landsat 7, a frame is one Virtual Channel Data Unit with a frame synchronizer pattern (frame marker) attached. This is the same as a Channel Access Data Unit (CADU).

## G

**geocentric.** Any coordinate frame whose origin is relative to the Earth's center of mass.

**geometric correction.** The transformation of image data, such as Landsat data, to match spatial relationships as they are on the Earth. Includes correction for band-to-band offsets, line length, Earth rotation, and detector-to-detector sampling delay. For ETM+ data, a distinction is made between data that have been geometrically corrected using systematic, or predicted, values and data that have been geometrically corrected using precise ground control point data and elevations models.

**geodetic coordinates.** Quantities, which define the position of a point on the spheroid of reference (for example, the Earth) with respect to the planes of the geodetic equator and of a reference meridian. Commonly expressed in terms of latitude and longitude.

**geodetic accuracy.** A measure of how closely a point on the Earth can be located relative to its true absolute location.

**geosynchronous.** An Earth satellite orbit in which the satellite remains in a fixed position over a geographic location on Earth.

**Global Position System (GPS).** A constellation of satellites that can be used to determine accurately the orbit data of satellites.

**ground control point (GCP).** A geographic feature of known location that is recognizable on images and can be used to determine geometric correction functions for those images.

**ground track.** The vertical projection of the actual flight path of a plane or space vehicle onto the surface of the Earth.

**ground truth.** Data, which are acquired from field checks, high-resolution remote sensing data, or other sources of known data. Ground truth is used as the basis for making decisions on training areas and evaluating classification results.

## H

**housekeeping data.** All data available onboard about health, safety, environment, or status of the platform and instruments.

**hue.** The attribute of a color that differentiates it from gray of the same brilliance and that allows it to be classed as blue, green, red, or intermediate shades of these colors.

## I

**image.** The recorded representation of an object produced by optical, electro-optical, optical-mechanical, or electronic means. It is the term generally used when the electromagnetic radiation emitted or reflected from a scene is not directly recorded on photographic film.

**image enhancement.** Any one of a group of operations, which improves the interpretability of an image or the detectability of targets or categories in the image. These operations include contrast enhancement, edge enhancement, spatial filtering, image smoothing, and image sharpening.

**image restoration.** A process by which a degraded image is restored to its original condition. Image restoration is possible only to the extent that the degradation transform is mathematically invertible.

**image-to-image registration.** The registration between images taken at different times.

**image transformation.** A function or operator, which takes an image as input and produces an image as its output. Depending on the transform chosen, the input and output images may appear entirely different and have different interpretations. Fourier, Hadamard, and Karhunen-Love transforms as well as various spatial filters, are examples of frequently used image transformation procedures.

**infrared.** Pertaining to energy in the 0.7 - 100  $\mu\text{m}$  wavelength region of the electromagnetic spectrum. For remote sensing, the infrared wavelengths are often subdivided into near infrared (0.7 - 1.3  $\mu\text{m}$ ), middle infrared (1.3-3.0  $\mu\text{m}$ ), and far infrared (7.0 - 15  $\mu\text{m}$ ). Far infrared is sometimes referred to as thermal or emissive infrared.

**instantaneous field of view (IFOV).** The solid angle through which a detector is sensitive to radiation. In a scanning system this refers to the solid angle subtended by the detector when the scanning motion is stopped. Instantaneous field of view is commonly expressed in milliradians. IFOV also refers to the ground area covered by this solid angle.

**international ground station (IGS).** Any Landsat ground station not belonging to the United States.

**interval.** Is a scheduled ETM+ image period along a WRS path, and may be from 1 to 90 full scenes in length.

**irradiance.** The measure, in units of power, of radiant flux incident on a surface.

## **J**

**jitter.** Small rapid variations in a variable (such as a waveform) due to deliberate or accidental electrical or mechanical disturbances or to changes in the supply of voltages, in the characteristics of components. Jitter effects arising from the oscillating mirrors and other movable parts aboard the Landsat spacecraft are often a cause of certain anomalies in the image data received and must be compensated for by the ground processing software.

## **K**

**K-band.** A radio frequency band extending from approximately 12.5 to 36 gigahertz.

**kernel.** In the spatial domain, a kernel is a  $M \times M$  operator, which can be used in the convolution or multiplication with a  $N \times N$  image to accentuate certain features or properties of an image. A kernel can also be represented in the frequency domain as a Fourier transform.

## L

**L-band.** A radio frequency band extending from approximately 1.0 to 2.0 gigahertz.

**Landsat 7.** Consists of the spacecraft and the ETM+ payload.

**level 0.** Space vehicle or instrument data at full space-time resolution with space-to-ground communication artifacts removed.

**light, transmitted.** Light that has traveled through a medium without being absorbed or scattered.

**long term acquisition plan.** The tasking of the sensor using cloud predictions to optimize the acquisition of cloud free scenes.

**lookup table.** An array of values from which functions corresponding to a given argument can be obtained.

## M

**major frame.** For ETM+, a major frame period is one complete scan of the ETM+ scan mirror (either direction), which includes not only the period during a scan but also the turnaround interval when the scan mirror changes direction for the next scan.

**map projection.** Any systematic arrangement of meridians and parallels portraying the curved surface of a sphere or spheroid upon a plane.

**metadata.** An archived set of descriptive information about a scene and the parent sub-interval that provides a user with geographic coverage, date of acquisition, sun angles, cloud cover, gain states, and other quality measurements.

**minor frame.** For ETM+ major frames are partitioned into minor frames, which is the most fundamental element of the data stream structure, in which specific data measurands (e.g. imagery, PCD, time codes) are extracted.

**mirror scan correction data.** This data includes scan start time, first half scan time error, second half scan time error, scan direction, and any other data which is required to perform mirror scan correction.

**modulate.** To vary, or control, the frequency, phase, or amplitude of an electromagnetic wave or other variable.

**modulation transfer function (MTF).** The modulation transfer function of an imaging system measures the spatial frequency modulation response of the system. As an imaging system processes or records an image, the contrast modulation of the processed or recorded image is different from the input image. The MTF can be thought of as a curve, indicating for each spatial frequency the ratio of the contrast modulation of the output image to the contrast modulation of the input image. It is formally defined as the magnitude of the Fourier transform of the line spread function of the imaging system.

**mosaic.** An image made by piecing together individual images covering adjacent areas.

**multiplexer.** An electronic device, which permits the transmission of multiple messages simultaneously on one communication channel.

**multispectral.** Generally denotes remote sensing in two or more spectral bands, such as visible and infrared.

## **N**

**nadir.** That point on the celestial sphere vertically below the observer, or 180° from the zenith.

**narrowband data.** The data includes the command or forward ranging in the narrowband forward link, and the telemetry or return ranging in the narrowband return link.

**near infrared.** The preferred term for the shorter wavelengths in the infrared region extending from about 0.7  $\mu\text{m}$  (visible red) to about 3  $\mu\text{m}$ . The longer wavelength end grades into the middle infrared. Sometimes called solar infrared, as it is only available for use during the daylight hours. Also known as the shortwave infrared (SWIR).

**node.** Either of the two points at which the orbit of a heavenly body intersects a given plane, especially the plane of ecliptic. With respect to Landsat, the orbital nodes occur at the equator, one on the descending, or daylight, track of the orbit and the other on the ascending, or nighttime, track.

**noise.** Any unwanted disturbance affecting a measurement (as of a frequency band), especially that which degrades the information-bearing quality of the data of interest.

**Nyquist interval.** The maximum time interval between equally spaced samples of a signal that will enable the signal waveform to be completely determined. The Nyquist interval is equal to the reciprocal of twice the highest frequency component of the sampled signal.

**Nyquist's theorem:** A theorem, developed by H. Nyquist, which states that an analog signal waveform may be uniquely reconstructed, without error, from samples taken at equal time intervals. The sampling rate must be equal to, or greater than, twice the highest frequency component in the analog signal.

## O

**optical transfer function (OTF).** A mathematical statement that describes the relationship between the input and the output of an imaging system. When the transfer function operates on the input, the output is obtained. Given any two of these three entities, the third can be obtained.

**orbit adjust.** The adding to or taking away of orbital velocity. This is normally done to maintain altitude or orbit phasing relationships.

**orbital period.** The interval in time between successive passages (orbits) of a satellite through a reference plane.

**orthorectified.** Describing an image in which terrain relief distortions have been removed.

## P

**panchromatic.** A single band covering a broad range of wavelengths; usually used in context of collecting information from the whole visible spectrum.

**parallax.** The apparent change in the position of one object, or point, with respect to another, when viewed from different angles.



**path.** The longitudinal center line of a Landsat scene of a Landsat scene, corresponding to the center of an orbital track. Sequential numbers from east to west are assigned to 233 nominal satellite tracks for Landsat 7. Path numbers are used with row numbers to designate nominal scene center points.

**payload.** That part of a spacecraft (e.g. ETM+) that is separate from the equipment or operations necessary to maintain the spacecraft in orbit.

**payload correction data.** Image support data imbedded in the wideband data stream. Includes satellite attitude, ephemeris, time, angular displacement sensor (ADS) data and payload state.

**perigee.** The point in the orbit of a heavenly body (e.g. satellite) at which it is nearest the Earth.

**pixel.** Picture element provided by a single detector scene sample output.

**pitch.** The rotation of a spacecraft about the horizontal axis normal to its longitudinal axis (in the along-track direction) so as to cause a nose-up or nose-down attitude.

**polar stereographic.** An azimuthal stereographic projection commonly used with Landsat data acquired about 65° latitude. In this projection, the meridians are straight lines converging at the pole (central point), and lines of latitude are concentric circles about this point. Like the UTM projection, the polar stereographic is a conformal projection, meaning that angular relationships are preserved.

**pole wander.** The apparent motion in the poles of the Earth relative to inertial coordinate system. Changes in moments of inertia are due to changes in moments of density due primarily to tides and liquid mass. The National Imager and Mapping Agency (NIMA) generates pole wander data which are used by the Landsat 7 system in the conversion of downlinked ephemeris from inertial to fixed reference, during Level 0R processing.

**precision correction.** Post-processed geometric correction of satellite data using ground control points to correlate the spacecraft's predicted position with its actual geodetic position.

**prime meridian.** Meridian of longitude 0 degrees, used as the origin for measurements of longitude. The meridian of Greenwich, England, is the internationally accepted prime meridian on most charts.

## Q

**quantization level.** The number of numerical values used to represent a continuous quantity.

**quaternion.** A vector of four components; the position is contained in the first three components and an associated scalar rater is located in the last component of this four element vector.

## R

**radian.** The angle subtended by an arc of a circle equal in length to the radius of the circle:  $57.3^\circ$

**radiance.** Measure of the energy radiated by an object. In general, radiance is a function of viewing angle and spectral wavelength and is expressed as energy per solid angle.

**Rayleigh scattering.** Selective scattering of light in the atmosphere by particles that are small compared with the wavelength of light.

**reflectance.** The ratio of the radiant energy reflected by a body to that incident upon it. In general, reflectance is a function of the incident angle of the energy, viewing angle of the sensor, spectral wavelength and bandwidth, and the nature of the object.

**registration.** The process of geometrically aligning two or more sets of image data such that resolution cells for a common ground area can be digitally or visually superimposed.

**roll.** The rotation of a spacecraft about its longitudinal axis (in the along-track direction) so as to cause a side-up or side-down attitude. The roll axis is referred to as the y axis.

**row.** The latitudinal (nominal) center line of a Landsat scene. Row 1 is at latitude  $80^\circ 47'N$ , row 60 is at the equator, and row 122 is at latitude  $81^\circ 51'S$ . In total there are 248 rows.

## S

**sampling rate.** The number of samples taken per unit time, i.e., the rate at which signals are sampled for subsequent use, such as for modulation, coding, and quantization.

**saturation.** The condition where energy flux exceeds the sensitivity range of a detector.

**S band.** A radio frequency band extending from approximately 2.0 to 4.0 gigahertz.

**sidelap.** The extent of lateral overlap between images acquired over adjacent ground tracks.

**signal-to-noise ratio.** The ratio of the level of the information-bearing signal power to the level of the noise power. More precisely, the signal-to-noise ratio of the mean DN to the standard deviation in DN. This is a temporal noise definition in that the mean DN is the time averaged value and the standard deviation in DN is the standard deviation in the time series.

**space oblique mercator.** A variation on the basic mercator map projection based on the dynamics of satellite motion. The movements of the satellite, sensor, and the Earth, expressed as functions of time, are used to calculate which latitudes and longitudes on the Earth correspond to locations in the projection plane.

**spectral band.** An interval in the electromagnetic spectrum defined by two wavelengths, frequencies, or wave numbers.

**spectral response.** The response of a material as a function of wavelength to incident electromagnetic energy, particularly in terms of the measurable energy reflected from and emitted by the material.

**spectral signature.** The quantitative measurement of the properties of an object at one or several wavelength intervals. Spectral signature analysis techniques use the variation in the spectral reflectance or emittance of objects as a method of identifying the objects.

**steradian.** A unit of measure of solid angles. Formally, it is the angle subtended at the center of the sphere by a portion of the surface whose area is equal to the square of the radius of the sphere. There are  $4\pi$  steradians in a sphere.

**subinterval.** Is a contiguous segment of raw wideband data received during a Landsat 7 contact period. Subintervals are caused by breaks in the wideband datastream due to communication dropouts and/or the inability of the spacecraft to transmit a complete observation (interval) within a single Landsat 7 contact period. The largest possible subinterval is 35 full scenes long with a partial scene preamble and postamble. The smallest possible subinterval is a single ETM+ scene.

**sun elevation angle.** The angle of the Sun above the horizon.

**solar zenith angle.** Reciprocal of the sun elevation angle.

**sun synchronous.** An Earth satellite orbit in which the orbital plane remains at a fixed angle with respect to the Sun, precessing through 360° during the period of a year.

**swath.** Refers to the 185 kilometer wide ETM+ imaging ground track.

## T

**telemetry.** The science of measuring a quantity, transmitting the measured value to a distant station, and there, interpreting or recording the quantity measured.

**temporal.** Pertaining to, concerned with, or limited by time.

**temporal resolution.** The expected repeat time between measurements over the same location.

**thermal band.** A general term for intermediate and long wavelength infrared-emitted radiation, as contrasted to short wavelength reflected infrared radiation. In practice, generally refers to infrared radiation emitted in the 3-5  $\mu\text{m}$  and 9-14  $\mu\text{m}$  atmospheric windows.

**thermal infrared.** The preferred term for the middle wavelength ranges of the infrared region extending roughly from 3  $\mu\text{m}$  at the end of the near infrared, to about 15 or 20  $\mu\text{m}$  where the far infrared commences. In practice the limits represent the envelope of energy emitted by the Earth behaving as a graybody with a surface temperature around 290 K. Seen from space, the radiance envelope has several brighter bands corresponding to windows in the atmospheric absorption bands. The thermal band most used in remote sensing extends from 8 to 15  $\mu\text{m}$ .

**time, Greenwich mean.** Mean solar time of the meridian of Greenwich, England (longitude 0), used by most navigators and adopted as the prime basis of standard time throughout the world. Abbreviated GMT.

**time, mean Sun.** The distance in longitude from the Greenwich meridian determines the mean Sun time at a given location on the Earth. The mean Sun time at any location is determined by dividing the difference in longitude from Greenwich (in degrees, moving east) by 15 and adding the result to the current GMT. This will be mean Sun time relative to Greenwich, expressed in hours.

**transmittance.** The ratio of the energy per unit time per unit area (radiant power density) transmitted through an object to the energy per unit time per unit area incident on the object. In general, transmittance is a function of the incident angle of the energy, viewing angle of the sensor, spectral wavelength and bandwidth, and the nature of the object.

## U

**ultraviolet radiation.** Electromagnetic radiation of shorter wavelength than visible radiation but longer than X-rays; roughly, radiation in the wavelength interval between 10 and 4,000 angstroms.

**umbra.** The complete or perfect shadow of an opaque body, as a planet, where the light from the source of illumination is completely cut off.

**universal transverse mercator.** A widely used map projection employing a series of identical projections around the world in the intermediate latitudes, each covering 6 degrees of longitude and oriented to a meridian. The UTM projection is characterized by its property of conformality, meaning that it preserves scale and angular relationships well, and by the ease with which it allows a useful rectangular grid to be superimposed on it. The UTM projection is most commonly used with landsat data.

**UT1-UTC time correction data.** Universal Time (UT) 1 is determined from observations of stellar transits to determine local mean sidereal time corrected to remove the effects of polar motion. Universal Time Coordinated (UTC) is defined to be equal to that of the International System used for atomic time, but it is kept with .9 seconds of UT1 by periodic leap-second adjustments.

## V

**virtual channel data unit (VCDU).** The CCSDS protocol data unit consisting of a fixed length data structure. It is used for bidirectionally space/ground communications on a CCSDS virtual channel.

**visible radiation.** Electromagnetic radiation of the wavelength interval to which the human eye is sensitive; the spectral interval from approximately 0.4 to 0.7  $\mu\text{m}$ .

## **W**

**wavelength.** Wavelength = 1/frequency. In general, the mean distance between maximums (or minimums) of roughly periodic pattern. Specifically, the shortest distance between particles moving in the same phase of oscillation in a wave disturbance.

**world geodetic system (WGS).** The reference Earth model used by the Landsat 7 system.

**worldwide reference system.** A global indexing system for Landsat data, which is based on nominal scene centers, defined by path and row coordinates.

## **X**

**X-band.** A radio frequency band extending from approximately 8.0 to 12.5 gigahertz.

## **Y**

**yaw.** The rotation of a spacecraft about its vertical axis so as to cause the spacecraft's longitudinal axis to deviate left or right from the direction of flight. The yaw axis is referred to as the z axis.

## **Z**

**zenith.** The point in the celestial sphere that is exactly overhead.

## Acronym Expansion

ACCA	Automatic Cloud Cover Assessment
AGS	Alaska Ground Station
AKM	Apogee Kick Motor
AU	Astronomical Unit
BRDF	Bidirectional Reflection Distribution Function
CADU	Channel Access Data Units
CCSDS	Consultative Committee for Space Data Systems
CN	Coherent Noise
COFUR	Cost Of Fulfilling User requests
CPF	Calibration Parameter File
CRAM	Combined Radiometric Correction Model
DFCB	Data Format Control Book
DN	Background Noise
DOQ	Digital Orthophoto Quadrangle
ECS	EOSDIS Core System
EDC	EROS Data Center
EDC-DAAC	EROS Data Center - Distributed Active Archive Center
EOS	Earth Observing System
EOSAT	Earth Observation Satellite Company
EOSDIS	EOS Data and Information System
EPGS	EOS Polar Ground Sites
EROS	Earth Resources Observation Systems
ETM	Enhanced Thematic Mapper
ETM+	Enhanced Thematic Mapper Plus
FAC	Full Aperture Calibrator
FASC	Full Aperture Solar Calibrator
FDF	Flight Dynamics Facility
FOM	Flight Operations Manager
FOT	Flight Operations Team
FTP	File Transfer Protocol
GeoTIFF	Geographic Tagged Image File Format
GSD	Ground Sample Distance
HDF	Hierarchical Data Format
IAD	Ion Assisted Deposition
IAS	Image Assessment System
IC	Internal Calibrator
IFOV	Instantaneous Field of View
IGS	International Ground Stations
IOC	Initial On-orbit Checkout
IR	Infrared
JPL	Jet Propulsion Laboratory
LGN	Landsat Ground Network
LGS	Landsat Ground Station

LP-DAAC	Land Processes Distributed Active Archive Center
LPGS	Level-1 Product Generation System
LPS	Landsat Processing System
LTAP	Long Term Acquisition Plan
ME	Memory Effect
MOC	Mission Operations Center
MMS	Multimission Modular Spacecraft
MSCD	Mirror Scan Correction Data
MSS	MultiSpectral Scanner
MTF	Modulation Transfer Function
NASCOM	NASA Communications Division
NCEP	National Centers for Environmental Prediction
NISN	NASA Integrated Services Network
NLAPS	National Landsat Archive Production System
NOAA	National Oceanic and Atmospheric Administration
PAC	Partial Solar Calibrator
PCD	Payload Correction Data
SBRS	Santa Barbara Remote Sensing
SCS	Scan Correlated Shift
SGS	Svalbard Ground Station
SLC	Scan Line Corrector
SMA	Scan Mirror Assembly
SME	Scan Mirror Electronics
SNR	Signal to Noise Ratio
SSR	Solid State Recorder
SWIR	Short Wave Infrared
SZA	Solar Zenith Angle
TDRS	Tracking Data and Relay Satellites
TM	Thematic Mapper
TOA	Top-of-Atmosphere
USAF	United State Air Force
USGS	United States Geological Survey
VNIR	Visible & Near Infrared
WFF	Wallops Flight Facility
WGS	World Geodetic System
WRS	Worldwide Reference System



## References

- Arvidson, T., Gasch, J., and Goward, S.N. (2001), Landsat 7's Long Term Acquisition Plan - An innovative approach to building a global imagery archive, in press Remote Sensing of the Environment.
- Campana, K. A. (1994), Use of cloud analyses to validate and improve model diagnostic clouds at NMC. Paper presented at the Joint ECMWF/GEWEX Workshop on Modelling, Validation, and Assimilation of Clouds, European Centre for Medium-Range Weather Forecasts, Reading, England, Oct. 31-Nov. 4, 1994.
- Chander, G., Helder, D.L., Markham, B.L., Dewald, J., Kaita, E., Thome, K.J., Micijevic, E., Ruggles, T., "Landsat-5 TM Reflective-Band Absolute Radiometric Calibration", IEEE Transactions on Geoscience and Remote Sensing, vol. 42, No. 12, pp. 2747-2760, Dec, 2004. (Invited paper) Available in [PDF](#) form.
- Chander, G., Meyer, D.J., Helder, D.L., "Cross-Calibration of the Landsat-7 ETM+ and EO-1 ALI sensors," IEEE Transactions on Geoscience and Remote Sensing, vol. 42, No. 12, pp. 2821-2831, Dec, 2004. (Invited paper) Available in [PDF](#) form.
- Chander, G., Markham, B. L., Barsi, J. A., "Revised Landsat 5 Thematic Mapper Radiometric Calibration," IEEE Transactions on Geoscience and Remote Sensing, vol. 4, no. 3, pp. 490–494, Jul. 2007. Available in [PDF](#) form.
- Chander, G., Markham, B.L., Helder, D.L., "Summary of current radiometric calibration coefficients for Landsat MSS, TM, ETM+, and EO-1 ALI sensors", Remote Sensing of Environment 113 (2009) 893 – 903. Available in [PDF](#) form.
- Ellison, J., Milstein, J. (1995), Improved Reduced-Resolution Satellite Imagery, The Aerospace Corporation. Available in [PDF](#) form.
- Gasch, J. and Campana, K. A. (2000), Cloud cover avoidance in space-based remote sensing acquisition. In Algorithms for Multispectral, Hyperspectral, and Ultraspectral Imagery IV, Sylvia S. Shen, Michael R. Descour, Editors, Proceedings of SPIE Vol. 4049, pp. 336-347.
- Goward, S. N., Haskett, J., Williams, D., Arvidson, T., Gasch, J., Lonigro, R., Reeley, M., Irons, J., Dubayah, R., Turner, S., Campana, K., and Bindschadler, R. (1999), Enhanced Landsat capturing all the Earth's land

- areas. EOS, 80 (26): 289, 293.
- Irish, R. (2000), Landsat 7 Automatic Cloud Cover Assessment. Algorithms for Multispectral, Hyperspectral, and Ultraspectral Imagery. SPIE Vol. 4049, pp. 348-355. Available in [PDF](#) form.
  - Irish, R.R., J.L. Barker, S.N. Goward, and T.J. Arvidson (2006). Characterization of the Landsat-7 ETM+ automated cloud-cover assessment (ACCA) algorithm, Photogrammetric Engineering & Remote Sensing, vol. 72, no. 10, pp: 1179–1188. Available in [PDF](#) form.
  - Markham, B. L., Barker, J. L. Landsat MSS and TM Post-Calibration Dynamic Ranges, Exoatmospheric Reflectances and At-Satellite Temperatures. EOSAT Landsat Technical Notes, No. 1, August 1986. Available in [PDF](#) form.
  - Markham, B.L., Chander, G. Revised Landsat 5 TM Radiometric Calibration Procedures and Post-Calibration Dynamic Ranges. White Paper, May, 2003. Available in [PDF](#) form.
  - Markham, B. L., Barker, J.L., Seiferth, J., and Morfitt, R. On-orbit Performance of the Landsat-7 ETM+ Radiometric Calibrators. International Journal of Remote Sensing, in press.
  - Rossow, W. B., Walker, A. W., Beuschel, D. E., and Roiter, M. D. (1996), International Satellite Cloud Climatology Project (ISCCP) Documentation of New Cloud Datasets, WMO/TD-No. 737, 115 pp., World Meteorol. Organ., Geneva, Switzerland, 1996
  - Schott, J.R., Barsi, J.A., Nordgren, B.L., Raqueno, N.G., and de Alwis, D. Calibration of Landsat Thermal Data and Application to Water Resource Studies. Remote Sensing of Environment, in press.
  - Storey, James, C., "Landsat 7 on-orbit modulation transfer function estimation", Proceedings of SPIE -- Volume 4540, Sensors, Systems, and Next-Generation Satellites V, Hiroyuki Fujisada, Joan B. Lurie, Konradin Weber, Editors, December 2001, pp. 50-61. Available in [PDF](#) form.
  - Thome, K.J., Whittington, E., LaMarr, J., Anderson, N., and Nandy, P. (2000). Early Ground-Reference Calibration Results for Landsat-7 ETM+ Using Small Test Sites. Proc. SPIE Conference, Vol. 4049, pp. 134-142.